
**UNIVERSITÀ DEGLI STUDI DI MILANO**

*Corso di Dottorato in Medicina Sperimentale e Biotecnologie Mediche*
*Ciclo XXXII*

*Dipartimento di Scienze Biomediche e Cliniche L. Sacco*

# UNRAVELING THE MECHANISMS INVOLVED IN ENDOTHELIAL RESPONSE TO MICROGRAVITY [MED/04]

Tutor: Prof. Jeanette A.M. Maier

Coordinatore: Prof. Massimo Locati

Laura Locatelli

Matricola R11767

Anno Accademico 2018 - 2019

# SUMMARY

# 1. ABSTRACT

Exposure to real or simulated microgravity is sensed as a stress by mammalian cells, which activate a complex adaptive response. Culture of human endothelial cells for 10 days in real microgravity onboard the ISS resulted in the modulation of more than a thousand genes, some of which involved in stress response. We cultured human endothelial cells for 4 and 10 days in the Rotating Wall Vessel, a NASA developed surrogate system for bench-top microgravity research on Earth. We highlight the crucial role of the early increase of HSP70, since its silencing markedly impairs cell survival. Once HSP70 upregulation fades away after 4 days of simulated microgravity, a complex and articulated increase of various stress proteins - SIRT2, PON2, SOD2, p21, HSP27, P-HSP27 all endowed with cytoprotective properties – occurs and counterbalances the upregulation of the pro-oxidant TXNIP. Interestingly, TXNIP was the most overexpressed transcript in endothelial cells after space flight. We conclude that HSP70 upregulation sustains the initial adaptive response of endothelial cells to mechanical unloading and drives them towards the acquisition of a novel phenotype that maintains cell viability and function through the involvement of different stress proteins.

We also demonstrated that mitophagy contributes to endothelial adaptation to gravitational unloading. After 4 and 10 days of exposure to simulated microgravity in the Rotating Wall Vessel, the amount of BNIP3, a marker of mitophagy, was increased and, in parallel, mitochondrial content and oxygen consumption were reduced, suggesting that HUVEC acquire a thrifty phenotype to meet the novel metabolic challenges generated by gravitational unloading. Moreover, we suggested that microgravity induced-disorganization of the actin cytoskeleton triggers stress adaptation and mitophagy, thus creating a connection between cytoskeletal dynamics and mitochondrial content upon gravitational unloading. We also found that Mg homeostasis was modulated in microgravity, since a reduction of total intracellular magnesium and modulation of its transporters was found in EC exposed to simulated

microgravity. We also investigated a new 3D cell culture method, a microfluidic system where EC are cultured in 3D and in presence of fluid laminar flow, in perspective of using these systems for experiments in microgravity.

# 2. INTRODUCTION

## 2.2. BLOOD VESSELS

The vascular system of human body is composed by arteries, veins and capillaries, three different types of blood vessels that differ in the function, structure and blood pressure to which they are subjected (Figure 1).

The blood vessels are characterized by the same three different layers, named *tunicae*: the intima, the media, and the adventitia [Tabrizchi 2005].

The intima, the innermost one, is composed by a single layer of endothelial cells laid on connective tissue (called lamina propria).

The media corresponds to the muscular layer of the vessel and is composed in different ways depending on the vessels: mainly smooth muscle cells for arteries of medium and small caliber; elastic fibers for large arteries; fibrous component for veins while the capillaries lack of this layer.

The adventitia constitutes the outer layer of blood vessels and is responsible of the interaction with the surrounding environment. Collagen and elastic fibers are the major component of the adventitia, that provides an additional protective layer to the vessels. Considering that in medium and large vessels it can become very thick, this layer is nourished by *vasa vasorum*, a network of small blood vessels necessary to provide additional supply of blood to the adventitia.

*Shear stress*, i.e. the frictional force generated by blood flow, and different blood pressure to which they are subjected diversify the endothelium in arteries, arterioles, post-capillaries venules and capillaries [Hinsbergh 2012].

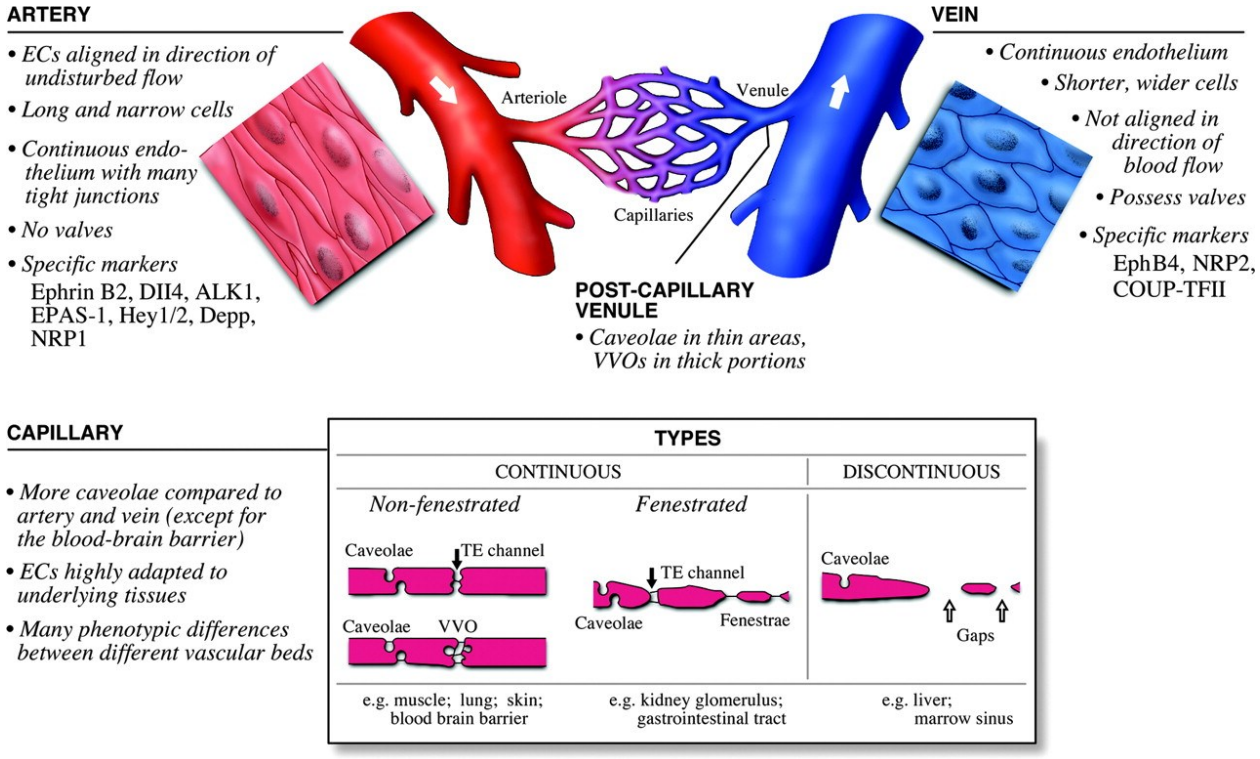


*Figure 1: Different types of blood vessels and their features.*
*Artery, vein and capillary differ for many parameters, among which the number and types of junctions, the alignment or not to the flow and the expression of specific markers [Aird 2007].*

## 2.3. ENDOTHELIUM

It has been estimated that endothelium surface is about 3000-6000 $m^2$ for about 720 g in an adult [Gimbrone 1986]. Most of it is represented by microvascular endothelial cells that line the capillaries [Hinsbergh 2012].

Endothelial and hematopoietic cells derive from hemangioblasts [Choi 1998], bipotent blasts which can originate either a pre-endothelial cell or an hematopoietic cell (Figure 2) [Psaltis 2011]. They can finally transdifferentiate in mesenchymal cells and intimal smooth muscle cells [Galley 2004].

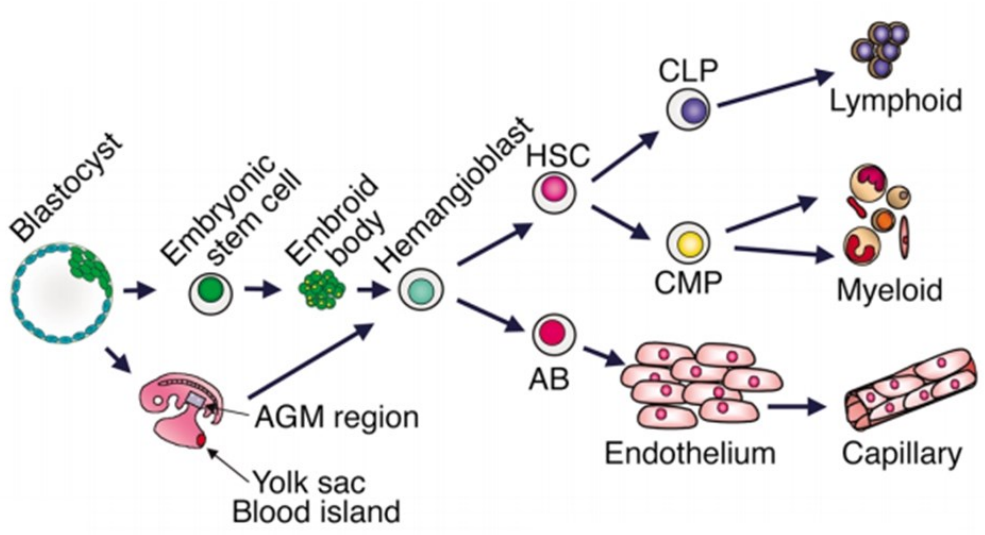


*Figure 2: Endothelial cell precursors.*
*Hemangioblast can derive from blastocyst-derived embryonic stem (ES) cells, or from the yolk sac or AGM region of the early embryo and it can differentiate in Hematopoietic Stem Cells (HSCs), giving rise to both red and white blood cells lineage, or in Angioblast (AB), the precursor of endothelial cells [Moore 2002].*

Von Willebrand Factor (vWF), platelet-endothelial cell adhesion molecule 1 (PECAM-1), endothelial Nitric Oxide Synthases (eNOS) and vascular endothelial-cadherin (VE-Cadherin) are specific markers of mature endothelial cells [Huang 2008, Bai 2010].

Endothelial cells (ECs) are normally quiescent *in vivo* with a turnover rate of approximately once every three years [Foreman 2003]. Most of ECs in the adult have a cell cycle variable from months to years, unless injury to the vessel wall or angiogenesis occur, with the exception of the endothelia of endometrium and corpus luteum, which have a turnover rate of weeks. ECs proliferation can be enhanced by different stimuli, such as Vascular Endothelial Growth Factor (VEGF) and Fibroblast Growth Factor (FGF); in particular, VEGF is highly specific for the endothelium.

## 2.4. ENDOTHELIAL CELL HETEREOGENEITY

Endothelial cells are different between different organs, segments and even in the same organ and this heterogeneity can be detected at different levels: morphology and structure, function, gene expression and antigen composition [Regan 2012].

Endothelial heterogeneity is mediated by two mechanisms: the effect of the surrounding environment and epigenetics (Figure 3).

For what concerns the microenvironment, different ECs located in different districts of the body are subjected to different type of stimuli that orchestrate different reaction and specific functions of ECs. This type of mechanism is dynamically regulated.

On the other hand, epigenetics modifications define the gene expression of ECs through hereditable changes in ECs phenotype determined by DNA and histone methylation, histone acetylation or deacetylation. Even if these epigenetic modifications are triggered by signals from the surrounding environment, as the first mechanism of heterogeneity, they can also persist after the removal of the signals and they are transmitted during mitosis [Aird 2012].

These two mechanisms are responsible of the different role and specific functions of endothelial cells of different districts.

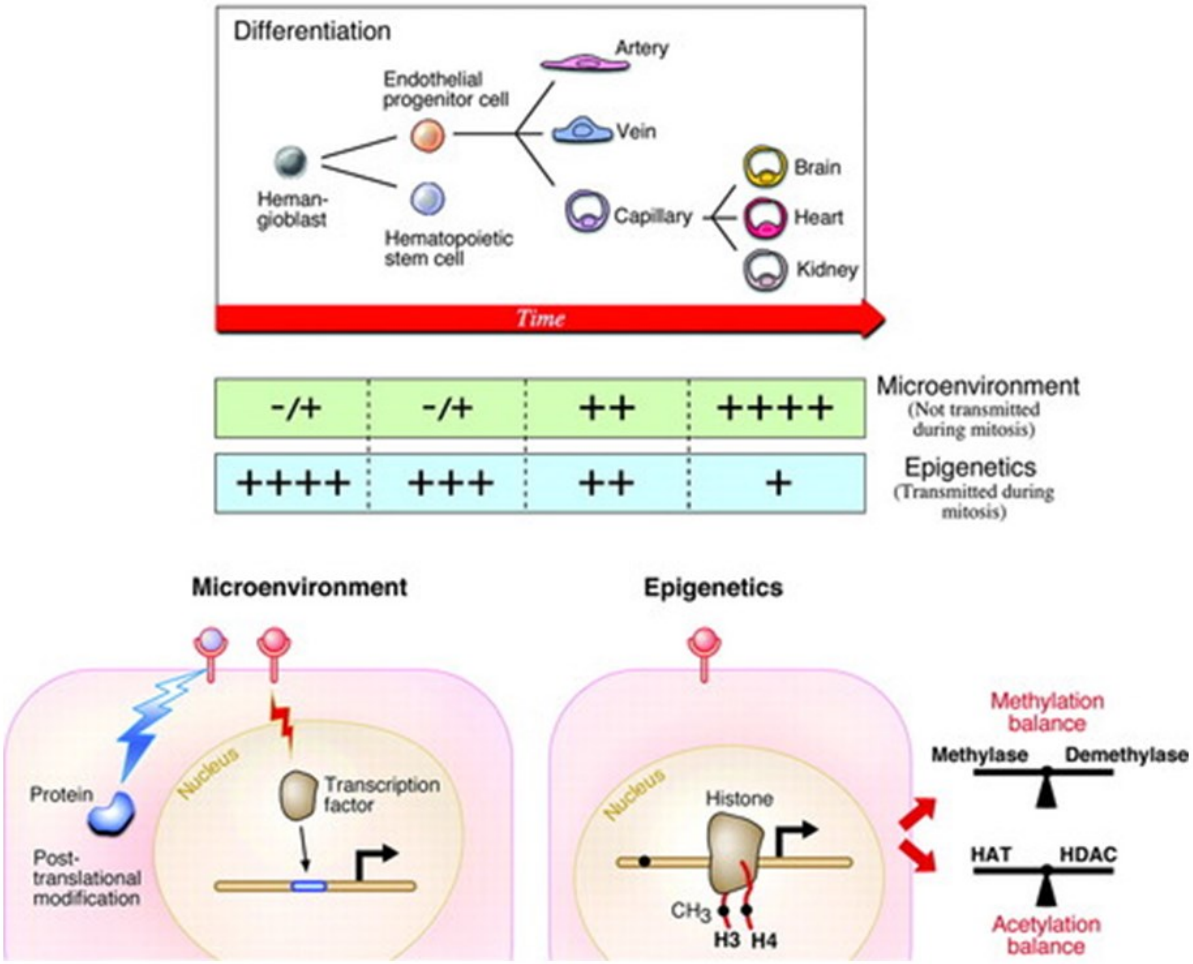


*Figure 3: Mechanisms of endothelial cell heterogeneity [Aird 2012].*
*Starting from the hemangioblast precursor to the terminally differentiated cells the effects of microenvironment and epigenetic are different. The effect of microenvironment is predominant in differentiated cells while epigenetics is fundamental in defining the genotypic and phenotypic features of the precursors cells and it is then transmitted to the progeny through mitosis.*

### 2.4.1. STRUCTURAL HETEREOGENEITY

The shape of ECs can vary very deeply across the vascular tree, depending on the segment and the type of vessels they line and also on the organ they are located in [Regan 2012]. They can display a flat morphology or they can appear plump and

cuboidal as in venules.
Even the thickness can vary, from 0.1 μm in capillaries and veins to 1 μm in big arteries such as aorta.

Moreover, blood-flow direct the alignment of ECs (and their nuclei) in the direction of flow in straight segments of arteries but not at branch points, so the ramification and the length of the vessels are important features in determining the effect of the alignment to the flow.

They can also vary for the type of junction they are composed by: tight junctions (also called *zonula occludens)* or adherens junction (or *zonula adherens*). The former type of junctions is fundamental for the function of barrier of ECs and they allow the cell to maintain a polarity of luminal and apical side [Aird 2007]. For example, within the microvasculature, blood vessels of the blood brain barrier are particularly rich in tight junction while in post-capillary venules they are absent, in order to allow the extravasation of leukocytes during inflammation.

Moreover, the endothelium could be continuous (fenestrated or non-fenestrated) or discontinuous, depending on the needs of the surrounding tissue [Hinsbergh 2012] (Figure 4). Fenestrated continuous endothelium is characteristic of locations where filtration or transendothelial transport are fundamental (for example capillaries of glands and kidney); while non-fenestrated endothelium is abundant in vessels of brain, heart, lung and skin [Hinsbergh 2012]. On the other hand, discontinuous endothelium may be found in certain sinusoidal beds.

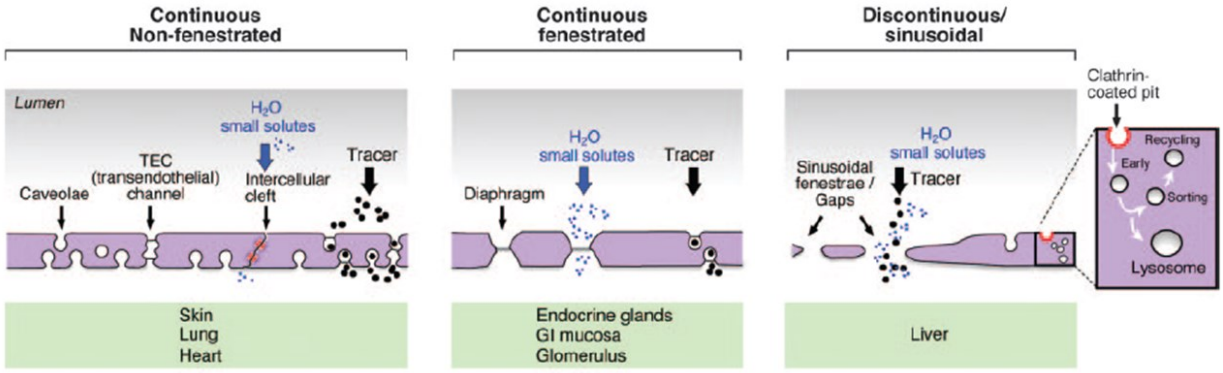


*Figure 4: Types of endothelium.*
*In continuous non-fenestrated capillaries small solutes and fluids pass constitutively between ECs while larger solutes are carried through transendothelial channels or transcytosis. Continuous fenestrated endothelium is highly permeable to water and small solutes but not to larger macromolecules. Discontinuous endothelium is characterized by fenestrae and it is rich of clathrin-coated pits, which play an important role in receptor-mediated endocytosis [Aird 2007].*

### 2.4.2. FUNCTIONAL HETEREOGENEITY

Endothelial cells are able to perform different function, such as regulation of vascular tone, coagulation and fibrinolysis, leukocytes' trafficking, and also immunoresponse, most of which are performed by specific subset of blood vessel or vascular beds [Sena 2013].

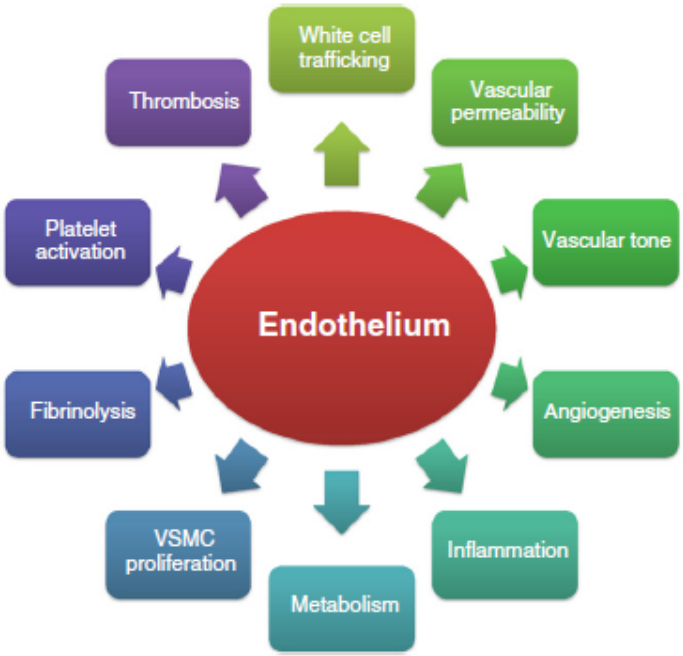


*Figure 5: Endothelial cells functions [Sena 2013].*
*ECs are able to perform different function in order to maintain tissue homeostasis, among which the regulation of coagulation, immunoresponse, permeability, angiogenesis and metabolism. To do these functions they interact with different cell types.*

Until 50 years ago the endothelium was considered as an inert barrier [Galley 2004]. Nowadays it is clear this is a dynamic and heterogeneous organ fundamental in maintaining the integrity of vessels and tissues homeostasis.

Endothelial cells have synthetic, metabolic, secretory and immunologic functions [Cines 1998] that allow the interaction of EC with the environment and their response after stimuli [Galley 2004].

The endothelium is a semipermeable barrier that regulates exchanges of different fluids and solutes between the blood and the surrounding tissues through the regulation of permeability. Fluids and small solutes pass passively across the endothelium through the paracellular pathway, while macromolecules are shuttled using the trans-cellular pathway. The former is mediated by homophilic adhesion of VE-Cadherin, which can be

stably associated to the membrane or can translocate (through the remodeling of actin cytoskeleton) to the cytosol in response of extracellular stimuli, mediating the increase of permeability. Particularly there are three different stimuli that lead to VE-cadherin translocation: c-Src and RhoA activation and/or increased calcium concentration (Figure 6).

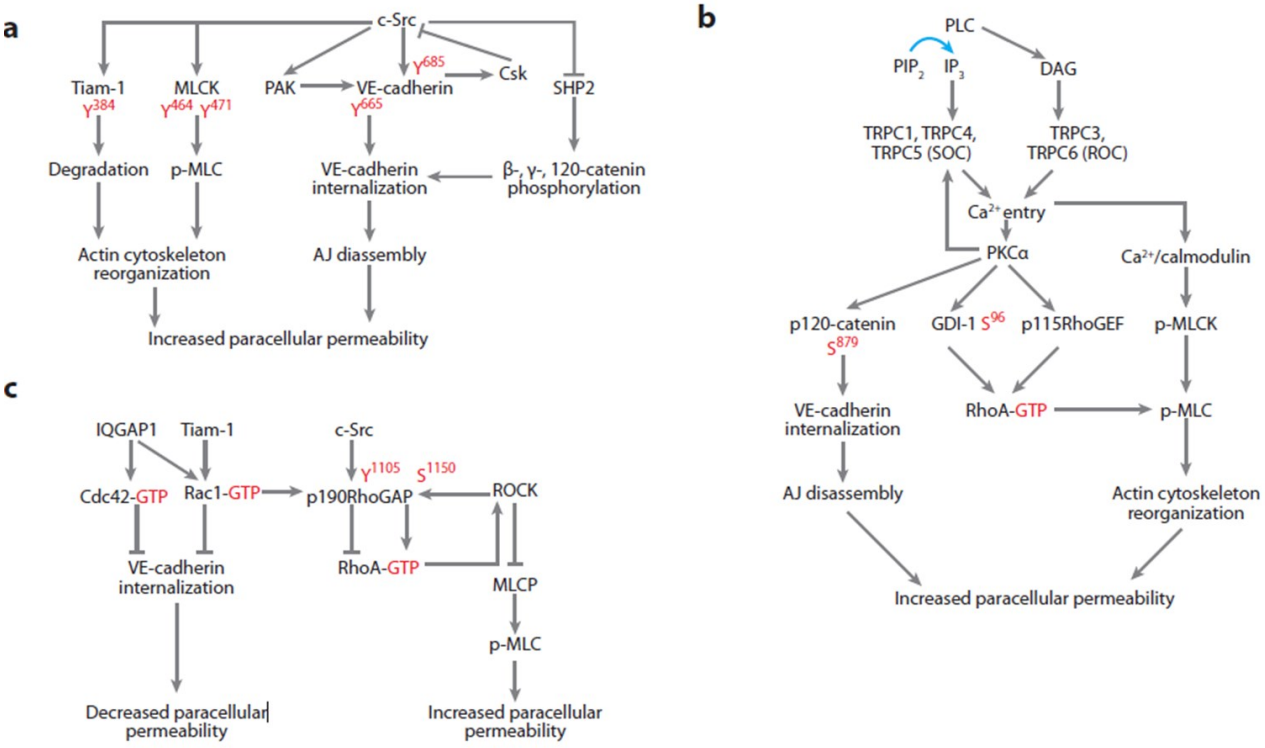


*Figure 6: Pathways leading to Ve-Cadherin translocation and increasing permeability [Komarova 2010].*

The latter may involve receptors (in the so-called receptor-mediated transcytosis) or may be receptor-independent (fluid-phase transcytosis). This mechanism is mediated by the presence of Caveolae (they represent ~20% of the cell volume), vesicles carriers composed by Caveolin-1, a scaffolding protein on the cytosolic side of the membrane that mediate the internalization of the cargo through the fusion of the plasma membrane. This

pathway is well known to be involved in the activation/inactivation process of endothelial Nitric Oxide Synthase (eNOS) in endothelial cells. The binding and the translocation of eNOS from the membrane to the cytosol through caveolae internalization is associated with enzyme inhibition, while Src-mediated phosphorylation of Caveolin-1 stimulates caveolae scission, eNOS release and activation and NO synthesis (Figure 7) [Frank 2006].

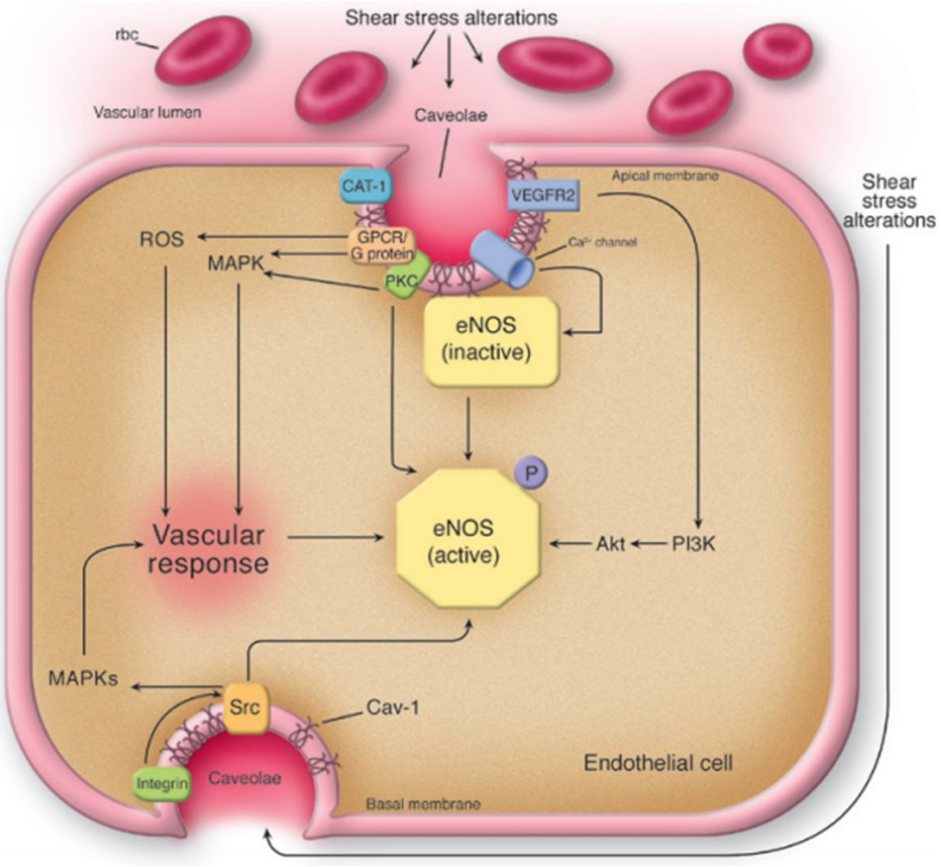


*Figure 7: Effect of shear stress on caveolae translocation.*
*Upon stimulation (e.g., shear stress), Caveolin-1 and caveolae may allow for the proper organization of various signal transduction pathways or organize the different regulatory proteins necessary for rapid and efficient eNOS activation [Frank 2006].*

In this point of view, the heterogeneity of junctional properties, the presence or not of fenestrae and different types of transcytosis in endothelial cells of different vascular beds define different basal permeability. For example, permeability is inversely proportional to the amount of tight junction and directly proportional to the presence of fenestrae. Moreover, in case of acute or chronic inflammation, endothelial cells are able to mediate inducible permeability, most of which takes place in the post-capillary venules.

## 2.5. ANGIOGENESIS

Angiogenesis is a complex multistep process of vascular growth by sprouting of preexisting vessels. Under normal circumstances, angiogenesis is a highly ordered and regulated process driving quiescent endothelial cells into a series of events culminating with the organization of a vascular network that responds to the demands of the growing or healing tissues. Metabolic stress has a role in influencing angiogenesis since various signals from the microenvironment including low oxygen tension, low extracellular pH, and low glucose concentration, trigger neovascularization. Angiogenesis occurs not only during fetal development but also physiologically during development and growth, in menstrual cycle, in wound healing and repair or pathologically, particularly in neoplastic and inflammatory diseases.

The steps leading to angiogenesis require cell proliferation, production of molecules able to degrade the extracellular matrix, modulation of adhesion and migration and finally differentiation to new functional vessels [Galley 2004]. All these processes are controlled by integration of signals from the microenvironment.

Component of the extracellular matrix and various soluble molecules activate or inhibit the angiogenic process and a balance between pro-angiogenic and anti-angiogenic factors tightly controls angiogenesis. Some angiogenic factors are endothelial specific, such as the members of the vascular endothelial growth factor (VEGF) and angiopoietin families, and Ephrin B2 and 4B. Many other growth factors modulate the function of different cell types including endothelial cells, such as members of the Fibroblast Growth Factor (FGF), PDGF or Transforming Growth Factor (TGF)β families. In addition, a myriad of other gene products - from Notch to transcription factors - have been shown crucial for vessel formation. In such a redundant system, VEGF maintains its position as the most critical driver of vascular formation, as it is necessary in both vasculogenesis, i.e. the formation of primitive vascular structures during embryogenesis via the differentiation of endothelial precursor cells, and angiogenesis during early development as well as in the adult. VEGF binds to its receptor type 2 (VEGFR-2) and generates a tyrosine kinase signalling cascade that stimulates the production of factors that variously stimulate vessel permeability (eNOS, producing NO), proliferation/survival, migration (MMPs) and finally differentiation into mature blood vessels. VEGF is a protagonist in angiogenesis in all its phases since it increases vascular permeability, stimulates ECM remodelling, induces endothelial proliferation and migration, inhibits apoptosis, enhances branching of the neoformed vessels, and regulates lumen diameter (Figure 8). Indeed, disruption of even a single VEGF allele in mice leads to embryonic death.

VEGF alone is unable to direct blood vessel organization and maturation and it works in concert with other factors. The angiopoietins (Ang) seem to be among VEGF's most important partners. These proteins bind the Ties, a family of receptor tyrosine kinases selectively expressed on the vascular endothelium. Specifically, Ang1 stabilizes the vessel, maximizes interactions between endothelial cells and the surrounding cells and matrix and maintains endothelial quiescence.

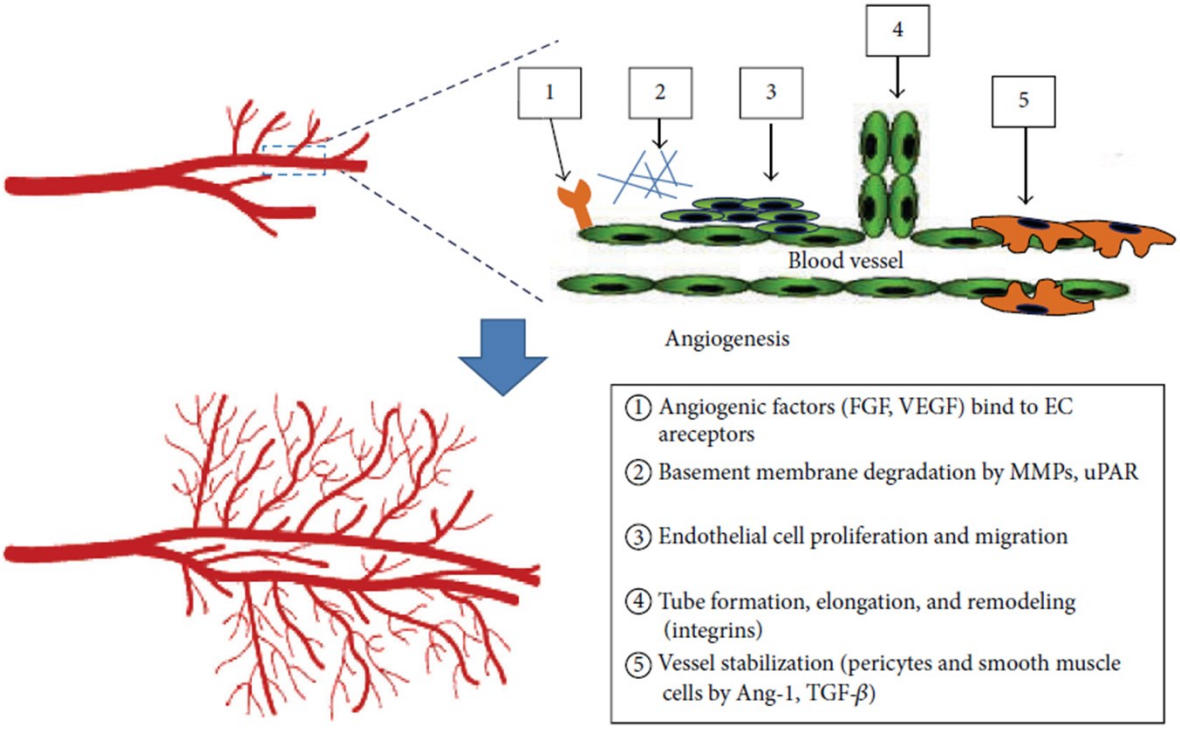


*Figure 8: Steps of angiogenic pathway [Yoo 2013].*

## 2.6. VASCULAR TONE

Another important function of endothelium is the regulation of vascular tone through the production of vasoactive molecules acting on smooth muscle cells of the tunica media, mediating their relaxation or contraction. In particular, the endothelium produces both vasodilator molecules (i.e. nitric oxide -NO- and prostacyclin) and vasoconstrictor molecules (endothelin-1, ET-1, and platelet activating factor, PAF).

NO, a soluble gas with a half-life of about 30 seconds, is continuously synthetized from the aminoacid L-arginine by the constitutive calcium-calmodulin dependent enzyme Nitric Oxide Synthase (NOS). In mammals, three different isoforms of NOS have been identified:

neuronal NOS (nNOS), inducible NOS (iNOS) and endothelial NOS (eNOS). eNOS and nNOS are $Ca^{2+}$- dependent constitutively active enzymes, whereas the inducible isoform iNOS is a $Ca^{2+}$-independent enzyme involved in inflammation and immune response [Shulz 1992]. NO, spreading rapidly from endothelial cells to smooth muscle cells, determines relaxation and vasodilation through the modulation of the activity of soluble Guanylyl Cyclase, producing increased concentrations of Cyclic Guanosin Monophosphate (cGMP) (Figure 9). cGMP interacts with three types of intracellular receptors: i) cGMP-dependent protein kinases; ii) cGMP-regulated ion channels and iii) cGMP-regulated cyclic nucleotide phosphodiesterases [Moncada 1991].

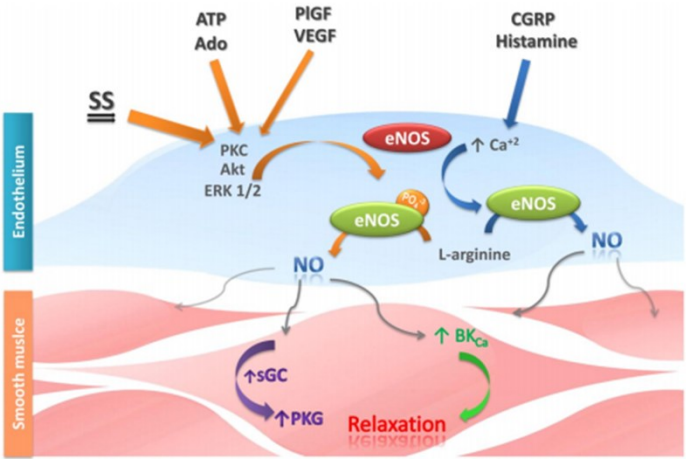


*Figure 9: NO production from eNOS in EC and its effect on smooth muscle cells (SMCs) [Krause 2011].*

Another vasodilatory molecule produced by endothelial cells is the prostacyclin $PGI_2$, produced from arachidonic acid, which is secreted and acts both on smooth muscle cells, inducing vasodilatation, and on platelets, delaying their aggregation.

From arachidonic acid it is also produced the vasoconstrictor PAF, a phospholipid that remains in the membrane and mediates the adhesion of leukocytes to the endothelium.

Another vasoconstrictor is endothelin (ET). There are three types (but vascular endothelial cells produce only ET-1) whose biological actions are mediated by two types of receptors: ETA, expressed on smooth muscle cells that mediate vasoconstriction and cell proliferation, and ETB, expressed predominantly at the endothelial level, which mediate vasodilation through production of NO and prostacyclin [Galley 2004]. ETB receptors are also present on the surface of smooth muscle cells where they exert the same vasoconstrictive role as ETA. ET-1 stimulates cell proliferation and the increase of expression of some genes such as collagenase and Platelet Derived Growth Factor (PDGF).

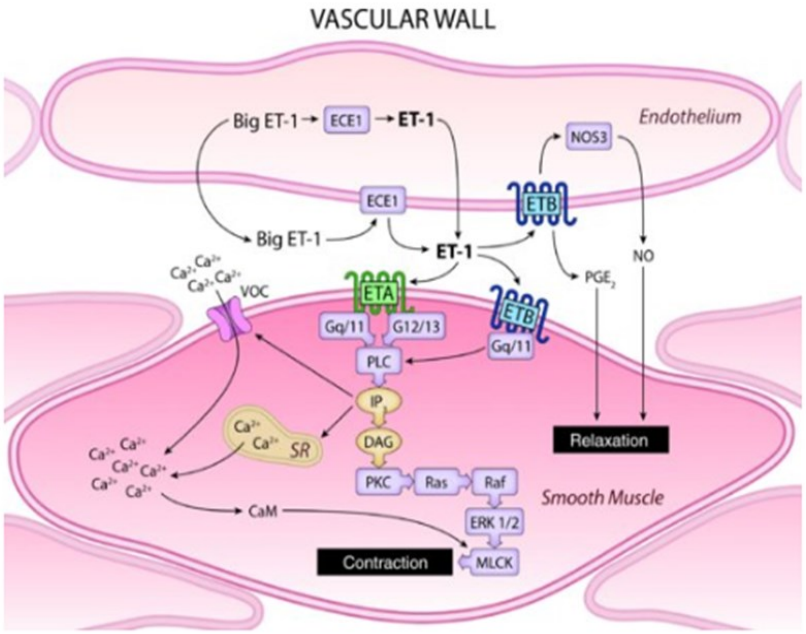


*Figure 10: Schematic mechanism of action on endothelin on ECs and SMCs [Kohan 2011].*

## 2.7. COAGULATION

Another fundamental role played by endothelium is the control of coagulation. In the absence of tissue damage, endothelial cells express antithrombotic and fibrinolytic

proteins, in order to avoid the erroneous triggering of the coagulation process. In the presence of an injury to the vessel, the endothelium triggers a cascade of events leading to the arrest of blood loss through clot formation and wall repair [Cines 1998; Levi 2002].

In basal conditions ECs express Tissue Factor Pathway Inhibitor (TFPI), a molecule able to bind the Xa factor forming the TF - FVIIa - FXa complex so that the conversion of prothrombin into thrombin is prevented and the conversion of fibrinogen in fibrin is inhibited. ECs also express Thrombomodulin, a membrane glycoprotein that is able to directly bind thrombin and addresses it to degradation, thus preventing its proteolytic activity on fibrinogen and the activation of platelets, factor V and XIII. Moreover, in basal conditions the endothelium produces Protein S, a cofactor that increases the activity of the C protein implicated in the blocking of factor VII and V of coagulation (Figure 11).

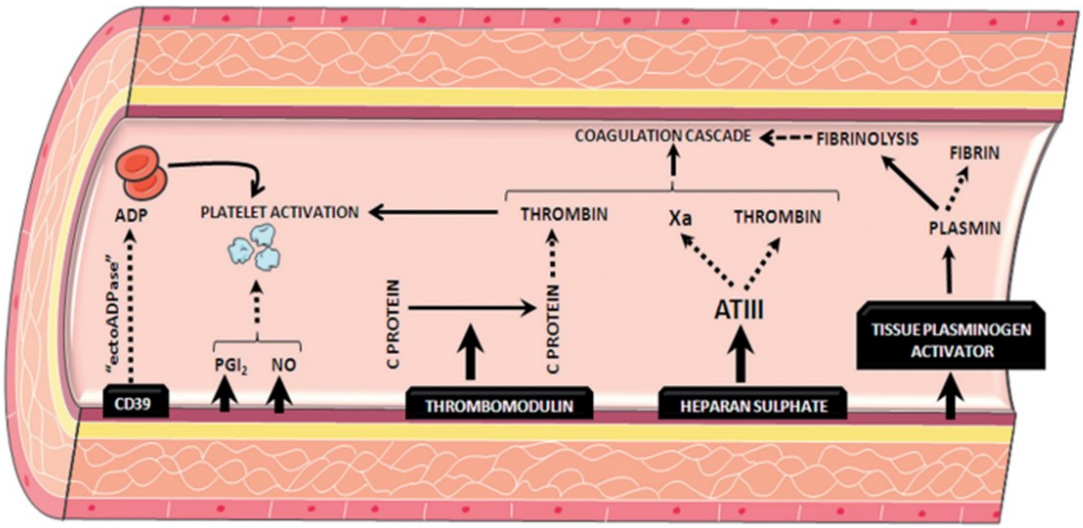


*Figure 11: Antithrombotic properties of the healthy vascular endothelium. Abbreviations: PGI2, prostacyclin; NO, nitric oxide; ATIII, antithrombin III; ADP, adenosine diphosphate [Badimon 2012].*

Following vascular damage, however, endothelial cells express a pro-coagulant surface by exposing Tissue Factor (TF) which initiates coagulation. Consequently, a cap of platelets adhering to the sub-endothelial surface is formed. Moreover, in this phase, the binding of thrombin to thrombomodulin expressed by endothelial cells leads to activation of the Thrombin-Activatable Fibrinolysis Inhibitor (TAFI), a molecule responsible for slowing down of fibrinolysis speed, in order to allow the complete resolution of the lesion.

When the lesion has been repaired, the clot removal is triggered by the activated plasmin, a serin protease that mediates the degradation of the fibrin and is produced from the plasminogen by proteolytic cut. The endothelial cells participate to this process exposing receptors for t-PA (Plasminogen Tissue Activator) and u-PA (Plasminogen Urokinase Activator) and blocking plasmin degradation mediated by the $\alpha$2-Plasmin Inhibitor [Cines 1998].

The fibrinolysis is also regulated by the levels of inhibitors of plasminogen activators (PAIs). Under basal conditions the liver is the major producer of PAIs but chemicals, among which thrombin, can increase their production by endothelial cells, inhibiting fibrinolysis [Fitzgerald 2000] (Figure 12).

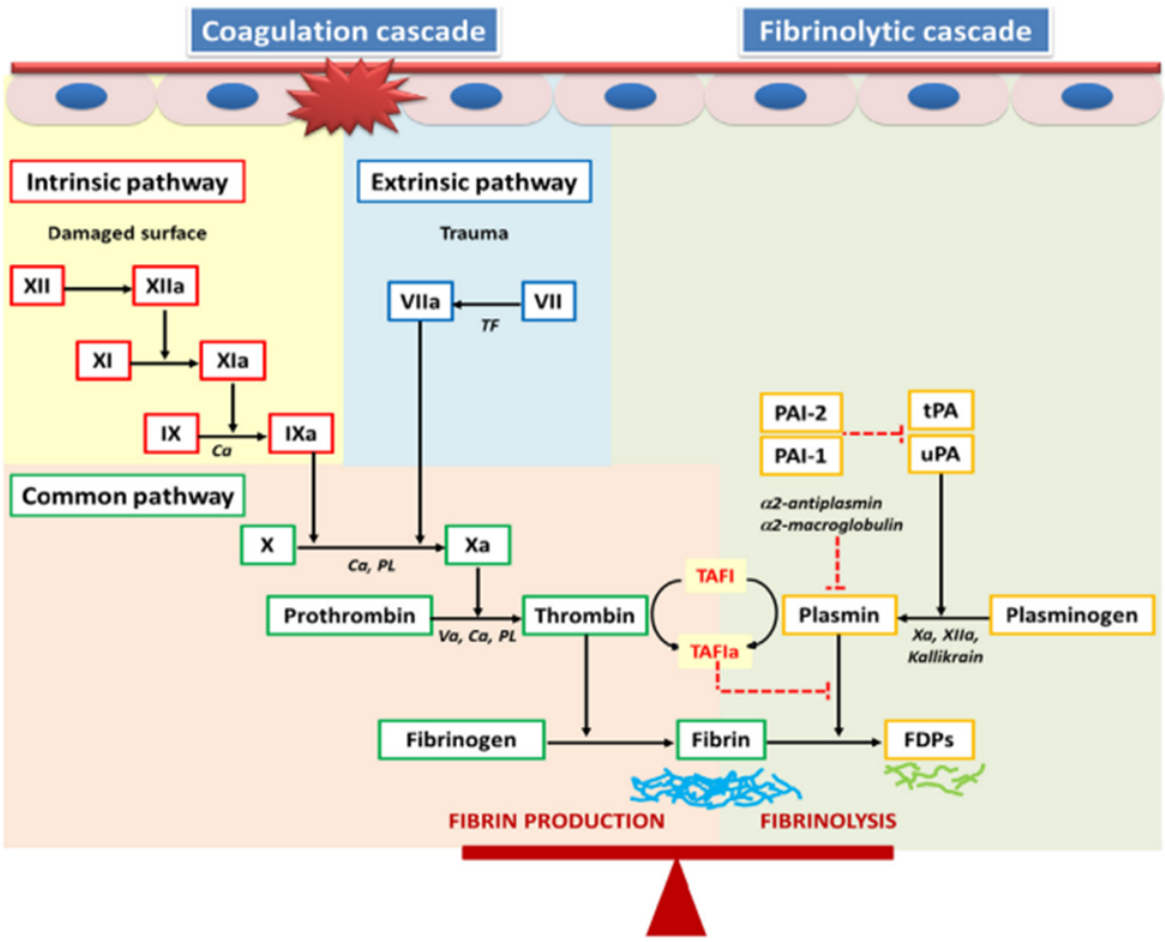


*Figure 12: Coagulation and fibrinolytic cascades* [Fawzy *2015*].

## 2.8. IMMUNORESPONSE

Endothelial cells have been shown to be important mediators of the immune response because they actively participate in leukocyte extravasation at the site of infection and because they can act as antigen-presenting cells.

For what regards the first function, endothelial cells, through the expression of different adhesion molecules, mediate the four different phases of leukocyte

extravasation: rolling, integrin activation, stable adhesion and trans-endothelial migration (Figure 13).

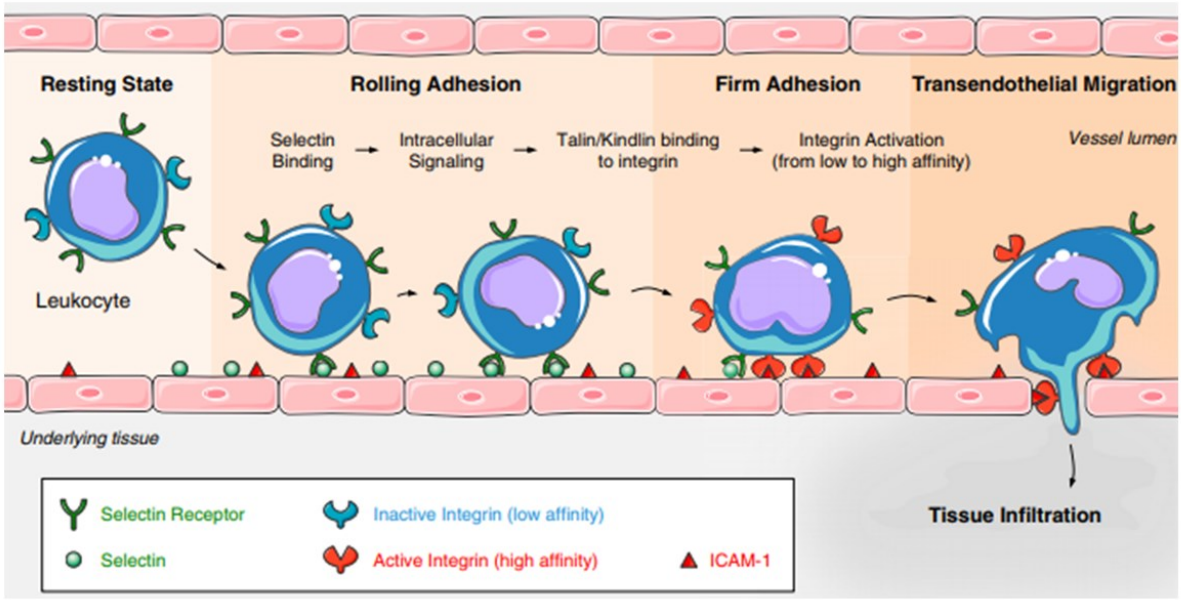


*Figure 13: Leukocyte trafficking during immune response [Lagarrigue 2016]*

Initially, the endothelial cell expresses cell adhesion molecules called selectins, belonging to the Cellular Adhesion Molecules family (CAM). During rolling phase weak bonds are established between the selectins of the endothelial cells and the leukocyte membrane's carbohydrates. Since the strength of the blood flow is greater than the bond strength between the adhesion molecules, the leukocyte rolls on the endothelial surface. During this phase, however, other membrane molecules of the ECs, the integrins, change conformation from the inactive to the active form in which the binding sites are exposed and to which the leukocyte can be associated with high affinity (stable adhesion phase). This leads to a stable adhesion that allows the leukocyte to cross the vessel wall to reach the tissue where they are recruited (trans-endothelial migration).

Endothelial cells can also act as antigen-presenting cells because, like all the cells of the organism, they express the MHC (Major Complex of Histocompatibility) class I on their surface, thereby acting as antigen presenting cells to effector lymphocytes $CD8^+$. Furthermore, in presence of an intense inflammatory response, endothelial cells also express class II MHC, necessary for the activation of the $CD4^+$ lymphocytes [Goldsby 2000].

## 2.9. ENDOTHELIAL METABOLISM

Most of the energy produced by endothelial cells derives from glycolysis, since 85% of their ATP is produced by converting glucose to lactate [De Bock 2013]. ECs do not continue generating ATP through oxidative phosphorylation (OXPHOS), i) to protect themselves from oxidative stress, keeping reactive oxygen species (ROS) under control and ii) to preserve oxygen for the diffusion in perivascular tissue that need oxygenation [De Bock 2013; Helmlinger 2000]. Moreover, glycolysis is fundamental in hypoxic tissue, where ECs need to produce ATP very fast to avoid tissue damage and necrosis.

The enzyme 6-phosphofructo-2-kinase/fructose-2,6- bisphosphatase 3 (PFKFB3) is the key stimulator of glycolysis in ECs. This enzyme produces fructose-2,6-bisphosphate (F2,6P2), a strong allosteric activator of phosphofructokinase-1 (PFK1), a rate-limiting enzyme of glycolysis. Another glycolytic regulator in EC is Hexokinase 2 (HK2) that phosphorylates glucose to glucose-6- phosphate (Figure 14) [Rohlenova 2018].

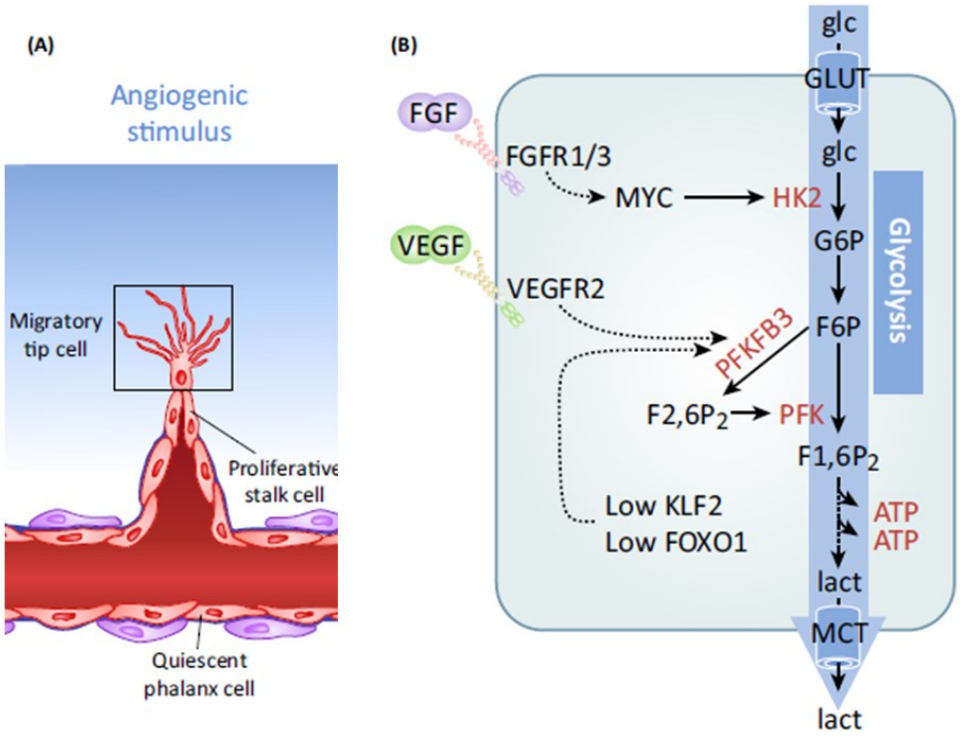


*Figure 14: Glycolysis is the main energy source in sprouting endothelium [Rohlenova 2018]. Abbreviations: F1,6P2, fructose-1,6-bisphosphate; F2,6P2, fructose-2,6-bisphosphate; F6P, fructose-6- phosphate; FGF, fibroblast growth factor; FGFR1/3, fibroblast growth factor receptor 1/3; FOXO1, forkhead box O1; G6P, glucose-6-phosphate; glc, glucose; GLUT, glucose transporter; HK2, hexokinase 2; KLF2, Krüppel-like factor; lact, lactate; MCT, monocarboxylate transporter; MYC, c-MYC; PFKFB3, phosphofructokinase-2/fructose-2,6-bisphosphatase; VEGF, vascular endothelial growth factor; VEGFR2, vascular endothelial growth factor receptor 2.*

Under laminar shear stress ECs are kept in a resting state through the activation of Krüppel-like Factor 2 (KLF2), a transcription factor responsible of the inhibition of the above-mentioned key genes and others [Doddaballapur 2015]. Another transcription factor inhibiting ECs glycolysis is Forkhead box O1 (FOXO1) that indirectly reduces glycolysis by inhibiting the transcription factor MYC.

It's now well established that ECs metabolism is a driving and controlling force of angiogenesis. For instance, VEGF stimulates PFKFB3 levels, FGF signaling promotes

MYC expression, thereby stimulating HK2 levels and glycolysis. Moreover, PFKFB3 and other glycolytic enzymes are compartmentalized in filopodia and lamellipodia in the so-called "ATP hot-spots", colocalizing with F-actin in membrane ruffles of lamellipodia.

In this point of view mitochondria in EC are more used as a biosynthetic center than energy generators. Proliferating endothelial cells (ECs) metabolize fatty acids to sustain the tricarboxylic acid cycle (TCA), producing the precursors aspartate and glutamate from its intermediates oxaloacetate (OAA) and a-ketoglutarate (a-KG), precursors of deoxynucleotide (dNTP) synthesis (Figure 15).

ECs use also amino acids for their metabolism, in particular they are able to use glutamine, the most abundant nonessential amino acid (NEAA) in the blood [Mayers 2015]. Through the enzyme glutaminase-1 (GLS1) ECs use glutamine as a source of carbons to sustain TCA cycle for protein and nucleotide synthesis. Furthermore, glutamine is essential for the production of glutathione (GSH), a key regulator of redox homeostasis.

Glucose however is not only used for glycolysis but, once converted in glucose-6-phosphate by the hexokinase (HK), it can be destined to the glycogen synthesis or can enter in pentose phosphate pathway (oxPPP) to generate ribulose-5-phosphate (Ru5P), used for nucleotide synthesis, and NADPH, fundamental to convert glutathione from its oxidized form, GSSG, to its reduced form, GSH, a key antioxidant [Riganti 2012].

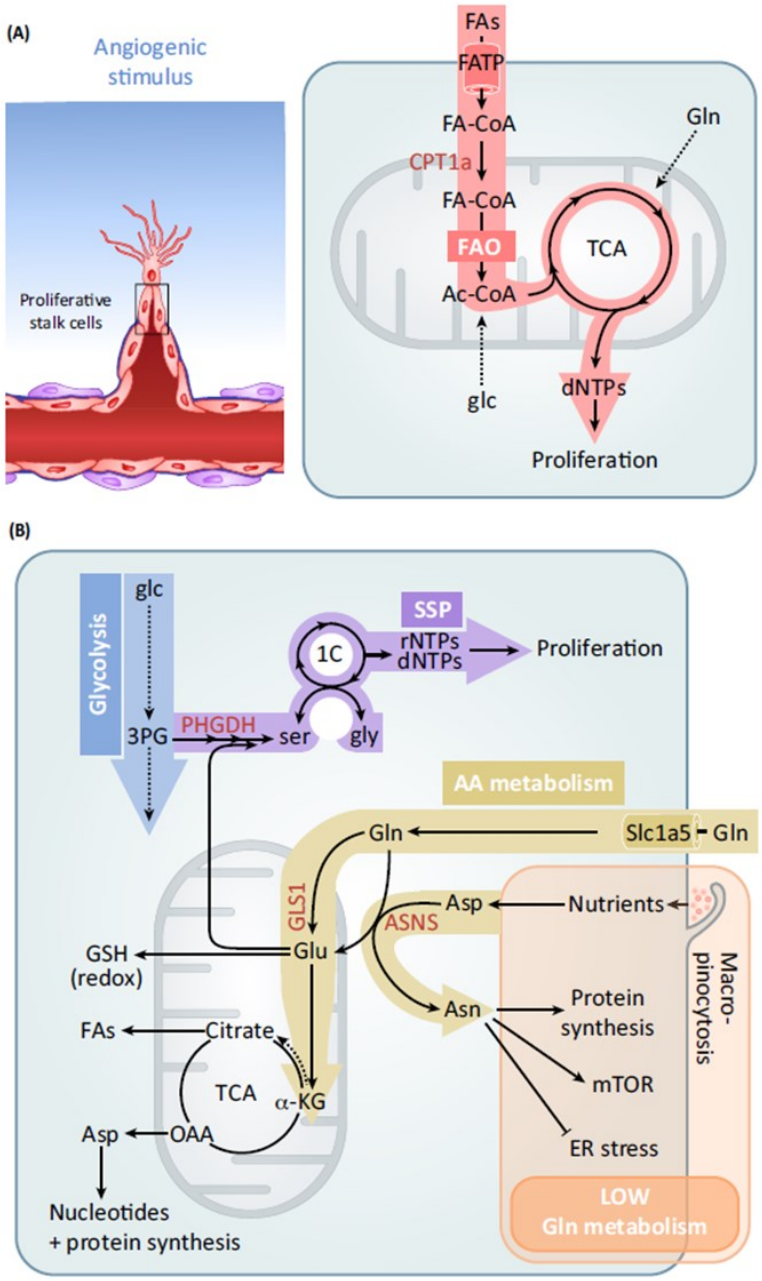


*Figure 15: Role of mitochondria in ECs metabolism [Rohlenova 2018].*
*In proliferating ECs fatty acid sustain the TCA cycle (A). Serine is directed to the serine synthesis pathway (SSP) to produce nucleotides while glutamine sustains TCA cycle in nucleotide synthesis or takes part in glutathione production (B).*
*Abbreviations: 1C, one-carbon; 3PG, 3-phosphoglycerate; a-KG, a-ketoglutarate; AA, amino acid; Ac-CoA, acetyl CoA; Asn, asparagine; ASNS, asparagine synthetase; Asp, aspartate; CPT1a, carnitine palmitoyltransferase 1a; dNTPs, deoxyribonucleotides; ER, endoplasmic reticulum; FA-CoA, fatty acid-CoA; FAO, fatty acid b-oxidation; FAs, fatty acids; FATP, fatty acid transporter;*

*glc, glucose; GLS1, glutaminase 1; gly, glycine; mTOR, mammalian target of rapamycin; OAA, oxaloacetate; PHGDH, phosphoglycerate dehydrogenase; rNTPs, ribonucleotides; ser, serine; Slc1a5, solute carrier family 1 (neutral amino acid transporter), member 5; TCA, tricarboxylic acid cycle.*

## 2.10. MITOCHONDRIA IN ENDOTHELIAL CELLS

Despite their secondary role in the energy production process, endothelial cell mitochondria are considered integrators of signaling from the environment, thus orchestrating cell response (Figure 16).

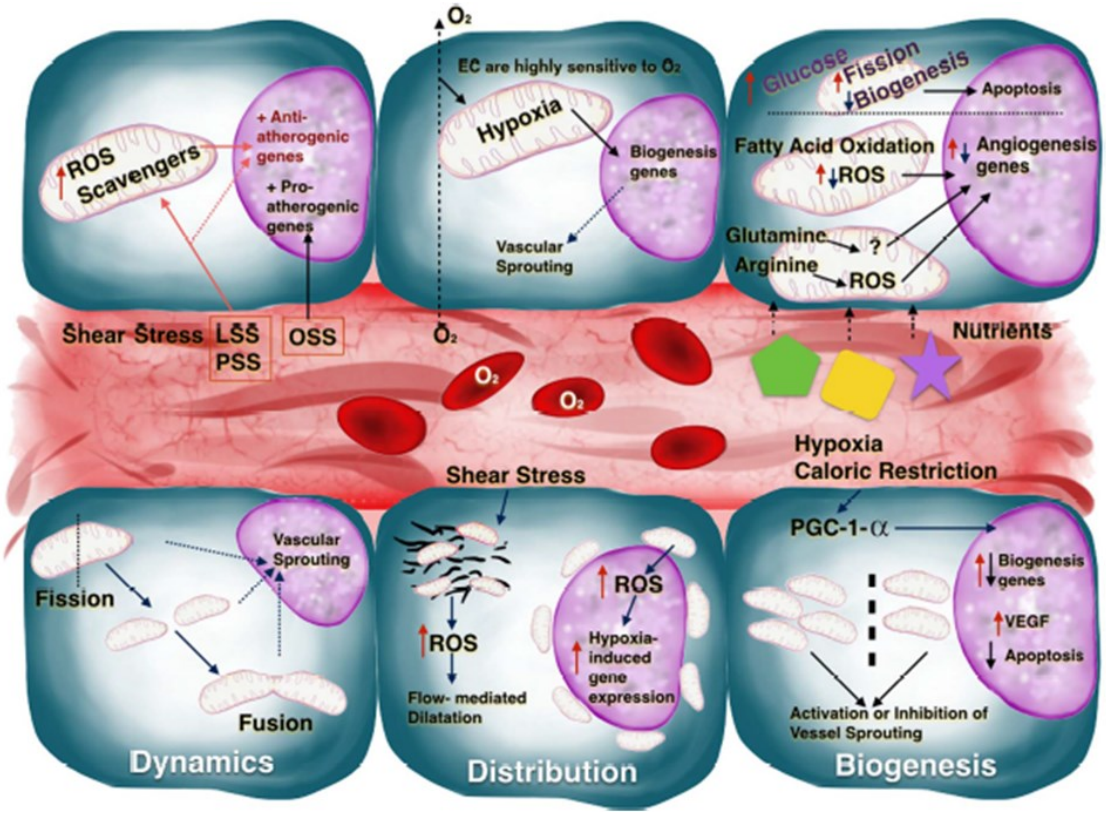


*Figure 16: ECs mitochondria as signaling organelles for environmental cues.*
*After different kind of stimuli such as oxygen, hemodynamics, and nutrients mitochondria in ECs modify their biogenesis, dynamics, and programmed degradation. Here the effects of LSS and PSS*

*on EC mitochondria are shown as examples. Abbreviations: LSS, laminar shear stress; PSS, pulsatile shear stress; OSS, oscillatory shear stress [Caja 2017].*

Mitochondrial content is determined by the balance between mitochondrial biogenesis and degradation (through the process called mitophagy). Biogenesis requires replication of mitochondrial DNA (mtDNA) and expression of mitochondrial and nuclear genes. The master regulator of this process is the peroxisome proliferator-activated receptor gamma coactivator-1$\alpha$ (PGC-1$\alpha$), a transcription factor responsible of the activation of nuclear respiratory factor (NRF)- 1 and −2 and transcription factor A, mitochondrial (TFAM) and transcription factor B, mitochondrial (TFBM) that coordinate the expression of genes necessary for the process of biogenesis (the former activate genes encoded by nuclear genes, the latter by mitochondrial genes).

PGC-1$\alpha$ expression is affected by several factors (such as hypoxia and caloric restriction) and is activated in case of energy demand to increase ATP production by ECs, modulating several genes related to lipid and glucose metabolism [Leone 2011; Patten 2012].
PGC-1$\alpha$ also modulates the expression of vascular endothelial growth factor-1 (VEGF-1) and stimulates angiogenesis [Widlansky 2012].

Additionally, PGC-1$\alpha$ arranges cellular defenses against oxidative stress, protects against apoptosis, limits inflammation, and improves nitric oxide bioavailability [Valle 2005, Shulz 2008].

Moreover, mitochondrial organization is dynamic because these organelles continuously undergo cycles of fusion and fission. Fusion allows the distribution of metabolites, proteins, and mtDNA within the cell and helps to maintain electrical and biochemical connectivity, while fission is important for normal cell functions like cell division,

movement and elimination of damaged or senescent mitochondria (Figure 17). Cytoskeletal organization is fundamental in orchestrating cycles of fusion and fission and determines mitochondrial network spatial organization [Moore 2018].

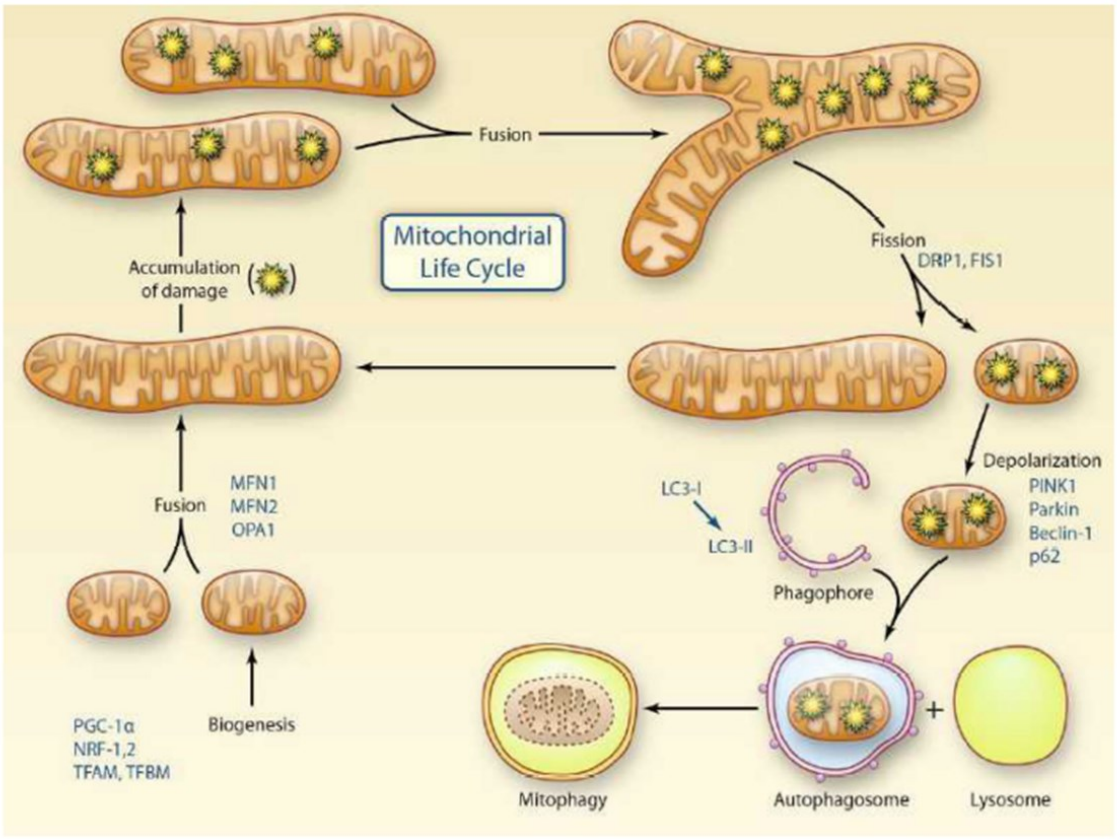


*Figure 17: Mitochondrial life cycle [Kluge 2018].*

In particular the process of degradation of mitochondria is named mitophagy, i.e. a particular form of autophagy specific for mitochondria. Autophagy is a well-controlled process that provides energy to the cell through degradation of damaged organelles. The process involves the formation of the double-membrane autophagosome where the cellular components targeted for degradation are engulfed and the fusion with a lysosome, where the contents and inner membrane are degraded by acid hydrolases and

recycled for use by the cell. The stimuli that activate mitophagy also activate PGC-1$\alpha$ and biogenesis to supply new mitochondria to replace the eliminated ones.

## 2.11. MICROGRAVITY

During evolution life on Earth became possible thanks to body's ability to adapt to changes of various environmental factors such as light, water, temperature and pH. A constant in the course of evolution was the force of gravity, which exerted its effects on all the organs and systems which, in turn, develop in order to optimally work in presence of a steady gravity that on Earth is represented by 1G.
For example, human circulatory system has evolved in order to ensure a constant supply of blood to all the tissues of the organism and its subsequent return to the hearth, counterbalancing the force of gravity that opposes it. Also the musculoskeletal system, which allows the maintenance of an upright posture and all the movements of the body, is opposed by gravity and integrates the information coming from the vestibular system, which informs on the position of the organism in space by exploiting the presence of the gravitational field to "orient".

In Space, where there is a reduction of gravity, our body experiences microgravity. All the phenomena that usually are linked and governed by gravity, such as floating and sedimentation appear negligible, thus allowing the study of those biological mechanisms that are masked by gravity on Earth. Moreover, the organism tries to adapt itself to this new condition reaching a new physiological balance that allows the permanence in orbit even for long periods. Among the adaptations developed by astronauts in microgravity there are modifications in the musculoskeletal system (astronauts experience muscular atrophy and osteoporosis due to the reduced mechanical stimulus given by

microgravity), in the immune system (astronauts are strongly immunosuppressed when return on Earth), in the endocrine and cardio-circulatory systems (Figure 18).

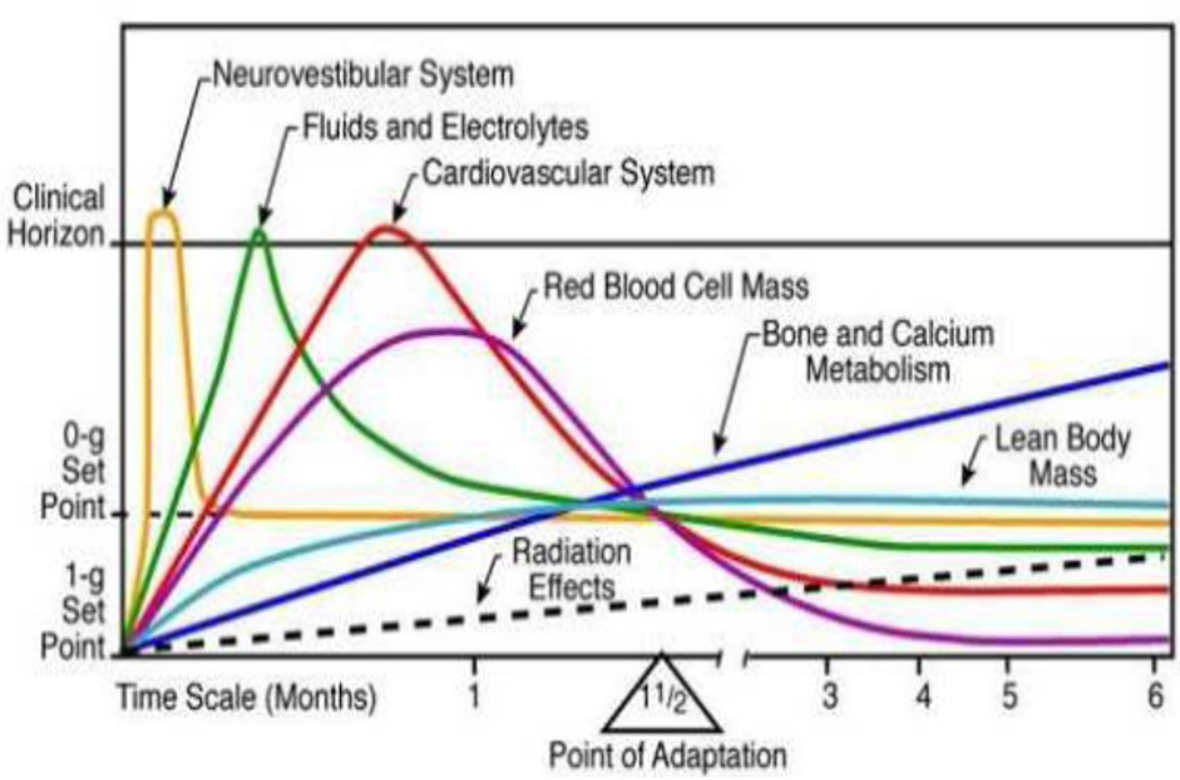


*Figure 18: Physiological changes associated with microgravity exposure.*
*Astronauts experience during and after space-flight different alterations in different systems of our body, that have different time of appearance and recovery upon return in normal gravity condition (from the Physiology Slide Set of the American Society of Gravitational and Space Biology) (http://asgsb.org/slidesets/slidesets.html).*

Particularly, the changes affecting the cardiovascular system in space caused after astronauts return on Earth a phenomenon known as cardiovascular deconditioning, which is characterized by a reduction in blood volume and circulating erythrocytes mass, by cardiac atrophy due to the reduction of the load to the heart, and by reduced vascular tone, all mechanisms involved in a disorder known as orthostatic hypotension, i.e. the

inability to maintain an upright position for long periods without the risk of losing consciousness.

Numerous experiments conducted both in real and simulated microgravity have shown that many cellular populations respond to the new environmental conditions by modifying various parameters such as the proliferative rate, cell differentiation, response and signal transduction, cytoskeletal organization and gene expression.

## 2.12. DEVICES TO SIMULATE MICROGRAVITY

Experiments in real microgravity are difficult to perform. They are expensive and experimental apparatus is limited. Moreover, all reagents must be safe for the crew and the number of samples is limited. Moreover, it is important to keep in mind that space environment is unique, because it is not only characterized by the lack of gravity but also by exposure to cosmic radiations. In addition, for what regards gravity, astronauts experience during the launch different g forces up to 12 g and then they stabilized in microgravity onboard the International Space Station (ISS). Other ways to perform experiments in real microgravity are parabolic flights and rockets, but the duration of microgravity is limited [Maier 2015].

For these reasons different bench-top systems were developed to study the effect of microgravity on different cell populations in laboratory. They can simulate microgravity in a range between $10^{-3}$ to $10^{-6}$ g and they are used to perform studies in preparation for spaceflight and to deepen the results obtained from experiments on the ISS. There are different bioreactors, which mimic some aspects of real microgravity [Herranz 2013].

### 2.12.1. CLINOSTAT

Clinostat is considered an effective tool to simulate microgravity and has been used in several studies. There are two types of this device: the 1-D clinostat, characterized by movements orientated along a single axis, and the 2-D clinostat, more commonly used, constituted by two different plans that rotate. These two types of clinostat are based on the randomization of the movements with a constant speed [Herranz 2013]. These two types of clinostat do not reproduce fully the lack of gravity because of their omnilateral rotation and, for this reason, a new clinostat has been developed [van Loon 2007]. The new bioreactor, called Random Positioning Machine (RPM), consists of a more internal plan where the samples are housed that rotate clockwise and counterclockwise and an outer plane that moves horizontally and vertically, both with random rotation speed and direction [Herranz 2013]. The cells are grown in flasks which must be completely filled with medium to decrease the risk of turbulence or shear forces during rotation and they are located in the center of the inner plane, where the reduction of gravity is bigger (Figure 19).

However, the samples are also subjected to vibrational forces caused by the movement of the arms of the device and for this reason controls in 1G condition should be kept at the basis of the RPM to be exposed to the same vibration. It has been observed that the effects of simulated microgravity with clinostat are comparable to those obtained in laboratories on the ISS in various cell types, including endothelial cells [Kraft 2000; Grimm 2002; Woods 2003; Morbidelli 2005; Versari 2007].

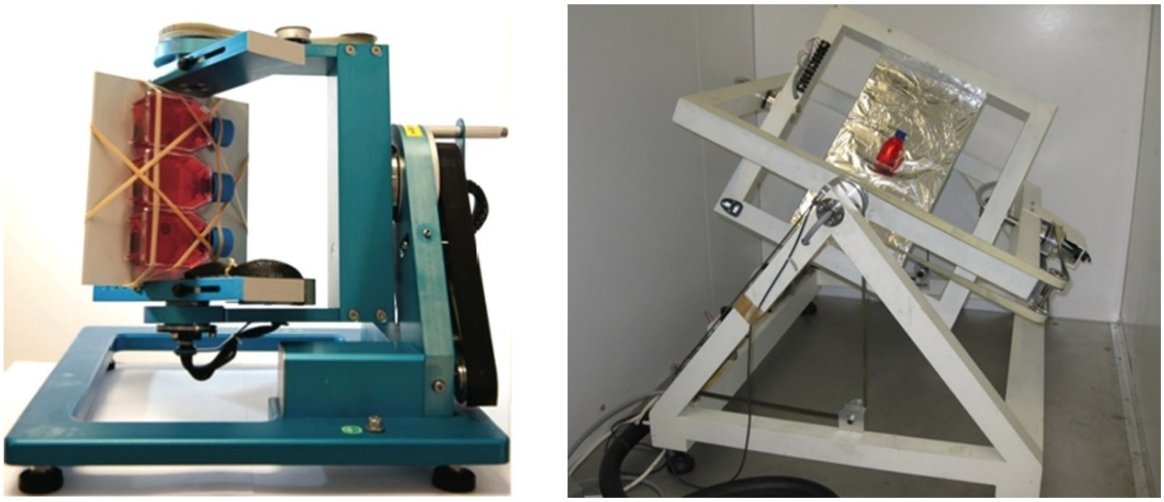

*Figure 19: 2D-clinostat (left) and RPM (right).*

### 2.12.2. ROTATING WALL VESSEL (RWV)

This bioreactor was developed by NASA to simulate the effects of microgravity on cells (Figure 20 A). The bioreactor, also called Rotating Cell Culture System (RCCS), consists of a cylindrical growth chamber (Figure 20 B), which keeps the cells in suspension by slow rotation around its horizontal axis, with a coaxial silicon membrane that allows gas exchange. The microgravity simulation is obtained thanks to the continuous change of orientation of the gravity vector generated by the combination of two different movements. Changes in direction are faster than the response time of the object to gravity and there are no constant directions for a specific time. Therefore, the simulation of microgravity within the RWV depends on the speed and distance of the sample from the center of rotation: rotation at 28 rpm produce a reduction of gravity that is comparable to the microgravity experienced by astronauts on the ISS. Adherent cells have to be cultured on microcarrier beads (Figure 20 C) that allow the maintenance in suspension of the cells into the RWV vessel. Even in this case, most of the results obtained with this bioreactor

have been confirmed by experiments in real microgravity in various cell types, including endothelial cells [Maier 2015].

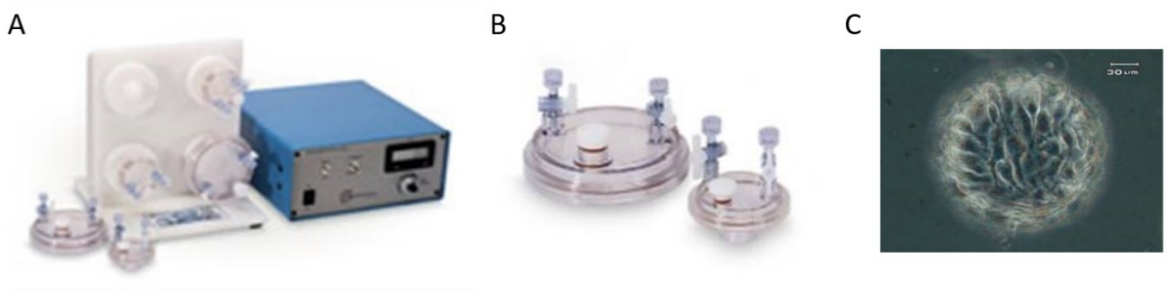


*Figure 20: RWV bioreactor from Synthecon (A), the vessels (B) and endothelial cells on microcarrier beads (C).*

### 2.12.3. MAGNETIC LEVITATION

Magnetic levitation is a relatively new technique used to investigate the biological response to weightlessness. Magnetic levitation occurs when the magnetic force counteracts the gravitational force [Herranz 2012] (Figure 21).

It should be taken in account that the magnetic field that is generated can influence the cellular behavior and this can confuse the effects due only to microgravity. Few studies are available on cells exposed to magnetic levitation on different cell types [Hammer 2009, Sun 2015, Qian 2009].

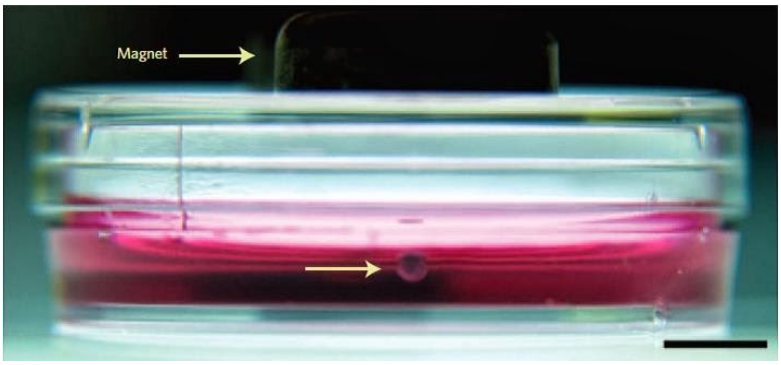

*Figure 21: Cells in magnetic levitation*

## 2.13. MECHANOSENSING

Endothelial cells, lining the inner surface of blood vessels, are constantly subjected to mechanical stimuli including shear stress, generated by blood flow and experienced by all the types of ECs, and circumferential stretch that is generated by blood pressure and experienced in major vessels but not in the microvasculature [Chatterjee 2018]. ECs are also known as mechanotransducers, since they perceive, interpret and react to mechanical signals coming from the environment, converting them into biochemical ones. In particular, mechanotransduction can be divided in three different steps: detection and transmission of the signal to specialized structures, translation of mechanical to biochemical signal and the subsequent cell response (Figure 22) [Alonso 2016].

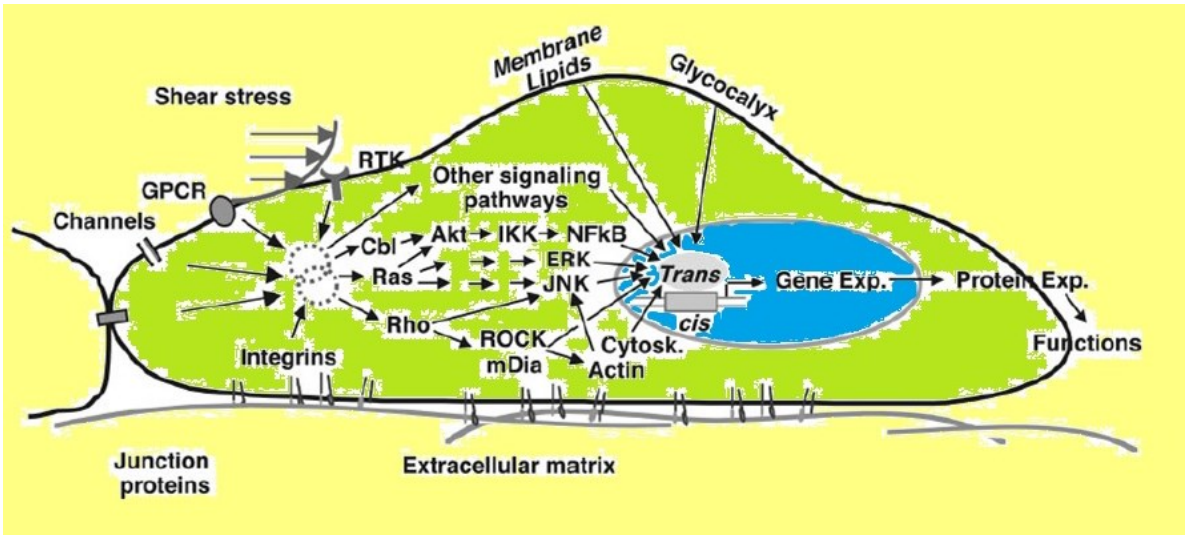


*Figure 22: steps of mechanotransduction.*
*Mechanical forces are detected in ECs through mechanosensors, including ion channels, junction proteins, integrins, glycocalyx, receptor tyrosine kinases (RTK) and G-protein-coupled receptor*

*(GPCR). These molecules transduce the signal to intracellular adaptors, signaling molecules and cytoskeleton, all of them with a downstream effect on transcription. Yellow: detection of mechanical stimuli from mechanosensors. Green: transmission. Blue: transcriptional regulation.*
*Modified from Am J Physiol Heart Circ Physiol 292: H1209–H1224, 2007 [Chien 2007].*

Mechanotransduction is mostly initiated at the cell surface, where the deformation of the cell surface and plasma membrane are transmitted along the cytoskeleton to the nucleus, where transcription takes place. Specifically, the different mediators of mechanotransduction are organized in microdomains and include cell surface itself, cytoplasmic receptors, ion channels, kinases, integrins and extracellular matrix components (Figure 23) [Ingber 2006].

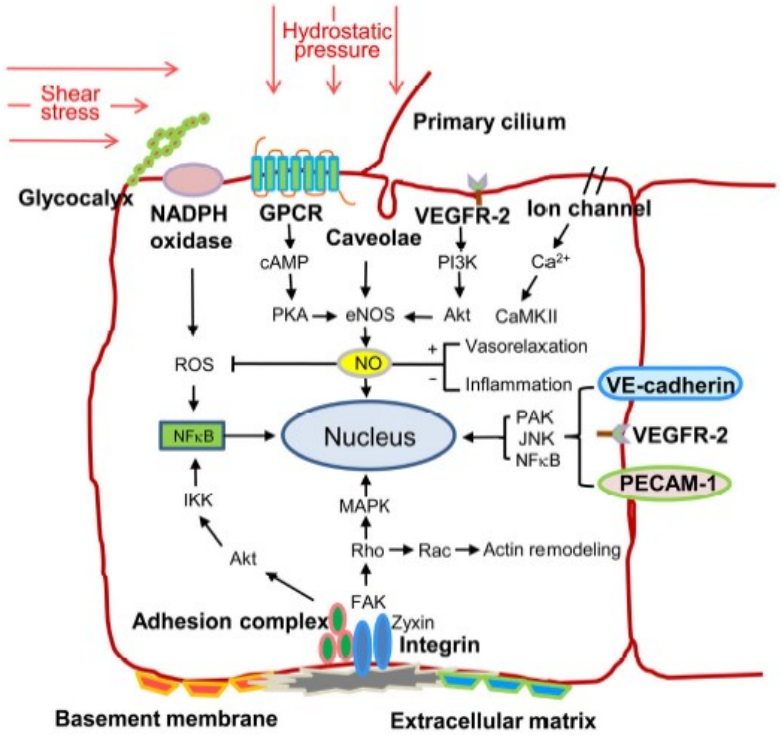


*Figure 23: Endothelial mechanosensors [Deng 2014]*

- TENSEGRITY: the cell, with its membrane and cytosolic components, is an integrated structure able to perceive mechanical forces through tensegrity, i.e. tensional-integrity. According to this theory the mechanical stress is loaded on cytoskeletal elements (actin-myosin microfilaments, microtubules and intermediate filaments) that transmit it to the cytoplasm and nucleus [Ingber 2006].
- CAVEOLAE: they are lipid rich invaginations and are important vesicle transporters for transcytosis in endothelial cells and they are reported to be platform of cellular function including mechanotransduction [Deng 2014]; caveolin-1 (Cav-1) is the major scaffold protein of these vesicles and regulates the internalization of the caveolae and the nitric oxide pathway, because they bind the type 3 NOS keeping it inactive. Furthermore, caveolae transport both channels and ionic pumps, which are other important mechanical sensors.
- INTEGRINS: these transmembrane heterodimeric receptors span across the membrane and connect the extracellular matrix to the intracellular cytoskeleton, mediating the bidirectional transmission of mechanical forces. They are constituted by an extracellular domain, implicated in the functions of adhesion and recognition of the ligand, a transmembrane domain and a cytoplasmic short domain, which lacks kinase activity but can physically bind cytoskeletal proteins and recruit proteins for signal transduction. In particular, mechanical forces are transmitted to the cytoskeleton through the rearrangement of actin microfilaments, microtubules and intermediate filaments mediated by integrins that activate focal adhesion kinase (FAK) and c-Src kinases [Simmons 2015].
- ION CHANNELS: they were proposed in the past as primary sensors of altered shear stress but their variation in activity represents also an early event in the signaling cascade in the mechanosensing of the endothelium [Chatterjee 2014]. They are responsible for some of the fastest response of ECs to shear. They are able

to perceive the mechanical stretching given by conformational changes of the lipid bilayer in which they are through the gate domain or through the channel itself. There are several channels that have been recognized as mechanically sensitive including TRP (Transient Receptor Potential Protein superfamily, are cation carrying channels), K(2P), MscS like proteins and DEG/ENaC channels [Ogneva 2013]. Moreover, recently different evidences emerged about a direct link existing between TRP family and Rho/ROCK pathway, suggesting a possible crosstalk between different mediators of mechanosensing such as integrins, ion channels and cytoskeleton [Alonso 2016].

- GLYCOCALYX: it is present on the surface of the EC, composed by various macromolecules such as glycoproteins, proteoglycans and glycosaminoglycans and is able to interact with molecules present in the plasma. Its thickness increases with vessel diameters, ranging from 2 to 4.5 μm in arteries. Through conformational changes the glycocalyx is able to act as a selective permeable barrier and as a mechanosensor in addition to transducing intracellular signals in response to flow variations. Indeed, flow can modulate glycocalyx production and distribution. Furthermore, the glycocalyx is in communication with both the cytoskeletal elements and the endoplasmic reticulum through their proteoglycans tails, therefore the mechanical signal may be propagated downstream [Fu 2013].
- PECAM1: it is a molecule present on the surface of the endothelial cell and located in the region of the junctions between ECs. The mechanical stimulus triggers the phosphorylation of PECAM1 that leads to the activation of ERK (when PECAM1 binds SHP-2), PI3K (when it is in a complex with VEGFR2 and VE-cadherin) and AKT (which leads to the cytoskeletal rearrangement).

## 2.14. ENDOTHELIUM IN MICROGRAVITY

To disclose the role of endothelial cells response to microgravity in the onset of cardiovascular deconditioning in astronauts during and after spaceflight, different studies in real and simulated microgravity were conducted on endothelial cells. Most of the experiments in real microgravity were performed on Human Endothelial Cells from Umbilical Vein (HUVEC), a model of macrovascular endothelial cells [Kapitonova 2011, Kapitonova 2012, Versari 2013]. These studies revealed that HUVEC after spaceflight undergo morphological modifications, among which they show an irregular surface and variable size and shape compared to Controls grown on Earth in normal 1G condition. Immunofluorescence for different markers were performed and revealed a decrease in mitochondria and in tubulin, which in parallel accumulated in the peripheral cytoplasmic surface in bundles of tubulin-positive structures [Kapitonova 2011, Kapitonova 2012]. In the SPHINX experiment [Versari 2013] HUVEC after 10 days of spaceflight were analyzed for modulation of gene expression using microarray and this study revealed that there were different modulated genes, among which the most upregulated was Thioredoxin Interacting Protein (TXNIP), an inhibitor of the anti-oxidant protein Thioredoxin (TRX), suggesting that HUVEC in real microgravity generate a pro-oxidative environment.
In 2015 also human microvascular endothelial cells (HMEC) were flown to the ISS and experiments are still in progress.

Many of the results obtained with studies in real microgravity were achieved after using devices to simulate microgravity on Earth. These bench systems are low cost compared to real microgravity experiments, they allow the generation of big amounts of samples for the experiments.
It has been shown that the simulation of microgravity impacts on different functions of

endothelial cells, which respond with morphological, functional and biochemical changes [Morbidelli 2005; Versari 2007; Cotrupi 2005; Carlsson 2003; Grenon 2013; Mariotti 2008].

Many studies on HUVEC in simulated microgravity, using either RWV or RPM, demonstrated that they grow faster in microgravity, they change morphology and display cytoskeletal disorganization (Figure 24) [Carlson 2003, Versari 2007].

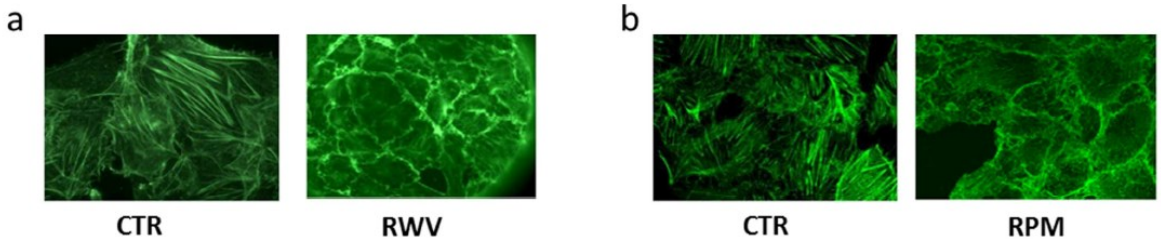


*Figure 24: Cytoskeletal alteration of HUVEC exposed to simulated microgravity. HUVEC grown in RWV (a, Carlsson 2003) or RPM (Versari 2007) were stained with phalloidin to visualize actin cytoskeleton.*

HUVEC in simulated microgravity show elongated morphology, disorganization of actin microfilaments that concentrate in the perinuclear area and a decrease in stress fibers. Furthermore, Caveolin-1 is less associated with the plasma membrane and is localized at perinuclear level as actin [Grenon 2013], so that the authors hypothesize that the disorganization of the cytoskeleton compromises the translocation of the caveolin-1 in the caveolae.

An increase in levels of endothelial nitric oxide synthase (eNOS) has been observed both in HUVEC and HMEC exposed to simulated microgravity in the RWV or RPM [Versari 2007]. The increase in expression of this enzyme is explained by Grenon et al. as a consequence of cytoskeletal changes. Other authors suggest that the increase in nitric oxide observed in endothelial cells in simulated microgravity is due to the induction of

the inducible form of the enzyme through a mechanism dependent on the suppression of the activity of the transcriptional factor AP-1 [Wang 2009].
Another study demonstrates that upon stimulation with TNF-$\alpha$, HUVEC grown in the RWV showed cytoskeletal actin rearrangement, associated with a concomitant change in levels and distribution of adhesion molecules, such as ICAM-1 and VCAM-1, which accumulate on the plasma membrane and may influence trans-endothelial migration processes [Kang 2011]. In other endothelial cell lines also proteins of the extracellular matrix (laminin, fibronectin and $\alpha$-tubulin) were found to be upregulated in simulated microgravity [Grosse 2012; Wehland 2013; Grimm 2010; Monici 2011]. All these changes, considered together, have led the authors to hypothesize that exposure to microgravity may cause a dysregulation in cell motility and adhesion to the substrate.

On the contrary, HMEC grown in the RPM and in RWV are growth inhibited, through the upregulation of p21, an effect that is supported by *in vivo* experiments showing a decrease in angiogenesis in space. In simulated microgravity in both RPM and RWV the decrease in PI3K-Akt pathway activity and the increase in NFkB expression have been shown to be the cause of apoptosis induction in pulmonary HMEC [Kang 2011], while apoptosis has not been observed in dermal HMEC [Maier 2015]. In HMEC grown in the RWV was observed the downregulation of IL-6 while NO synthesis was increased [Cotrupi 2005].

All these data were confirmed also in the animal model. Indeed, microvascular endothelial dysfunction was detected in rats during spaceflight [Vernikos 2010].

It is pivotal to continue studies on endothelial cell in microgravity to disclose the role of endothelial function/dysfunction in the onset of cardiovascular deconditioning, but also other disorders observed in space that involve other apparati, as bone and muscle, considering the relevance of the cross-talk of endothelial cells with other cell types as well

as their pivotal role in maintaining vascular integrity and, consequently, adequate tissue perfusion.

# 3. MATERIAL AND METHODS

## 3.1. CELL CULTURE

Human Endothelial Cells from Umbilical Vein (HUVEC) were used as a model for macrovascular EC, while HMEC, i.e. Human Dermal Microvascular Endothelial Cells, for microvascular ECs.

HUVEC were from ATCC and serially passaged in M199 containing 10% of fetal bovine serum (FBS), Endothelial Cell Growth Factor (ECGF) (150 μg/ml), glutamine (2 mM), sodium pyruvate (1 mM), and heparin (5 U/ml) on 2% gelatin coated dishes. HMEC were obtained from CDC (Atlanta, USA) and grown in MCDB131 containing epidermal growth factor (EGF) (10 ng/mL) and 10% FBS and glutamine (2 mM) on 2% gelatin-coated dishes. All culture reagents were from Gibco (Thermo Fisher Scientific, Waltham, Massachusetts, USA).

Different conditions of cell culture were studied: i) normal 1G condition ii) simulation of microgravity, both in classic 2D condition. In addition, 3D-microfluidic cell culture conditions were established. To this purpose, ECs were cultured in a 3D structure that resembles vessel network in the presence of fluid flow.

## 3.2. SIMULATION OF MICROGRAVITY

To generate microgravity, we utilized the Rotating Wall Vessels (RWV) (Synthecom Inc, Houston, TX, USA) after seeding on beads (Cytodex 3, Sigma Saint Louis, Missouri, USA). As controls in 1G condition, HUVEC grown on beads were cultured in the vessels not undergoing rotation. Both RWV sample and the control were cultured at 37°C and 5% $CO_2$. The experiments were performed at different time points.

## 3.3. 3D-MICROFLUIDIC CELL CULTURE

In 3D experiments, HUVEC and HMEC were seeded in a microfluidic device fabricated using a standard soft-lithography technique [Tsvirkun 2017] After the seeding cells were subjected to a constant flow of supplemented medium at 1 μL/min, corresponding to a wall shear stress of about 0.2 Pa (representative of physiological conditions for venous endothelial cells) in channels of nominal section 30 × 30 μm. Cells were cultured in the microfluidic device for 7 days and fixed for immunofluorescence.

## 3.4. SILENCING HSP70, PROLIFERATION AND APOPTOSIS

The cells on beads were transfected with HSP70 siRNA (1 μg, 5'-TTCAAAGTAAATAAACTTTAA -3' from Qiagen, Milan, Italy) using HiPerfect Transfection Reagent (Qiagen, Milan, Italy) according to the manufacturer's recommendations. After 8h with the siRNA transfection mix, the medium was replaced with fresh standard medium and the cells transferred into the RWV.

After 48h the cells were trypsinized, stained with trypan blue solution (0,4%) and counted using a LUNA™ Automated Cell Counter (Logos Biosystems, Villeneuve d'Ascq, France). In parallel, apoptosis was assessed using the Cell Death Detection ELISA Photometric enzyme immunoassay (Sigma Aldrich, Saint Louis, Missouri, USA), which measures cytoplasmic histone-associated DNA fragments (mono- and oligonucleosomes) in the cytoplasmic fraction of cell lysates. The experiment was performed in triplicate two times. Data are expressed as the mean ± standard deviation.

## 3.5. REAL TIME-PCR

Total RNA was extracted by the PureLink RNA Mini kit (Ambion, Thermo Fisher Scientific, Waltham, Massachusetts, USA). Single-stranded cDNA was synthesized from 1 μg RNA in a 20 μl final volume using High Capacity cDNA Reverse Transcription Kit, with RNase inhibitor (Applied Biosystems, Thermo Fisher Scientific, Waltham, Massachusetts, USA) according to the manufacturer's instructions. Real-time PCR was performed in triplicate three times using the 7500 FAST Real Time PCR System instrument using TaqMan Gene Expression Assays (Life Technologies - Thermo Fisher Scientific, Waltham, Massachusetts, USA).

On HUVEC TaqMan Gene Expression Assays (Life Technologies - Thermo Fisher Scientific, Waltham, Massachusetts, USA) was utilized: Hs00197750_m1 (TXNIP), Hs00247263_m1 (SIRT2), Hs00165563_m1 (PON2), Hs00167309_m1 (SOD2), Hs00359147_s1 (HSP1A1). The housekeeping gene GAPDH was used as an internal reference gene. Relative changes in gene expression were analysed by the 2-ΔΔCt method.

## 3.6. REACTIVE OXYGEN SPECIES (ROS) PRODUCTION

ROS production was quantified using 2'-7'-dichlorofluorescein diacetate (DCFH) on HUVEC cultured in simulated microgravity for various times. At the end of the experiment the cells were rapidly transferred into black bottomed 96 plates (Greiner bio-one, Frickenhausen, Germany) and exposed for 30 min to 20 μM DCFH solution. The emission at 529 nm of the DCFH dye was monitored using Promega Glomax Multi

Detection System (Promega, Madison, Wisconsin, USA). The results are the mean of three independent experiments performed in quadruplicate. Data are shown as the % of ROS levels in HUVEC cultured in the RWV *vs* static 1G conditions (CTR) ± standard deviation.

## 3.7. REDUCED *vs* OXIDIZED GLUTATHIONE QUANTIFICATION

Reduced glutathione (GSH)/oxidized glutathione (GSSG) was measured using the GSH/GSSG-Glo™ Assay, which is a luminescence-based system (Promega, Madison, Wisconsin, USA) according to the manufacturers' instructions. Data are shown as the % of GSH/GSSG levels in HUVEC cultured in the RWV vs static 1G conditions (CTR) ± standard deviation. The results are the mean of three independent experiments performed in quadruplicate.

## 3.8. COMET ASSAY

Comet assay was performed after various times of culture in the RWV. HUVEC were mixed with low melting-point agarose and spread on pretreated slides which were died, immersed in ice cold lysis solution (Tris-HCl 0.01 M pH 10, NaCl 2.5 M, EDTA 0.1 M, NaOH 0.3 M, Triton 1%, DMSO 10%) and incubated at 4°C for 60 min. Electrophoresis was conducted in ice cold running buffer (NaOH 0.3 M, EDTA 0.001 M) for 30 min at 300 mA. The slides were then rinsed, fixed in ice-cold methanol for 3 min, dried at room temperature, stained with ethidium bromide and analysed with a fluorescence microscope.

## 3.9. PROTEIN ARRAY

After various times of culture in the RWV or in static 1G conditions, conditioned media were collected and HUVEC were lysed in a buffer containing 50 mM Tris-HCl pH 8.0, 150 mM NaCl, 1 mM EDTA, 1% NP-40. Cell extracts (80 μg) were utilized to incubate the membranes on which 26 antibodies against human cell stress-related proteins were spotted in duplicate (R&D systems, Space Import Export, Milan, Italy), according to the manufacturer's instructions. Densitometry was performed by the ImageJ software. Two separate experiments were performed, and data are expressed as % of the fold increase in the signal intensity of RWV vs static 1G conditions. Both cell extracts and conditioned media were used to incubate the membrane on which 40 antibodies against cytokines, chemokines and adhesion molecules were spotted in duplicate (RayBiotech, Inc, Norcross, Georgia, USA). Two separate experiments were performed and representative blots are shown. By the ImageJ software no significant differences were detected in any spot.

## 3.10. WESTERN BLOT

HUVEC were lysed in 10 mM Tris-HCl (pH 7.4) containing 3 mM MgCl2, 10 mM NaCl, 0.1% SDS, 0.1% Triton X-100, 0.5 mM EDTA and protein inhibitors, separated on SDS-PAGE and transferred to nitrocellulose sheets at 400 mA for 2 h at 4°C.

- To study the stress adaptive response of HUVEC to simulated microgravity, western analysis was performed on stress protein using antibodies against heat shock protein (HSP)70, p21Cip1 (p21) (Tebu Bio-Santa Cruz, Magenta, Italy), Thioredoxin interacting protein (TXNIP) and paraoxonase (PON) 2 (Invitrogen, Carlsbad, California, USA), sirtuin (SIRT)2 (Millipore, Vimodrone, Italy),

superoxide-dismutase (SOD) 2 (BD Transduction Laboratories, Milano, Italy), HSP27 and phospho (P)-HSP27 (Cell Signaling, Euroclone, Pero, Italy)

- To study mitochondrial content, antibodies against Cyclophilin D (CYP D) (Invitrogen, Carlsbad, California, USA), Mitochondrially Encoded Cytochrome C Oxidase I (MTCO1) and Voltage-Dependent Anion Channels (VDAC) (Abcam, Cambridge, UK), were used.
- To investigate modulation in the autophagy/mitophagy pathway, microtubule-associated proteins 1A/1B light chain 3B (LC3 B) (Cell Signaling, Euroclone, Pero, Italy), Sequestosome 1 (p62) and BCL2 Interacting Protein 3 (BNIP3) (Sigma Aldrich, St Louis, Missouri, USA) were used as marker of these processes to perform western blot.
- Different magnesium transporters were also tested in HUVEC and HMEC in different culture conditions: Transient Receptor Potential Melastatin 7 (TRPM7) (Bethyl, Montgomery, Texas, USA), Magnesium Transporter 1 (MagT) (Abcam, Cambridge, UK), Magnesium Transporter MRS2 (MRS2) (Thermo Fisher Scientific, Waltham, Massachusetts, USA).

Glyceraldehydes-3-phosphate dehydrogenase (GAPDH) was used as internal control of loading. After extensive washing, secondary antibodies labelled with horseradish peroxidase (Amersham Pharmacia Biotech Italia, Cologno Monzese, Italy) were used. Immunoreactive proteins were detected by the SuperSignal chemiluminescence kit (Pierce, Thermo Fisher Scientific, Waltham, Massachusetts, USA).

All the experiments were performed at least 3 times and a representative blot is shown. Images were analysed using ImageJ.

## 3.11. NOS ACTIVITY

NOS activity was measured in the conditioned media by using the Griess method. Briefly, conditioned media were mixed with an equal volume of freshly prepared Griess reagent. The absorbance was measured at 550 nm. The concentrations of nitrites in the samples were determined using a calibration curve generated with standard $NaNO_2$ solutions. The experiment was performed in triplicate and repeated 5 times with similar results. Data are shown as the % of $NaNO_2$ release in HUVEC cultured in the RWV vs static 1G conditions (CTR) ± standard deviation.

## 3.12. CONFOCAL IMAGING IN SIMULATED MICROGRAVITY

After 4 and 10 days in the RWV or in 1G, HUVEC were trypsinized and cytospun on Frosted microscope glasses, fixed in phosphate-buffered saline containing 3% paraformaldehyde and 2% sucrose pH 7.6, permeabilized with HEPES-Triton 1%, incubated with anti-TXNIP, anti-Cyclophilin D or anti-LC3 immunopurified IgGs overnight at 4°C, and stained with an Alexa Fluor secondary antibody (Thermo Fisher Scientific, Waltham, Massachusetts, USA). Finally, cells were mounted with moviol and images were acquired using a different objective in oil by a SP8 Leica confocal microscope.

## 3.13. CONFOCAL IMAGING IN 3D-MICROFLUIDIC DEVICES

HUVEC and HMEC were cultured in the microfluidic device for 7 days and fixed in phosphate-buffered saline containing 4% paraformaldehyde and 2% sucrose pH 7.6, permeabilized with Triton 0.3%, incubated with phalloidin-TRIC or anti-TXNIP immunopurified IgGs overnight at 4°C, and stained with an Alexa Fluor 488 (Thermo Fisher Scientific, Waltham, Massachusetts, USA). Nuclei were stained using DAPI. Finally, cells were mounted with ProLong™ Gold Antifade Mountant (Invitrogen, Carlsbad, California, USA) and images were acquired using a 63X objective in oil by a ZEISS 710 confocal microscope. Images were analysed using ImageJ.

## 3.14. OXYGEN CONSUMPTION MEASUREMENTS ON CELLS

The respiratory chain capacity was determined by high-resolution respirometry on HUVEC grown in 1G condition (CTR) or in the RWV for 4 and 10 days. The beads were collected from the RWV vessels, trypsinized and $1x10^6$ cells for each sample were used. The mitochondria respiration rates were measured using the O2K oxygraph chambers (Oroboros, Instruments, Innsbruck, Austria). The cells were transferred into oxygraph chambers and resuspended in the respiration medium MiR06 (0.5 mM EGTA, 3 mM MgCl2, 60 mM K-lactobionate, 20 mM taurine, 10 mM KH2PO4 20 mM Hepes, 110 mM sucrose and 1 g/l bovine serum albumin fatty acid-free, 280 U/ml catalase (pH 7.1)). The sequential addition of pyruvate (10 mM), malate (2 mM), oligomycin (0.5 μM), the uncoupler FCCP (Carbonyl cyanide-4-(trifluoromethoxy) phenylhydrazone, 0.5 μM),

rotenone (0.5 μM) and antimycin A (AA) (2.5 μM) allows the measurement of basal, leak and maximal respiration respectively. All the reagents used for respirometry assay were purchased from Sigma.

## 3.15. MITOCHONDRIA EXTRACTION AND OXYGEN CONSUMPTION MEASUREMENTS ON PURIFIED FRACTION OF MITOCHONDRIA

Oxygen consumption was measured also on extracted mitochondria of HUVEC grown in 1G condition (CTR) or in the RWV for 4 days. The cells were trypsinized, permeabilized, resuspended in isolation buffer (100mM KCl, 50mM TRIS, 5mM MgCl2, 1.8mM ATP, 1mM EDTA) and centrifuged at 600xg for 10 minutes at 4°C. Then the supernatant was centrifuged at 10000xg for 15 minutes at 4°C to allow the sedimentation of the mitochondria which were resuspended in Mito Preservation Medium (MiR06 supplemented with 20 mM Histidine, 20 μM Vitamin E succinate, 3mM Glutathione, 1μM Leupeptin, 2 mM Glutamate, 2mM Malate, 2 mM Mg-ATP) and 150 μg of mitochondria were used for high-resolution respirometry analysis. The efficiency of the different components of the respiratory chain was measured: complex I respiration (state2), maximal oxidative phosphorylation capacity of complex I (state3), complexes I and II (state3+Succ), complex II function (state3+Succ+Rot) and proton leak across the inner mitochondrial membrane (state4). Then respiratory chain was inhibited by antimycin A (2.5 μM) to obtain the residual oxygen flux that was subtracted to each steady state to correct oxygen fluxes. The respiratory control ratio was calculated as the ratio between state3 and state4 showing a general measure of mitochondrial function. The oxygen

consumption measurements were performed three times and the results are shown as the mean ± standard deviation.

## 3.16. STUDY OF AUTOPHAGY/MITOPHAGY

In some experiments, to allow the accumulation of autophagosomes and study the autophagic process, HUVEC were treated with 40μM of chloroquine (CQ) (Sigma Aldrich, St Louis, Missouri, USA) for 1h and then collected for protein extraction and western blot. To inhibit autophagy/mitophagy, HUVEC in the RWV were treated with 40 μM of chloroquine for 4 days and collected for western blot and immunofluorescence. In other experiments, HUVEC in 1G condition were treated with 0.5 μM of Cytochalasin D (Sigma Aldrich, St Louis, Missouri, USA).

## 3.17. CYTOSKELETAL DISRUPTION

We mimicked cytoskeletal disruption in 1G condition using Cytochalasin D (Sigma Aldrich, St Louis, Missouri, USA), a toxin that binds actin and induces its depolymerization. We performed dose- and time-dependent experiments to test cell viability on both HUVEC and HMEC, and found that in HUVEC 0.5μM Cytochalasin D was not cytotoxic up to 96h while for HMEC we selected a treatment with 10nM of Cytochalasin D up to 72h. Different time points were studied.

## 3.18. MTT ASSAY

To test cell viability upon different treatment (Chloroquine or Cytochalasin D), we used the MTT assay. HUVEC and HMEC were seeded in 96 well/plates and 24 h later exposed to different doses of each compound. After 96h (HUVEC) or 72h (HMEC) of treatment, 3-(4,5-Dimethylthiazol-2-yl)-2,5-Diphenyltetrazolium Bromide was added (MTT, 0.5 mg/mL) (Sigma-Aldrich, St. Louis, MO, USA) in the culture medium in ratio 1:10. After 3-4h of incubation with MTT solution, formazan crystals, derived by the degradation of MTT into the mitochondria of living cells, were dissolved in EtOH:DMSO (1:1) and absorbance was measured at 550 nm. Viability was calculated comparing absorbance of each treatment to CTR one. Every experiment was repeated three times in triplicate.

## 3.19. QUANTIFICATION OF TOTAL INTRACELLULAR MAGNESIUM

The total amount of intracellular Mg was evaluated using the fluorescent chemosensor DCHQ5. Cells were trypsinized and resuspended in MeOH:MOPS (methanol: $H_2O$ 1:1 buffered at pH 7.4 with 2mM 3-morpholinopropane1-sulfonic acid at room temperature) (Sigma Aldrich, St Louis, Missouri, USA).

Cells suspension was sonicated and then loaded in black bottomed 96 plates (Greiner bio-one, Frickenhausen, Germany) in the presence of 15 μM of DCHQ5 [Sargenti 2017]. After 20 seconds of shaking, fluorescence intensity was read using Promega Glomax Multi Detection System (Promega, Madison, Wisconsin, USA) ($\lambda$exc=360 nm, $\lambda$emm=510nm).

For each sample measurement the numbers of micromoles of magnesium ion was calculated by interpolation of the calibration curve equation; magnesium sulfate ($MgSO_4$, Sigma Aldrich, St Louis, Missouri, USA) was used to create a standard curve.

## 3.20. GLUCOSE TREATMENT

In some experiments in 2D Static Cell culture, D-Glucose (Sigma Aldrich, St. Louis, Missouri, USA) was added to normal medium, in which the concentration of glucose is 1 mg/mL (5.5 mM), to obtain a final concentration of 5.4 mg/mL (30 mM) and the effect of the high-glucose medium was studied after overnight or 24h of treatment.
In 3D-Flow Cell culture experiments, after 7 days in culture with normal medium, D-Glucose was added overnight or for 24h.

## 3.21. ACTIN ALIGNMENT QUANTIFICATION

Images derived from immunofluorescence for F-actin performed on HMEC and HUVEC grown in 3D-flow condition, in control medium and in presence of 5.4 mg/mL of D-glucose, were analysed using the OrientationJ plugin of ImageJ. The direction of flow within the 30 × 30 μm channels was assumed as theta=0 and the angular distributions of actin fibers was calculated as the deviation of fiber orientation compared to theta=0.

## 3.22. STATISTICAL ANALYSIS

Statistical significance was determined using the Student's t test and set at p values less than 0.05. In the figures *p<0.05; **p<0.01; ***p<0.001.

# 4. RESULTS (1): STRESS PROTEINS AND ADAPTATION TO SIMULATED MICROGRAVITY

# 4.1. PRO- AND ANTI- OXIDANT SPECIES IN HUVEC EXPOSED FOR 4 AND 10 DAYS TO SIMULATED MICROGRAVITY

It is well known that microgravity is perceived by different cell types as a stressful situation and for this reason a factor promoting apoptosis. Despite this, HUVEC in simulated microgravity are able not only to survive, but also grow faster than controls in 1G [Carlsson 2003; Versari 2007], thus suggesting that HUVEC in simulated microgravity activate an adaptive response to counterbalance the stress raising from the exposure to gravitational unloading.

Moreover, it is reported that in some cell types microgravity induces oxidative stress [Wang 2009; Liu 2008; Beck 2014] that may be due to an unbalance between pro- and anti-oxidant species production. Therefore, we initially measured Reactive Oxygen Species (ROS) production, markers of a pro-oxidant environment, in HUVEC cultured in the RWV for various times. Using 2'-7'-dichlorofluorescein diacetate (DCFH) we found a modest, albeit statistically significant, increase of ROS after 2 h in cells in simulated microgravity (RWV) *vs* 1G conditions (CTR) and no differences thereafter (Figure 25 A). To have an overview of the antioxidant response of HUVEC in simulated microgravity, we measured GSH, the most abundant antioxidant in aerobic cells [Ballatori 2009], with a focus on the ratio between the reduced *vs* oxidized form (GSH/GSSG). Even in this case only at 2h in the RWV, but not at later times we found GSH/GSSG ratio significantly decreased (Figure 25 B), proving the ability of HUVEC cultured in the RWV of buffering pro-oxidant species using GSH/GSSG system.

In addition, we measured possible oxidative damage of DNA by comet assay, but we found no DNA damage in HUVEC exposed to RWV compared to 1G condition (Figure 25 C).

We therefore conclude that in the early exposure to simulated microgravity, HUVEC accumulate more ROS than controls, but rapidly counterbalance the establishment of a pro-oxidant environment by upregulating anti-oxidant systems, as the GSH. Indeed, for exposure longer than 2h, HUVEC in the RWV exhibit the same amounts of ROS as CTR and no DNA damage occurs.

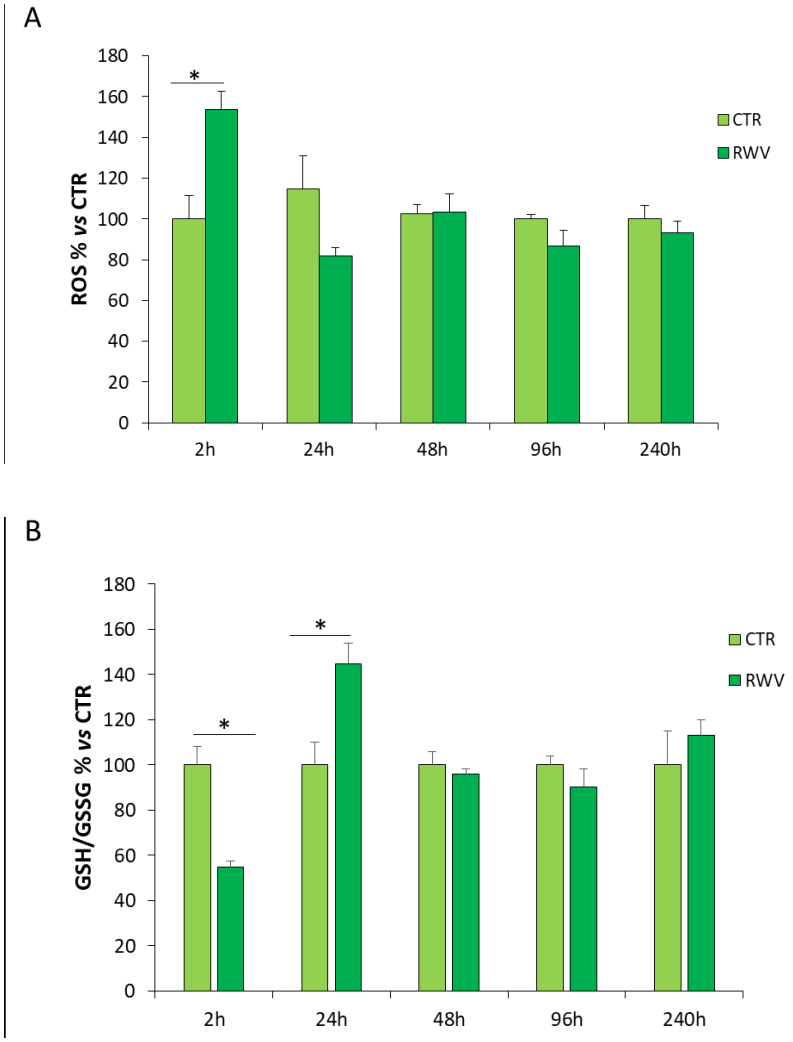

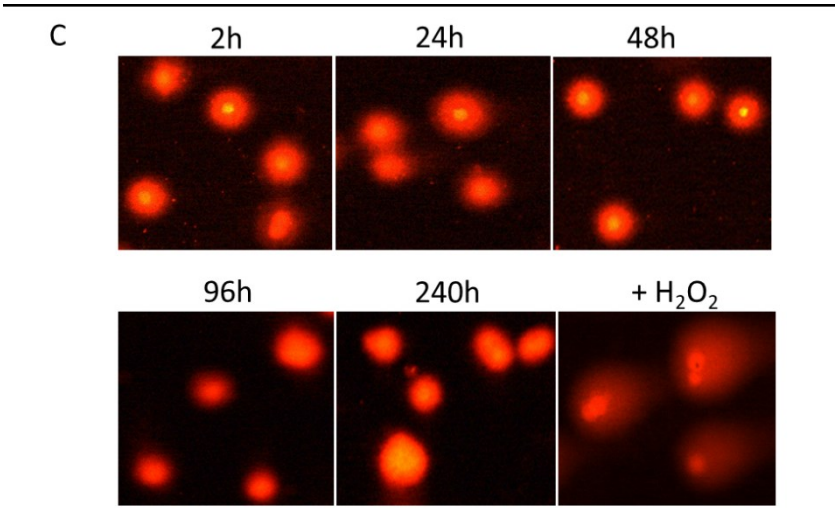


*Figure 25: Pro- and Anti-oxidant species in HUVEC exposed for 4 and 10 days to simulated microgravity.*
*HUVEC were cultured for various times in the RWV or in static 1G conditions (CTR) and then analysed for ROS production (A), GSH/GSSG ratio (B) and DNA damage (C). In C exposure to H2O2 (100 μM) for 2 h was used as a positive control.*

## 4.2. THE MODULATION OF STRESS PROTEINS IN HUVEC EXPOSED FOR 4 AND 10 DAYS TO SIMULATED MICROGRAVITY

Next, we investigated the levels of stress proteins by utilizing a specifically tailored protein array (Figure 26A).

HUVEC were cultured for 4 and 10 days in 1G condition (CTR) or in simulated microgravity (RWV) and lysed. 80 μg of cell extract were used for the analysis. The protein array, designed to detect modulation in 26 proteins known to be involved in stress pathways, highlighted the modulation of six proteins: HSP70, SIRT2, PON2, SOD2,

p21 and P-HSP27, all upregulated in HUVEC exposed to RWV compared to respective controls (Figure 26 B, C).

A

| | 1 | 2 | 3 | 4 | 5 | 6 | 7 | 8 | 9 | 10 | 11 | 12 | 13 | 14 | 15 | 16 | 17 | 18 | 19 | 20 | 21 | 22 |
|---|---|---|---|---|---|---|---|---|---|---|---|---|---|---|---|---|---|---|---|---|---|---|
| A | Ctr (+) | | | | | | | | | | | | | | | | | | | | Ctr (+) | |
| B | | | ADAMTS1 | | Bcl-2 | | CA9 | | Cited-2 | | COX-2 | | Cyt-C | | Dkk-4 | | FABP-1 | | HIF-1α | | | |
| C | | | HIF-2α | | P-HSP27 | | HSP60 | | HSP70 | | IDO | | P-JNKPan | | NFkB1 | | p21/CIP | | p27 | | | |
| D | | | P-p38α | | P-p53 | | PON1 | | PON2 | | PON3 | | TXN-1 | | SIRT2 | | SOD2 | | Ctr (-) | | | |
| E | Ctr (+) | | | | | | | | | | | | | | | | | | | | | |

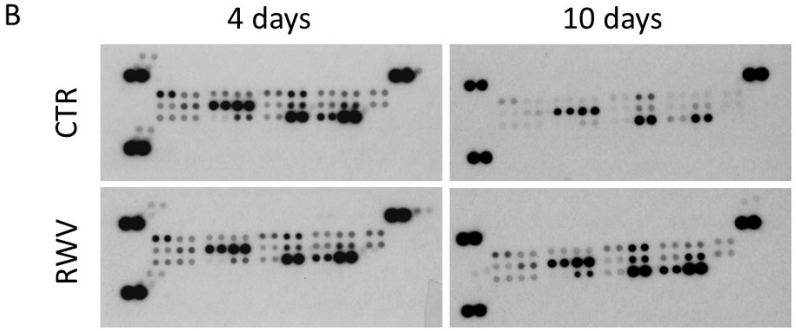


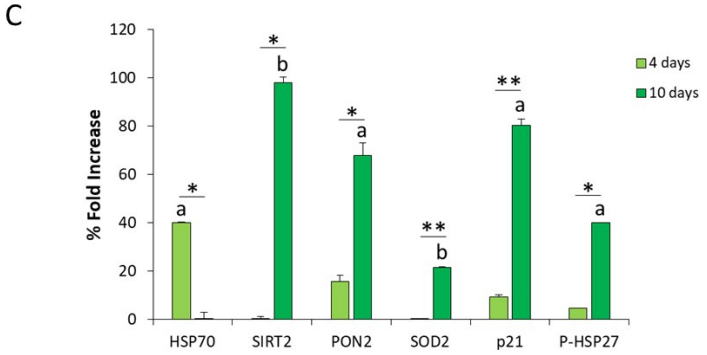


*Figure 26: Stress protein array.*

*(A) Scheme of the 26 proteins spotted in duplicate on the membrane of the array. (B) Representative blots of HUVEC in 1G condition (CTR) or in the RWV for 4 and 10 days are shown.*

*(C) Densitometric analysis; the fold increase of the mostly upregulated proteins in simulated microgravity compared to respective control are shown. Data are expressed as % of the fold increase of the signal intensity obtained in cells in the RWV vs static 1G-conditions. Different*

*letters indicate the statistically significant effect of RWV vs 1G conditions (a: p<0.05; b: p<0.01) while the symbol * indicates the statistically significant variation of RWV 4 days vs RWV 10 days.*

## 4.3. HSP70 EXPRESSION IN HUVEC EXPOSED TO SIMULATED MICROGRAVITY

It was previously shown that HSP70 is induced in HUVEC after 24 h of exposure in simulated microgravity and remains elevated up to 96 h [Carlsson 2003]. As shown in Figure 26, using protein array on cell lysates, one of the most upregulated protein in HUVEC exposed to simulated microgravity is HSP70, mostly after 4 days. To validate this result, we performed Real time-PCR, which demonstrates the overexpression of *HSPA1A* (*HSP70)* after 4 days in the RWV (Figure 27 A) and western blot (B), which shows the upregulation of HSP70 after 4 days of culture in the RWV. Both RNA and protein return to baseline after 10 days in simulated microgravity (Figure 27).

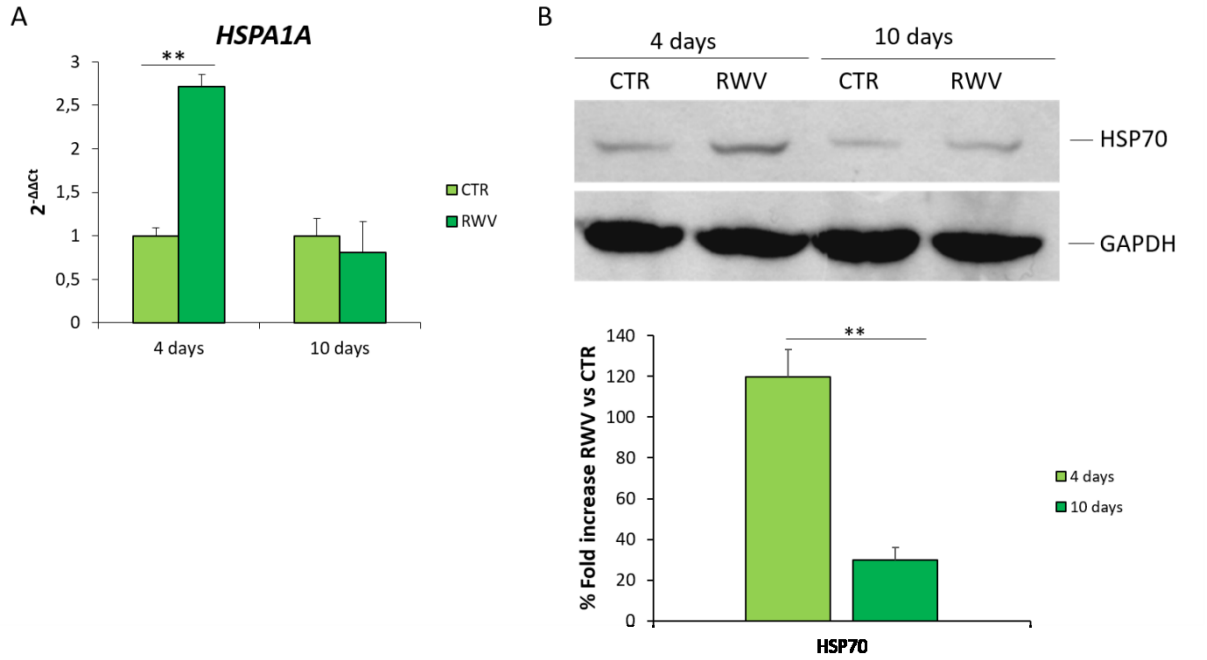

*Figure 27: HSP70 expression in HUVEC exposed to simulated microgravity.*
*(A) Real-Time PCR was performed using primers designed on HSPA1A sequence on RNA extracted from HUVEC cultured in the RWV or in static 1G condition (CTR) for 4 and 10 days. (B) Western blot was performed using specific antibodies against HSP70. GAPDH is used as marker of loading. A representative blot and relative quantification are shown.*

## 4.4. EFFECT OF HSP70 SILENCING IN HUVEC EXPOSED TO SIMULATED MICROGRAVITY

Considering that HSP70 rapidly increases in HUVEC in simulated microgravity [Carlsson 2003], we decided to unravel its role in the early phases of HUVEC exposure to simulated microgravity.

For this reason we transiently silenced *HSP70* using a specific siRNA before exposing HUVEC to gravitational unloading for 48 h. As a control, the cells were exposed to a non-interfering, scrambled sequence. We confirmed HSP70 downregulation at RNA level using real-time PCR in silenced HUVEC (Figure 28 A).

We then tested the effect of HSP70 silencing on cell proliferation in HUVEC in 1G condition or in simulated microgravity. We found that HUVEC in the RWV grow faster than static 1G conditions (CTR), as previously reported [Carlsson 2003; Versari 2007]. On the contrary, silencing *HSP70* completely prevented this effect and HUVEC in the RWV grow less than in 1G condition when *HSP70* is silenced (Figure 28 B).

HSP70 is an important molecular chaperone also implicated in the control of apoptosis. It inhibits AIF (apoptotic inducer factor) and APAF (activator factor of apoptotic proteases) [Beere 2000; Saleh 2000; Ravagnan 2001], thus protecting cells from apoptosis. To test the effect of the silencing of *HSP70* on apoptosis, we measured cleaved nucleosomes in HUVEC silencing or not *HSP70* after 48 h in the RWV using an ELISA.

TNFα (50 ng/ml) was used as a positive control to induce apoptosis. We found that after *HSP70* silencing HUVEC cultured for 48 h in the RWV show cleavage of nucleosomes, an index of apoptosis (Figure 28 C).

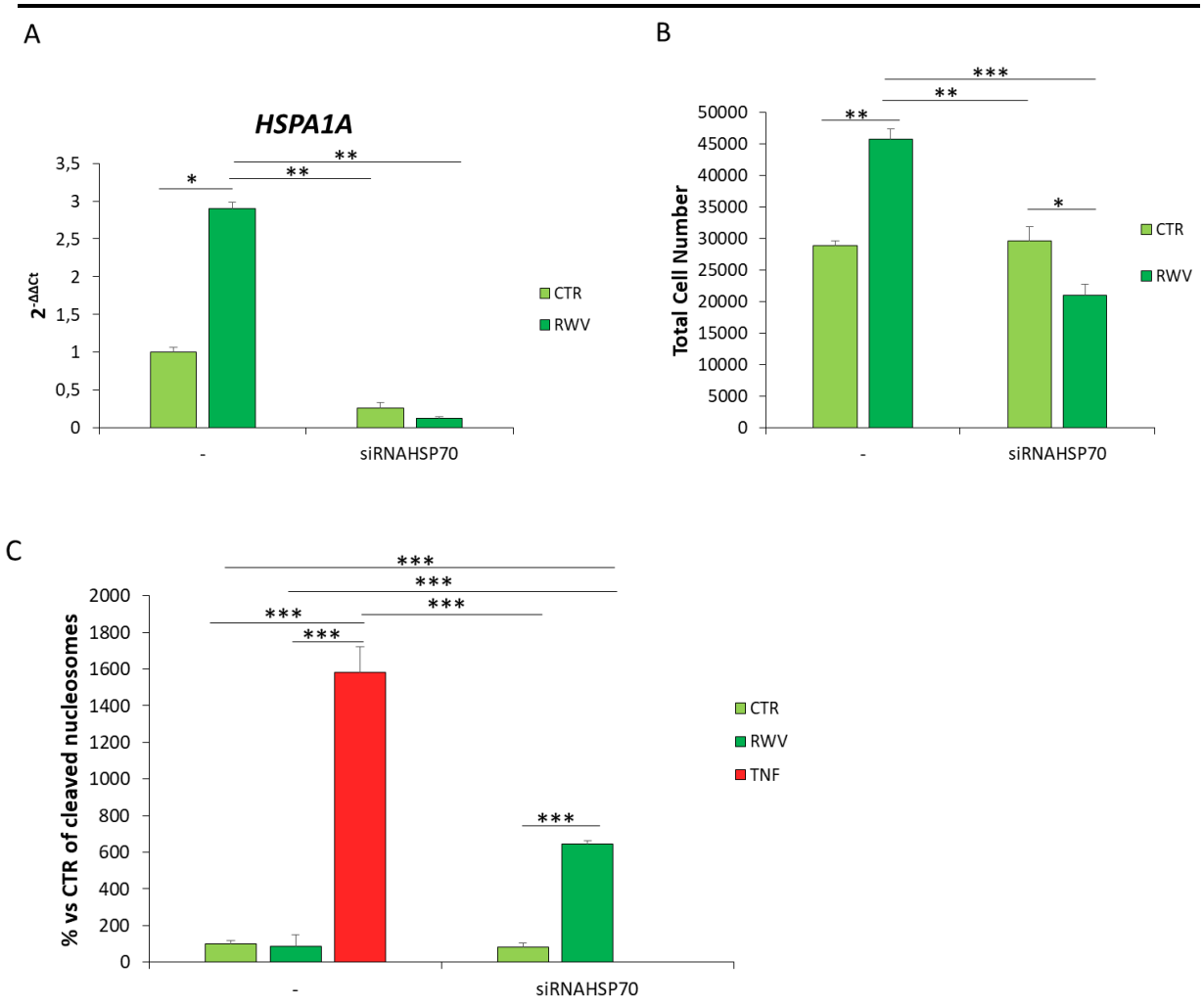


*Figure 28: Effect of HSP70 silencing on cell growth and survival.*
*HUVEC were transfected with siRNA against HSPA1A or with a scrambled non silencing sequence (-) and maintained in the RWV or in 1G conditions for 48 h.*
*(A) To assess silencing, Real-Time PCR was performed using primers designed on the HSPA1A sequence.*
*(B) Cells were counted using a cell counter.*
*(C) ELISA was used to test apoptotic cells. The amount of cleaved DNA/histone complexes was*

*measured after 48 h and the % fold increase compared to CTR was plotted. TNFα (50 ng/ml) was used as positive control.*

## 4.5. SIRT2, PON2, SOD2, P21 AND HSP27 IN HUVEC EXPOSED TO SIMULATED MICROGRAVITY

Next, we examined the levels of the other stress proteins which resulted upregulated by protein array, i.e. SIRT2, PON2, SOD2, p21 and HSP27.
SIRT2 is a NAD-dependent deacetylase involved in the regulation of various biological processes including cell cycle control, genomic integrity, microtubule dynamics, differentiation and autophagy [North 2007; Dryden 2003; Inoue 2007; Pandithage 2008].

PON2 is a calcium-dependent enzyme with a dual function. PON2 is predominantly localized in the endoplasmic reticulum, mitochondria and perinuclear region, where it exerts its functions [Aviram 2004; Horke 2007; Rothem 2007].
As a lactonase it has an hydrolytic activity of lactones, while as antioxidant PON2 reduces oxidative stress damage and promotes cell survival, by indirectly but specifically reducing superoxide release from the internal mitochondrial membrane [Altenhöfer 2010].

p21 is potent inhibitor of kinase-cyclin dependent (CDK) that binds and inhibits CDK2 and 4 thus blocking the cell in the G1 phase of the cell cycle. The expression of this gene is mainly controlled by the p53 protein, a transcription factor that is activated in case of DNA damage.
Superoxide dismutase 2 (SOD2), also known as manganese-dependent superoxide

dismutase (MnSOD), is a mitochondrial enzyme, which binds the superoxide produced during the mitochondrial electron transport chain and converts it in hydrogen peroxide and oxygen. SOD2 is fundamental in buffering mitochondrial ROS and protecting cells from oxidative stress and apoptosis.

Hsp27 belongs to the family of small Hsp. In addition to its role as a molecular chaperon, it is implicated in several processes such as protection from apoptosis (by inhibition of both the intrinsic and the extrinsic pathway), protection from oxidative stress (by lowering ROS levels and directing oxidized proteins to degradation via proteasome) and regulation of actin cytoskeleton (by promoting polymerization of F-actin and its stability) [Haslbeck 2002; Rogalla 1999; Arrigo 2001; Lavoie 1993; Sun 2015]. Stress induces both an increase in the expression and in the phosphorylation of Hsp27.

Western blot confirms that PON2, SOD2, p21, HSP27 and its phosphorylated form are upregulated after 10, but not 4, days of exposure to simulated microgravity, as detected using protein array. The total amounts of SIRT2 decrease in CTR after 10 days, while in HUVEC cultured in the RWV SIRT2 remains elevated (Figure 29 A).

By Real Time-PCR no significant modulation of *SIRT2*, *PON2*, *SOD2* and *HSPB1 (HSP27)* was found (Figure 29 B), thus confirming the results of the SPHINX experiment [Versari 2013]. On the contrary, *CDKN1A (p21)* was markedly overexpressed after 10 days of culture in the RWV.

We also investigated the protein level of SIRT2, PON2, SOD2, HSP70, HSP27 and its phosphorylated form in proliferating *vs* quiescent HUVEC under physiological 1G conditions, to distinguish the effects of microgravity from those determined by quiescence, considering the faster proliferation of HUVEC grown in the RWV compared to 1G cultured HUVEC.

No modulation in PON2, SOD2, HSP70, HSP27 and its phosphorylated form was found in proliferating *vs* quiescent HUVEC using western blot, while SIRT2 was downregulated

and p21 upregulated in quiescent cells (Figure 29 C). We then conclude that the upregulation of PON2, SOD2, HSP70, HSP27 observed in HUVEC cultured in the RWV was due to gravitational unloading itself.

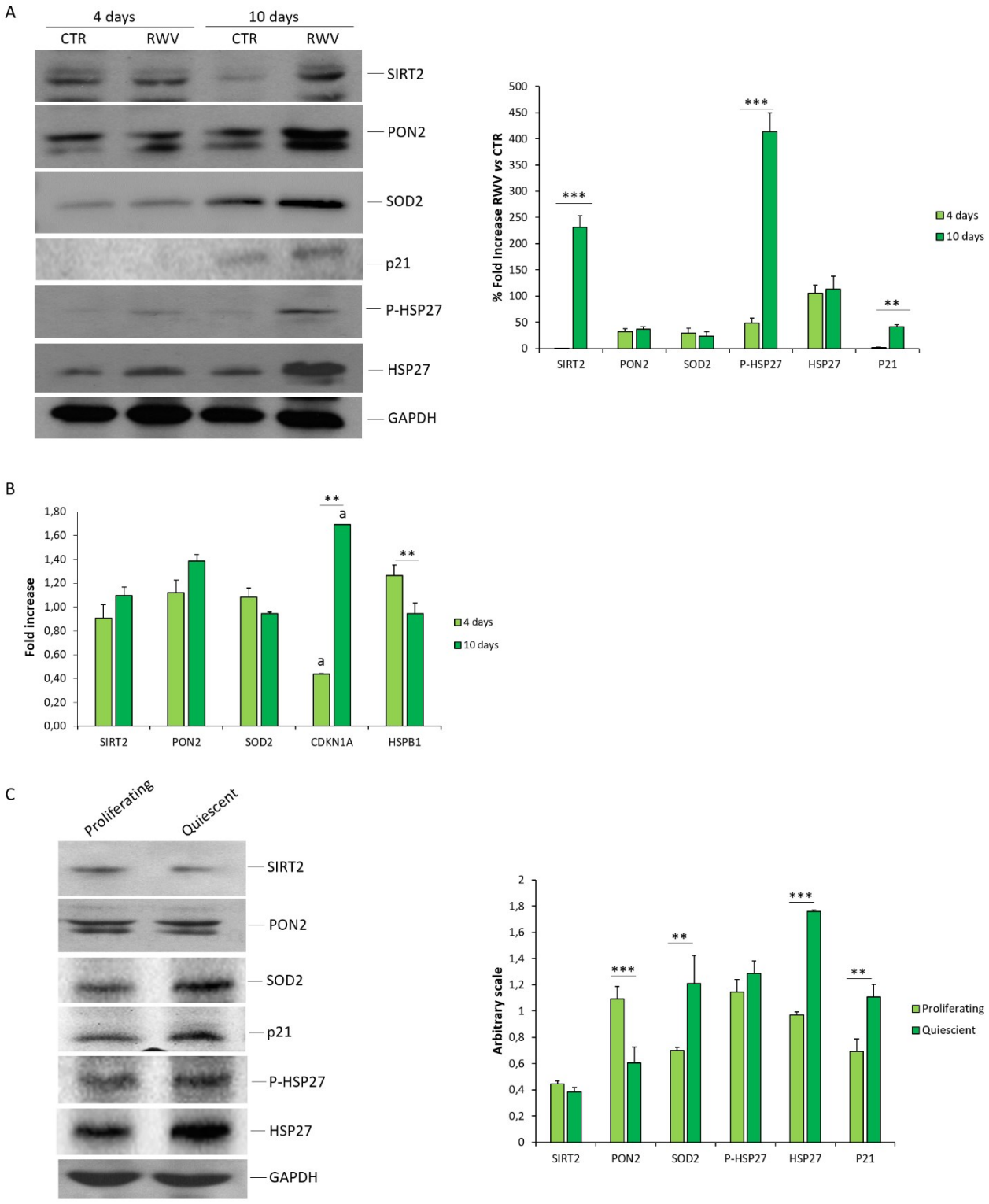


*Figure 29: Stress proteins in HUVEC exposed to simulated microgravity.*
*Western blot (A) and Real Time PCR (B) were performed on HUVEC cultured in the RWV or in static 1G condition (CTR) for 4 and 10 days. All the values were normalized with respect to their*

*controls cultured in static 1G conditions. a: p<0.05 indicates the significant effect of RWV vs static 1G conditions while the symbol * indicates the statistically significant variation of RWV 4 days vs RWV 10 days. (C) The total amounts of stress proteins by western blot were studied in proliferating and quiescent HUVEC. In A and C blots quantification are shown on the right.*

## 4.6. TXNIP IN HUVEC EXPOSED TO SIMULATED MICROGRAVITY

The SPHINX experiment performed on the ISS [Versari 2013] studied the modulation of gene expression in HUVEC cultured in space for 10 days and highlighted that the most overexpressed gene was *TXNIP*. TXNIP is produced in response to cellular stress. It inhibits the antioxidant action of Thioredoxin (TRX), an ubiquitous oxidoreductase expressed in EC responsible for the control of migration, growth, angiogenesis and apoptosis [Dunn 2010]. TXNIP is implicated in various diseases associated with aging [Salminen 2012] and in cardiovascular diseases [Wang 2012; World 2011; Yamawaki 2005; Yoshioka 2004; Zschauer 2011], thus it may be a pivotal player in the onset of cardiovascular deconditioning detected in astronauts during and after space flight.

We examined the levels of its transcript, using Real Time PCR, and the total amounts of the protein, by western blot. In agreement with Versari we found that *TXNIP* was overexpressed in HUVEC after 10 days in the RWV, while no modulation of *TXNIP* was detected at day 4 (Figure 30 A). Similarly, the protein is upregulated in HUVEC after 10 days in the RWV (Figure 30 B). TXNIP is localized both in the nucleus and in the cytoplasm, where it exerts different functions [Spindel 2012]. For this reason we analysed TXNIP localization in HUVEC grown in 1G condition or in RWV for 4 and 10 days (Figure 30 C). We found that TXNIP localizes in the nucleus and in the cytoplasm, both in CTR and in HUVEC in the RWV. Furthermore, immunofluorescence confirmed no differences

in TXNIP amount after 4 days in simulated microgravity and its increase in HUVEC grown in the RWV for 10 days (Figure 30C).

Even in this case we compared the total amounts of TXNIP in proliferating *vs* quiescent HUVEC to discern the effect of microgravity and we found that TXNIP decreases in quiescent cells (Figure 30 D), thus reinforcing the hypothesis that simulated microgravity is directly responsible for the upregulation of TXNIP after 10 days in RWV.

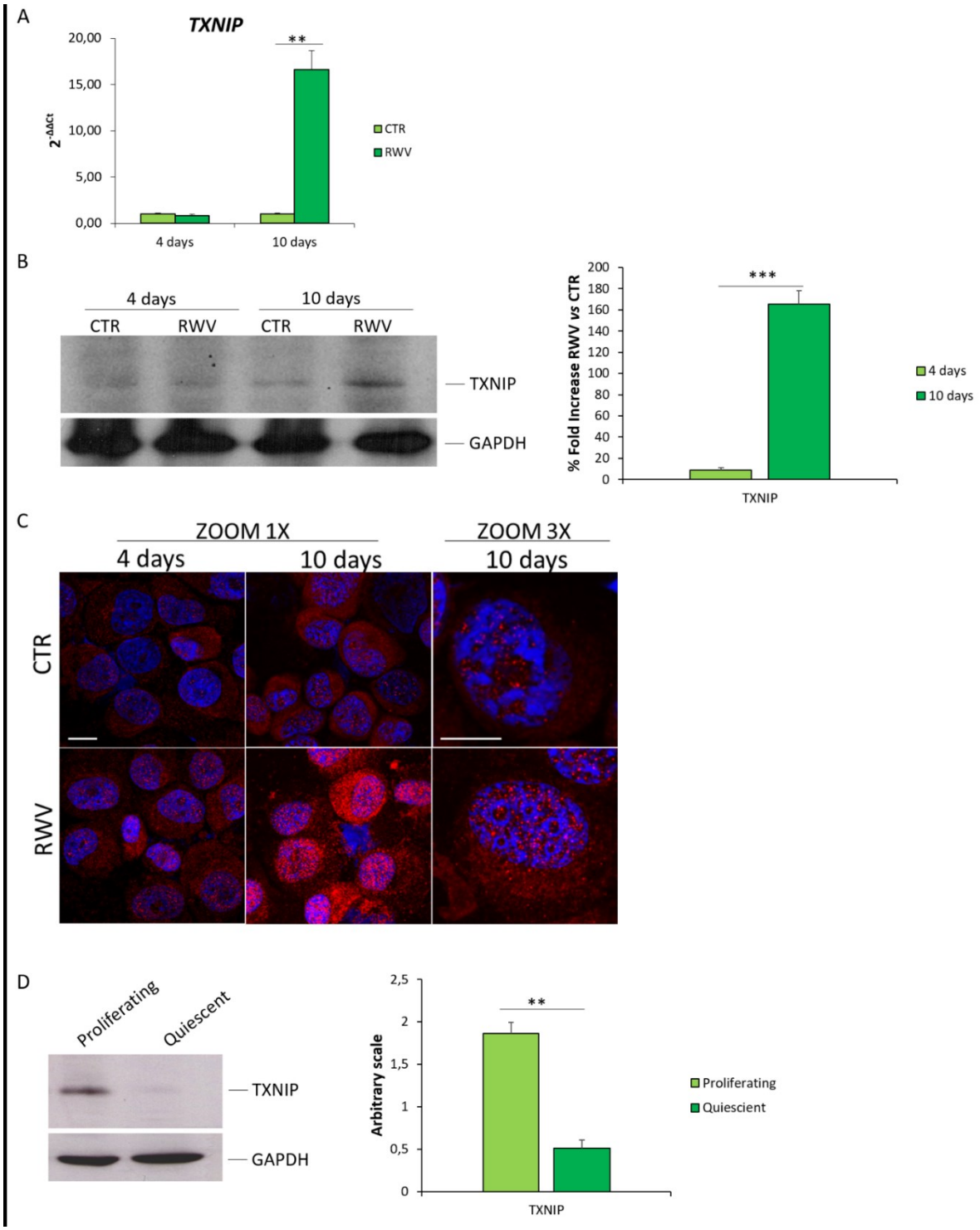


*Figure 30: TXNIP expression in HUVEC.*
*HUVEC were cultured in the RWV or in static 1G conditions (CTR) for 4 and 10 days and Real Time PCR (A) and western blot (B) were performed as described in the methods. Quantification is shown on the right.*

*(C) Immunofluorescence was performed on HUVEC cultured as above, cytospun, and stained with DAPI and TXNIP antibody. Images were acquired using a 63X objective in oil by a SP8 Leica confocal microscope; right panel: zoom 3X. Scale bar: 10μm*
*(D) Proliferating and quiescent HUVEC were analysed for the total amounts of TXNIP by western blot. Quantification is shown on the right.*

## 4.7. ENDOTHELIAL FUNCTION IN HUVEC EXPOSED TO SIMULATED MICROGRAVITY

We analysed also nitric oxide (NO) production, because NO is a multifunctional molecule which influences vascular functions. We have previously shown that HUVEC cultured in simulated microgravity for 24 and 48 h release higher amounts of NO than controls. We show that after 4 days in the RWV HUVEC continue to release more NO than controls, while at day 10 no significant differences were detected (Figure 31 A).

Endothelial function is affected also by inflammatory mediators and alterations of the cytokine network have been described in endothelial cells exposed to simulated microgravity for 24 and 48 h [Carlsson 2003; Grenon 2013; Cotrupi 2005]. To obtain a broad profile of cytokine synthesis and release in HUVEC cultured in the RWV for 4 and 10 days, we utilized a human inflammation antibody array on both conditioned media and cell extracts. No significant alterations were detected in the total amounts of cytokines, chemokines and adhesion molecules in HUVEC exposed to simulated microgravity *vs* 1G conditions (Figure 31 B-D).

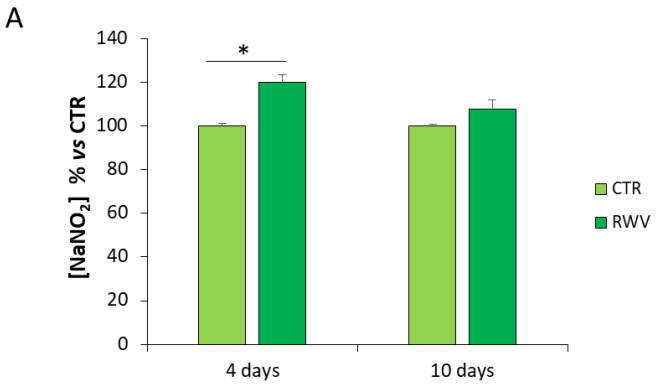


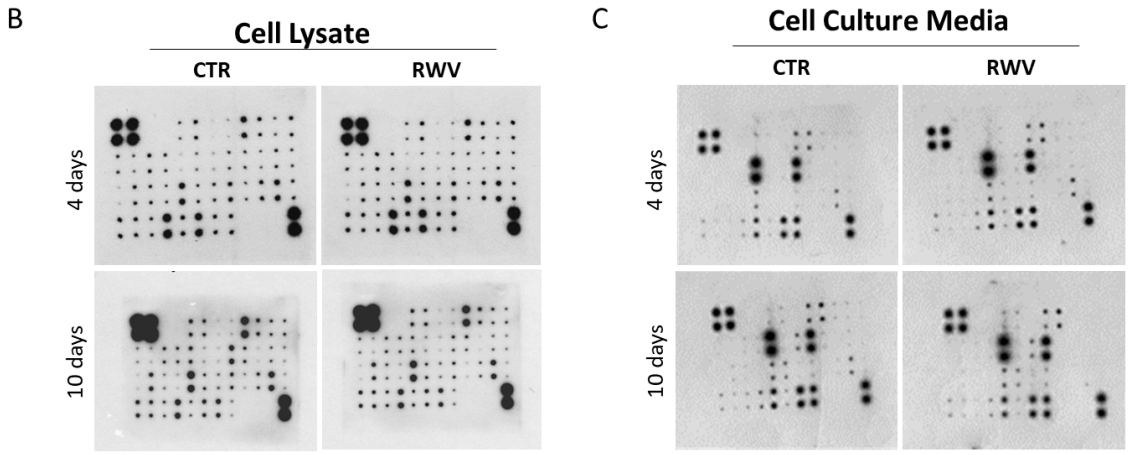


D

| | A | B | C | D | E | F | G | H | I | J | K | L |
|---|---|---|---|---|---|---|---|---|---|---|---|---|
| 1 | POS | POS | NEG | NEG | Eotaxin-1 | Eotaxin-2 | GCSF | GM-CSF | ICAM-1 | INF-γ | CCL1 | IL-1α |
| 2 | | | | | | | | | | | | |
| 3 | IL-1β | IL-2 | IL-3 | IL-4 | IL-6 | IL-6R | IL-7 | IL-8 | IL-10 | IL-11 | IL-12 p40 | IL-12 p70 |
| 4 | | | | | | | | | | | | |
| 5 | IL-13 | IL-15 | IL-16 | IL-17 A | IP-10 | MCP-1 | MCP2 | M-CSF | MIG | MIP-1α | MIP-1β | MIP-1δ |
| 6 | | | | | | | | | | | | |
| 7 | RANTES | TGF-β1 | TNFα | TNFβ | TNFRI | TNFRII | PDGF-BB | TIMP-2 | BLANK | BLANK | NEG | POS |
| 8 | | | | | | | | | | | | |

*Figure 31: Nitric oxide production and cytokine network in HUVEC exposed to simulated microgravity.*

*(A) Nitric oxide was measured by Griess method in HUVEC cultured in RWV or in static 1G conditions (CTR) for 4 and 10 days. Data are shown as the % of $NaNO_2$ release in HUVEC cultured in the RWV vs static 1G conditions (CTR). (B, C) Inflammatory protein arrays were performed both on cell lysate and on conditioned media. Representative membranes are shown. (D) Map of the membrane array.*

**These data were published in FASEB J. 2019 May; 33(5):5957-5966.**

**doi: 10.1096/fj.201801586RR.**

**The agreement to publish these data on the thesis is attached. (Appendix A)**

# 5. RESULTS (2): METABOLIC ADAPTATION

# 5.1. MITOCHONDRIAL CONTENT IN HUVEC EXPOSED TO SIMULATED MICROGRAVITY

In endothelial cells mitochondria are not primary used to produce energy, since 85% of ATP needed by EC derives from glycolysis [De Bock 2013]. Endothelial mitochondria produce the precursors necessary for the synthesis of various molecules required for cellular necessities [Rohlenova 2018]. Therefore, mitochondria in EC are used as integrators of signaling from the environment, since they are able to perceive chemical and mechanical stimuli and orchestrate cell response. At the moment no data are available on HUVEC bioenergetics in microgravity. For this reason we investigated mitochondrial content and function in HUVEC exposed to simulated microgravity.

To have an overview of the effect of simulated microgravity on mitochondrial content in HUVEC, we performed immunofluorescence. After 4 and 10 days, HUVEC cultured in the RWV or in 1G condition (CTR) were trypsinized and cytospun on a glass coverslip. We used an antibody against Cyclophilin D (CYP D), a protein that is part of the permeability transition pore in the inner membrane of the mitochondria, as a marker of mitochondria. We show that HUVEC grown in the RWV have fewer mitochondria than their control (CTR) (Figure 32 A).

We also performed western blot for different markers of mitochondria, such as CYP D, Mitochondrially Encoded Cytochrome C Oxidase I (MTCO1), a protein encoded by mitochondrial DNA, and Voltage-Dependent Anion Channels (VDAC), located on the outer mitochondrial membrane. MTCO, VDAC and CYP D were all significantly downregulated in HUVEC cultured in the RWV for 4 and 10 days (Figure 32 B), confirming the results obtain by immunofluorescence also at the biochemical level.

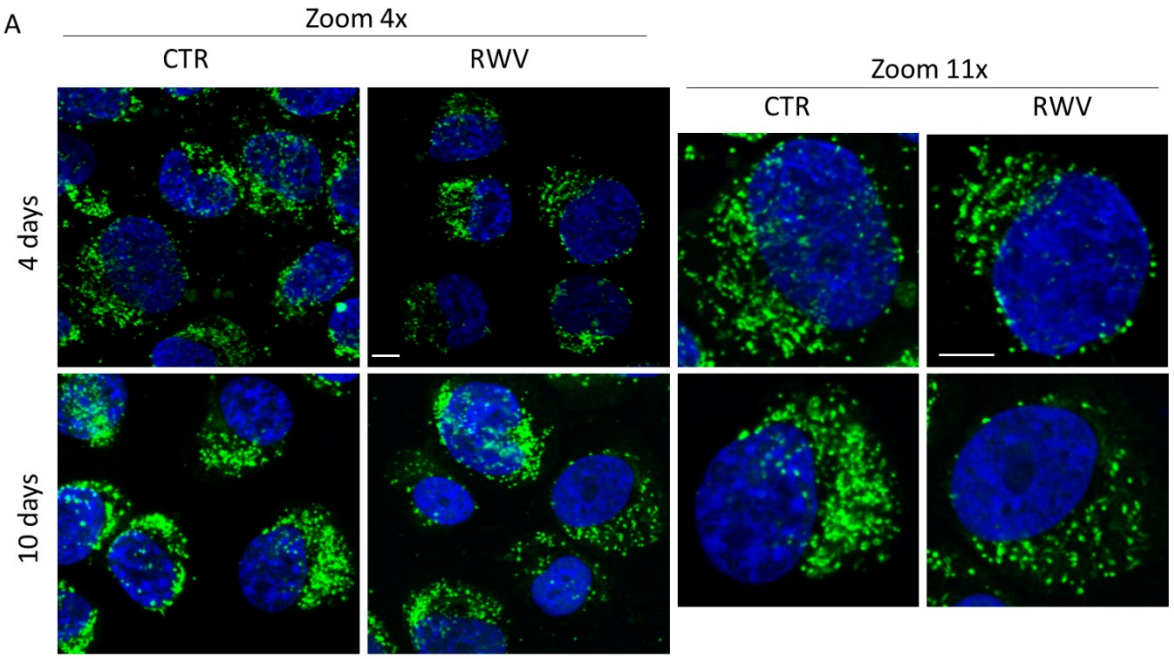
A
Zoom 4x
CTR
RWV
Zoom 11x
CTR
RWV
4 days
10 days

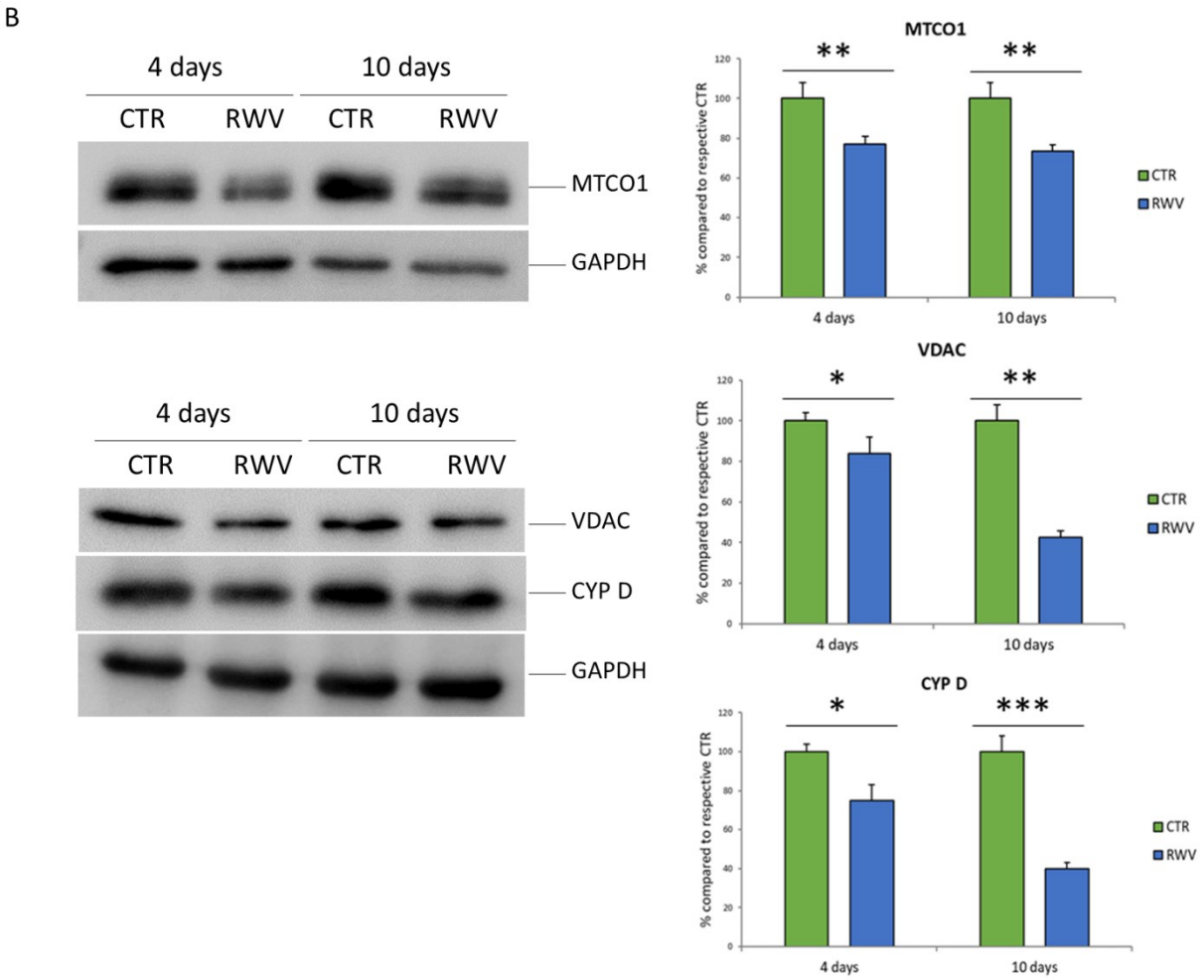
B
4 days
10 days
CTR
RWV
CTR
RWV
MTCO1
GAPDH
4 days
10 days
CTR
RWV
CTR
RWV
VDAC
CYP D
GAPDH
MTCO1
% compared to respective CTR
**
**
4 days
10 days
CTR
RWV
VDAC
% compared to respective CTR
*
**
4 days
10 days
CTR
RWV
CYP D
% compared to respective CTR
*
***
4 days
10 days
CTR
RWV

*Figure 32: Immunofluorescence and western blot of mitochondrial markers in HUVEC grown in 1G or RWV.*
*HUVEC were grown in RWV or in 1G condition (CTR) for 4 and 10 days. In A cells cytospun on glass coverslips at the end of the experiment were labeled with Dapi (for nuclei) and with antibodies against CYP D (for mitochondria). Images were acquired using a 40X objective in oil with different magnification by a SP8 Leica confocal microscope.*
*In B representative western blots for different mitochondrial markers (left) and relative quantification (right) are shown.*

## 5.2. MITOCHONDRIAL FUNCTION IN HUVEC EXPOSED TO SIMULATED MICROGRAVITY

Mechanical and biochemical stimuli are known to modulate not only mitochondrial content but also their function. For this reason, we decided to use O2K oxygraph chambers to test mitochondrial function in HUVEC. We measured different respiration states: maximal respiration, corresponding to the maximal activity of the electron transport chain, basal respiration, i.e. oxygen consumption at steady state, and leak respiration, which measures oxygen consumption not linked to ATP production. We found that HUVEC exposed to simulated microgravity tend to have a minor basal and leak capacity, without reaching statistical significance, compared to their controls, while their maximal respiratory capacity is significantly reduced (Figure 33 A).

Considering that we have previously shown that HUVEC in the RWV have a lower mitochondrial amount (Figure 32) and that the previous experiment was conducted using the same amount of cells ($1x10^6$) for both 1G and RWV samples, we decided to perform respirometry also on a purified fraction of mitochondria, to avoid bias due to different mitochondrial content. We then evaluated the function of isolated mitochondria in HUVEC grown in 1G condition or the RWV for 4 days, testing the functionality of the

different components of the respiratory chain: complex I respiration (state2) and its maximal oxidative phosphorylation capacity (state3); the function of complexes I and II together (state3+Succ) and complex II alone (state3+Succ+Rot); finally proton leakage was measured using an inhibitor of ATP synthase (state4). The respiratory control ratio was calculated as the ratio between state3 and state4 and used as a general indicator of mitochondrial function. This parameter was similar in controls and in cells in the RWV, indicating that single mitochondria are as efficient in cells cultured in the RWV as in 1G condition (CTR) (Figure 33 B).

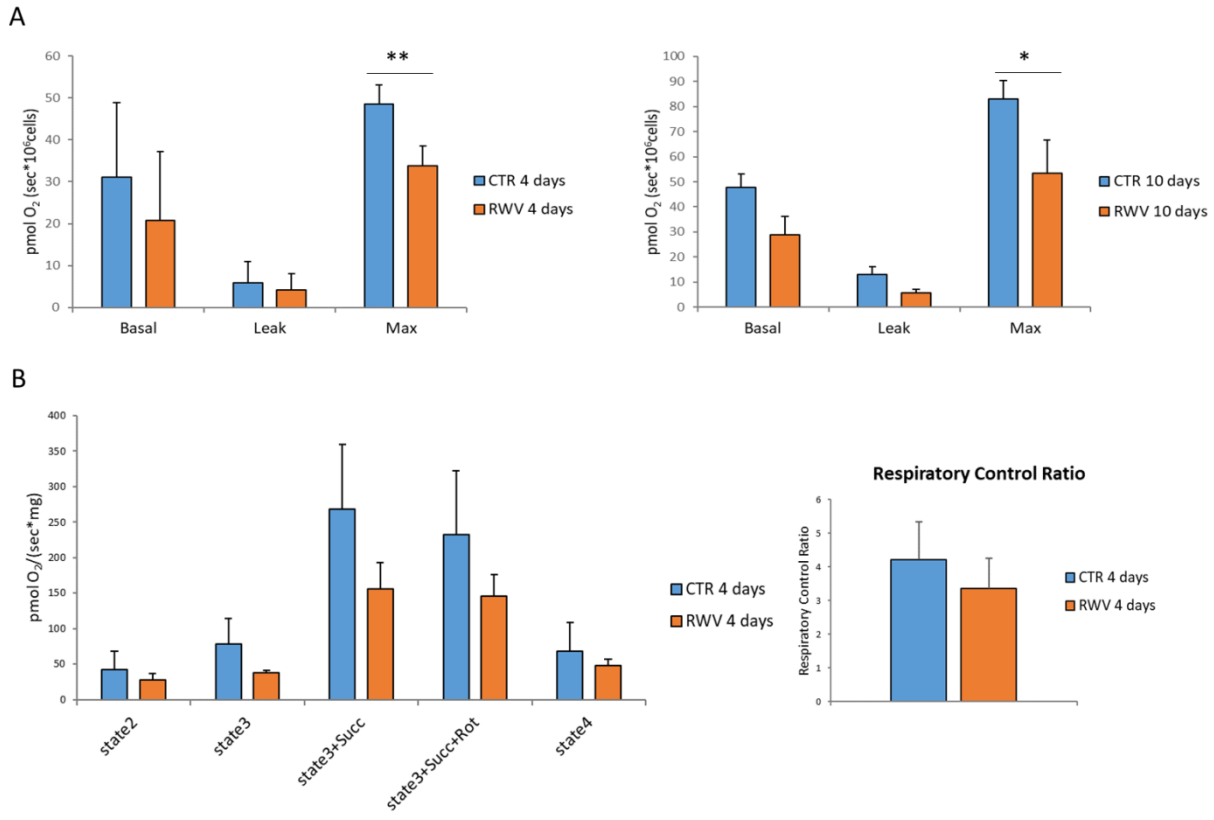


*Figure 33: High resolution respirometry on HUVEC and on isolated mitochondria after exposure to simulated microgravity.*

*(A) High resolution respirometry was performed on 1x10⁶ cells and basal, leak and maximal respiration were measured as described on HUVEC cultured in 1G condition (CTR) or in the RWV for 4 and 10 days.*

*(B) Mitochondria were extracted from HUVEC grown for 4 days in 1G condition (CTR) or in the*

*RWV and oxygen consumption was measured on a purified fraction of mitochondria (150 μg). The experiments were repeated three times ± standard deviation.*

## 5.3. AUTOPHAGY/MITOPHAGY IN HUVEC EXPOSED TO SIMULATED MICROGRAVITY

Mitochondrial content is determined by the balance between mitochondrial biogenesis and degradation. We hypothesized that the decreased number of mitochondria in HUVEC exposed to simulated microgravity could be due to an increased degradation of mitochondria through the autophagic flow and, specifically, mitophagy.

In the literature it was already reported that HUVEC in simulated microgravity activate autophagy [Wang 2013; Li 2018; Jeong 2018]. To confirm these results, we evaluated the levels of two markers of autophagy by western blot, i.e. microtubule-associated proteins 1A/1B light chain 3B (LC3 B) that triggers the formation of autophagosomal vacuoles, and Sequestosome 1 (p62), which is expressed with the cargo within the vesicle. In particular, LC3 B exists in two forms: total (LC3 B-I) and cleaved (LC3 B-II) form, which is specifically produced when autophagy occurs. Western Blot revealed no significant modulation of these proteins in HUVEC exposed for 4 days to simulated microgravity *vs* their controls (Figure 34 A). We hypothesized that autophagy in simulated microgravity was fast to the point that the autophagosomes were very rapidly degraded, preventing any possibility of detecting an increase of LC3 B-II or p62 changes. Therefore, on the basis of previous studies reporting how to study autophagy [Klionsky 2016], we treated the cells with chloroquine, which blocks the binding of autophagosomes to lysosomes by altering the acidic environment of the lysosomes, thus allowing the accumulation of autophagosomes to detect both LC3 B-II and p62 even in the case of very fast autophagic flow. For these experiments chloroquine (40 μM) was added to the culture media 1 h

before ending the experiment in HUVEC cultured for 4 and 10 days in 1G condition (CTR) and in the RWV. Then the cells were lysed and western blot was performed. HUVEC cultured in the RWV significantly increased LC3 B-II and p62 compared to controls (Figure 34 B), suggesting that the decreased amount of mitochondria in simulated microgravity is due to increased autophagy. Moreover, we also analysed the level of the mitophagy BCL2 Interacting Protein 3 (BNIP3), which targets mitochondria to autophagosomes by interacting directly with LC3 [Rikka 2011], and we found higher amount of BNIP3 in HUVEC cultured in the RWV for 4 and 10 days *vs* their controls (Figure 34 B).

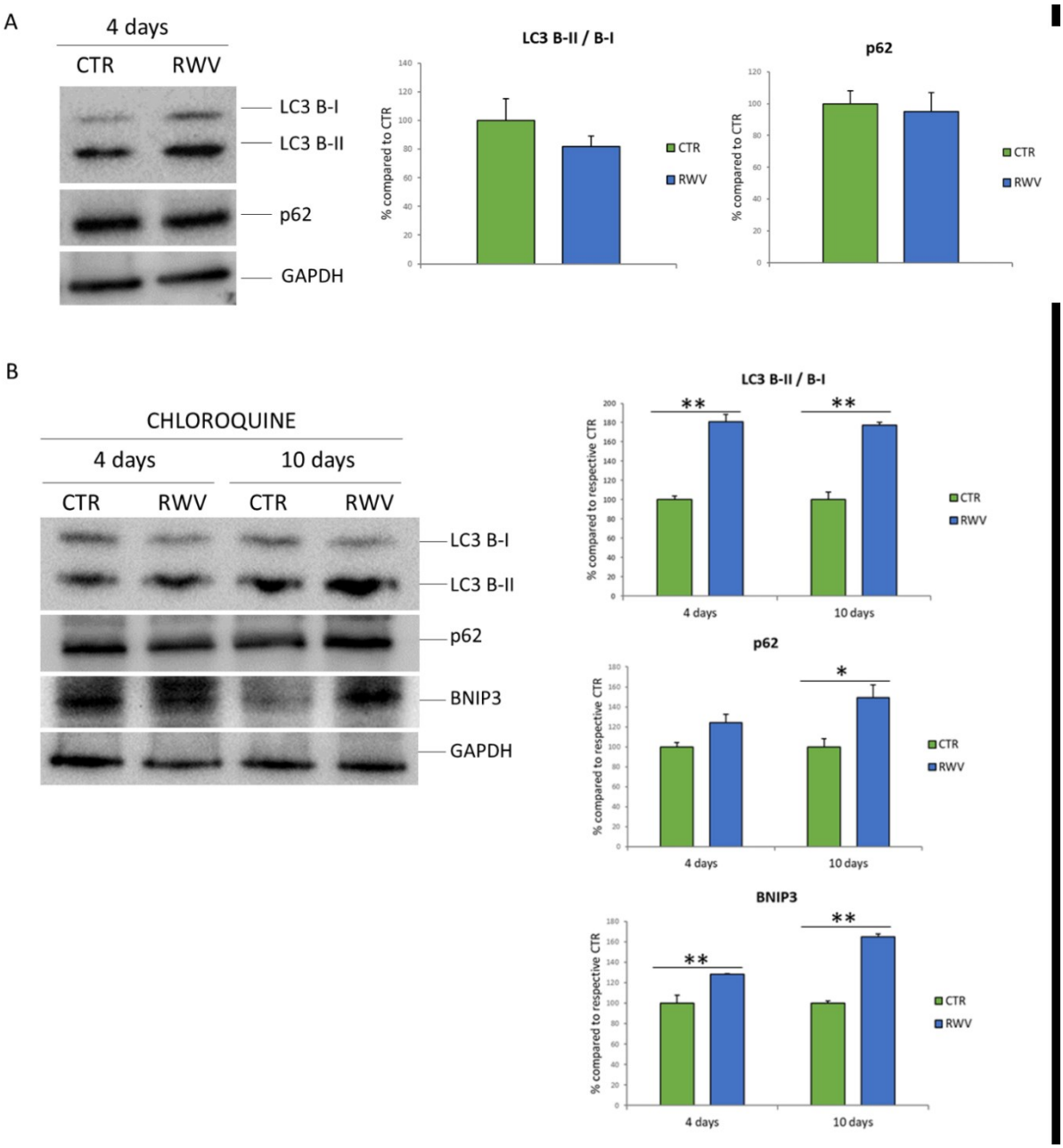


*Figure 34: Autophagic flow in HUVEC in simulated microgravity.*
*Autophagy was monitored in the presence (B) or in the absence (A) of chloroquine for 1 h. On the left representative blots for LC3 B, p62 and BNIP3 are shown; on the right relative quantification obtained by ImageJ.*

## 5.4. THE ROLE OF MITOPHAGY IN MODULATING MITOCHONDRIAL CONTENT IN HUVEC EXPOSED TO SIMULATED MICROGRAVITY

To test whether mitophagy was really responsible for the decrease of mitochondria in simulated microgravity, we used chloroquine to inhibit autophagy/mitophagy [Georgakopoulos 2017]. We performed dose- and time-dependent cell viability experiments, and found that 40 μM was the ideal concentration of chloroquine to inhibit mitophagy without affecting HUVEC survival up to 4 days of treatment (Figure 35 A). HUVEC were cultured with (RWV+CQ) or without (CTR and RWV) chloroquine (40 μM) for 4 days. Then immunofluorescence and western blot were performed. Immunofluorescence for LC3 B (Figure 35 B) demonstrates that treatment with chloroquine for 4 days increases the number of autophagosomes in RWV+CQ compared to both CTR and RWV. Then, the mitochondrial protein CYP D was analysed both by immunofluorescence and western blot (Figure 35 C). HUVEC cultured in the RWV have a lower mitochondrial content than HUVEC grown in 1G and this event is prevented by the addition of chloroquine, which blocks autophagy and restores a mitochondrial content similar to the control. These results demonstrate that autophagy is responsible for the degradation of mitochondria in simulated microgravity.

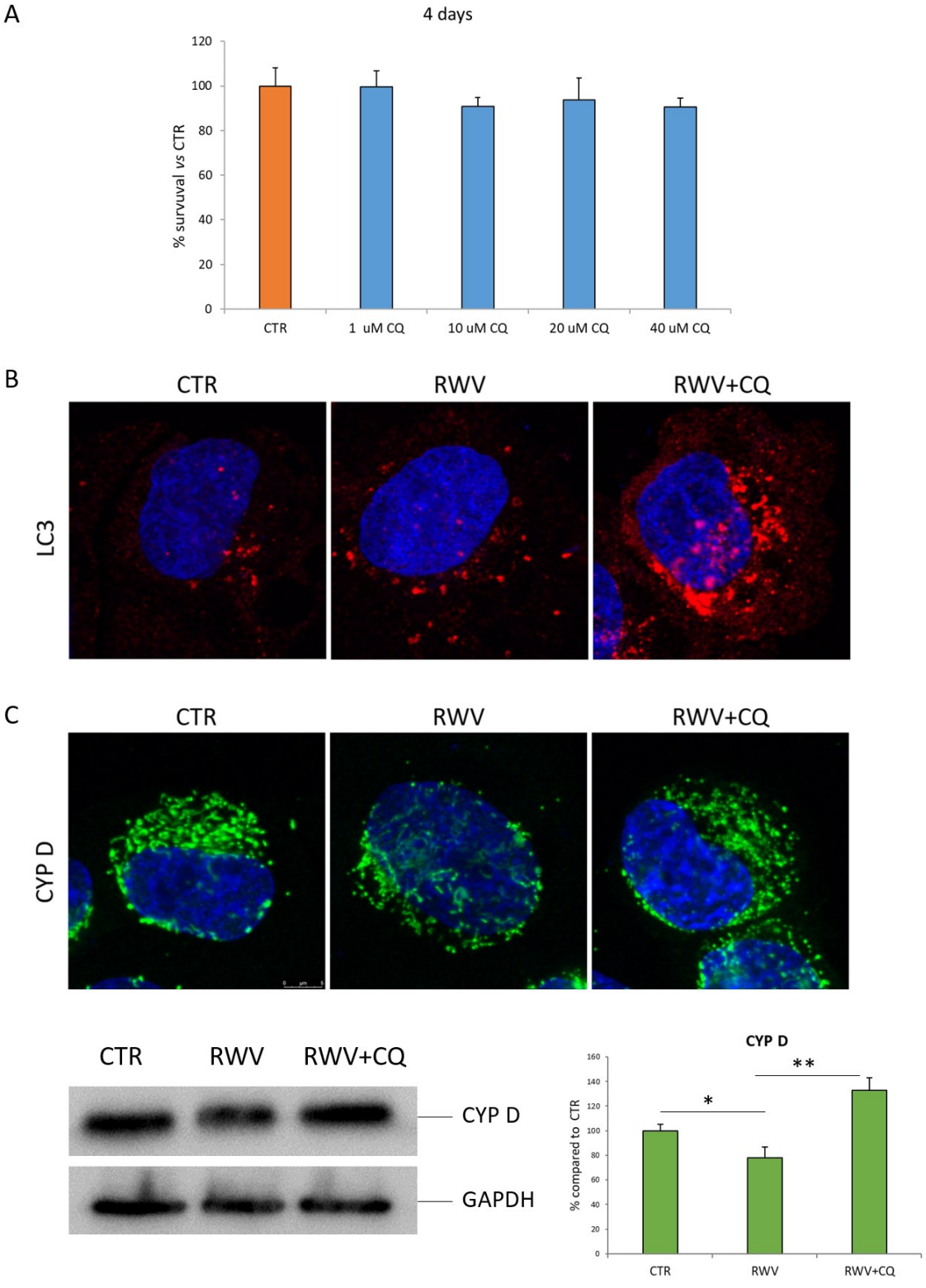


*Figure 35: Mitochondrial content in HUVEC cultured with (RWV+CQ) or without (CTR and RWV) chloroquine (40 μM) for 4 days.*

*(A) Cell survival after 4 days of chloroquine (CQ) treatment was tested. Different concentrations were used and 40 μM of CQ was chosen to perform the experiment.*
*(B) The efficiency of 40 μM chloroquine in inhibiting autophagy was tested by immunofluorescence for LC3 B. Nuclei were stained by DAPI.*
*(C) Mitochondria were visualized utilizing antibodies against CYP D (upper panel) and Western blot was performed on cell lysates (lower panel). Densitometry was performed using Image J and is shown on the right.*

## 5.5. DEGRADATION OF MITOCHONDRIA IN HUVEC IN SIMULATED MICROGRAVITY IS REVERSIBLE UPON RETURN TO 1G CONDITION

To determine whether the mitochondrial degradation of HUVEC exposed to simulated microgravity was reversible upon return to normal 1G conditions, we cultured HUVEC in the RWV for 7 days and then returned them to normal 1G condition for the following 3 days. We then performed immunofluorescence (upper panel) and western blot (lower panel) to visualize mitochondrial content in CTR and RWV HUVEC after 7 and 10 days and in HUVEC cultured for 7 days in the RWV and 3 days in 1G (Figure 36). We show that 3 days in 1G condition are sufficient to increase mitochondrial content compared to respective RWV, becoming more comparable to CTR.

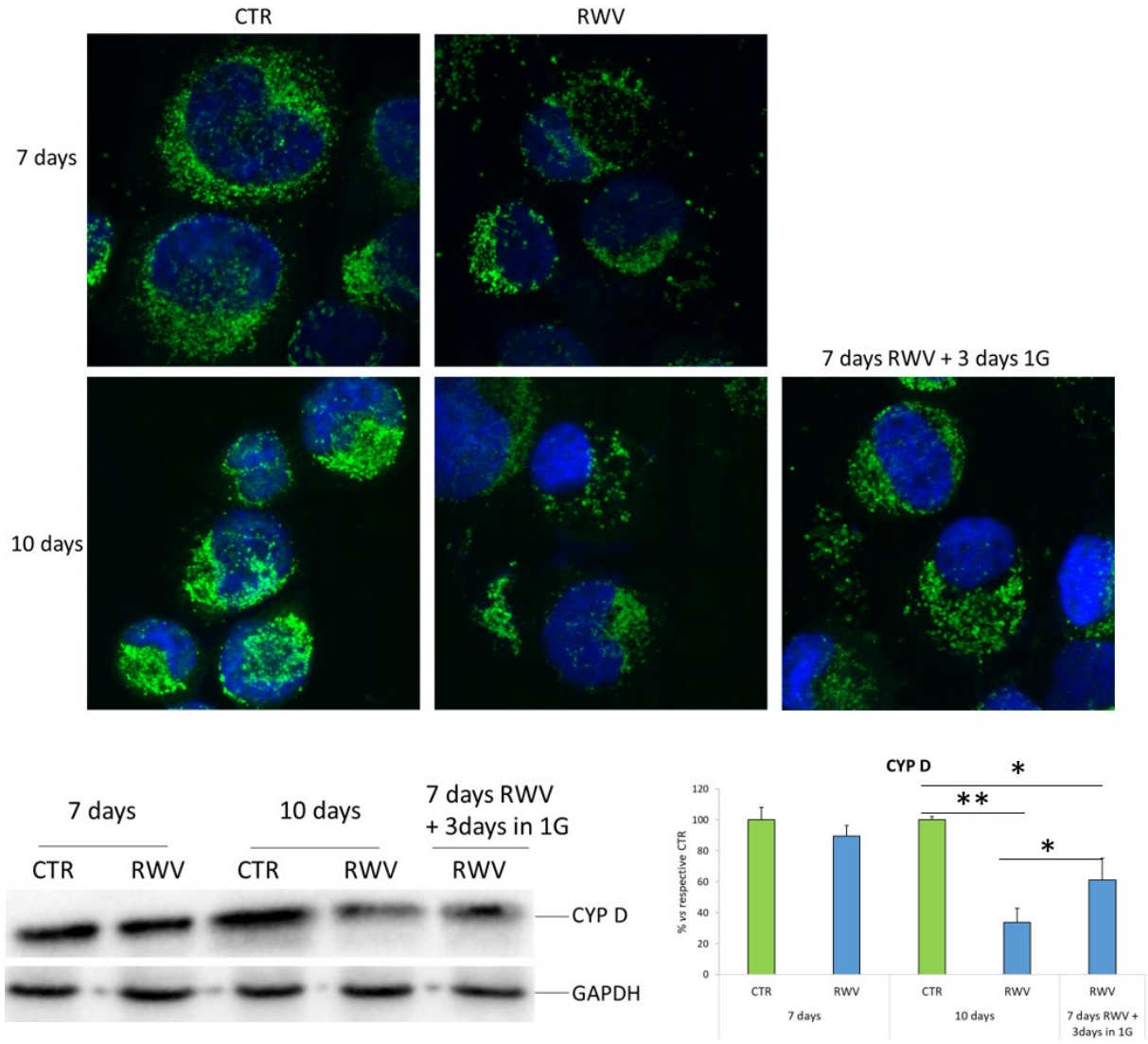


*Figure 36: Mitochondrial content in HUVEC cultured in 1G condition and in the RWV. Mitochondria were visualized utilizing antibodies against CYP D (immunofluorescence, upper panel) and Western blot was performed on cell lysates (lower panel). Densitometry was performed using Image J and is shown on the right.*

## 5.6. THE ROLE OF CYTOSKELETAL DISORGANIZATION IN DRIVING MITOPHAGY AND REDUCING MITOCHONDRIAL CONTENT

Mitochondrial dynamics is strictly linked to cytoskeletal organization, which has a relevant role in maintaining mitochondrial network and function [Moore 2018]. For this reason we asked whether cytoskeletal disorganization, which occurs upon exposure to microgravity [Maier 2015; Carlsson 2003; Versari 2007; Kapitonova 2012], might play a role in driving mitophagy. We used Cytochalasin D, a toxin that binds actin and induces its depolymerization, to mimic cytoskeletal disruption in 1G condition. After performing dose- and time-dependent experiments to test cell viability, we selected 0.5 μM Cytochalasin D as the ideal concentration to use, since it not cytotoxic up to 96 h (Figure 37 A). After treating HUVEC with 0.5 μM Cytochalasin D for 24 h, we performed immunofluorescence and western blot. Using phalloidin, which labels F-actin, we confirmed a massive disorganization of actin fibers associated with modifications of cell shape (Figure 37 B), a scenario that closely recalls the results obtained in microgravity. We then analysed CYP D by immunofluorescence (Figure 37 A) and western blot (Figure 37 C). CYP D is reduced upon cytoskeletal disruption compared to control, indicating a reduced mitochondrial mass. Interestingly, Cytochalasin D upregulates BNIP3 (Figure 37 C), thus suggesting that cytoskeletal disruption leads to increased mitophagy which results in a decreased content of mitochondria.

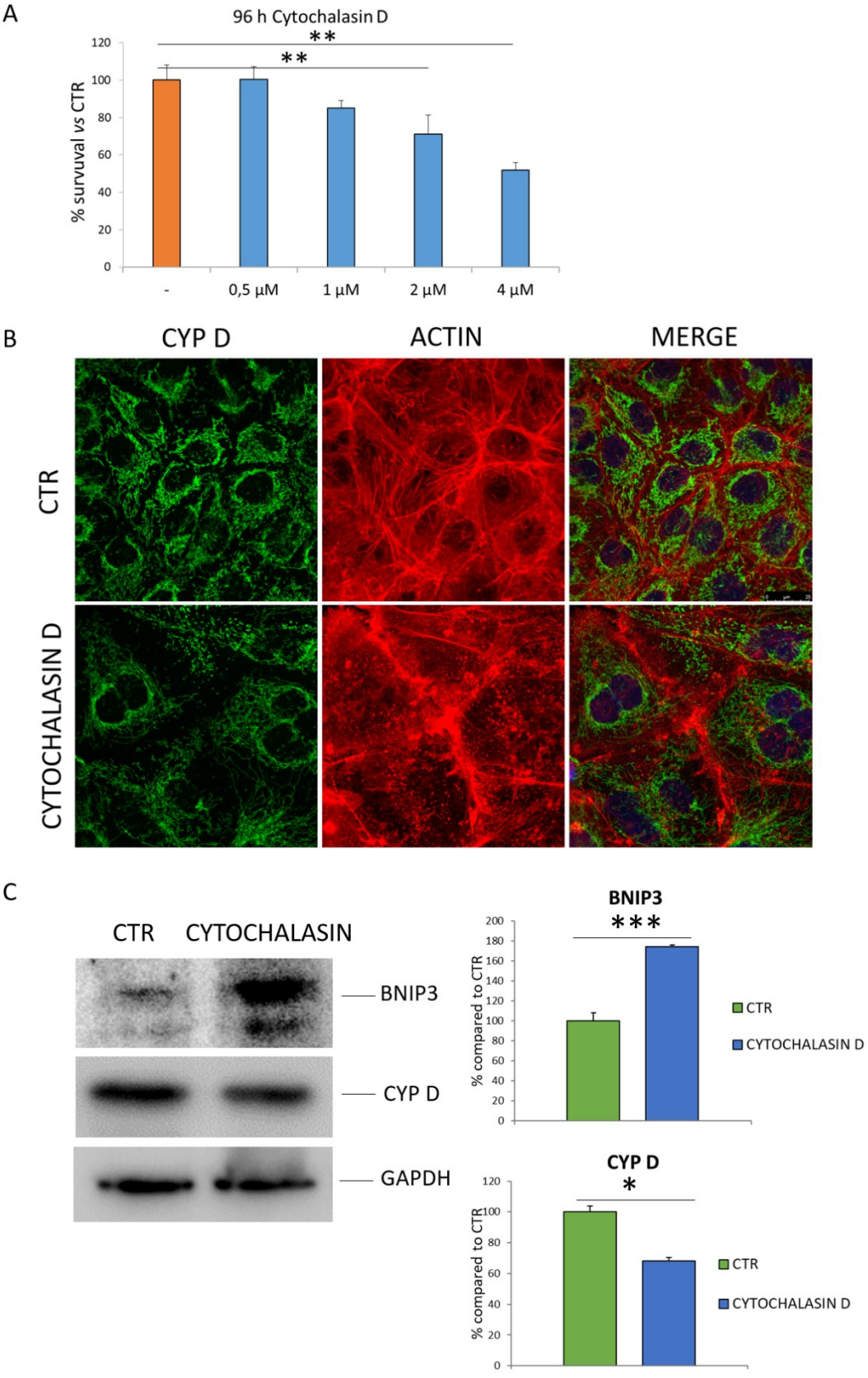
A
96 h Cytochalasin D
**
**
% survuval vs CTR
120
100
80
60
40
20
0
-
0,5 µM
1 µM
2 µM
4 µM
B
CYP D
ACTIN
MERGE
CTR
CYTOCHALASIN D
C
CTR
CYTOCHALASIN
BNIP3
CYP D
GAPDH
BNIP3
***
% compared to CTR
200
180
160
140
120
100
80
60
40
20
0
CTR
CYTOCHALASIN D
CYP D
*
% compared to CTR
120
100
80
60
40
20
0
CTR
CYTOCHALASIN D

*Figure 37: Mitochondrial content and mitophagy in HUVEC exposed to Cytochalasin D. HUVEC were treated or not with Cytochalasin D for 24 h.*
*(A) Cytotoxicity of different concentration of Cytochalasin D were tested on HUVEC for 96h. (B) Cells were stained to detect CYP D (left) and actin (middle). The merge is shown in the right panels.*
*(C) BNIP3 and CYP D were analysed by western blot. GAPDH was used as a control of loading. The experiments were repeated at least three times. Representative blots and relative quantification obtained by ImageJ are shown.*

**These data are accepted for the publication in FASEB J. The FASEB Journal. 2019;00:1–13. https ://doi.org/10.1096/fj.20190 1785RRR**

**The original draft is attached. (Appendix B)**

# 6. RESULTS (3): THE ROLE OF CYTOSKELETON IN MEDIATING MICROGRAVITY EFFECTS ON HUVEC

# 6.1. CYTOSKELETAL REMODELING IN 1G CONDITION

Disorganization of the cytoskeleton is one of the earliest events induced by a stress. Cytoskeletal disorganization in simulated microgravity is an event which occurs early and evolves rapidly after culture in the RWV. Indeed, we have previously shown that in HUVEC in the RWV, actin fibers' disorganization begins after 4 h and clusters of actin become evident in perinuclear position within 24 h. After 144 h in the RWV, these clusters disappear and stress fibers are markedly decreased [Carlsson 2003]. Intriguingly, the cytoskeleton has been proposed as a sensor of changes of gravity [Vorselen 2014] and for this reason we asked whether cytoskeletal disruption could orchestrate endothelial response to microgravity.

As previously described, we used Cytochalasin D to induce actin depolymerization and cytoskeletal remodeling in 1G condition. We treated HUVEC with different doses of Cytochalasin D for different times and, after staining with phalloidin-TRIC, we visualized actin disorganization by confocal microscopy (Figure 38 A).

On the basis of a dose dependent experiment (Figure 38 B), we utilized 0.5 μM Cytochalasin D as the ideal concentration to mimic in 1G condition the cytoskeletal remodeling happening in microgravity. Thereafter we compared HUVEC treated with 0.5 μM Cytochalasin D for 24 and 96h with HUVEC cultured in the RWV for 4 and 10 days and tested the effect of actin dysregulation on stress response, mitochondrial content and magnesium homeostasis.

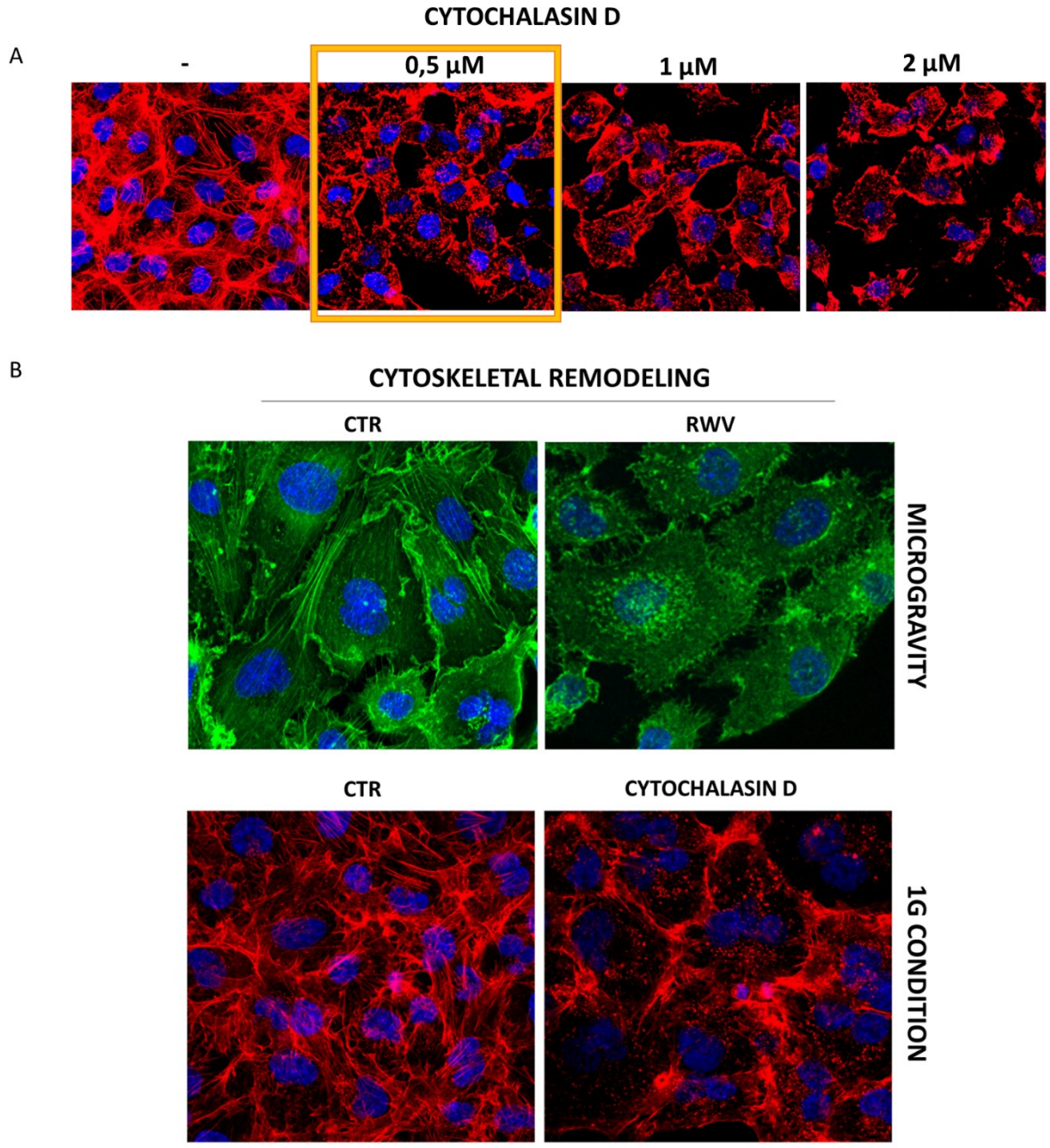


*Figure 38: Cytoskeletal remodeling in presence of mechanical (microgravity) or biochemical (Cytochalasin D) signals.*

*Different doses of Cytochalasin D were tested on HUVEC and staining for actin was performed (A). In B comparison of cytoskeletal remodeling obtained with simulated microgravity or Cytochalasin D.*

## 6.2. THE EFFECT OF CYTOSKELETAL REMODELING ON STRESS RESPONSE

Cytoskeleton is continually remodeled to respond to different signals. As a consequence, several cytoskeleton-interacting proteins are involved in stabilizing the system, among which molecular chaperons are counted as one of the most important proteins that interact closely with the cytoskeleton network [Quintà 2011]. In particular, chaperone proteins help the assembly/disassembly of cytoskeletal proteins and are key factors for many structural and functional rearrangements of actin during different physiological processes.

HSP70 is thought to participate in *de novo* folding pathways of cytoskeletal proteins [Quintá 2011]. HSP27 is known to stabilize actin microfilaments [Sun 2015]. Even TXNIP was proposed to be a biomechanical regulator of Src activity, thus able to affect and be affected by cytoskeleton [Spindel 2012].

As previously shown our data suggest that microgravity induces the sequential involvement of various anti-oxidant proteins that end up in counterbalancing the increase of pro-oxidant TXNIP. For this reason, we selected HSP70, HSP27 and TXNIP, proteins that are linked to stress pathway as well as to cytoskeletal organization, to be analysed after exposure to Cytochalasin D, to highlight if their modulation in HUVEC cultured in the RWV was due to microgravity-induced cytoskeletal remodeling.

We cultured HUVEC for 24 and 96 h in control condition (CTR) or in presence of 0.5 μM Cytochalasin D (CYTOCHALASIN D) and then we performed western blot on cell lysates (Figure 39).

We found that cytoskeletal disruption by Cytochalasin D was associated with the upregulation of TXNIP, mostly after 96 h, which corresponds to 10 days exposure to microgravity. HSP70 was increased by Cytochalasin D within 24 h and then returned to

basal level (96 h), consistently with HSP70 expression in HUVEC exposed to simulated microgravity (RWV). After 4 days of simulated microgravity, we observe a mild increase of HSP27, which culminates at day 10. A similar result was obtained in cells treated with Cytochalasin D. We hypothesize that, in face of a decrease of HSP70, HSP27 is increased in an attempt to maintain the stability of the remaining actin fibers.

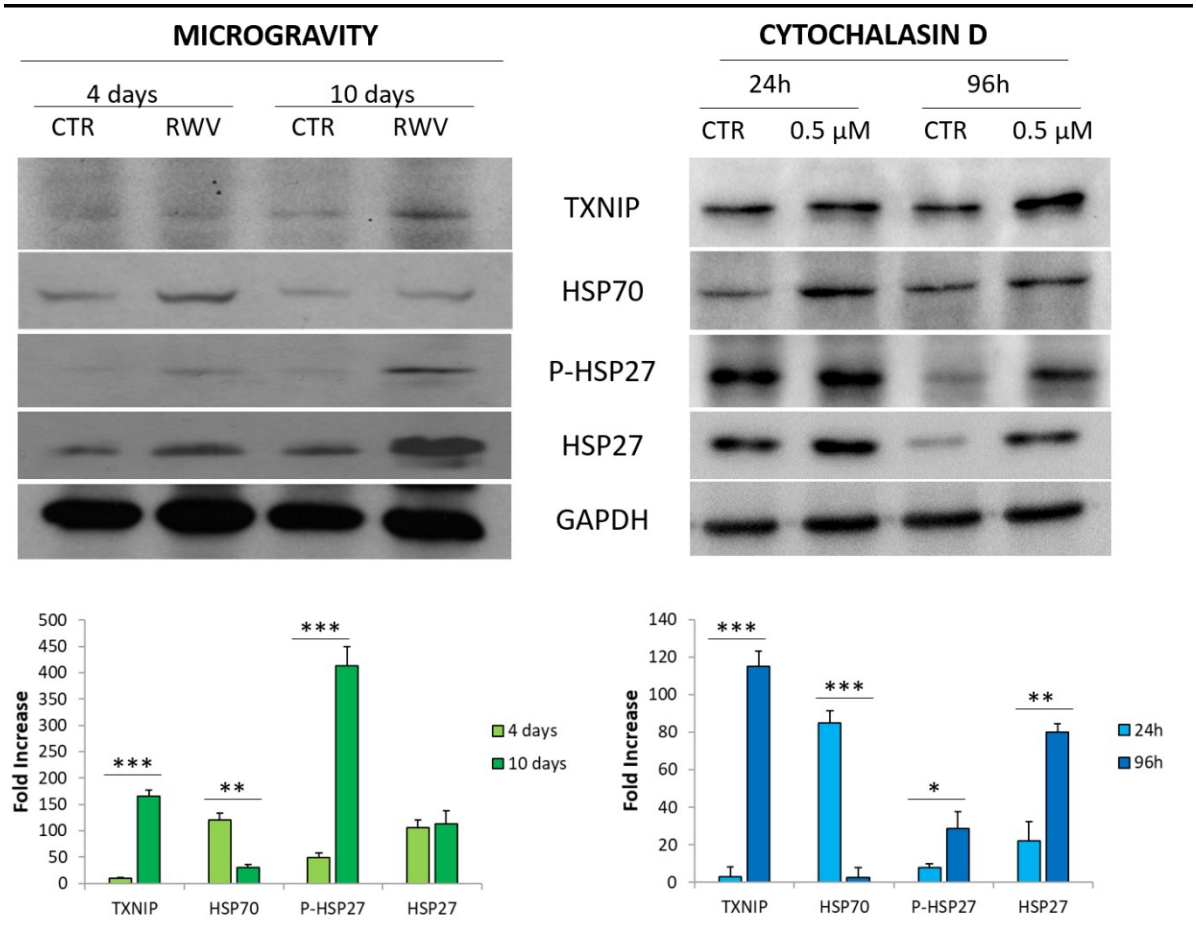


*Figure 39: The effect of cytoskeletal disruption on the amounts of stress proteins.*
*Using Cytochalasin D to destabilize actin fibers is possible to achieve many of the modulation in stress protein observed in simulated microgravity. Western blot was performed on HUVEC cultured in 1G condition or in simulated microgravity (RWV) (left panels) or in the presence or not of 0.5 µM Cytochalasin D (right panels). Antibodies against TXNIP, HSP70, HSP27 and P-HSP27 were used. Under the blots relative quantifications are shown.*

## 6.3. THE EFFECT OF CYTOSKELETAL REMODELING ON MITOCHONDRIA

Not only the cytoskeleton has been proposed as a gravity-sensor [Vorselen 2014] but cytoskeletal dynamics have also an important role in autophagy [Kast 2017]. The cytoskeleton interacts with the mitochondria [Moore 2018], and mitophagy is regulated by cytoskeletal components [Strzyz 2018]. We tested whether a link might exist between autophagy, mitochondrial content and cytoskeletal remodeling in our experimental model.

As previously shown (Figure 37) HUVEC treated with 0.5 μM Cytochalasin D for 24 h display a decrease in CYP D protein level paralleled by an increase of BNIP3 (Figure 37 B), suggesting that cytoskeletal disruption activates mitophagy thus reducing mitochondrial content. We then analysed the effect of 96h treatment with Cytochalasin D and performed western bot (Figure 40 A) and immunofluorescence (Figure 40 B) using antibodies against CYP D. We found that CYP D decreased upon Cytochalasin D treatment for 24 and 96 h, recapitulating what happens to HUVEC exposed to simulated microgravity.

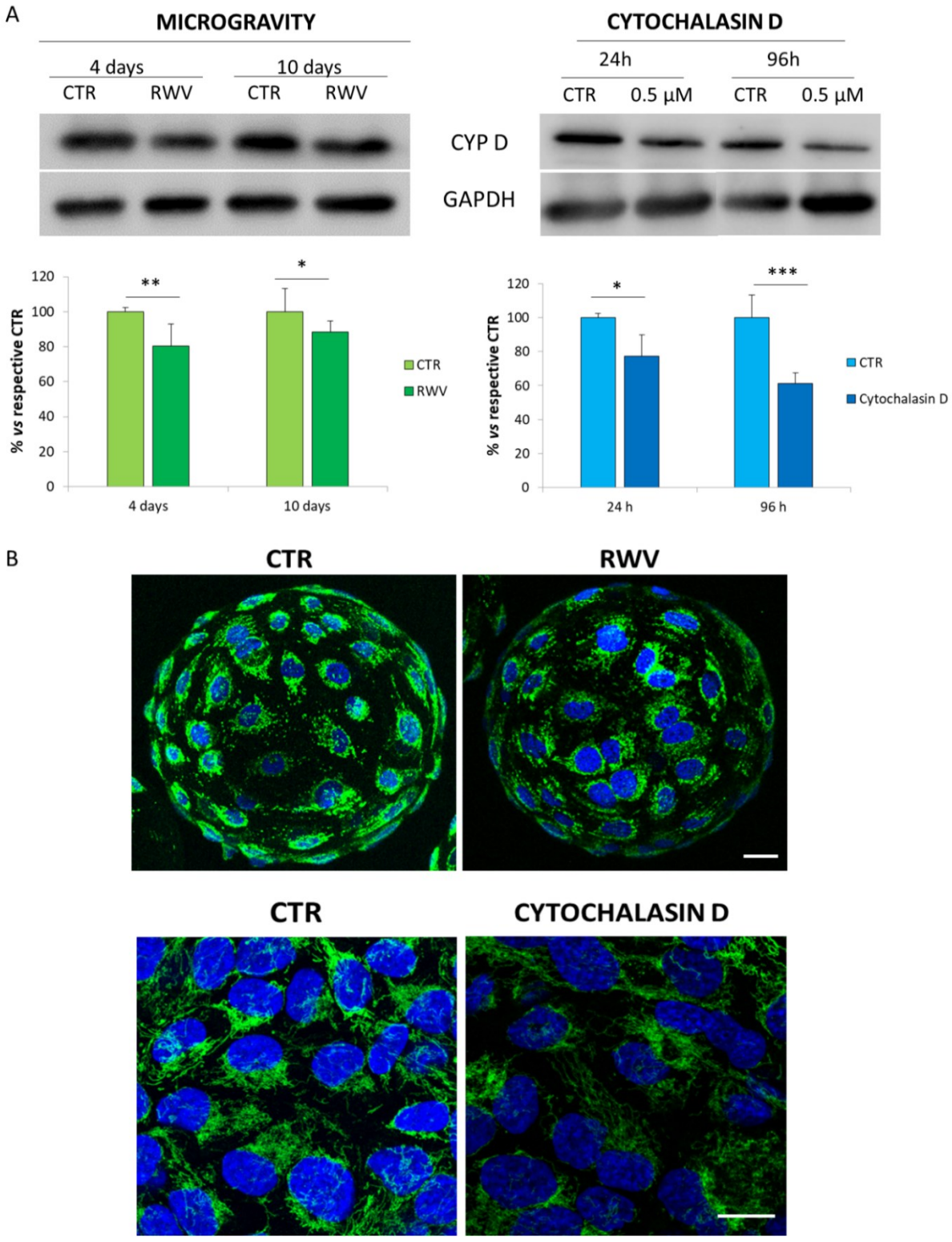


*Figure 40: The effect of cytoskeletal disruption on mitochondria.*
*Western blot (A) and immunofluorescence (B) were performed on HUVEC exposed to simulated*

*microgravity or Cytochalasin D. In B images were acquired using 63X objective in a SP8 Leica confocal microscope with different magnification. Scale bar = 30 μm.*

## 6.4. THE EFFECT OF CYTOSKELETAL REMODELING ON MAGNESIUM HOMEOSTASIS

Magnesium (Mg) is the most abundant intracellular bivalent cation and is involved in a wide of variety of biochemical reactions. In particular, Mg plays a major role in regulating endothelial functions [Maier 2012]. This is why Mg homeostasis in cells is tightly regulated. Different studies have shown that an altered homeostasis of Mg is a risk factor for endothelial dysfunction and cardiovascular diseases [Romani 2013]. For this reason, we decided to study if microgravity could affect Mg homeostasis, with a specific focus on the amounts and function of the Mg transporter MagT1 and of the Transient Receptor Potential Melastatin 7 (TRPM7) channel, the two most important Mg transporters expressed in endothelial cells. TRPM7 possesses the functional duality of being an ion channel and a kinase and is responsible for the transport of different divalent cations [Nadler 2001; Runnels 2001; Schmitz 2014], while MagT1 is a highly selective transporter for Mg [Goytain 2005].

By western blot, we observed that after 4 and 10 days of culture in simulated microgravity, HUVEC downregulate TRPM7 protein and upregulate MagT1, suggesting a compensatory mechanism to maintain the intracellular homeostasis of Mg (Figure 41 A, left panel).

Determinations of total and free $Mg^{2+}$ concentrations consistently indicate that the majority of $Mg^{2+}$ is located within mitochondria, nucleus, and endo-(sarco)-plasmic reticulum [Romani 2011]. Mitochondria are one of the major intracellular $Mg^{2+}$ store; furthermore, their function, content and spatial organization within the cell is tightly

regulated by $Mg^{2+}$ availability [Pilchova 2017]. Many of the cellular energy production processes are composed by many $Mg^{2+}$ - dependent enzymatic reactions and ATP is active only when linked to $Mg^{2+}$ [Gout 2014].

We also studied the effect of microgravity on the Mg Transporter MRS2 (MRS2), a protein located in the mitochondria and mediates the influx of Mg into the mitochondrial matrix [Piskacek 2009]. It is also required for normal expression of the mitochondrial respiratory complex I subunits and thus it is fundamental for physiological functions of the cell. We found that MRS2 levels decrease when HUVEC are cultured in simulated microgravity for 4 and 10 days, and this could be explained with the decreased mitochondrial content found in HUVEC grown in RWV. Indeed, normalizing MRS2 for CYP D content, no differences were detectable between CTR and RWV samples (Figure 41 B, C).

We evaluated the total amount of intracellular Mg using the fluorescent chemosensor DCHQ5 to unravel if the modulation on aforementioned Mg transporters impact on Mg homeostasis. We found a decrease of total intracellular Mg in HUVEC grown for 4 and 10 days in microgravity compared to 1G HUVEC (Figure 41 D). This result could have different explanations:

- MagT1 increase in simulated microgravity is not sufficient to compensate TRPM7 decrease;
- Intracellular Mg in proliferating cells is usually higher than quiescent cells, and it is copiously reported that HUVEC in RWV grow faster than relative CTR [Carlsson 2003, Maier 2014];
- The decrease of mitochondrial mass upon gravitational unloading means a decrease in one of the major store of Mg within the cells.

We then evaluated the same parameters also in presence of Cytochalasin D, in order to disclose a possible role of cytoskeleton in affecting Mg homeostasis. We found that after 24 and 96 h of treatment HUVEC downregulate TRPM7 and MRS2 and upregulate

MagT1, as evaluated using western blot, with a consequent reduction of total intracellular magnesium concentration compared to respective controls (Figure 41, right panels). Again, treatment with Cytochalasin D phenocopies the effects of culture in the RWV.

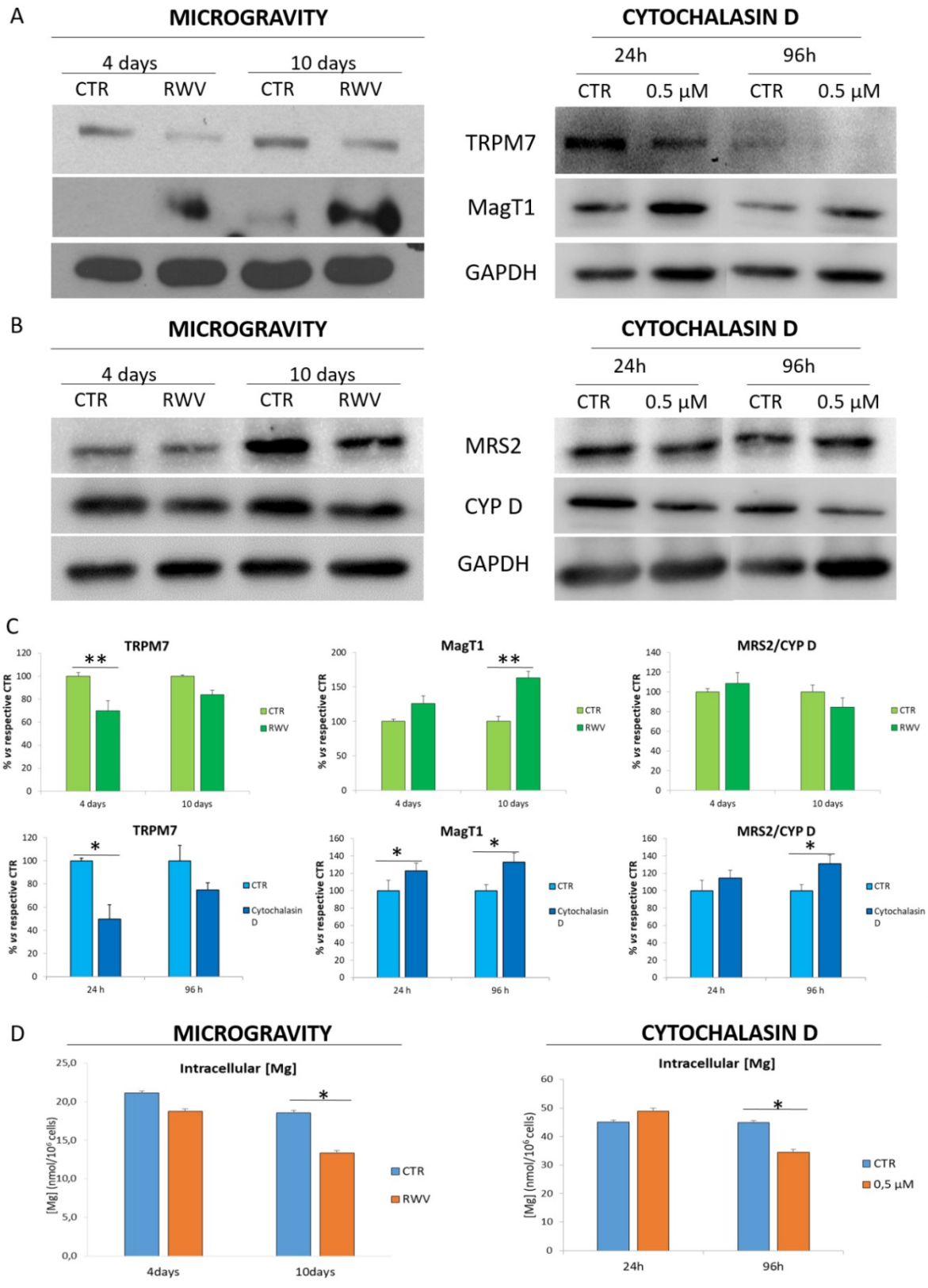
A
MICROGRAVITY
4 days
10 days
CTR
RWV
CTR
RWV
CYTOCHALASIN D
24h
96h
CTR
0.5 µM
CTR
0.5 µM
TRPM7
MagT1
GAPDH
B
MICROGRAVITY
4 days
10 days
CTR
RWV
CTR
RWV
CYTOCHALASIN D
24h
96h
CTR
0.5 µM
CTR
0.5 µM
MRS2
CYP D
GAPDH
C
TRPM7
MagT1
MRS2/CYP D
% vs respective CTR
4 days
10 days
CTR
RWV
TRPM7
MagT1
MRS2/CYP D
% vs respective CTR
24 h
96 h
CTR
Cytochalasin D
D
MICROGRAVITY
Intracellular [Mg]
[Mg] (nmol/10⁶ cells)
4days
10days
CTR
RWV
CYTOCHALASIN D
Intracellular [Mg]
[Mg] (nmol/10⁶ cells)
24h
96h
CTR
0,5 µM

*Figure 41: The effect of cytoskeletal disruption on Mg homeostasis.*
*(A-B) The levels of the Mg transporters TRPM7, MagT1 and MRS2 were analysed by western blot in HUVEC exposed to simulated microgravity or to Cytochalasin D. In B western blot for CYP D was used as internal reference to evaluate MRS2 in relation of mitochondrial content. In C blots relative quantification were shown. In D the fluorescent chemosensor DCHQ5 was used to measure total intracellular Mg.*

# 7. RESULTS (4): MICROGRAVITY AND MICROVASCULAR ENDOTHELIAL CELLS

# 7.1. THE EFFECT OF MICROGRAVITY AND CYTOSKELETAL DISRUPTION ON HUMAN MICROVASCULAR ENDOTHELIAL CELLS (HMEC)

The endothelium is very heterogeneous. Morphological and functional differences as well as different responses to growth factors have been observed in endothelial cells derived from micro and macro circulation [Ribatti 2002].

It is noteworthy that the microvasculature represents the majority of the total endothelial surface [Danese 2007]. It is a crucial player in inflammation [Danese 2007] and angiogenesis [Carmeliet 2005]. An impairment of microvasculature functions is supposed to occur in microgravity, since angiogenesis, wound healing, impairment of cell growth and inflammation are reported [Davidson 1999; Kirchen 1995; Unsworth 1998; Cotrupi 2005].

On these bases, we analysed the response of Human Dermal Microvascular Endothelial Cell (HMEC) to simulated microgravity. We performed the same experiments conducted on HUVEC, i.e. simulation of microgravity using the RWV for 4 and 10 days, analysis of stress response, mitochondrial content, magnesium homeostasis and the role of the cytoskeleton in orchestrating HMEC response in microgravity.

We started analysing the red-ox status. We found that HMEC grown in simulated microgravity (RWV) for 10 days produce more ROS than controls (Figure 42 A). This result could explain, in part, the growth-retardation of microvascular EC exposed to simulated microgravity reported in literature.

Subsequently, we analysed stress response at the protein level, performing western blot on the same proteins modulated after the exposure of HUVEC to microgravity, i.e.

HSP70, TXNIP, SIRT2, PON2, SOD2, P-HSP27 and HSP27. Apart from SOD2, the other proteins resulted upregulated also in HMEC grown in RWV for 4 and 10 days compared to 1G control. In addition, if compared to HUVEC, HMEC response seems accelerated, since the majority of these proteins were increased at 4 days and remained elevated at 10 days (Figure 42 B).

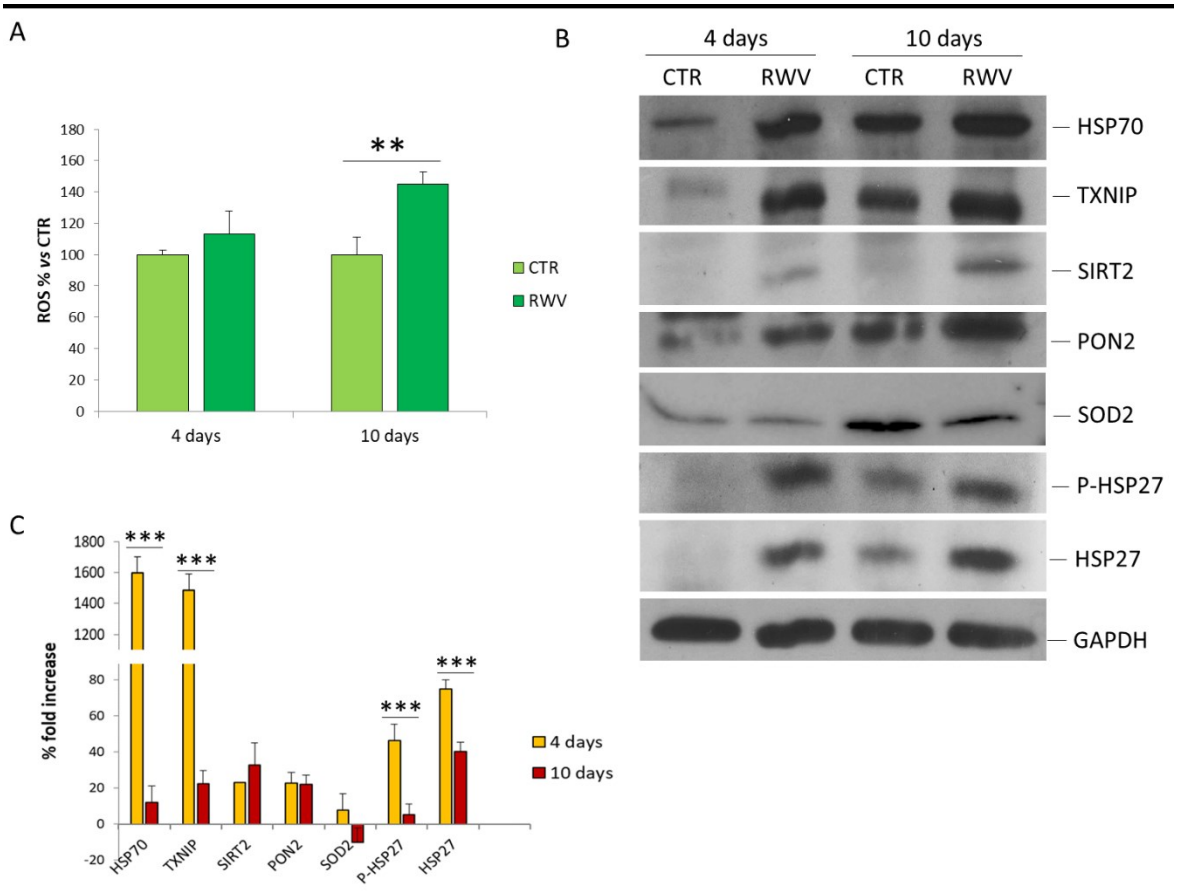


*Figure 42: ROS production and stress proteins in HMEC.*
*HMEC grown in 1G condition (CTR) or in simulated microgravity (RWV) for 4 and 10 days were analysed for ROS production using DCFDA (A) and for the total amounts of proteins linked to stress response by western blot (B). In C quantification of western blots showed in B and C obtained using ImageJ software.*

We then selected stress proteins known to be linked to cytoskeletal regulation and performed western blot on cell extracts from HMEC treated or not with Cytochalasin D, in order to define the potential role of cytoskeletal remodeling in modulating HMEC response. HMEC were tested for dose- and time-dependent response to Cytochalasin D and 10 nM was found as the higher dose not cytotoxic up to 72 h using MTT assay (Figure 43 A). Cytochalasin D treatment seemed to recapitulate the majority of the stress response observed in HMEC grown in microgravity, since Cytochalasin D increased the pro-oxidant protein TXNIP mostly at 24h (in microgravity TXNIP increased at 4 days and then remained elevated) and also the stress proteins HSP70 and HSP27 (Figure 43 B).

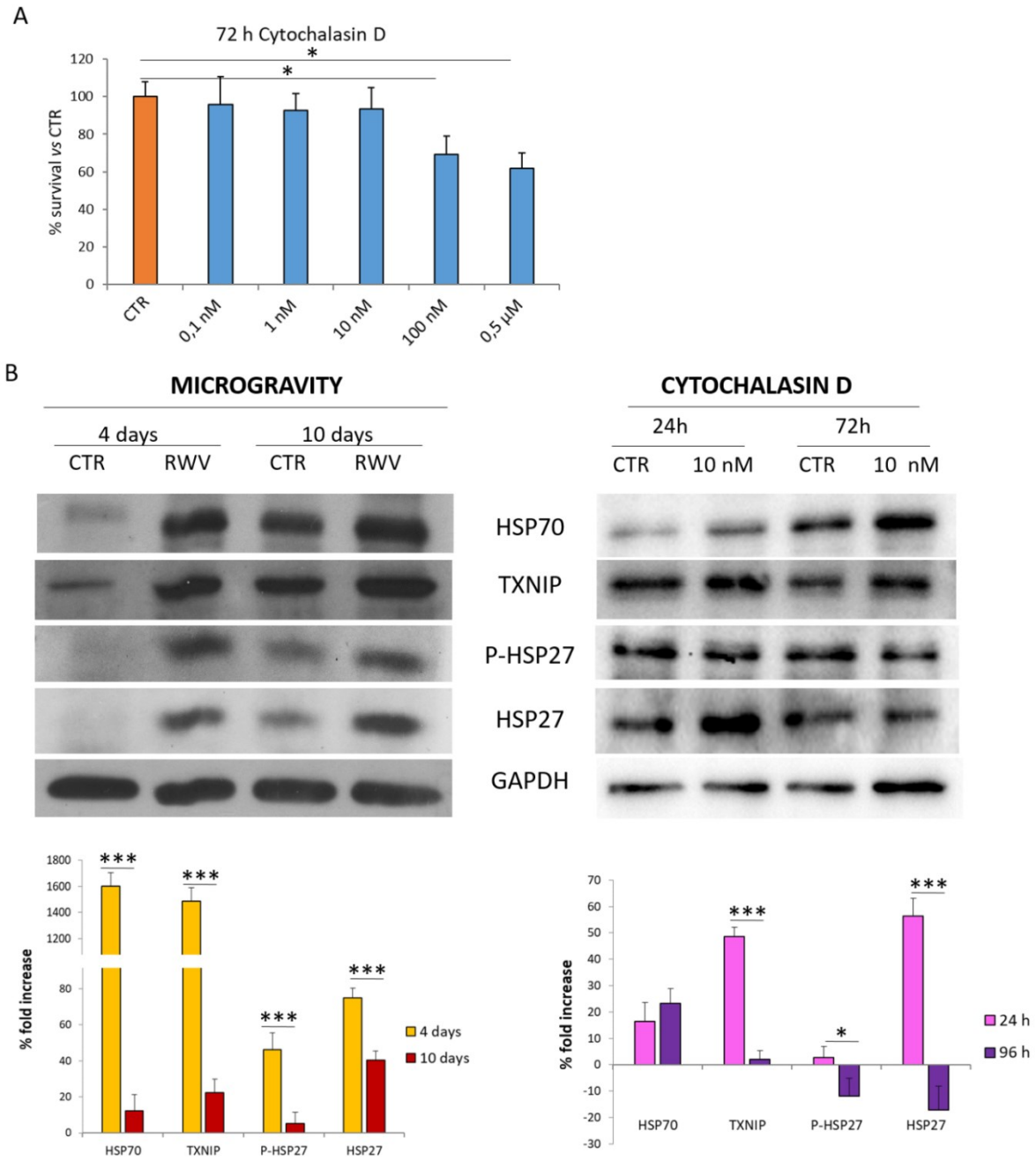


*Figure 43: The effect of cytoskeletal disruption on stress response of HMEC.*
*Cytotoxicity of Cytochalasin D was tested on HMEC for 72 h (A) Western blot (B) was performed on HMEC cultured in 1G condition on in simulated microgravity (RWV) on the left or in presence or not of 10 nM Cytochalasin D (on the right). Antibodies against TXNIP, HSP70, HSP27 and P-HSP27 were used. Densitometric analysis was performed and quantification are reported (lower panel).*

We also studied Mg homeostasis and mitochondrial content in HMEC grown in simulated microgravity or in presence of Cytochalasin D. Figure 44 A shows that HMEC after 4 days in the RWV upregulate TRPM7 that remains elevated also at day 10 if compared to controls. MagT1 was increased both at 4 and 10 days in the RWV. Similarly to HUVEC, we found less mitochondria in HMEC cultured in the RWV for 4 and 10 days vs their controls as detected by immunofluorescence using antibodies against CYP D (Figure 44 C, left panel). Western blot for CYP D confirmed this result (Figure 44 A, left panel).

In addition, we found that disorganizing the cytoskeleton by culturing the cells in the presence of Cytochalasin D mimics what happens under simulated microgravity. Indeed, HMEC upregulate TRPM7 and MagT1 both at 24 and 72 hours of treatment compared to controls. More studies are ongoing to define Mg homeostasis in Cytochalasin D-treated HMEC. Moreover, Cytochalasin D decreases mitochondrial content. By immunofluorescence this event is visualized after 24 h and, more evident, after 72 h. By western blot, we detected a modest decrease of CYP D after 24 h exposure to Cytochalasin D while at 72h the difference is more pronounced.

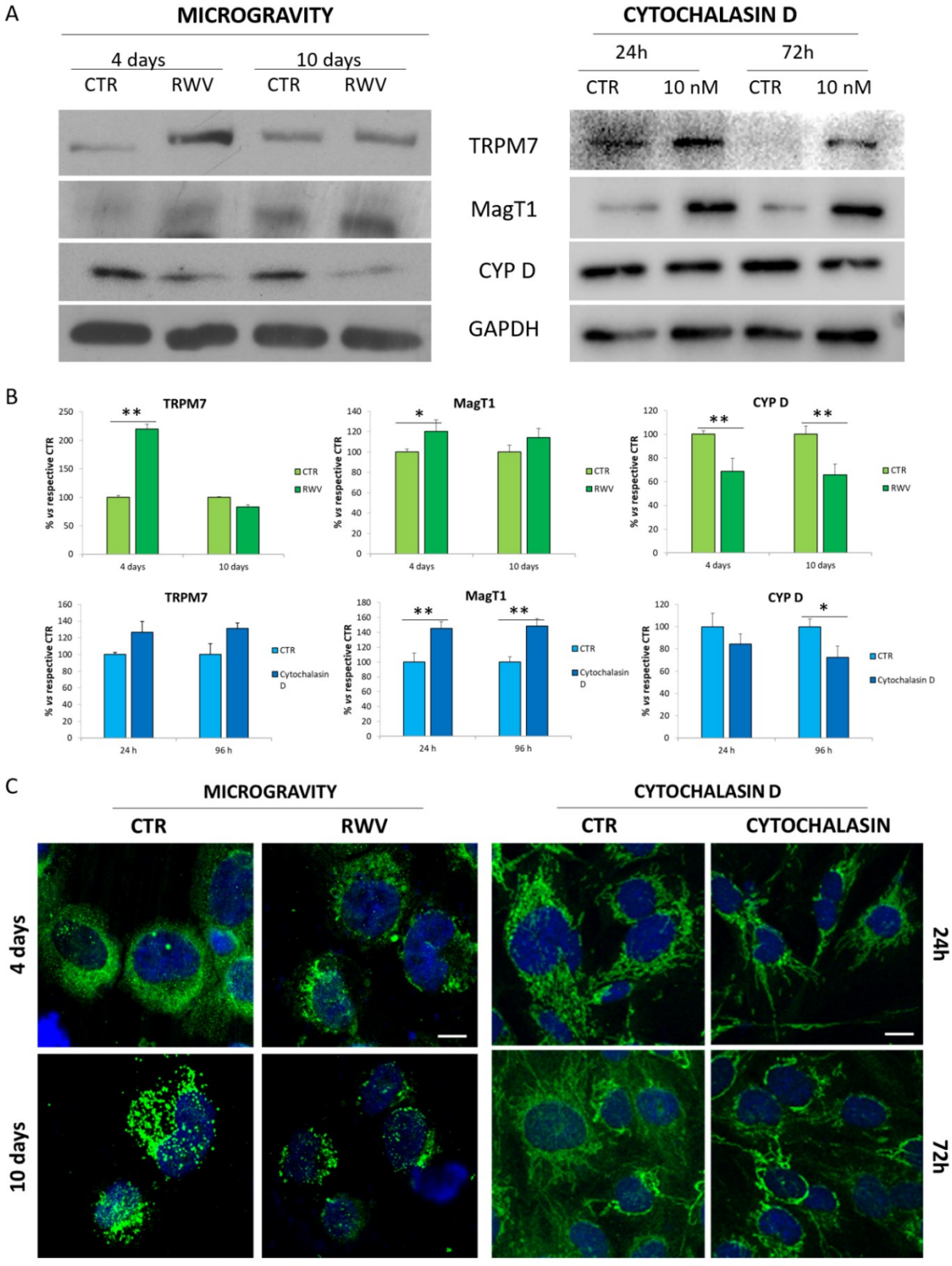
A
MICROGRAVITY
4 days
10 days
CTR
RWV
CTR
RWV
CYTOCHALASIN D
24h
72h
CTR
10 nM
CTR
10 nM
TRPM7
MagT1
CYP D
GAPDH
B
TRPM7
MagT1
CYP D
% vs respective CTR
CTR
RWV
4 days
10 days
Cytochalasin D
24 h
96 h
C
MICROGRAVITY
CYTOCHALASIN D
CTR
RWV
CTR
CYTOCHALASIN
4 days
10 days
24h
72h

*Figure 44: The effect of cytoskeletal disruption on magnesium homeostasis and mitochondrial content of HMEC.*
*(A) The levels of the magnesium transporters TRPM7, MagT1 were analysed using western blot in HMEC exposed to simulated microgravity or to Cytochalasin D. CYP D was used as marker to analyze mitochondrial content. In B quantifications of western blots obtained using ImageJ. In C the immunofluorescence for CYP D was performed to visualize mitochondria network. Scale bar = 30 μm.*

# RESULTS (5):

# MOVING

# FROM

# 2D TO 3D

## 7.2. WHY WORKING IN 3D?

Different aspects of cell behavior, such as proliferation rate, specific functions, metabolism, drugs sensitivity and differentiation, are strongly dependent on the effect of the microenvironment [Jeanes 2011]. For what regards endothelial cells a more physiological condition is represented by 3D organization in vessels and the presence of a steady flow. Mechanical forces, including fluid flow, strongly influence ECs [Davies 1995]. Indeed, ECs are constantly subjected to mechanical stimuli, including shear force, generated by blood and tangential to the endothelial surface [Song 2011], and circumferential stretch generated by blood pressure. These mechanical forces induce ECs to modulate their functions, secreting biomolecular signals [Resnick 2003], remodeling vascular structure [Carmeliet 2000, Tzima 2005; DuFort 2011; Blackman 2002] and modulating transcription [Adams 2007]. ECs are also sensitive to biochemical stimuli, coming from the extracellular matrix (ECM) or other cells that interact with them [Chatterjee 2018].

During the past decades, scientists started to face the limitation of two dimensional (2D) cells culture and began to approach three dimensional (3D) systems, more physiological method of cell culture. These 3D systems may be used for many applications, starting from basic research to clinic, screening of new drugs, development of new systems for regenerative medicine and so on [Rimann 2012].

It is imperative to continue to disclose the mechanisms underlying ECs response to different stimuli, using systems that are as similar as possible to the physiological conditions, in order to have a better overview of EC behavior in normal, but also in pathological condition.

## 7.3. WHAT TO STUDY IN 3D?

Many studies try to elucidate the mechanisms underlying endothelial dysfunction and related diseases using different approaches, starting from the type and method of cell culture [Hansen 2013; Shen 2008; Kim 2012; Colace 2011]. The idea of using 3D system in microgravity experiments is at the moment remote, because of technical constraints that prevent the application of 3D culture system of endothelium in real and simulated microgravity (microfluidic devices where endothelial cells are cultured are not sealed and liquid leakage and air bubbles formation are problems that should still be solved).

For this reason, with the aim of working in the future with these systems in microgravity, we decided to optimized the culture model and expose the cells to a biochemical challenge known to induce endothelial dysfunction, i.e. high extracellular glucose.

We tested the effect of high concentration of glucose on both micro- and macro- vascular ECs culture in 2D classic condition and in 3D microfluidic device that resemble the physiological spatial organization of ECs in ramification of vessels of different calibers and apply shear stress generated by fluid flow.

We focus our attention on the cytoskeleton, one of the first and key mediator of both mechanical and biochemical signals arising from endothelial microenvironment [Ingber 2006].

## 7.4. THE EFFECT OF GLUCOSE ON THE ACTIN CYTOSKELETON IN HUVEC TREATED FOR 24H

We decided to investigate the effect of high glucose on actin cytoskeleton. To achieve this goal we seeded HUVEC in 2D static petri dish and we treated them for 24 h with normal

medium (CTR) or with normal medium supplemented with 5.4 mg/mL D-glucose (High Glucose). We then analysed the effect of this treatment on actin expression and organization (Figure 45). We found that D-glucose has no significative effect in 2D on both total actin content (upper panel), as detected by western blot, and its organization in fibers (lower panel), evaluated using confocal microscopy.

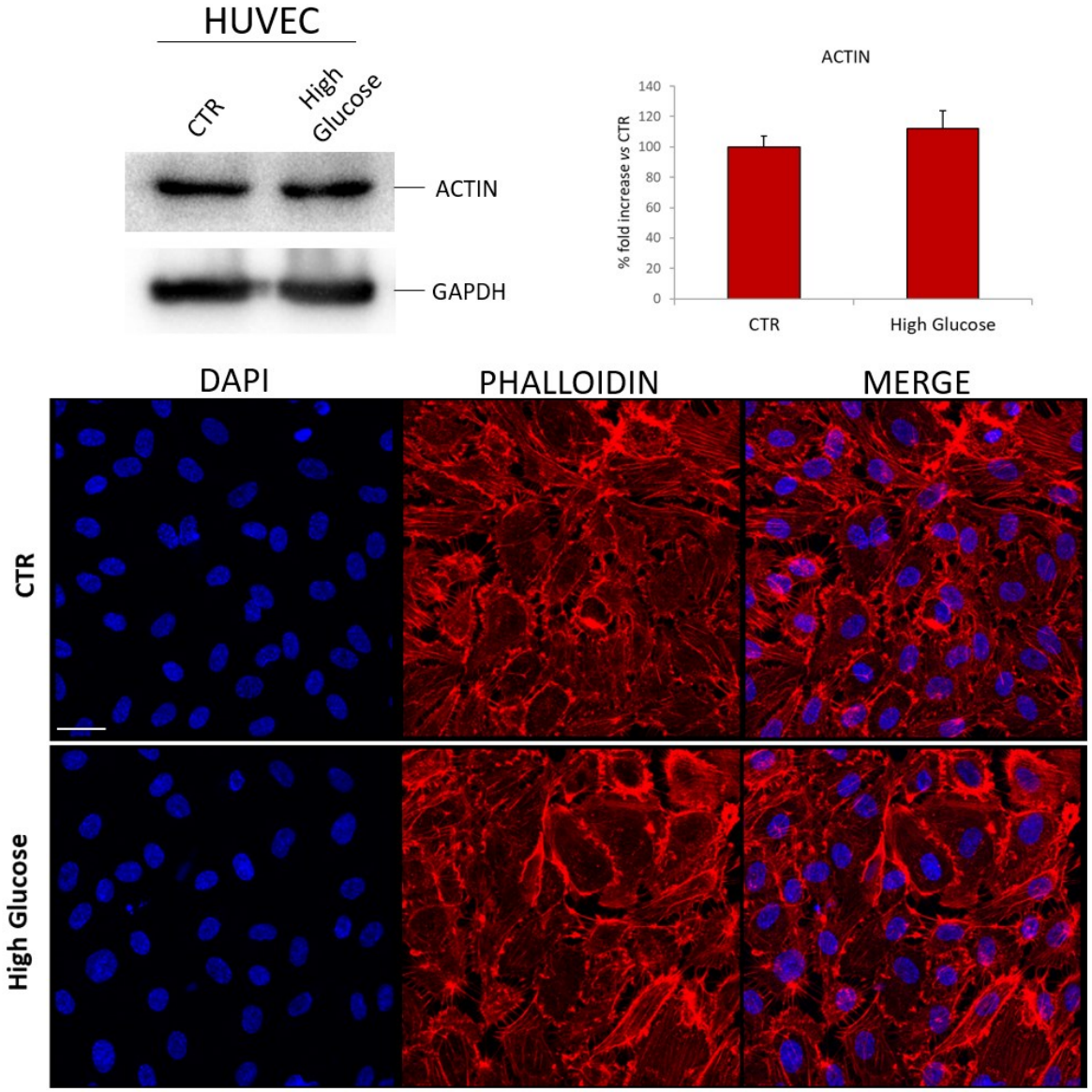


*Figure 45: Effect of glucose on actin content and cytoskeleton organization in HUVEC. HUVEC in 2D static condition were cultured for 24h in presence or not of high concentration of D-Glucose and Actin content and organization were studied. In the upper panel western blot*

*shows no modulation of total actin upon the treatment with High glucose compared to control and in parallel no modulation of actin organization in fibers was detected by confocal microscopy (lower panel). Nuclei were labeled with DAPI (blue) and Actin using Phalloidin-TRIC (Red). Scale bar = 40μm.*

## 7.5. THE EFFECT OF GLUCOSE ON THE ACTIN CYTOSKELETON IN HMEC TREATED FOR 24H

We evaluated the effect of high glucose-containing medium on the actin cytoskeleton and the nuclei also on HMEC. Confluent HMEC in 2D static condition were treated for 24h with normal medium (CTR) or medium supplemented with 5.4 mg/mL of D-glucose (High Glucose). Western Blot for actin and fluorescence microscopy after labeling with phalloidin were performed (Figure 46). In HMEC treated with high glucose a slight but not significant decrease of total actin content was detected (upper panel) as well as an altered organization of F-actin. Indeed, fluorescence microscopy shows that upon the treatment with high glucose actin fibers tend to be less organized than the controls. Moreover, in high glucose treated samples, fragmented nuclei, a marker of apoptosis, are observed, suggesting a possible effect of high glucose on HMEC survival.

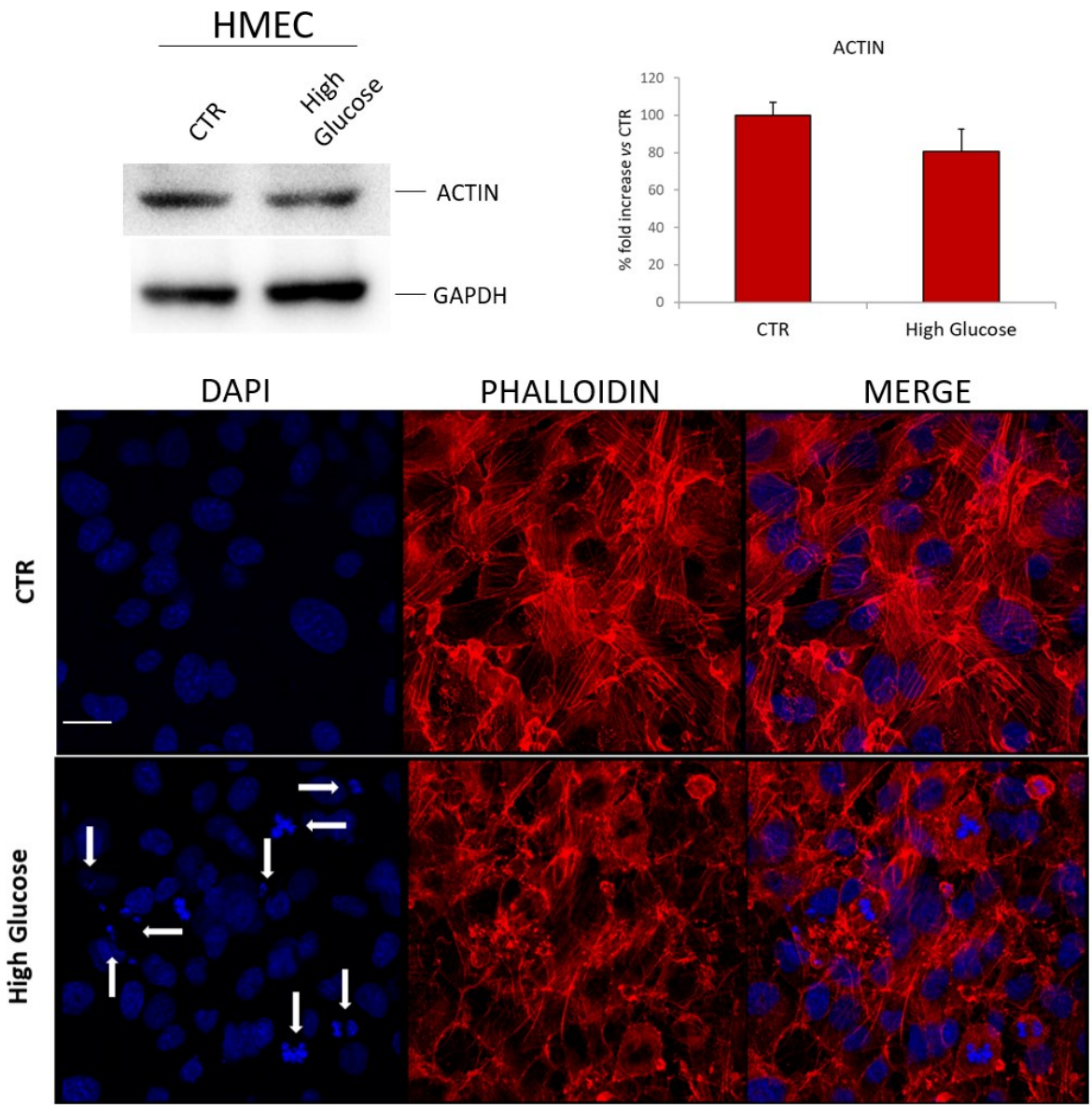


*Figure 46: Effect of glucose on actin content and cytoskeleton organization in HMEC. HMEC in 2D condition were cultured for 24h in the presence or not of D-Glucose, lysed for protein extraction or fixed for fluorescence microscopy. Western blot shows a slight decrease in total actin upon the treatment with High glucose (upper panel) and fluorescence microscopy shows a consistent reorganization of actin cytoskeleton, with less bundles of F-actin and less organized. DAPI staining revealed also fragmented nuclei in HMEC exposed to high glucose compared to control. Nuclei were labeled with DAPI (blue) and Actin using Phalloidin-TRIC (Red). Scale bar = 40μm*

# 7.6. THE EFFECT OF GLUCOSE ON ACTIN CYTOSKELETON IN HUVEC AND HMEC CULTURED IN 3D MICROFLUIDIC DEVICES

To study EC behavior in a more physiological condition, both HUVEC and HMEC were cultured in microfluidic devices that recapitulate vascular 3D organization better than culture in 2D static petri dish. In this system, cells were seeded in channels with different calibers and cultured until confluence in presence of a steady flow of culture medium. Channels of nominal section 30 × 30 μm were taken as the ideal channels were cells were subjected to a wall shear stress of about 0.2 Pa representative of physiological conditions for venous endothelial cells.

The process of fabrication of this microfluidic device could be sum up in different steps: mold fabrication, chip preparation, coating, seeding, cell culture and then analysis by fluorescence microscopy (Figure 47).

In the beginning, a mold is generated using classic soft lithography, recapitulating 6 identical networks of vessels (step 1). These networks are composed by ramifications of vessels of different calibers, starting from the biggest (2 channels of 200 μm in the inlet and outlet of the chip) to the smallest (16 channels of 30 μm in the center of the chip). Then a mixture of Polydimethylsiloxane (PDMS) and curling agent is prepared, deprived of air bubbles using a vacuum pump and poured slowly upon the mold. The PDMS mixture requires about 3 hours at 56°C to completely solidify. Then the chip is carved out the mold, the inlet and outlet are created removing PDMS and the chip is attached on a glass coverslip at 56°C for 1 hour (step 2).

After this step at the inlet and outlet of the chip a thin tube is connected: the inlet will provide medium influx to the chip while the outlet will discard the medium coming from

the chip into a syringe that will create the fluid flow by connection to a pump. Then fibronectin (20 μg/ml) is injected in the microfluidic devices overnight (step 3). The day after the cells are introduced once in the chip and their sedimentation is supported by complete stillness in the incubator for 30 minutes at 37°C (step 4). The seeding process is repeated 3 times and then the chip is connected to the fluid pump to maintain the culture (step 5). After 7 days HUVEC and HMEC are completely confluent in every channel of the chip and they can be used for the experiments.

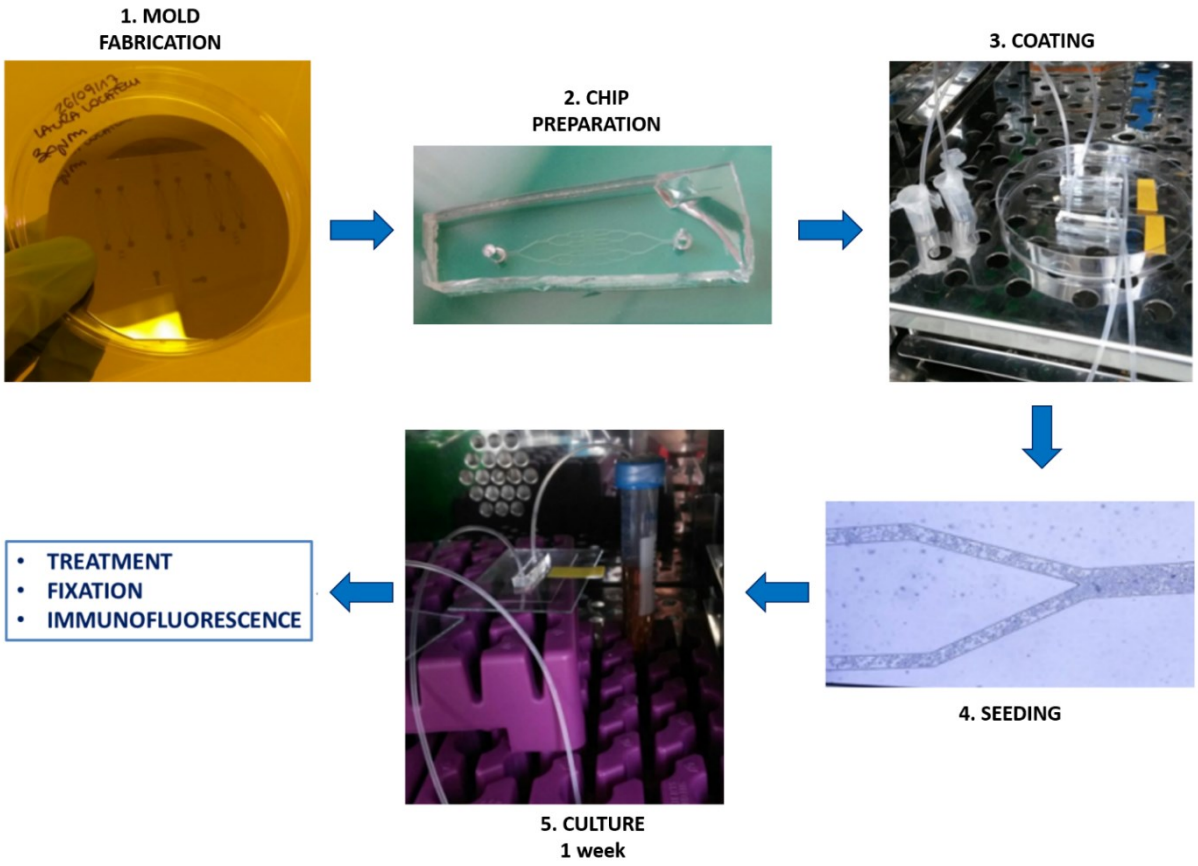


*Figure 47: steps of microfluidic device fabrication and cell culture.*

In this 3D-flow model, the effect of glucose on actin cytoskeleton was studied. In particular, HUVEC and HMEC were perfused with medium containing normal or high concentrations of D-glucose for 24h. HMEC seemed more susceptible to the detrimental effects of high glucose. Indeed, after 24h of treatment HMEC presented many apoptotic/fragmented nuclei and most of the channels in the microfluidic device were blocked by cells detached from the wall of the channel, making the analysis of the actin cytoskeleton impossible and useless. For this reason, we decided to treat HUVEC for 24h with normal or high glucose containing medium and HMEC for 16 h, and then perform the analyses.

Figure 48 shows phalloidin-labelled F-actin in HMEC (left panel) and HUVEC (right panel) in control medium (a, e) and in presence of D-glucose (c, g). The orientation of F-actin was studied using ImageJ (b, f, d, h) and the angle assumed by actin fibers compared to flow direction was plotted (i, j).

It is possible to observe that actin fibers in control HUVEC and HMEC align with the direction of flow. Upon glucose treatment, distributions of actin fibers in both HUVEC and HMEC are less peaked around theta=0, i.e. the direction of flow along the channel, and more populated at larger angles than the respective control distributions. This quantifies the fact that, for HMEC, flow-aligned stress fibers seen in the control tend to disappear for more isotropic cortical and protrusion-involved actin, whereas for HUVEC stress fibers are clearly visible in both conditions but tend to be less flow-aligned in the presence of high glucose.

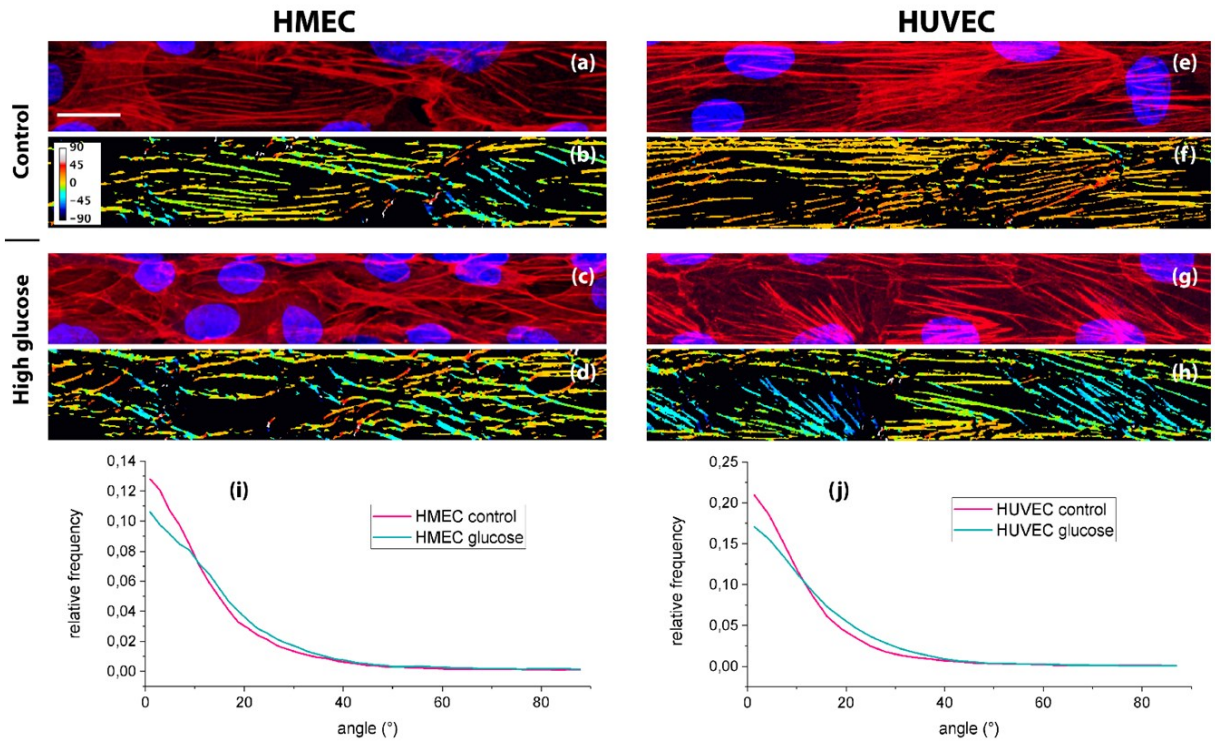


*Figure 48: Actin organization and orientation analysis in HUVEC and HMEC grown in 3D microfluidic chips in the presence of normal or high glucose.*
*Fluorescence microscopy of phalloidin-labelled HMEC (left panel) and HUVEC (right panel) was performed in control medium (a, e) and in the presence of 5.4 mg/mL of D-glucose (c, g) for 16h and 24h respectively. The respective orientation analysis perfomed using Image are shown (b, f, d, h). Considering the flow direction as theta=0, the angular distributions of actin fibers shown in panels (i) and (j) are built by counting in the same (positive) angular bin the data having +theta or -theta orientation.*

## 7.7. TXNIP EXPRESSION IN HMEC EXPOSED TO HIGH GLUCOSE FOR 24H

Since in 2D static condition HMEC showed many fragmented nuclei upon 24h high glucose treatment and in 3D-flow condition this treatment led to cell detachment, we

studied the expression of TXNIP (Figure 49). TXNIP increase is associated with reactive oxygen species (ROS) production and apoptosis, events already reported in literature in both HUVEC and HMEC treated with high glucose.

Figure 49 shows that the treatment with high glucose in 2D static condition has no significant effect in modulating TXNIP amounts as detected by western blot (A) and immunofluorescence (B). Also TXNIP subcellular localization is not affected by high glucose concentration. Cells were seeded in the microfluidic device, subjected for 6 days to steady flow of control medium and before the end of the experiment they were subjected to a steady flow of control medium (CTR) or medium supplemented with 5.4 mg/mL of D-glucose (High glucose). After overnight treatment cells were fixed and immunofluorescence for TXNIP was performed. We show that HMEC grown in 3D condition do not upregulate TXNIP after the treatment with glucose. We hypothesized that the effect of glucose on HMEC survival does not involve TXNIP.

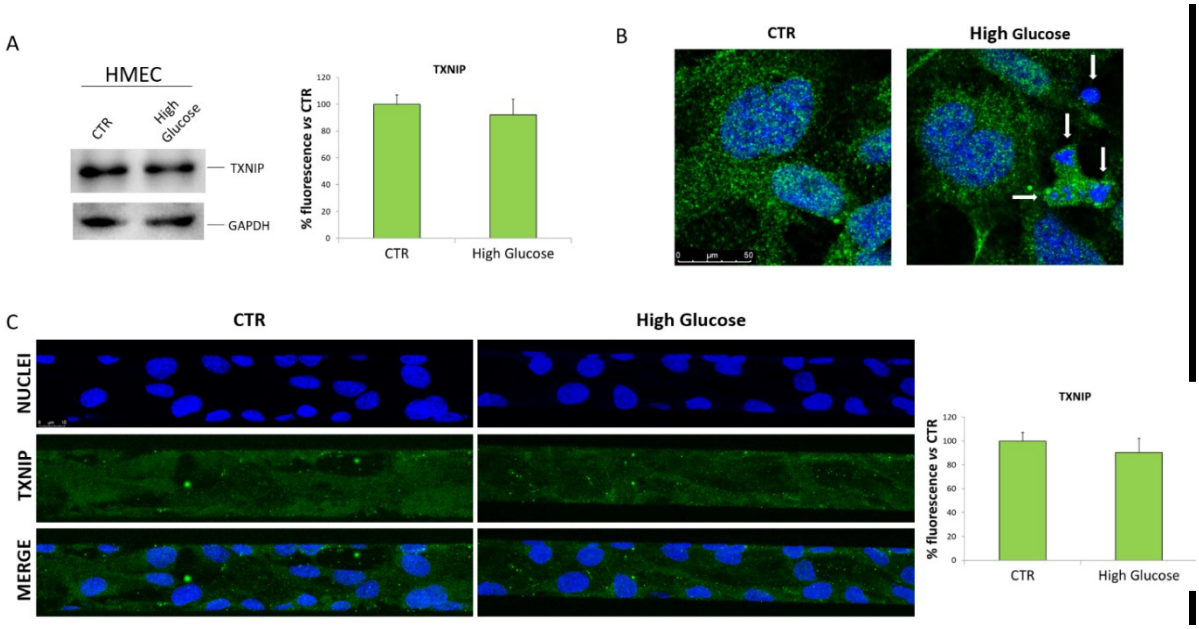


*Figure 49: Txnip in HMEC exposed for 24h to high concentration of glucose.*
*A) Western Blot on cell lysates was performed on HMEC cultured in 2D static condition after 24h of treatment with D-glucose. Representative blot (left) and relative quantification (right) are*

*shown.*
*B) Immunofluorescence for HMEC in 2D static condition shows no modulation in the amount and localization of TXNIP in HMEC cultured for 24h with high glucose compared to CTR. Immunofluorescence for TXNIP was performed on HMEC cultured in 3D-flow condition for 7 days and treated with 5.4 mg/mL of glucose overnight. Representative images (left) and relative quantification (right) are shown.*

It can be concluded that both 2D and 3D culture systems show the detrimental effect of high glucose in HUVEC and HMEC, with a higher sensitivity of HMEC if compared to HUVEC. In 2D high glucose promotes apoptosis of HMEC, and in 3D HMEC detach from the substrate indicating that their viability is markedly impaired. While culture in 2D does not significantly alter actin fibers' organization, the orientation of the fibers is clearly influenced by high glucose in 3D. The effect is more evident in HMEC in 3D, where not only altered distribution and orientation but also fragmentations of actin fibers are observed. Briefly, culture in 3D exacerbates the influence of high glucose on ECs. These results suggest that moving from 2D to 3D is fundamental to better disclose ECs behavior in both physiological and pathological conditions. Furthermore, since ECs are heterogeneous, it is not surprising that HUVEC and HMEC behave differently. Work is in progress to utilize 3D systems to perform experiments in microgravity to better reflect what happens *in vivo*, but many constraints and difficulties still have to be overcome.

# 8. DISCUSSION

Human space missions unveiled that microgravity exerts unique relevant effects on physical and biological phenomena. Understanding these effects is critical for human space exploration, and also advances knowledge on Earth. It is known that spaceflight induces modifications in body systems that lead to bone and skeletal muscle loss, immune dysfunction, cardiovascular deconditioning, among others. These responses of humans and model organisms to microgravity resemble the onset of age-related disorders and debilitating chronic human diseases on Earth. Therefore, spaceflight provides opportunities both for analysis of these changes and for testing of therapeutics in accelerated models of aging or disease. Moreover, research in space, in addition to projecting us towards the future, might also help to disclose the mechanisms underlying the transition from aquatic to terrestrial habitats during evolution [Bouillon 2014].

What we define space-associated diseases should actually be viewed as the result of a complex adaptive process that allows to thrive in such an extreme environment and tends to gradually revert upon return to normal 1G condition on Earth. We focus our attention on the endothelium, the thin layer that lines the inner surface of the blood vessels, because of the important role fulfilled by endothelial cells in maintaining homeostasis, by providing an antithrombotic surface to the blood, conveying adequate blood supply to all the tissues, secreting paracrine signals acting on neighboring cells, and many others [Galley 2004; Shulz 1992; Moncada 1991; Cines 1998; Levi 2002; Goldsby 2000].

Many studies of both real and simulated microgravity focused on different types of endothelial cells and in particular HUVEC, a consolidated model of macrovascular endothelial cells, were widely used [Carlsson 2003; Versari 2007; Grenon 2011; Versari 2013]. These studies reported that HUVEC in simulated microgravity undergo cytoskeletal remodeling, modulate the synthesis of vasoactive and inflammatory mediators and grow faster, thus suggesting that these cells engage an adaptive response to gravitational unloading. In particular, the SPHINX experiment [Versari 2013] offered

an overview of the transcriptional modulation of HUVEC after 10 days of culture onboard the ISS, i.e. under real microgravity. This experiment revealed the transcriptional regulation of hundreds genes among which the most overexpressed gene was TXNIP, a transcript coding for a pro-oxidant protein that binds to and inhibits the thiol-reducing and anti-oxidant capacity of thioredoxin (Trx) and causes cellular oxidative/nitrosative stress [Lee 2013].

Rather than being the endpoint, experiments in space generate a lot of puzzling questions. Obviously, the overexpression and the role of TXNIP are some of these. The first issue we faced was the following: in spite of the upregulation of TXNIP in HUVEC in microgravity, the overall amount of free radicals is similar to the controls. Consequently, we concentrated on the stress pathway activated in HUVEC cultured in the RWV and found that these cells engage a complex dynamic adaptive response to reach a new equilibrium that allows their survival in microgravity. In particular, early after exposure to simulated microgravity, HSP70, a chaperon protein, is upregulated. HSP70 is pivotal in ensuring HUVEC survival, as demonstrated by the occurrence of apoptosis in HUVEC grown in the RWV after HSP70 silencing. In a later phase, HSP70 returns to basal levels and the antioxidant proteins SIRT2, PON2, SOD2, HSP27 and its phosphorylated form P-HSP27 are upregulated. Also the pro-oxidant protein TXNIP accumulates, thus mimicking what happens in space. Our data indicate that antioxidant proteins counterbalance the pro-oxidant effect of the increase of TXNIP, since, apart from an early modest and transient increase, no accumulation of ROS occurs in HUVEC cultured in the RWV. It should be noted that, beyond its role as an endogenous inhibitor of Trx, TXNIP also regulates metabolism and cell behavior. In particular, in HUVEC under stress, TXNIP stimulates the expression of type 2 VEGF receptor, which is fundamental for endothelial survival and growth [Galley 2004]. Therefore also TXNIP might contribute to endothelial survival in microgravity-stressed HUVEC.

All these studies lead to the conclusion that HSP70 upregulation is required in the early steps of endothelial adaptation to microgravity. Then, the sequential contribution of different stress proteins drives HUVEC toward the acquisition of novel homeostatic features that maintain cell viable and functional. Also microvascular endothelial cell activate a stress response in simulated microgravity with some significant differences. Indeed, in HMEC in the RWV for 10 days we detected higher amounts of ROS than in 1G controls. While more studies are necessary, we propose that oxidative stress might be due to the imbalance between the increase of TXNIP and the reduction of SOD2.

Interestingly, many of the stress proteins upregulated after the exposure to simulated microgravity have a link with mitochondria, rod-shaped organelles that convert oxygen and nutrients into ATP.

PON2 is localized in the inner mitochondrial membrane, where it associates with mitochondrial respiratory complex II and III, binds Coenzyme Q10, regulates the respiratory complex activity and prevents oxidative stress in vascular cells and the liver [Devarajan 2018]. Interestingly, PON2 protects against atherosclerosis [Aviram 2004; Ng 2006], but may also support apoptosis evasion by its anti-oxidative and anti-apoptotic function [Horke 2007]. PON2 might be necessary to maintain the function of mitochondrial complex II. Indeed PON2 presence in complex II promotes rapid cellular response to external insults such as hypoxia, contributing to the reduction of ROS generation by mitochondria [Li 2018].

SOD2 plays an essential role in cells' protection against mitochondrial oxidative damage [Mukherjee 2011, Smith 2017]. SOD2 activation occurs exclusively inside the mitochondria [Kamati 2013]. SOD2 is synthesized in the cytosol and, upon stimulation, it crosses the outer and inner mitochondrial membranes to reach the mitochondrial matrix, where manganese (Mn2+) is incorporated into the enzyme [Culotta 2006]. It is noteworthy that inducible Hsp70 has a pivotal role in SOD2 shuttling from the cytosol to

the mitochondria [Zemanovic 2018].

SIRT2 is a NAD-dependent protein deacetylase, which deacetylates internal lysines on histone and alpha-tubulin as well as many other proteins such as key transcription factors. It participates to the modulation of multiple and diverse biological processes such as cell cycle control, genomic integrity, microtubule dynamics, cell differentiation, metabolic networks, and autophagy. The enzymatic reaction catalyzed by SIRT2 requires NAD+ as substrate, and, consequently, SIRT2 function is strictly linked to the energy/redox status of the cell [Webstrer 2012; Gomes 2015]. In general, sirtuins are considered to be metabolic and stress-sensor proteins and, after stimuli from the microenvironment, they may target proteins involved in cell cycle progression pathway, mitochondrial function, metabolism and energy homeostasis [Gomes 2015].

HSP27 is involved in various biological functions such as oxidative stress response, heat shock, and hypoxic/ischemia injury [You 2009, Benjamin 1998]. It is reported that HSP27 has an antioxidant activity, suppresses inflammatory response, improves survival, activates autophagy/mitophagy and increases mitochondrial activity [You 2009; Hollander 2004; Liu 2007; Vernon 2013; Mehlen 1996; Préville 1999, Lin 2016]. Furthermore, as a cytoskeleton regulator, HSP27 is critical for dynamic intracellular trafficking during autophagy and mitophagy [Kang 2011].

As far as TXNIP is concerned, under stress TXNIP shuttles to the mitochondrion and determines mitochondrial dysfunction, membrane depolarization, release of pro-apoptotic proteins in the cytosol [Saxena 2010], mitochondrial damage and mitophagy [Devi 2017].

Therefore, we focused on the mitochondria of HUVEC in simulated microgravity. It is well known that mitochondria orchestrate cell behavior not only because of their bioenergetics function, but also because they integrate signals from the environment, sense cellular stresses and contribute cell death signaling. In the endothelium,

mitochondria are biosynthetic factories rather than powerhouse, since endothelial cells obtain most of the energy by glycolysis, with the dual aim of protecting themselves from oxidative stress and preserving oxygen for the diffusion into the perivascular tissues. Therefore, endothelial mitochondria mainly function as a biosynthetic center to produce the precursors of various molecules required for cellular necessities.

Only a few studies are available on mitochondria in microgravity. Mitochondrial mass was reduced in Hodgkin's lymphoma cells cultured in a clinostat [Jeong 2018]. Mitochondrial functions of osteoblasts cultured in the RPM were impaired [Michaletti 2017], with important metabolic consequences. On the contrary, rat cardiomyocytes cultured in the RWV upregulated mitochondrial proteins to maintain the energetics of the cells at the expense of protein synthesis [Feger 2016]. Oligodendrocytes, the myelin-forming cells in the central nervous system, increased mitochondrial respiration in simulated microgravity, suggesting an increase in Krebs cycle flux [Espinosa-Jeffrey 2016].

HUVEC in the RWV exhibit a reduction of mitochondrial mass paralleled by a reduced consumption of oxygen. Nevertheless, isolated mitochondria of HUVEC in simulated microgravity are as efficient those of controls, suggesting that the decreased mitochondrial mass might represent an adaptive response to maintain fundamental functions and protect HUVEC from an overproduction of reactive oxygen species, thus integrating the complex events induced by the sequential intervention of stress proteins.

The mechanisms underlying the reduction of mitochondrial mass were investigated. Mitochondrial content is determined by the balance between mitochondrial biogenesis and degradation through mitophagy, i.e. the autophagic removal of damaged or superfluous mitochondria. Also autophagy, a process which allows the cell to raze redundant and/or dysfunctional components, is considered an adaptive response that contributes to stress resistance [Murrow 2013]. Accordingly, various types of stress - such

as heat shock and mechanical cues - activate autophagy in various cell types [Dokladny 2015; King 2012]. Therefore, it is not surprising that simulated microgravity induces autophagy [Wang 2013; Li 2018; Jeong 2018]. We show that culture in the RWV induces autophagy in HUVEC and that the inhibition of autophagy with chloroquine prevents mitochondrial loss. Accordingly, BNIP3, a mitochondrial stress sensor and a crucial player in mitophagy [Rikka 2011], is upregulated in HUVEC exposed to microgravity. We reasoned on the biological relevance of these findings and propose that the mitophagy contributes to endothelial adaptation to microgravity because a lower amount of mitochondria protects HUVEC from an overproduction of reactive oxygen species. On the other hand, our results indicate that having less mitochondria results in a reduced capacity to face an overload of substrates, which means that the new equilibrium reached by the cells might be not sufficient to deal with additional metabolic or environmental challenges. This consideration raises the possibility that HUVEC adapted to gravitational unloading are viable but frail and eventually unfit to respond to unfavourable conditions. The good news is that these effects of microgravity on mitochondria are reversible upon return to 1G conditions.

To unveil the mechanisms involved in activating mitophagy/autophagy, we focused on the cytoskeleton, which has been proposed as a sensor of changes of gravity [Vorselen 2014] since i) cytoskeletal dynamics have an important role in autophagy [Kast 2017], ii) mitochondria interact with cytoskeletal components [Strzyz 2018], iii) mitophagy is regulated by cytoskeletal components [Moore 2018], and iv) microgravity rapidly and steadily disassembles HUVEC cytoskeleton [Maier 2015; Carlsson 2003; Kapitonova 2012; Versari 2007]. Moreover, cytoskeleton interacts with several proteins, which are involved in stabilizing the system, among which molecular chaperons [Quintà 2011]. Considering that i) HSP70 participates in *de novo* folding of cytoskeletal proteins [Quintá 2011], ii) HSP27 stabilizes actin microfilaments [Sun 2015] and iii) TXNIP is a biomechanical

regulator of Src activity, thus able to affect and be affected by the cytoskeleton [Spindel 2014], we decided to study whether cytoskeletal dysregulation has a role in modulating stress response of EC in simulated microgravity.

We anticipate that cytoskeletal remodeling that occurs from the very beginning of microgravity exposure plays a pivotal role in orchestrating endothelial cell response, and this is true not only for HUVEC but also for HMEC. We utilized Cytochalasin D, which disassembles actin fibers, to mimic the effects of microgravity on HUVEC and HMEC cytoskeleton. Focusing on HUVEC, we detected an early upregulation of hsp70 that is maintained for all the duration of the experiment, while TXNIP increases at later time, similarly to what happens in microgravity. In addition, we provide evidence indicating a reduction of mitochondrial mass. Similar results were obtained also in HMEC.

Mitochondria are the primary intracellular stores of magnesium, which controls hundreds of enzymes involved in all the metabolic pathways. Moreover, Mg is necessary for $ATP^{2-}$, being this the form responsible for the energy production. We found that total Mg is reduced in HUVEC cells in microgravity in parallel with the reduction of mitochondrial mass. This finding further support the possibility that endothelial cells in microgravity are frail and might have reached their limit of adaptive capabilities.

In conclusion, we hypothesize that simulated microgravity affects endothelial cells behavior by remodeling the cytoskeleton, a common feature observed in different cell types early after the exposure to both real and simulated microgravity. Disorganized cytoskeleton in turn affects stress response, mitochondria and magnesium homeostasis (Figure 50) and results in the acquisition of a new homeostatic phenotype that allows the cells to cope with gravitational unloading.

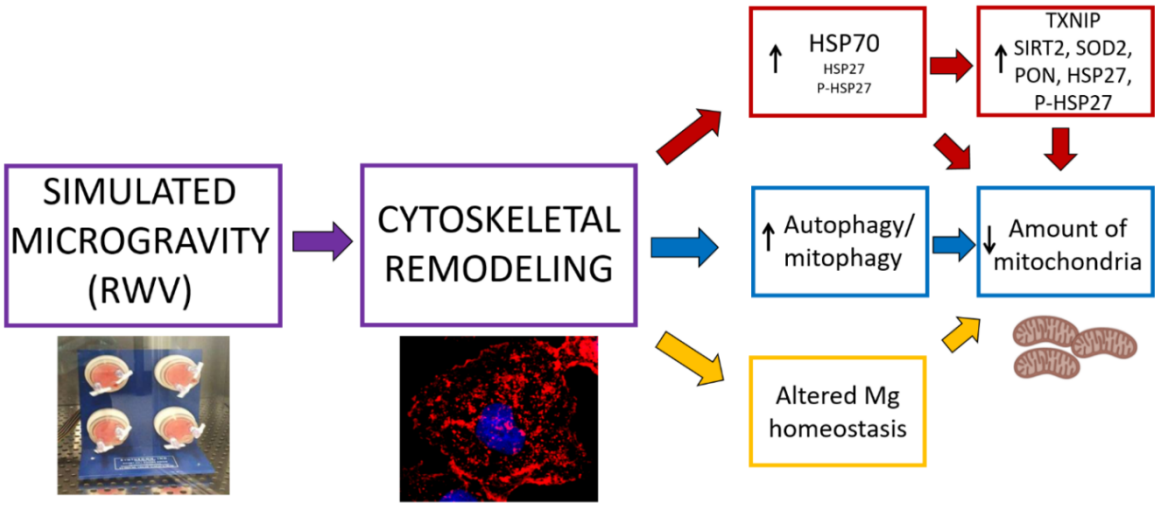


*Figure 50: Hypothesis of mechanisms engaged by endothelial cells in simulated microgravity.*

Many open questions are still to be solved, such as the meaning of the upregulation of TXNIP, detected both in real and in simulated microgravity. Silencing TXNIP might help to understand this issue. Another aspect to investigate is endothelial function. We did not detect any alteration in the synthesis and secretion of inflammatory cytokines and chemokines, as well as in the amount of adhesion molecules, but other functions - such as regulation of permeability, coagulation, antigen presentation - need to be studied. Last, we think that it would be extremely interesting to culture HUVEC in a 3D microfluidic system in microgravity, since this system better reflects the physiology of the endothelium and seems to be more sensitive to environmental cues.

A big question remains: why to invest time and money in space research? As Stephen Hawking said "We explore because we are human, and we want to know". Probably our ancestors in 1492 were asking a similar question when money fueled Columbus and his three ships to the New World. We now know that the discovery of Americas changed the history of our civilization.

Spreading out into space might have an even greater effect. Considering our immediate problems on Earth -global warming, pollution, limited drinking water supply, overpopulation- space might represent a sort of “life insurance” for the survival of humanity.

"I expect that within the next hundred years we will be able to travel anywhere in the solar system, except maybe the outer planets," Hawking explained. This might be feasible only if we can solve all the heath challenges that space imposes, from microgravity to radiations.

# 9. REFERENCES


- Adams RH, Alitalo K. Molecular regulation of angiogenesis and lymphangiogenesis. Nat. Rev. Mol. Cell Biol. 2007;8:464–478.
- Aird WC. Phenotypic Heterogeneity of the Endothelium II. Representative Vascular Beds. Circ Res. 2007;100:174-190.
- Aird WC. Endothelial cell heterogeneity. Cold Spring Harb Perspect Med. 2012 Jan;2(1):a006429.
- Aird WC. Phenotypic heterogeneity of the endothelium: I. Structure, function, and mechanisms. Circ Res. 2007 Feb 2;100(2):158-73.
- Alonso JL, Goldmann WH. Cellular mechanotransduction. AIMS Biophysics, 2016, 3(1): 50-62.
- Altenhöfer S, Witte I, Teiber JF, Wilgenbus P, Pautz A, Li H, Daiber A, Witan H, Clement AM, Förstermann U, Horke S. One enzyme, two functions: PON2 prevents mitochondrial superoxide formation and apoptosis independent from its lactonase activity. J Biol Chem 2010; 285, 24398-403.
- Arrigo AP. In search of the molecular mechanism by which small stress proteins counteract apoptosis during cellular differentiation. J Cell Biochem. 2005 Feb 1;94(2):241-6. Review.
- Aviram M, Rosenblat M. Paraoxonases 1, 2 and 3, oxidative stress, and macrophage foam cell formation during atherosclerosis development. Free Radic Biol. Med 2004; 37, 1304–1316.
- Aviram M, Rosenblat M. Paraoxonases 1, 2, and 3, oxidative stress, and macrophage foam cell formation during atherosclerosis development. Free Radic Biol Med. 2004 Nov 1;37(9):1304-16.

Badimon L, Padró T, Vilahur G. Atherosclerosis, platelets and thrombosis in acute ischaemic heart disease. Eur Heart J Acute Cardiovasc Care. 2012 Apr;1(1):60-74.

Bai K, Huang Y, Jia X, Fan Y, Wang W. Endothelium oriented differentiation of bone marrow mesenchymal stem cells under chemical and mechanical stimulations. J Biomech. 2010. 43:1176-81.

Ballatori N, Krance SM, Notenboom S, Shi S, Tieu K, Hammond CL. Glutathione dysregulation and the etiology and progression of human diseases. Biol Chem. 2009; 390, 191-214.

Beck M, Moreels M, Quintens R, Abou-El-Ardat K, El-Saghire H, Tabury K, Michaux A, Janssen A, Neefs M, Van Oostveldt P, De Vos WH, Baatout S. Chronic exposure to simulated space conditions predominantly affects cytoskeleton remodeling and oxidative stress response in mouse fetal fibroblasts. Int J Mol Med 2014; 34, 606-15.

Beck M, Moreels M, Quintens R, Abou-El-Ardat K, El-Saghire H, Tabury K, Michaux A, Janssen A, Neefs M, Van Oostveldt P, De Vos WH, Baatout S. Chronic exposure to simulated space conditions predominantly affects cytoskeleton remodeling and oxidative stress response in mouse fetal fibroblasts. Int J Mol Med 2014; 34, 606-15.

Beere HM, Wolf BB, Cain K, Mosser DD, Mahboubi A, Kuwana T, Tailor P, Morimoto RI, Cohen GM, Green DR. Heat-shock protein 70 inhibits apoptosis by preventing recruitment of procaspase-9 to the Apaf-1 apoptosome. Nat Cell Biol. 2000; 2(8):469-75.

Benjamin IJ, McMillan DR. Stress (heat shock) proteins: molecular chaperones in cardiovascular biology and disease. Circulation Research. 1998;83(2):117–132.

Blackman BR. A new in vitro model to evaluate differential responses of endothelial cells to simulated arterial shear stress waveforms. J. Biomech. Eng. 2002;124:397–407.

Bouillon R, Suda T. Vitamin D: calcium and bone homeostasis during evolution. Bonekey Rep. 2014 Jan 8;3:480.

Caja S, Enríquez JA. Mitochondria in endothelial cells: Sensors and integrators of environmental cues. Redox Biol. 2017 Aug; 12:821-827.

- Carlsson SI, Bertilaccio MT, Ballabio E, Maier JA. Endothelial stress by gravitational unloading: effects on cell growth and cytoskeletal organization. Biochim Biophys Acta. 2003. 1642: 173-9.
- Carmeliet P. Angiogenesis in life, disease and medicine. Nature 2005; 438:932–936.
- Carmeliet P. Mechanisms of angiogenesis and arteriogenesis. Nat. Med. 2000;6:389–396.
- Chatterjee S, Fisher AB. Mechanotransduction in the endothelium: role of membrane proteins and reactive oxygen species in sensing, transduction, and transmission of the signal with altered blood flow. Antioxid Redox Signal. 2014 Feb 20;20(6):899-913.
- Chatterjee S. Endothelial Mechanotransduction, Redox Signaling and the Regulation of Vascular Inflammatory Pathways. Front Physiol. 2018 Jun 7;9:524.
- Chien S. Mechanotransduction and endothelial cell homeostasis: the wisdom of the cell. Am J Physiol Heart Circ Physiol. 2007 Mar;292(3):H1209-24.
- Choi K. Hemangioblast development and regulation. Biochem Cell Biol. 1998; 76 (6): 947-57
- Cines DB, Pollak ES, Buck CA, Loscalzo J, Zimmerman GA, McEver RP, Pober JS, Wick TM, Konkle BA, Schwartz BS, Barnathan ES, McCrae KR, Hug BA, Schmidt AM, Stern DM. Endothelial cells in physiology and in the pathophysiology of vascular disorders. Blood. 1998 May 15;91(10):3527-61.
- Cines Douglas B., Pollak Eleanor S., Buck Clayton A., Loscalzo Joseph, Zimmerman Guy A., McEver Rodger PPober., Jordan S., Wick Timothy M., Konkle Barbara A., Schwartz Bradford S., Barnathan Elliot S., McCrae Keith R., Hug Bruce A., Schmidt Ann-Marie, and Stern David M. Endothelial cells in physiology and in the pathophysiology of vascular disorders. Blood 1998; 91: 3527–3561.
- Colace TV, Jobson J, Diamond SL. Relipidated tissue factor linked to collagen surfaces potentiates platelet adhesion and fibrin formation in a microfluidic model of vessel injury. Bioconjug. Chem. 2011;22:2104–2109.

- Cotrupi S, Ranzani D, Maier JA. Impact of modeled microgravity on microvascular endothelial cells. Biochim Biophys Acta. 2005. 1746: 163-8.
- Culotta VC, Yang M, O'Halloran TV. Activation of superoxide dismutases: Putting the metal to the pedal Biochim. Biophys. Acta 2006, 1763, 747-758.
- Danese S, Dejana E, Fiocchi C. Immune regulation by microvascular endothelial cells: Directing innate and adaptive immunity, coagulation, and inflammation. J Immunol 2007; 178:6017–6022.
- Davidson JM, Aquino AM, Woodward SC, Wilfinger WW. Sustained microgravity reduces intrinsic wound healing and growth factor responses in the rat. FASEB J 1999; 13:325–329.
- Davies PF. Flow-mediated endothelial mechanotransduction. Physiol. Rev. 1995;75:519–560.
- De Bock K, Georgiadou M, Carmeliet P. Role of endothelial cell metabolism in vessel sprouting. Cell Metab. 2013 Nov 5;18(5):634-47.
- De Bock K, Georgiadou M, Carmeliet P. Role of endothelial cell metabolism in vessel sprouting. Cell Metab. 2013;18(5):634-47.
- De Bock K, Georgiadou M, Schoors S, Kuchnio A, Wong BW, Cantelmo AR, Quaegebeur A, Ghesquière B, Cauwenberghs S, Eelen G, Phng LK, Betz I, Tembuyser B, Brepoels K, Welti J, Geudens I, Segura I, Cruys B, Bifari F, Decimo I, Blanco R, Wyns S, Vangindertael J, Rocha S, Collins RT, Munck S, Daelemans D, Imamura H, Devlieger R, Rider M, Van Veldhoven PP, Schuit F, Bartrons R, Hofkens J, Fraisl P, Telang S, Deberardinis RJ, Schoonjans L, Vinckier S, Chesney J, Gerhardt H, Dewerchin M, Carmeliet P. Role of PFKFB3-driven glycolysis in vessel sprouting. Cell. 2013 Aug 1;154(3):651-63.
- Dejeans N, Maier JA, Tauveron I, Milenkovic D., Mazur A. Modulation of gene expression in endothelial cells by hyperlipaemic postprandial serum from healthy volunteers. Genes Nutr 2010; 5, 263-74.

Deng Q, Huo Y, Luo J. Endothelial mechanosensors: the gatekeepers of vascular homeostasis and adaptation under mechanical stress. Sci China Life Sci. 2014 Aug;57(8):755-62.

Devarajan A, Su F, Grijalva V, Yalamanchi M, Yalamanchi A, Gao F, Trost H, Nwokedi J, Farias-Eisner G, Farias-Eisner R, Fogelman AM, Reddy ST. Paraoxonase 2 overexpression inhibits tumor development in a mouse model of ovarian cancer. Cell Death Dis. 2018 Mar 12;9(3):392.

Devi TS, Somayajulu M, Kowluru RA, Singh LP. TXNIP regulates mitophagy in retinal Müller cells under high-glucose conditions: implications for diabetic retinopathy. Cell Death Dis. 2017;8(5):e2777.

Doddaballapur A, Michalik KM, Manavski Y, Lucas T, Houtkooper RH, You X, Chen W, Zeiher AM, Potente M, Dimmeler S, Boon RA. Laminar shear stress inhibits endothelial cell metabolism via KLF2-mediated repression of PFKFB3. Arterioscler Thromb Vasc Biol. 2015 Jan;35(1):137-45.

Dokladny K, Myers OB, Moseley PL. Heat shock response and autophagy--cooperation and control. Autophagy. 2015;11(2):200-13..

Dryden SC, Nahhas FA, Nowak JE, Goustin AS, Tainsky MA. Role for human SIRT2 NAD-dependent deacetylase activity in control of mitotic exit in the cell cycle. Mol. Cell. Biol. 2003; 23:3173-3185.

DuFort CC, Paszek MJ, Weaver VM. Balancing forces: Architectural control of mechanotransduction. Nat. Rev. Mol. Cell Biol. 2011;12:308–319.

Dunn LL, Buckle AM, Cooke JP, Ng MK. The emerging role of the thioredoxin system in angiogenesis. Arterioscler. Thromb. Vasc. Biol. 2010; 30, 2089–2098.

Espinosa-Jeffrey A., Nguyen K., Kumar S., Toshimasa O., Hirose R., Reue K., Vergnes L., Kinchen J., Vellis J. (2016) Simulated microgravity enhances oligodendrocyte mitochondrial function and lipid metabolism. J Neurosci Res94(12):1434-1450.

- Fawzy MS, Toraih EA. Data supporting the structural and functional characterization of Thrombin-Activatable Fibrinolysis Inhibitor in breast cancer. Data Brief. 2015 Nov 14;5:981-9.
- Feger B.J., Thompson J.W., Dubois L.G., Kommaddi R.P., Foster M.W., Mishra R., Shenoy S.K., Shibata Y., Kidane Y.H., Moseley M.A., Carnell L.S., Bowles D.E. (2016) Microgravity induces proteomics changes involved in endoplasmic reticulum stress and mitochondrial protection. Sci Rep6:34091.
- Fitzgerald U., Hettle S, MacDonald C, McLean JS (2000). Umbilical cord endothelial cells expressing large T antigen: comparison with primary cultures and effect of cell age. In Vitro Cell Dev Biol Anim. 36(4):222-7. 81
- Foreman KE, Tang J. Molecular mechanisms of replicative senescence in endothelial cells. Exp Gerontol. 2003. 38: 1251-7.
- Frank PG, Lisanti MP. Role of caveolin-1 in the regulation of the vascular shear stress response. J Clin Invest. 2006 May;116(5):1222-5.
- Fu BM, and Tarbell JM. Mechano-sensing and transduction by endothelial surface glycocalyx: composition, structure, and function. Wiley Interdiscip. Rev. Syst. Biol. Med.2013; 5, 381–390.
- Galley HF, Webster NR. Physiology of the endothelium. Br J Anaesth 2004; 93(1):105-13.
- Georgakopoulos ND, Wells G, Campanella M. The pharmacological regulation of cellular mitophagy. Nat Chem Biol 2017; 13(2):136-146.
- Gimbrone MA. Vascular endothelium: nature's blood container. In: Vascular endothelium in hemostasis and thrombosis. Churchill Livingstone 1986, New York, pp 1–13.
- Goldsby R.A., Kindt T.J., Osborne B.A. (2000). Kuby Immunologia. Seconda Edizione UTET.
- Gomes P, Fleming Outeiro T, Cavadas C. Emerging Role of Sirtuin 2 in the Regulation of Mammalian Metabolism. Trends Pharmacol Sci. 2015 Nov;36(11):756-768.

Gout E, Rébeillé F, Douce R, Bligny R. Interplay of Mg2+, ADP, and ATP in the cytosol and mitochondria: unravelling the role of Mg2+ in cell respiration. Proc Natl Acad Sci U S A. 2014 Oct 28;111(43):E4560-7.

Goytain A, Quamme GA. Identification and characterization of a novel mammalian Mg2+ transporter with channel-like properties. BMC Genomics. 2005 Apr 1;6:48.

Grenon SM, Jeanne M, Aguado-Zuniga J, Conte MS, Hughes-Fulford M. Effects of gravitational mechanical unloading in endothelial cells: association between caveolins, inflammation and adhesion molecules. Sci Rep. 2013. 3:1494.

Grimm D, Bauer J, Ulbrich C, Westphal K, Wehland M, Infanger M, Aleshcheva G, Pietsch J, Ghardi M, Beck M, El-Saghire H, de Saint-Georges L, Baatout S. Different responsiveness of endothelial cells to vascular endothelial growth factor and basic fibroblast growth factor added to culture media under gravity and simulated microgravity. Tissue Eng Part A. 2010 May;16(5):1559-73.

Grimm D., Kossmehl P., Shakibaei M., et al. Effects of simulated microgravity on thyroid carcinoma cells. Journal of Gravitational Physiology. 2002;9(1):P253–P256.

Grosse J, Wehland M., Pietsch J. et al. Short-term weightlessness produced by parabolic flight maneuvers altered gene expression patterns in human endothelial cells. FASEB Journal 2012, vol. 26, no. 2, pp. 639–655.

Hammer BE, Kidder LS, Williams PC, Xu WW. Magnetic Levitation of MC3T3 Osteoblast Cells as a Ground-Based Simulation of Microgravity. Microgravity Sci Technol. 2009 Nov;21(4):311-318.

Hansen RR, Wufsus AR, Barton ST, Onasoga AA, Johnson-Paben RM, Neeves KB. High content evaluation of shear dependent platelet function in a microfluidic flow assay. Ann. Biomed. Eng. 2013;41:250–262.

Haslbeck M. sHsps and their role in the chaperone network. Cell Mol Life Sci. 2002 Oct;59(10):1649-57. Review.

Helmlinger G, Endo M, Ferrara N, Hlatky L, Jain RK. Formation of endothelial cell networks. Nature 2000; 405 (6783), 139–141.

Herranz R, Anken R, Boonstra J, Braun M, Christianen PC, de Geest M,et al. Hemmersbach R. Ground-based facilities for simulation of microgravity: organism specific recommendations for their use, and recommended terminology. Astrobiology. 2013. 13: 1-17.

Herranz R, Larkin OJ, Dijkstra CE, Hill RJ, Anthony P, Davey MR, et al. Microgravity simulation by diamagnetic levitation: effects of a strong gradient magnetic field on the transcriptional profile of Drosophila melanogaster. BMC Genomics. 2012. 13: 52.

Hinsberg VW. Endothelium-role in regulation of coagulation and inflammation. Semin Immunopathol. 2012. 34: 93-106.

Hollander JM, Martin JL, Belke DD, et al. Overexpression of wild-type heat shock protein 27 and a nonphosphorylatable heat shock protein 27 mutant protects against ischemia/reperfusion injury in a transgenic mouse model. Circulation. 2004; 110(23):3544–3552.

Horke S, Witte I, Wilgenbus P, Krüger M, Strand D, Förstermann U. Paraoxonase-2 Reduces Oxidative Stress in Vascular Cells and Decreases Endoplasmic Reticulum Stress–Induced Caspase Activation. Circulation 2007; 115, 2055-2064.

Horke S, Witte I, Wilgenbus P, Krüger M, Strand D, Förstermann U. Paraoxonase-2 reduces oxidative stress in vascular cells and decreases endoplasmic reticulum stress-induced caspase activation. Circulation. 2007 Apr 17;115(15):2055-64.

Huang NF and Li S. Mesenchymal stem cells for vascular regeneration. Regen Med. 2008. 3: 877-92.

Ingber DE. Cellular mechanotransduction: putting all the pieces together again. FASEB J. 2006 May;20(7):811-27. Review.

- Inoue T, Hiratsuka M, Osaki M, Yamada H, Kishimoto I, Yamaguchi S, Nakano S, Katoh M, Ito H, Oshimura M. SIRT2, a tubulin deacetylase, acts to block the entry to chromosome condensation in response to mitotic stress. Oncogene 2007; 26:945-957.
- Jeanes AI, Maya-Mendoza A, Streuli CH. Cellular microenvironment influences the ability of mammary epithelia to undergo cell cycle. PLoS One. 2011 Mar 29;6(3):e18144.
- Jeong AJ, Kim YJ, Lim MH, Lee H, Noh K, Kim BH, Chung JW, Cho CH, Kim S, Ye SK. Microgravity induces autophagy via mitochondrial dysfunction in human Hodgkin's lymphoma cells. Sci Rep. 2018; 8(1):14646.
- Jeong AJ, Kim YJ, Lim MH, Lee H, Noh K, Kim BH, Chung JW, Cho CH, Kim S, Ye SK. Microgravity induces autophagy via mitochondrial dysfunction in human Hodgkin's lymphoma cells. Sci Rep. 2018 Oct 2;8(1):14646.
- Kang C.-Y., Zou L., Yuan M. et al. Impact of simulated microgravity on microvascular endothelial cell apoptosis. European Journal of Applied Physiology 2011, vol. 111, no. 9, pp. 2131–2138.
- Kang R, Livesey KM, Zeh HJ 3rd, Lotze MT, Tang D. Metabolic regulation by HMGB1-mediated autophagy and mitophagy. Autophagy. 2011 Oct;7(10):1256-8
- Kapitonova MY, Kuznetsov SL, Froemming GR, Muid S, Nor-Ashikin MN, Otman S, et al. Effects of space mission factors on the morphology and function of endothelial cells. Bull Exp Biol Med. 2013. 154: 796-801.
- Kapitonova MY, Muid S, Froemming GR, Yusoff WN, Othman S, Ali AM,et al. Real space flight travel is associated with ultrastructural changes, cytoskeletal disruption and premature senescence of HUVEC. Malays J Pathol. 2012. 34: 103-13.
- Karnati S, Lüers G, Pfreimer S, Baumgart-Vogt E. Mammalian SOD2 is exclusively located in mitochondria and not present in peroxisomes Histochem. Cell Biol. 2013, 140, 105-117.
- Kast DJ, Dominguez R. The Cytoskeleton-Autophagy Connection. Curr Biol. 2017 Apr 24;27(8):R318-R326.

Kast DJ, Dominguez R. The Cytoskeleton-Autophagy Connection. Curr Biol. 2017 Apr 24;27(8):R318-R326.

Kim SK, Moon WK, Park JY, Jung H. Inflammatory mimetic microfluidic chip by immobilization of cell adhesion molecules for T cell adhesion. Analyst. 2012;137:4062–4068.

King JS. Mechanical stress meets autophagy: potential implications for physiology and pathology. Trends Mol Med. 2012 Oct;18(10):583-8.

Kirchen ME, O'Connor KM, Gruber HE, Sweeney JR, Fras IA, Stover SJ, Sarmiento A, Marshall GJ. Effects of microgravity on bone healing in a rat fibular osteotomy model. Clin Orthop Relat Res 1995; 318:231–242.

Klionsky D.J., Abdelmohsen K., Abe A., Abedin M.J., Abeliovich H., Acevedo Arozena A. et al. (2016) Guidelines for the use and interpretation of assays for monitoring autophagy (3rd edition). Autophagy12(1):1-222.

Klionsky DJ, Abdelmohsen K, Abe A, Abedin MJ, Abeliovich H, Acevedo Arozena A et al. Guidelines for the use and interpretation of assays for monitoring autophagy (3rd edition). Autophagy. 2016;12(1):1-222.

Kluge MA, Fetterman JL, Vita JA. Mitochondria and endothelial function. Circ Res. 2013 Apr 12;112(8):1171-88.

Kohan DE, Inscho EW, Wesson D, Pollock DM. Physiology of endothelin and the kidney. Compr Physiol. 2011 Apr;1(2):883-919.

Komarova Y, Malik AB. Regulation of endothelial permeability via paracellular and transcellular transport pathways. Annu Rev Physiol. 2010;72:463-93.

Kraft T. F. B., van Loon J. J. W. A., Kiss J. Z. Plastid position in Arabidopsis columella cells is similar in microgravity and on a random-positioning machine. Planta. 2000;211(3):415–422.

Krause BJ, Hanson MA, Casanello P. Role of nitric oxide in placental vascular development and function. Placenta. 2011 Nov;32(11):797-805.

- Lagarrigue F, Kim C, Ginsberg MH. The Rap1-RIAM-talin axis of integrin activation and blood cell function. Blood. 2016 Jul 28;128(4):479-87.
- Lavoie JN, Hickey E, Weber LA, Landry J. Modulation of actin microfilament dynamics and fluid phase pinocytosis by phosphorylation of heat shock protein 27. J Biol Chem. 1993 Nov 15;268(32):24210-4.
- Lee S, Kim SM, Lee RT. Thioredoxin and thioredoxin target proteins: from molecular mechanisms to functional significance. Antioxid Redox Signal. 2013. 18: 1165-207.
- Leone TC, Kelly DP. Transcriptional control of cardiac fuel metabolism and mitochondrial function. Cold Spring Harb. Symp. Quant. Biol. 76 (2011) 175–182.
- Levi M., Ten Cate H., van der Poll T. (2002). Endothelium: interface between coagulation and inflammation. Crit. Care Med., 30(5), [Suppl.]: S220-S224.
- Li CF, Sun JX, Gao Y, Shi F, Pan YK, Wang YC, Sun XQ. Clinorotation-induced autophagy via HDM2-p53-mTOR pathway enhances cell migration in vascular endothelial cells. Cell Death Dis. 2018; 9(2):147.
- Li CF, Sun JX, Gao Y, Shi F, Pan YK, Wang YC, Sun XQ. Clinorotation-induced autophagy via HDM2-p53-mTOR pathway enhances cell migration in vascular endothelial cells. Cell Death Dis. 2018 Feb 2;9(2):147.
- Li W, Kennedy D, Shao Z, Wang X, Kamdar AK, Weber M, Mislick K, Kiefer K, Morales R, Agatisa-Boyle B, Shih DM, Reddy ST, Moravec CS, Tang WHW. Paraoxonase 2 prevents the development of heart failure. Free Radic Biol Med. 2018 Jun;121:117-126.
- Lin S, Wang Y, Zhang X, Kong Q, Li C, Li Y, Ding Z, Liu L. HSP27 Alleviates Cardiac Aging in Mice via a Mechanism Involving Antioxidation and Mitophagy Activation. Oxid Med Cell Longev. 2016;2016:2586706.
- Liu L, Zhang X, Qian B, et al. Over-expression of heat shock protein 27 attenuates doxorubicin-induced cardiac dysfunction in mice. European Journal of Heart Failure. 2007;9(8):762–769.

- Liu Y, Wang E. Transcriptional analysis of normal human fibroblast responses to microgravity stress. Genomics Proteomics Bioinformatics 2008; 6, 29-41.
- Liu Y, Wang, E. Transcriptional analysis of normal human fibroblast responses to microgravity stress. Genomics Proteomics Bioinformatics 2008; 6, 29-41.
- Maier JA, Cialdai F, Monici M, Morbidelli L. The impact of microgravity and hypergravity on endothelial cells. Biomed Res Int. 2015;2015:434803.
- Maier JA, Cialdai F, Monici M, Morbidelli L. The impact of microgravity and hypergravity on endothelial cells. Biomed Res Int. 2015. 2015: 434803.
- Maier JA. Endothelial cells and magnesium: implications in atherosclerosis. Clin Sci (Lond). 2012 May;122(9):397-407.
- Malcolm A.S. Moore. Putting the neo into neoangiogenesis. J Clin Invest. 2002; 109(3):313-315.
- Mariotti M and Maier JA. Gravitational unloading induces an anti-angiogenic phenotype in human microvascular endothelial cells. J Cell Biochem. 2008. 104: 129-35.
- Mayers, J.R. and Vander Heiden, M.G. Famine versus feast: understanding the metabolism of tumors in vivo. Trends Biochem. Sci. 2015; 40, 130–140.
- Mehlen P, Kretz-Remy C, Préville X, Arrigo AP. Human hsp27, Drosophila hsp27 and human $\alpha$B-crystallin expression-mediated increase in glutathione is essential for the protective activity of these proteins against TNF$\alpha$-induced cell death. The EMBO Journal. 1996;15(11):2695–2706.
- Mehlen P, Preville X, Chareyron P, Briolay J, Klemenz R, Arrigo AP. Constitutive expression of human hsp27, Drosophila hsp27, or human $\alpha$B-crystallin confers resistance to TNF- and oxidative stress-induced cytotoxicity in stably transfected murine L929 fibroblasts. Journal of Immunology. 1995;154(1):363–374.
- Michaletti A., Gioia M., Tarantino U., Zolla L. (2017) Effects of microgravity on osteoblast mitochondria: a proteomic and metabolomics profile. Sci Rep7(1):15376.

- Moncada S, Palmer RM, Higgs EA. Nitric oxide physiology, pathophysiology and pharmacology. Pharmacol Rev. 1991; 43: 109-42.
- Monici M, Cialdai F., Romano G. et al. An in vitro study on tissue repair: impact of unloading on cells involved in the remodelling phase. Microgravity Sci. Technol. 2011; 23:391–401.
- Moore A.S., Holzbaur E.L.F. (2018) Mitochondrial-cytoskeletal interactions: dynamic associations that facilitate network function and remodeling. Curr Opin Physiol3:94-100.
- Moore AS, Holzbaur ELF. Mitochondrial-cytoskeletal interactions: dynamic associations that facilitate network function and remodeling. Curr Opin Physiol. 2018; 3:94-100.
- Moore AS, Holzbaur ELF. Mitochondrial-cytoskeletal interactions: dynamic associations that facilitate network function and remodeling. Curr Opin Physiol. 2018 Jun;3:94-100.
- Moore AS, Holzbaur ELF. Mitochondrial-cytoskeletal interactions: dynamic associations that facilitate network function and remodeling. Curr Opin Physiol. 2018 Jun;3:94-100.
- Morbidelli L, Monici M, Marziliano N, Cogoli A, Fusi F, Waltenberger J, et al. Simulated hypogravity impairs the angiogenic response of endothelium by up-regulating apoptotic signals. Biochem Biophys Res Commun. 2005. 334: 491-9.
- Morbidelli L., Monici M., Marziliano N., et al. Simulated hypogravity impairs the angiogenic response of endothelium by up-regulating apoptotic signals. Biochemical and Biophysical Research Communications. 2005;334(2):491–499.
- Mukherjee S, Forde R, Belton A, Duttaroy A. SOD2, the principal scavenger of mitochondrial superoxide, is dispensable for embryogenesis and imaginal tissue development but essential for adult survival Fly (Austin) 2011, 5(1), 39-46.
- Murrow L, Debnath J. Autophagy as a stress-response and quality-control mechanism: implications for cell injury and human disease. Annu Rev Pathol. 2013 Jan 24;8:105-37..
- Nadler MJ, Hermosura MC, Inabe K, Perraud AL, Zhu Q, Stokes AJ, Kurosaki T, Kinet JP, Penner R, Scharenberg AM, Fleig A. LTRPC7 is a Mg.ATP-regulated divalent cation

channel required for cell viability. Nature. 2001 May 31;411(6837):590-5. Erratum in: Nature 2001 Aug 9;412(6847):660.

- Ng CJ, Bourquard N, Grijalva V, Hama S, Shih DM, Navab M, Fogelman AM, Lusis AJ, Young S, Reddy ST. Paraoxonase-2 deficiency aggravates atherosclerosis in mice despite lower apolipoprotein-B-containing lipoproteins: anti-atherogenic role for paraoxonase-2. J Biol Chem. 2006 Oct 6;281(40):29491-500.
- North BJ, Verdin E. Mitotic regulation of SIRT2 by cyclin-dependent kinase 1-dependent phosphorylation. J. Biol. Chem. 2007; 282:19546-19555.
- Ogneva IV. Cell mechanosensitivity: mechanical properties and interaction with gravitational field. Biomed Res Int. 2013;2013:598461.
- Pandithage R, Lilischkis R, Harting K, Wolf A, Jedamzik B, Luscher-Firzlaff J, Vervoorts J, Lasonder E, Kremmer E, Knoll B, Luscher B. The regulation of SIRT2 function by cyclin-dependent kinases affects cell motility. J. Cell Biol. 2008; 180:915-929.
- Patten IS, Arany Z. PGC-1 coactivators in the cardiovascular system. Trends Endocrinol. Metab. 2012; 23(2): 90–97.
- Pilchova I, Klacanova K, Tatarkova Z, Kaplan P, Racay P. The Involvement of Mg2+ in Regulation of Cellular and Mitochondrial Functions. Oxid Med Cell Longev. 2017; 2017: 6797460.
- Piskacek M, Zotova L, Zsurka G, Schweyen RJ. Conditional knockdown of hMRS2 results in loss of mitochondrial Mg(2+) uptake and cell death. J Cell Mol Med. 2009 Apr;13(4):693-700.
- Préville X, Salvemini F, Giraud S, et al. Mammalian small stress proteins protect against oxidative stress through their ability to increase glucose-6-phosphate dehydrogenase activity and by maintaining optimal cellular detoxifying machinery. Experimental Cell Research. 1999;247(1):61–78.

- Psaltis PJ, Harbuzariu A, Delacroix S, Holroyd EW, Simari RD. Resident vascular progenitor cells: diverse origins, phenotype and function. J Cardiovasc Transl Res. 2011; 4(2): 161-76.
- Qian A, Di S, Gao X, Zhang W, Tian Z, Li J, Hu L, Yang P, Yin D, Shang P. cDNA microarray reveals the alterations of cytoskeleton-related genes in osteoblast under high magneto-gravitational environment. Acta Biochim Biophys Sin(Shanghai). 2009 Jul;41(7):561-77.
- Quintá HR, Galigniana NM, Erlejman AG, Lagadari M, Piwien-Pilipuk G, Galigniana MD. Management of cytoskeleton architecture by molecular chaperones and immunophilins. Cell Signal. 2011 Dec;23(12):1907-20.
- Ravagnan L, Gurbuxani S, Susin SA, Maisse C, Daugas E, Zamzami N, Mak T, Jäättelä M, Penninger, JM, Garrido C, Kroemer G. Heat-shock protein 70 antagonizes apoptosis-inducing factor. Nat Cell Biol 2001; 3, 839-43.
- Regan ER and Aird WC. Dynamical systems approach to endothelial heterogeneity. Circ Res. 2012. 111: 110-30.
- Resnick N, Yahav H, Shay-Salit A, Shushy M, Schubert S, Zilberman LCM, Wofovitz E. Fluid shear stress and the vascular endothelium: For better and for worse. Prog. Biophys. Mol. Biol. 2003;81:177–199.
- Ribatti D, Nico B, Vacca L, Roncali L, Dammacco F. Endothelial cell heterogeneity and organ specificity. J Hematother Stem Cell Res 2002; 11:81–90.
- Riganti C, Gazzano E, Polimeni M, Aldieri E, Ghigo D. The pentose phosphate pathway: an antioxidant defense and a crossroad in tumor cell fate. Free Radic Biol Med. 2012 Aug 1;53(3):421-36.
- Rikka S, Quinsay MN, Thomas RL, Kubli DA, Zhang X, Murphy ANet al. Bnip3 impairs mitochondrial bioenergetics and stimulates mitochondrial turnover. Cell Death Differ 2011; 18: 721–731.

- Rikka S., Quinsay M.N., Thomas R.L., Kubli D.A., Zhang X.., Murphy A.N., Gustafsson Å.B. (2011) Bnip3 impairs mitochondrial bioenergetics and stimulates mitochondrial turnover. Cell Death Differ18(4):721-31.
- Rimann M, Graf-Hausner U. Synthetic 3D multicellular systems for drug development. Curr Opin Biotechnol. 2012 Oct;23(5):803-9.
- Rogalla T, Ehrnsperger M, Preville X, Kotlyarov A, Lutsch G, Ducasse C, Paul C, Wieske M, Arrigo AP, Buchner J, Gaestel M. Regulation of Hsp27 oligomerization, chaperone function, and protective activity against oxidative stress/tumor necrosis factor alpha by phosphorylation. J Biol Chem. 1999 Jul 2;274(27):18947-56.
- Rohlenova K, Veys K, Miranda-Santos I, De Bock K, Carmeliet P. Endothelial Cell Metabolism in Health and Disease. Trends Cell Biol. 2018 Mar;28(3):224-236.
- Rohlenova K, Veys K, Miranda-Santos I, De Bock K, Carmeliet P. Endothelial Cell Metabolism in Health and Disease. Trends Cell Biol. 2018;28(3):224-236.
- Romani AM. Cellular magnesium homeostasis. Arch Biochem Biophys. 2011 Aug 1;512(1):1-23.
- Romani AM. Magnesium in health and disease. Met Ions Life Sci. 2013;13:49-79.
- Rothem L, Hartman C, Dahan A, Lachter J, Eliakim R, Shamir R. Paraoxonases are associated with intestinal inflammatory diseases and intracellularly localized to the endoplasmic reticulum. Free Radic. Biol. Med. 2007; 43, 730–739.
- Runnels LW, Yue L, Clapham DE. TRP-PLIK, a bifunctional protein with kinase and ion channel activities. Science. 2001 Feb 9;291(5506):1043-7.
- Saleh A, Srinivasula SM, Balkir L, Robbins PD, Alnemri ES. Negative regulation of the Apaf-1 apoptosome by Hsp70. Nat Cell Biol. 2000; 2(8):476-83.
- Salminen A, Ojala J, Kaarniranta K, Kauppinen A. Mitochondrial dysfunction and oxidative stress activate inflammasomes: impact on the aging process and age-related diseases. Cell. Mol. Life Sci. 2012; 69, 1–15. 86.

- Sargenti A, Farruggia G, Zaccheroni N, Marraccini C, Sgarzi M, Cappadone C, Malucelli E, Procopio A, Prodi L, Lombardo M, Iotti S. Synthesis of a highly Mg(2+)-selective fluorescent probe and its application to quantifying and imaging total intracellular magnesium. Nat Protoc. 2017 Mar;12(3):461-471.
- Saxena G, Chen J, Shalev A. Intracellular shuttling and mitochondrial function of thioredoxin-interacting protein. The Journal of biological chemistry. 2010;285(6):3997–4005.
- Schmitz C, Brandao K, Perraud AL. The channel-kinase TRPM7, revealing the untold story of Mg(2+) in cellular signaling. Magnes Res. 2014 Jan-Mar;27(1):9-15.
- Schulz E, Dopheide J, Schuhmacher S, Thomas SR, Chen K, Daiber A, Wenzel P, Munzel T, Keaney JF Jr. Suppression of the JNK pathway by induction of a metabolic stress response prevents vascular injury and dysfunction. Circulation. 2008; 118:1347–1357.
- Sena CM, Pereira AM, Seica R. Endothelial dysfunction – a major mediator of diabetic
- Shen F, Kastrup CJ, Liu Y, Ismagilov RF. Threshold response of initiation of blood coagulation by tissue factor in patterned microfluidic capillaries is controlled by shear rate. Arterioscler. Thromb. Vasc. Biol. 2008;28:2035–2041.
- Simmons RD, Kumar S, Jo H. The role of endothelial mechanosensitive genes in atherosclerosis and omics approaches. Arch Biochem Biophys. 2016 Feb 1;591:111-31.
- Smith MR, Fernandes J, Go YM, Jones DP. Redox dynamics of manganese as a mitochondrial life-death switch Biochem. Biophys. Res. Commun. 2017, 482, 388-398.
- Song JW, Munn L.L. Fluid forces control endothelial sprouting. Proc. Natl. Acad. Sci. USA. 2011;108:15342–15347.
- Spindel ON, Burke RM, Yan C, Berk BC. Thioredoxin-interacting protein is a biomechanical regulator of Src activity: key role in endothelial cell stress fiber formation. Circ Res. 2014 Mar 28;114(7):1125-32.
- Spindel ON, World C, Berk BC. Thioredoxin interacting protein: redox dependent and independent regulatory mechanisms. Antioxid Redox Signal. 2012;16(6):587–596.

- Spindel ON, Yan C, Berk BC. Thioredoxin-interacting protein mediates nuclear-to-plasma membrane communication: role in vascular endothelial growth factor 2 signaling. Arterioscler Thromb Vasc Biol 2012; 32, 1264-70.
- Strzyz P. Autophagy: Mitochondria encaged. Nat Rev Mol Cell Biol. 2018 Apr;19(4):212.
- Strzyz P. Autophagy: Mitochondria encaged. Nat Rev Mol Cell Biol. 2018 Apr;19(4):212.
- Sun HB, Ren X, Liu J, Guo XW, Jiang XP, Zhang DX, Huang YS, Zhang JP. HSP27 phosphorylation protects against endothelial barrier dysfunction under burn serum challenge. Biochem Biophys Res Commun. 2015 Jul 31;463(3):377-83.
- Sun HB, Ren X, Liu J, Guo XW, Jiang XP, Zhang DX, Huang YS, Zhang JP. HSP27 phosphorylation protects against endothelial barrier dysfunction under burn serum challenge. Biochem Biophys Res Commun. 2015 Jul 31;463(3):377-83.
- Sun YL, Chen ZH, Chen XH, Yin C, Li DJ, Ma XL, Zhao F, Zhang G, Shang P, Qian AR. Diamagnetic levitation promotes osteoclast differentiation from RAW264.7 cells. IEEE Trans Biomed Eng. 2015 Mar;62(3):900-8.
- Tabrizchi R. Ecosinoids and blood vessel structure. Vasc Health Risk Manag. 2005; 1(2): 91-2.
- Tsvirkun D, Grichine A, Duperray A, Misbah C, Bureau L. Microvasculature on a chip: study of the Endothelial Surface Layer and the flow structure of Red Blood Cells. Sci Rep. 2017 Mar 24;7:45036.
- Tzima E, Irani-Tehrani M, Kiosses WB, Dejana E, Schultz DA, Engelhardt B, Cao G, DeLisser H, Schwartz MA. A mechanosensory complex that mediates the endothelial cell response to fluid shear stress. Nature. 2005;437:426–431.
- Unsworth BR, Lelkes PI. Growing tissues in microgravity. Nat Med 1998; 4:901–907.
- Valle I, Alvarez-Barrientos A, Arza E, Lamas S, Monsalve M. PGC-1alpha regulates the mitochondrial antioxidant defense system in vascular endothelial cells. Cardiovasc Res. 2005; 66:562–573.

van Loon JJ. Some history and use of the random positioning machine, RPM, in gravity related research. Advances in Space Research. 2007. 39: 1161- 65.

vascular disease. Biochim Biophys Acta. 2013; 1832: 2216-31.

Vernikos J and Schneider VS. Space, gravity and the physiology of aging: parallel or convergent disciplines?. A Mini-Review. Gerontology. 2010. 56: 157-66.

Vernon PJ, Tang D. Eat-me: autophagy, phagocytosis, and reactive oxygen species signaling. Antioxidants and Redox Signaling. 2013;18(6):677–691.

Versari S, Longinotti G, Barenghi L, Maier JA, Bradamante S. The challenging nvironment on board the International Space Station affects endothelial cell function by triggering oxidative stress through thioredoxin interacting protein overexpression: the ESA-SPHINX experiment. FASEB J. 2013. 27: 4466-75.

Versari S, Villa A, Bradamante S, Maier JA. Alterations of the actin cytoskeleton and increased nitric oxide synthesis are common features in human primary endothelial cell response to changes in gravity. Biochim Biophys Acta. 2007. 1773: 1645-52.

Versari S., Villa A., Bradamante S., Maier J. A. M. Alterations of the actin cytoskeleton and increased nitric oxide synthesis are common features in human primary endothelial cell response to changes in gravity. Biochimica et Biophysica Acta. 2007;1773(11):1645–1652.

Vorselen D, Roos WH, MacKintosh FC, Wuite GJ, van Loon J.J. The role of the cytoskeleton in sensing changes in gravity by nonspecialized cells. FASEB J2014; 28(2):536-47.

Vorselen D, Roos WH, MacKintosh FC, Wuite GJ, van Loon JJ. The role of the cytoskeleton in sensing changes in gravity by nonspecialized cells. FASEB J. 2014Feb;28(2):536-47.

Wang J, Zhang J, Bai S, Wang G, Mu L, Sun B, Wang D, Kong Q, Liu Y, Yao X, Xu Y, Li H. Simulated microgravity promotes cellular senescence via oxidant stress in rat PC12 cells. Neurochem Int 2009; 55, 710–6.

Wang J, Zhang J, Bai S, Wang G, Mu L, Sun B, Wang D, Kong Q, Liu Y, Yao X, Xu Y, Li H. Simulated microgravity promotes cellular senescence via oxidant stress in rat PC12 cells. Neurochem Int 2009; 55, 710–6.

Wang XQ, Nigro P, Fujiwara K, Yan C, Berk BC. Thioredoxin interacting protein promotes endothelial cell inflammation in response to disturbed flow by increasing leukocyte adhesion and repressing Kruppel-like factor 2. Circ. Res. 2012; 110, 560–568.

Wang YC, Lu DY, Shi F, Zhang S, Yang CB, Wang B, Cao XS, Du TY, Gao Y, Zhao JD, Sun XQ. Clinorotation enhances autophagy in vascular endothelial cells. Biochem Cell Biol. 2013;91(5):309-14.

Wang YC, Lu DY, Shi F, Zhang S, Yang CB, Wang B, Cao XS, Du TY, Gao Y, Zhao JD, Sun XQ. Clinorotation enhances autophagy in vascular endothelial cells. Biochem Cell Biol. 2013 Oct;91(5):309-14.

Wang YC, Zhang S, Du TY, Wang B, Sun XQ. Clinorotation upregulates inducible nitric oxide synthase by inhibiting AP-1 activation in human umbilical vein endothelial cells. J Cell Biochem. 2009. 107: 357-63.

Webster BR, Lu Z, Sack MN, Scott I. The role of sirtuins in modulating redox stressors. Free Radic Biol Med. 2012 Jan 15;52(2):281-90.

Wehland M, Ma X, Braun M, Hauslage J, Hemmersbach R, Bauer J, Grosse J, Infanger M, Grimm D. The impact of altered gravity and vibration on endothelial cells during a parabolic flight. Cell Physiol Biochem. 2013;31(2-3):432-51.

Widlansky ME, Gutterman DD. Regulation of endothelial function by mitochondrial reactive oxygen species. Antioxid Redox Signal. 2011 Sep 15;15(6):1517-30.

Woods C. C., Banks K. E., Gruener R., DeLuca D. Loss of T cell precursors after spaceflight and exposure to vector-averaged gravity. The FASEB Journal. 2003;17(11):1526–1528.

World C, Spindel ON, Berk BC. Thioredoxin interacting protein mediates TRX1 translocation to the plasma membrane in response to tumor necrosis factor-alpha: a key

mechanism for vascular endothelial growth factor receptor-2 transactivation by reactive oxygen species. Arterioscler. Thromb. Vasc. Biol. 2011; 31, 1890–1897.

- Yamawaki H, Pan S, Lee RT, Berk BC. Fluid shear stress inhibits vascular inflammation by decreasing thioredoxin-interacting protein in endothelial cells. J. Clin. Invest. 2005; 115, 733–738.
- Yoo SY, Kwon SM. Angiogenesis and its therapeutic opportunities. Mediators Inflamm. 2013; 2013:127170.
- Yoshioka J, Schulze PC, Cupesi M, Sylvan JD, MacGillivray C, Gannon J, Huang H, Lee RT. Thioredoxin-interacting protein controls cardiac hypertrophy through regulation of thioredoxin activity. Circulation 2004; 109, 2581–2586.
- You W, Min X, Zhang X, et al. Cardiac-specific expression of heat shock protein 27 attenuated endotoxin-induced cardiac dysfunction and mortality in mice through a PI3K/Akt-dependent mechanism. Shock. 2009;32(1):108–117.
- Zemanovic S, Ivanov MV, Ivanova LV, Bhatnagar A, Michalkiewicz T, Teng RJ, Kumar S, Rathore R, Pritchard KA Jr, Konduri GG, Afolayan AJ. Dynamic Phosphorylation of the C Terminus of Hsp70 Regulates the Mitochondrial Import of SOD2 and Redox Balance. Cell Rep. 2018 Nov 27;25(9):2605-2616.e7.
- Zschauer TC, Kunze K, Jakob S, Haendeler J, Altschmied J. Oxidative stress-induced degradation of thioredoxin-1 and apoptosis is inhibited by thioredoxin-1-actin interaction in endothelial cells. Arterioscler. Thromb. Vasc. Biol. 2011; 31, 650–656.

# 10. APPENDIX

**APPENDIX A:**

FASEB J. 2019 May; 33(5):5957-5966. doi: 10.1096/fj.201801586RR.

**APPENDIX B:**

FASEB J, accepted for publication.

THE FASEB JOURNAL • RESEARCH • www.fasebj.org

# The dynamic adaptation of primary human endothelial cells to simulated microgravity

**Alessandra Cazzaniga,[1] Laura Locatelli,[1] Sara Castiglioni, and Jeanette A. M. Maier[2]**
Dipartimento di Scienze Biomediche e Cliniche L. Sacco, Università di Milano, Milano, Italy

**ABSTRACT: Culture of human endothelial cells for 10 d in real microgravity onboard the International Space Station modulated more than 1000 genes, some of which are involved in stress response. On Earth, 24 h after exposure to simulated microgravity, endothelial cells up-regulate heat shock protein (HSP) 70. To capture a broad view of endothelial stress response to gravitational unloading, we cultured primary human endothelial cells for 4 and 10 d in the rotating wall vessel, a U.S. National Aeronautics and Space Administration–developed surrogate system for benchtop microgravity research on Earth. We highlight the crucial role of the early increase of HSP70 because its silencing markedly impairs cell survival. Once HSP70 up-regulation fades away after 4 d of simulated microgravity, a complex and articulated increase of various stress proteins (sirtuin 2, paraoxonase 2, superoxide dismutase 2, p21, HSP27, and phosphorylated HSP27, all endowed with cytoprotective properties) occurs and counterbalances the up-regulation of the pro-oxidant thioredoxin interacting protein (TXNIP). Interestingly, TXNIP was the most overexpressed transcript in endothelial cells after spaceflight. We conclude that HSP70 up-regulation sustains the initial adaptive response of endothelial cells to mechanical unloading and drives them toward the acquisition of a novel phenotype that maintains cell viability and function through the sequential involvement of different stress proteins.—Cazzaniga, A., Locatelli, L., Castiglioni, S., Maier, J. A. M. The dynamic adaptation of primary human endothelial cells to simulated microgravity. FASEB J. 33, 000–000 (2019). www.fasebj.org**

**KEY WORDS:** HUVEC · RWV · stress response

The importance of human exploration of space has been underscored by many successful missions over the past 50 yr. With the increased duration of these missions, it has become evident that space affects the health of astronauts. Space represents a unique environment where various hazardous stimuli coexist. Besides radiation, microgravity importantly contributes to activating an adaptive response, which might be beneficial in space but might exert detrimental effects on tissues and cells when returning to Earth (1). To get insights into the cellular and molecular events involved in human adaptation to weightlessness, many human cell types have been studied in real or simulated microgravity (1). It is now clear that mammalian cells sense alterations of gravity as a stressful event and turn physical cues into biochemical signals, which reprogram their activities (2).

Endothelial cells (ECs), crucial for the integrity of the vascular wall, are very sensitive to mechanical hints (3). In response to different hemodynamic forces, such as fluid shear stress and blood pressure, ECs convert mechanical forces into various biochemical signals, which govern endothelial function and vascular remodeling. Just after the beginning of space missions, it became evident that another physical force (*i.e.*, gravity) is important in regulating endothelial behavior (1). Similar to what happens in response to disturbed shear stress or high blood pressure, gravitational unloading impairs endothelial homeostasis, and this has a role in the onset of spaceflight-associated cardiovascular deconditioning (4). Several studies have investigated the impact of simulated and real microgravity on the function of primary human ECs (5). In particular, the HUVEC is a consolidated model of macrovascular ECs, because HUVEC gene expression clusters tightly with that of other large-vessel ECs (6). In HUVECs, simulated microgravity remodels the cytoskeleton, modulates cell proliferation and cytokine expression, enhances NO production, and up-regulates heat shock protein (HSP) 70 (7–11). Under normal conditions, HSP70 is barely detectable, whereas in response to cellular stress, HSP70 is rapidly up-regulated. In addition to serving as a chaperonin, HSP70 protects ECs from apoptosis by interfering with

**ABBREVIATIONS:** CDKN1A, cyclin-dependent kinase inhibitor 1A; CTR, static 1 *g* conditions; DCFH, 2′-7′-dichlorofluorescein diacetate; EC, endothelial cell; GAPDH, glyceraldehyde-3-phosphate dehydrogenase; GSH, reduced glutathione; GSSG, oxidized glutathione; HSP, heat shock protein; ICAM-1, intercellular adhesion molecule 1; P-HSP27, phosphorylated HSP27; PON2, paraoxonase 2; ROS, reactive oxygen species; RWV, rotating wall vessel; siRNA, small interfering RNA; SIRT2, sirtuin 2; SOD2, superoxide dismutase 2; SPHINX, Spaceflight of HUVECs, Integrated Experiment; TXNIP, TXR interacting protein; TXR, thioredoxin

[1] These authors contributed equally to this work.

[2] Correspondence: Dipartimento di Scienze Biomediche e Cliniche L. Sacco, Università di Milano, Via GB Grassi 74, 20157 Milano, Italy. E-mail: jeanette.maier@unimi.it

doi: 10.1096/fj.201801586RR

key apoptotic proteins (12), and, accordingly, no apoptosis was detected in HUVECs in simulated microgravity (13). However, it is not yet known if HSP70 up-regulation is directly implicated in preventing cell death in simulated microgravity.

All of these results have been obtained using both the rotating wall vessel (RWV) and the random positioning machine to simulate microgravity for times ranging between 4 and 96 h. These surrogate systems for benchtop microgravity research reduce the average gravitational force acting on the cells to about $10^{-2}$–$10^{-3}$ $g$ (8). It is noteworthy that culture of HUVECs, human microvascular ECs, and U937 cells either in the RVW or in the random positioning machine yielded similar results (8, 14, 15). In the case of U937 cells, data obtained in these bioreactors reflect the findings obtained in true microgravity (16).

Two experiments on HUVECs have been performed in space (17–19). The first one lasted 12 d, and the cells displayed profound cytoskeletal alterations, reduced metabolic activity, and increased permeability, which were not reversible upon return to Earth (17, 18). In "Spaceflight of HUVEC: an Integrated Experiment (SPHINX)" (19), HUVECs were cultured for 10 d on the International Space Station. Postflight analysis demonstrated that spaceflight modulates the expression of more than 1000 genes (19), among which the most overexpressed is thioredoxin interacting protein (TXNIP) (19), a stress-responsive gene encoding a protein that contrasts the antioxidant action of thioredoxin (TXR). Currently, no data are available about TXNIP expression in HUVECs in simulated microgravity.

In this work, we aim to define HUVEC stress response after 4 and 10 d of culture in the RWV. Four days is the maximal time length utilized in simulated microgravity, whereas 10 d corresponds to the duration of SPHINX. Moreover, because experiments in space are demanding and subject to several restraints, including the difficulty of culturing enough cells to perform quantitative studies at the protein level, we here extend previous studies limited to gene expression to the assessment of the proteins.

## MATERIALS AND METHODS

### Cell culture

HUVECs were from the American Type Culture Collection (Manassas, VA, USA) and serially passaged in M199 containing 10% fetal bovine serum, 150 μg/ml EC growth factor, 2 mM glutamine, 1 mM sodium pyruvate, and 5 U/ml heparin on 2% gelatin-coated dishes. The cells were routinely tested for the expression of endothelial markers and used for 5–6 passages. All culture reagents were from Thermo Fisher Scientific (Waltham, MA, USA). To generate microgravity, we utilized the RWV (Synthecon, Houston, TX, USA) after seeding on beads (Cytodex 3; MilliporeSigma, Burlington, MA, USA) (7, 8, 20). As controls, HUVECs grown on beads were cultured in the vessels not undergoing rotation. By 3-[4,5-dimethylthiazole-2-*yl*]-2,5-diphenyltetrazolium bromide assay, HUVECs cultured in static 1 $g$ conditions (CTR) and RWV-cultured HUVECs are viable after 4 and 10 d (unpublished results). In addition, the cells were trypsinized, stained with trypan blue solution (0, 4%), and counted using a Luna Automated Cell Counter (Logos Biosystems, Anyang, South Korea). After 4 d, a 2-fold induction was observed in HUVECs cultured in the RWV *vs.* their controls (7, 8), but at d 10 the cell number was similar as confluence was reached.

### Silencing HSP70

The cells were treated with HSP70 small interfering RNA [siRNA; 1 μg, 5′-TTCAAAGTAAATAAACTTTAA-3′ (Qiagen, Germantown, MD, USA)] and 6 μl HiPerfect Transfection Reagent (Qiagen), according to the manufacturer's recommendations. After 8 h, the siRNA transfection medium was replaced with fresh standard medium, and the cells were transferred into the RWV. After 48 h the cells were trypsinized, stained with trypan blue solution (0, 4%), and counted as described above. In parallel, apoptosis was assessed using the Cell Death Detection ELISA photometric enzyme immunoassay (MilliporeSigma), which measures cytoplasmic histone-associated DNA fragments (mono- and oligonucleosomes) in the cytoplasmic fraction of cell lysates (21). The experiment was performed in triplicate 2 times. Data are expressed as means ± SD.

### Real-time PCR

Total RNA was extracted by the PureLink RNA Mini Kit (Thermo Fisher Scientific). Single-stranded cDNA was synthesized from 1 μg RNA in a 20-μl final volume using the High-Capacity cDNA Reverse Transcription Kit with RNase inhibitor (Thermo Fisher Scientific), according to the manufacturer's instructions. Real-time PCR was performed in triplicate on the 7500 Fast Real-Time PCR System instrument using TaqMan Gene Expression Assays (Thermo Fisher Scientific). **Table 1** summarizes the primers used. The housekeeping gene glyceraldehyde-3-phosphate dehydrogenase (*GAPDH*) was used as an internal reference gene. Relative changes in gene expression were analyzed by the $2^{-\Delta\Delta Ct}$ method (22). The experiment was performed in triplicate 2 times. Data are expressed as means ± SD.

### Reactive oxygen species production, reduced *vs.* oxidized glutathione, and comet assay

Reactive oxygen species (ROS) production was quantified using 2′-7′-dichlorofluorescein diacetate (DCFH) on HUVECs cultured in simulated microgravity for various times. The cells were rapidly transferred into black-bottomed 96-well plates (Greiner Bio-One, Kremsmünster, Austria) and exposed for 30 min to 20 μM DCFH solution. The emission at 529 nm of the DCFH dye was monitored using the Glomax-Multi Detection System (Promega, Madison, WI, USA) (23). The results are the means of 3 independent experiments performed in quadruplicate. Data are shown as percentages of ROS levels in HUVECs cultured in the RWV *vs.* CTR ± SD.

TABLE 1. *List of the primers used for real-time PCR*

| Gene | Primer |
|---|---|
| *TXNIP* | Hs00197750_m1 |
| *SIRT2* | Hs00247263_m1 |
| *HSPA1A* | Hs00197750_m1 |
| *CDKN1A* | Hs00355782_m1 |
| *PON2* | Hs00165563_m1 |
| *SOD2* | Hs00167309_m1 |
| *HSPB1* | Hs00356629_g1 |
| *GAPDH* | Hs99999905_m1 |

Reduced glutathione (GSH) and oxidized glutathione (GSSG) were measured using the GSH/GSSG-Glo Assay (Promega), which is a luminescence-based system, according to the manufacturer's instructions. Data are shown as percentages of GSH/GSSG levels in HUVECs cultured in the RWV *vs.* CTR ± SD.

Comet assay was performed after various times of culture in the RWV. HUVECs were mixed with low-melting-point agarose and spread on pretreated slides, which were dyed, immersed in ice-cold lysis solution (0.01 M Tris-HCl, pH 10; 2.5 M NaCl; 0.1 M EDTA; 0.3 M NaOH; 1% Triton; 10% DMSO), and incubated at 4°C for 60 min. Electrophoresis was conducted in ice-cold running buffer (0.3 M NaOH, 0.001 M EDTA) for 30 min at 300 mA. The slides were then rinsed, fixed in ice-cold methanol for 3 min, dried at room temperature, stained with ethidium bromide, and analyzed with a fluorescence microscope (23).

### Protein array

After various times of culture in the RWV or in CTR, conditioned media were collected, and HUVECs were lysed in a buffer containing 50 mM Tris-HCl (pH 8.0), 150 mM NaCl, 1 mM EDTA, and 1% NP-40. Cell extracts (80 μg) were utilized to incubate the membranes on which 26 antibodies against human cell stress-related proteins were spotted in duplicate (R&D Systems, Minneapolis, MN, USA) (22), according to the manufacturer's instructions. Densitometry was performed using ImageJ software (National Institutes of Health, Bethesda, MD, USA). Two separate experiments were performed, and data are expressed as percentages of the fold increase in the signal intensity of RWV *vs.* CTR. Conditioned media were used to incubate the membrane on which 40 antibodies against proteins involved in inflammation were spotted in duplicate (RayBiotech, Norcross, GA, USA). Two separate experiments were performed, and representative blots are shown. According to the ImageJ software, no significant differences were detected in any spot (unpublished results). ELISA was utilized to measure the amounts of intercellular adhesion molecule 1 (ICAM-1) (LifeSpan BioSciences, Seattle, WA, USA), according to the manufacturer's instructions. Data are shown as percentages of ICAM-1 levels in HUVECs cultured in the RWV *vs.* CTR ± SD.

### Western blot

HUVECs were lysed in 10 mM Tris-HCl (pH 7.4) containing 3 mM $MgCl_2$, 10 mM NaCl, 0.1% SDS, 0.1% Triton X-100, 0.5 mM EDTA, and protein inhibitors, separated on SDS-PAGE, and transferred to nitrocellulose sheets at 400 mA for 2 h at 4°C. Western analysis was performed using antibodies against HSP70 and cyclin-dependent kinase inhibitor-1 p21 (Santa Cruz Biotechnology, Dallas, TX, USA), TXNIP and paraoxonase 2 (PON2) (Thermo Fisher Scientific), sirtuin 2 (SIRT2) (MilliporeSigma, Vimodrone, Italy), superoxide dismutase 2 (SOD2) (BD Biosciences, San Jose, CA, USA), HSP27 and phosphorylated HSP27 (P-HSP27) (Cell Signaling Technology, Danvers, MA, USA), and GAPDH (Santa Cruz Biotechnology). After extensive washing, secondary antibodies labeled with horseradish peroxidase (GE Healthcare, Waukesha, WI, USA) were used. Immunoreactive proteins were detected by the SuperSignal Chemiluminescence Kit (Thermo Fisher Scientific) (24).

### NOS activity

NOS activity was measured in the conditioned media by using the Griess method (25). Briefly, conditioned media were mixed with an equal volume of freshly prepared Griess reagent. The absorbance was measured at 550 nm. The concentrations of nitrites in the samples were determined using a calibration curve generated with standard $NaNO_2$ solutions. The experiment was performed in triplicate and repeated 5 times with similar results. Data are shown as percentages of $NaNO_2$ release in HUVECs cultured in the RWV *vs.* CTR ± SD.

### Confocal imaging

After 4 and 10 d in the RWV, HUVECs were trypsinized and cytospun on frosted microscope glasses, fixed in PBS containing 3% paraformaldehyde and 2% sucrose (pH 7.6), permeabilized with 4-(2-hydroxyethyl)-1-piperazineethanesulfonic acid–Triton 1%, incubated with anti-TXNIP immunopurified IgGs overnight at 4°C, and stained with an Alexa Fluor 546 secondary antibody (Thermo Fisher Scientific). Finally, cells were mounted with moviol, and images were acquired using a ×63 objective in oil by an SP8 confocal microscope (Leica Microsystems, Buffalo Grove, IL, USA).

### Statistical analysis

Statistical significance was determined using the Student's *t* test and set at a value of $P < 0.05$.

## RESULTS

### The activation of stress response in HUVECs exposed to simulated microgravity

To have a rapid overview of HUVEC stress response in simulated microgravity, we utilized a protein array specifically tailored for stress proteins. Eighty micrograms of lysates from cells cultured in the RWV for 4 and 10 d were utilized. Out of 26 proteins investigated, HSP70, SIRT2, PON2, SOD2, p21, and P-HSP27 were up-regulated (**Fig. 1**).

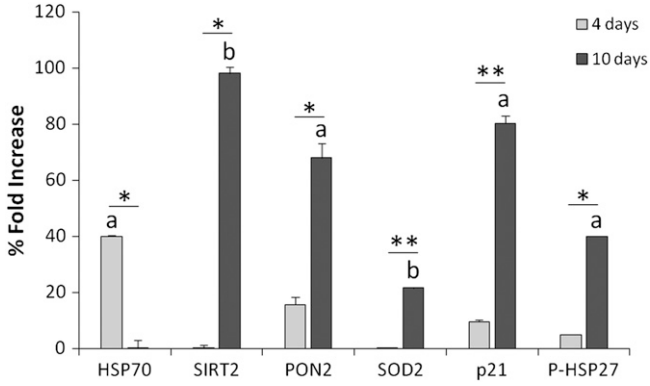


**Figure 1.** Stress response in HUVECs exposed to simulated microgravity. HUVECs were cultured in the RWV or in CTR for 4 and 10 d. Protein array was performed on cell extracts. Densitometric analysis on array spots was performed, and data are expressed as percentages of the fold increase of the signal intensity obtained in cells in the RWV *vs.* CTR. Different letters (*a*, *b*) indicate the statistically significant effect of RWV *vs.* CTR ($^aP < 0.05$, $^bP < 0.01$). $*P < 0.05$, $**P < 0.01$ (indicates the statistically significant variation of RWV 4 d *vs.* RWV 10 d).

In some cell types, microgravity induces oxidative stress (26–28). Therefore, we measured ROS production by DCFH fluorescence in HUVECs cultured in the RWV for various times. We found a modest, albeit statistically significant, increase of ROS after 2 h in cells in simulated microgravity (RWV) *vs.* CTR and no differences thereafter (**Fig. 2*A***). Because GSH is the most abundant antioxidant in aerobic cells (29), we measured the ratio GSH/GSSG and found it significantly decreased after 2 h in the RWV but not at later times (Fig. 2*B*), thus reinforcing the results obtained using DCFH.

In addition, no oxidative damage of DNA was detected by comet assay (Fig. 2*C*). We propose that the increased amounts of ROS detected after 2 h of culture in the RWV did not reach the threshold to damage DNA.

## HSP70 in HUVECs exposed to simulated microgravity

We have previously shown that HSP70 is induced in HUVECs after 24 h of exposure in simulated microgravity and remains elevated up to 96 h (7). In this study, experiments were performed after 4 and 10 d of culture in the RWV. Real-time PCR demonstrates the overexpression of *HSPA1A* (*HSP70*) and Western blot shows the up-regulation of HSP70 (2.1-fold induction) after 4 d of culture in the RWV. Both RNA and proteins return to baseline after 10 d in simulated microgravity (**Fig. 3*A*, *B***).

To understand the role of HSP70 in the early response to simulated microgravity, we transiently silenced *HSP70* using a specific siRNA before exposing HUVECs to gravitational unloading for 48 h. As a control, the cells were exposed to a noninterfering, scrambled sequence. By real-time PCR, *HSP70* expression was down-regulated in silenced HUVECs (Fig. 3*C*). We then counted the cells. As expected (7, 8), HUVECs in the RWV proliferated faster than those in CTR. Silencing *HSP70* completely prevented this effect and cell number was lower than in the controls (Fig. 3*D*). One of the roles of HSP70 is to protect the cells from apoptosis (12). To understand the behavior of HUVEC-silencing *HSP70*, we measured cleaved nucleosomes as an index of apoptosis in HUVECs after 48 h in the RWV using an ELISA. TNF-α (50 ng/ml) was used as a positive control. Figure 3*E* shows that silencing *HSP70* induced the cleavage of

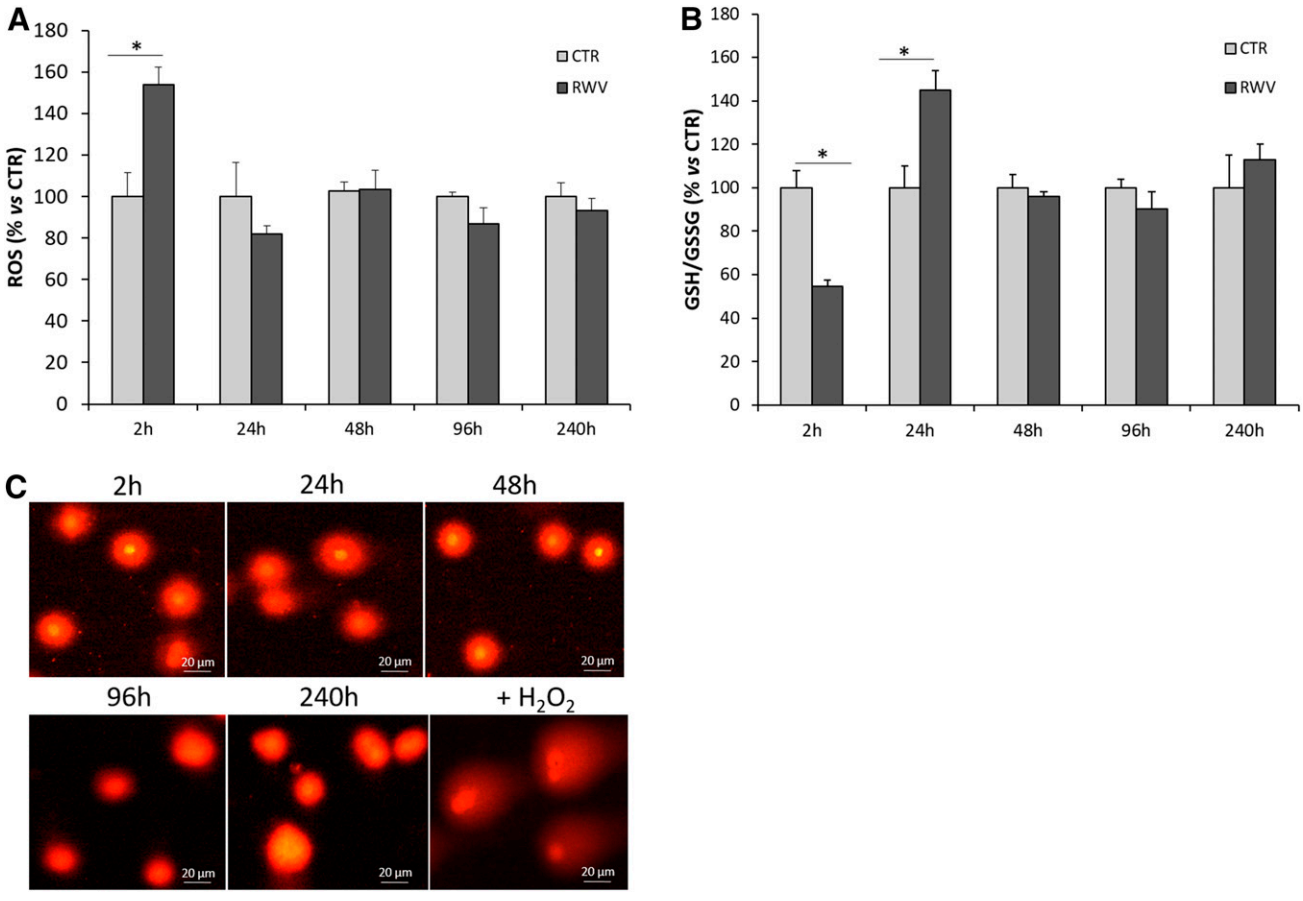


**Figure 2.** ROS generation, GSH/GSSG ratio, and oxidative damage to DNA in HUVECs exposed to simulated microgravity. HUVECs were cultured for various times in the RWV or in CTR. *A*) ROS generation was measured by DCFH. Data are shown as percentages of ROS levels in HUVECs cultured in the RWV *vs.* CTR. *B*) GSH/GSSG ratio was calculated as described in the Materials and Methods. Data are shown as percentages of GSH/GSSG levels in HUVECs cultured in the RWV *vs.* CTR. *C*) Comet assay was performed. After staining with ethidium bromide, the slides were analyzed using a fluorescence microscope. Exposure to $H_2O_2$ (100 μM) for 2 h was used as a positive CTR. Scale bars, 20 μm. $^*P < 0.05$.

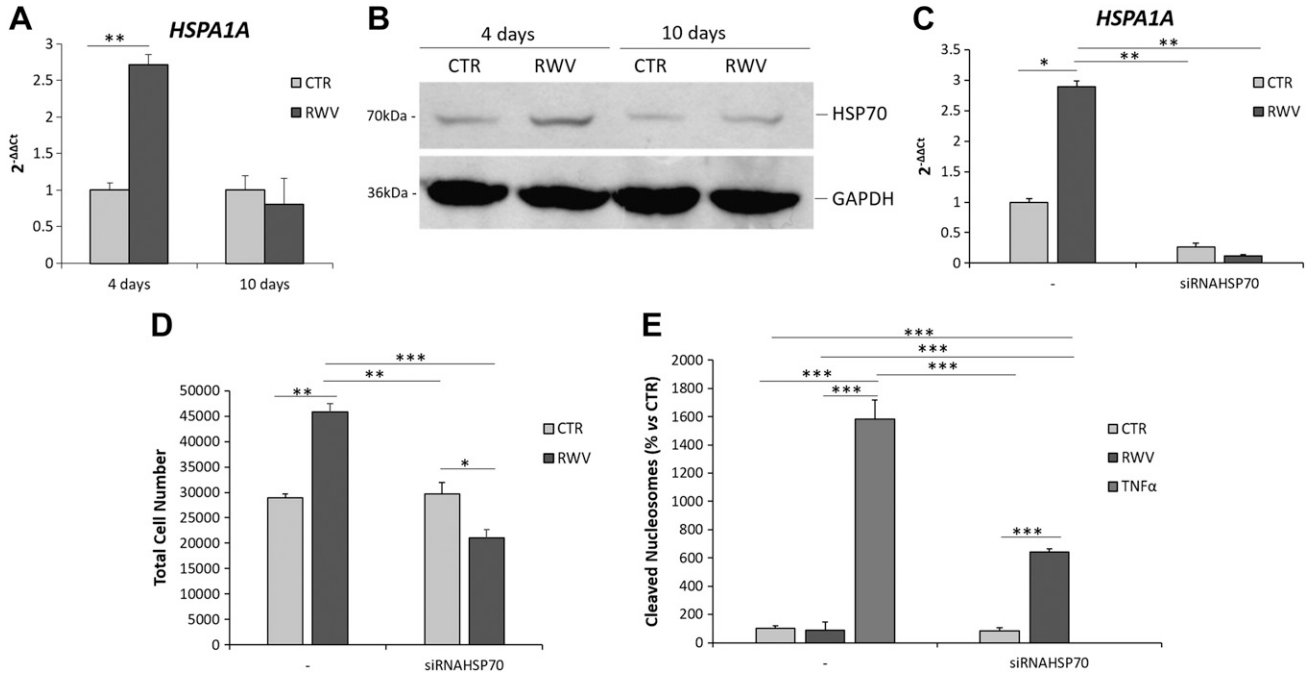


**Figure 3.** The levels and the role of HSP70 in HUVECs exposed to simulated microgravity. *A*) HUVECs were cultured in the RWV or in CTR for 4 and 10 d. Real-time PCR was performed using primers designed on the *HSPA1A* sequence. The experiment was repeated 3 times in triplicate. *B*) Western blot was performed using specific antibodies against HSP70. GAPDH was used as marker of loading. A representative blot is shown. *C*) HUVECs were transfected with siRNA against *HSP70* or with a scrambled nonsilencing sequence (−) and maintained in the RWV or in CTR for 48 h. To assess silencing, real-time PCR was performed using primers designed on the *HSPA1A* sequence. *D*) Cells treated as in *C* were trypsinized and counted. *E*) Cell death in extracts from HUVECs treated as in *C* was assessed using a Cell Death Detection ELISA Kit, which measures the amount of cleaved DNA and histone complexes. TNF-α (50 ng/ml) for 48 h was the positive CTR. $*P < 0.05$, $**P < 0.01$, $***P < 0.001$.

nucleosomes in HUVECs exposed for 48 h to simulated microgravity.

## SIRT2, PON2, SOD2, p21, and HSP27 in HUVECs exposed to simulated microgravity

Next, we examined the levels of the other stress proteins that were increased by protein array. Western blot confirmed that PON2, SOD2, HSP27, and its phosphorylated form are up-regulated after 10, but not 4, d of exposure to simulated microgravity (**Fig. 4*A***). The total amounts of SIRT2 decreased in CTR after 10 d, whereas in HUVECs cultured in the RWV, SIRT2 remained elevated. After 10 d in the RWV, we also detected higher amounts of p21, a cyclin-dependent kinase inhibitor, which also plays a role in stress response (Fig. 4*A*).

It is noteworthy that no significant modulation of *SIRT2*, *PON2*, *SOD2*, and *HSPB1* (*HSP27*) was found by real-time PCR (Fig. 4*B*), thus confirming the results of SPHINX (19). On the contrary, cyclin-dependent kinase inhibitor 1A (*CDKN1A*) (*p21*) was markedly overexpressed after 10 d of culture in the RWV. Our results indicate that *1*) apart from *CDKN1A*, the induction of these proteins is not transcriptionally regulated, and 2) studies limited to gene expression as in Versari *et al.* (19) might hinder our understanding of the complex network of events activated in microgravity.

To understand whether the up-regulation of stress proteins depends on quiescence, which is reached after 8 d in culture (5, 7), we compared the total amounts of SIRT2, PON2, SOD2, HSP70, HSP27, and its phosphorylated form in proliferating *vs.* quiescent HUVECs under physiologic 1 *g* conditions. Whereas SIRT2 was down-regulated and p21 up-regulated in quiescent cells, the other proteins did not change in proliferating *vs.* quiescent cells (Fig. 4*C*). We propose that the up-regulation of PON2, SOD2, HSP70, and HSP27 observed in HUVECs cultured in the RWV is due to gravitational unloading itself.

## TXNIP in HUVECs exposed to simulated microgravity

Because *TXNIP* is overexpressed in HUVECs cultured in space (19), we examined the levels of its transcript and the total amounts of the protein by real-time PCR and Western blot, respectively. In agreement with Versari *et al.* (19), we found that *TXNIP* was overexpressed in HUVECs after 10 d in the RWV (**Fig. 5*A***), whereas no modulation of *TXNIP* was detected at d 4 (Fig. 5*A*). Western blot shows that the increase of the RNA correlated with the increase of the protein (2-fold induction at d 10; Fig. 5*B*). Because TXNIP is localized both in the nucleus and in the cytoplasm of HUVECs (30), it is noteworthy that we found the increase of both nuclear and cytosolic TXNIP in HUVECs cultured in the RWV for 10 d by confocal microscopy. No differences emerged after 4 d in simulated microgravity (Fig. 5*C*).

We then compared the total amounts of TXNIP in proliferating *vs.* quiescent HUVECs (Fig. 5*D*) and found

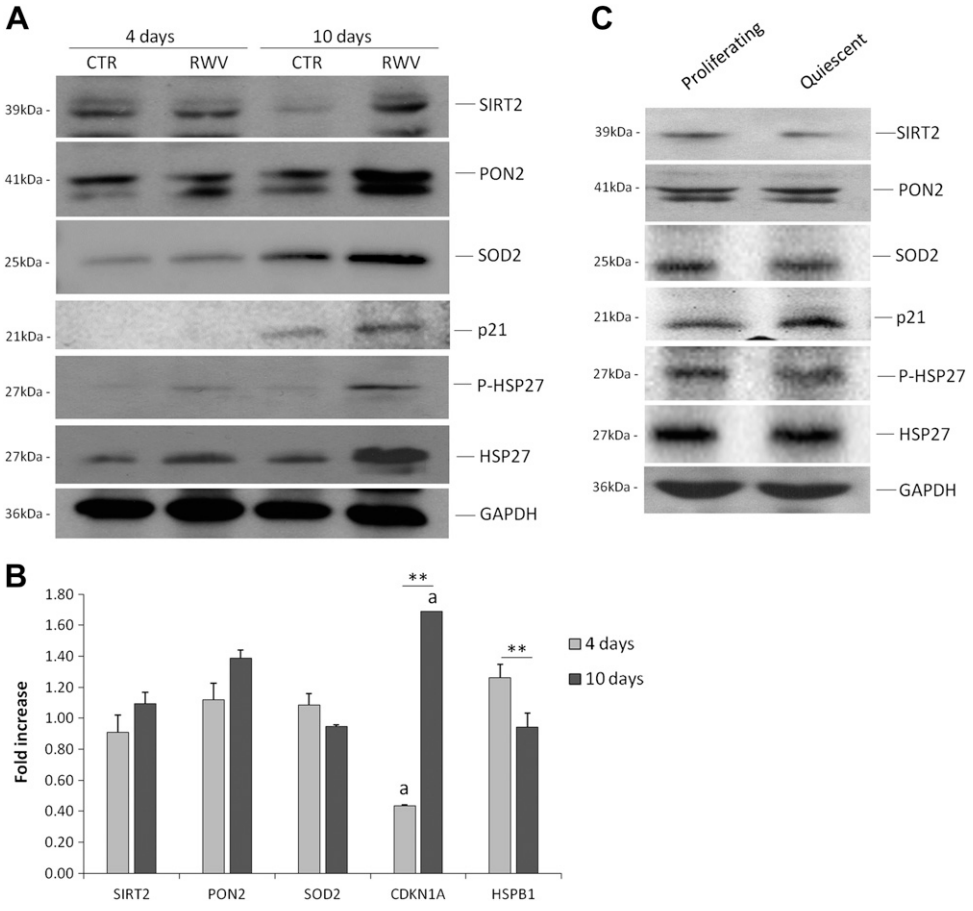


**Figure 4.** Stress proteins in HUVECs exposed to simulated microgravity. *A*, *B*) HUVECs were cultured in the RWV or in CTR for 4 and 10 d. Western blot and real-time PCR were performed as described in the Materials and Methods. All the values were normalized with respect to their controls cultured in CTR. $^{a}P < 0.05$ (indicates the significant effect of RWV *vs.* CTR). $^{*}P < 0.05$, $^{**}P < 0.01$ (indicates the statistically significant variation of RWV 4 d *vs.* RWV 10 d). *C*) Proliferating and quiescent HUVECs were analyzed for the total amounts of stress proteins by Western blot.

that TXNIP decreases in quiescent cells, thus suggesting that simulated microgravity is directly responsible for the up-regulation of TXNIP after 10 d in RWV.

## Endothelial function in HUVECs exposed to simulated microgravity

NO is a multifunctional molecule that influences vascular functions. We have previously shown that HUVECs cultured in simulated microgravity for 24 and 48 h release higher amounts of NO than those cultured in CTR (8). After 4 d of culture in the RWV, HUVECs continued to release more NO than CTR, whereas at d 10, no significant differences were detected (**Fig. 6*A***).

Inflammatory mediators affect endothelial function, and alterations of the cytokine network have been described in ECs exposed to simulated microgravity for 24 and 48 h (7, 9, 20).

In HUVECs cultured in simulated microgravity for 24 and 48 h, a decrease of ICAM-1 was described (9). By ELISA, we did not find any difference in the total amount of ICAM-1 in cells maintained in the RWV for 4 and 10 d (Fig. 6*B*).

To obtain a broad profile of the cytokine network in HUVECs cultured in the RWV for 4 and 10 d, we utilized a human inflammation antibody array. After centrifugation, conditioned media were analyzed. We did not detect any significant alteration in the total amounts of cytokines and chemokines secreted in the conditioned media by HUVECs exposed to simulated microgravity (RWV) *vs.* CTR (Fig. 6*C*, *D*), as confirmed by the ImageJ software (unpublished results).

## DISCUSSION

Until now, HUVECs have been cultured in simulated microgravity for various times but not longer than 96 h (5, 7–9). In this study, we focus on the stress response activated by HUVECs exposed to simulated microgravity for 4 and 10 d and demonstrate the crucial early role of HSP70 and the involvement of other stress proteins thereafter.

HSP70 is induced in HUVECs after 24 h of exposure to simulated microgravity (7), is still elevated at d 4, and decreases to baseline at d 10, as suggested by SPHINX (19). We hypothesize that mechanical unloading determines alterations of protein folding, protein aggregation, or both and that this is the trigger for HSP70 up-regulation. Indeed, in HUVECs in microgravity, we and others have reported the early disorganization of the cytoskeleton with the formation of perinuclear clusters of actin (5, 7, 17). HSP70 is thought to participate in folding pathways of cytoskeletal proteins (31). Accordingly, we found that cytoskeletal disruption by cytochalasin D is associated with an increase of HSP70 (unpublished results). We anticipate that the cytoskeleton senses the altered mechanical loading and converts the reduced mechanical stimuli in chemical signals that activate the stress response necessary to maintain the cells' viability. The pivotal role of the

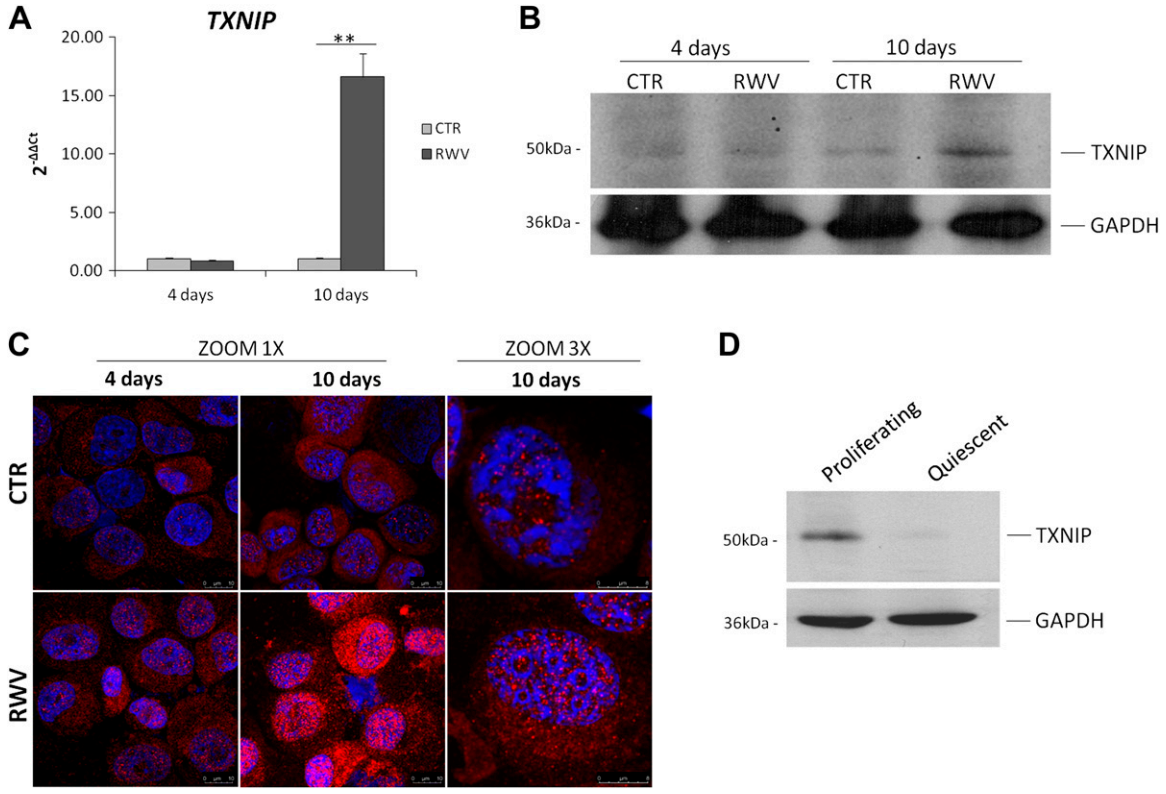


**Figure 5.** TXNIP in HUVECs exposed to simulated microgravity. *A*, *B*) HUVECs were cultured in the RWV or in CTR for 4 and 10 d. Real-time PCR and Western blot were performed as described in the Materials and Methods. *C*) HUVECs cultured as above were cytospun and stained with DAPI to detect the nuclei and with antibodies against TXNIP. Images were acquired using a ×63 objective in oil by an SP8 confocal microscope (left and center panels, ×1 magnification; right panels, ×3 magnification). *D*) Proliferating and quiescent HUVECs were analyzed for the total amounts of TXNIP by Western blot. $^{**}P < 0.01$.

increase of HSP70 is underlined by the demonstration that silencing *HSP70* induces apoptosis in HUVECs in simulated microgravity. Indeed, HSP70 not only buffers protein misfolding but also inhibits apoptosis acting on caspase-dependent and independent pathways. Altogether, these results indicate that HSP70 is an early gatekeeper for HUVEC

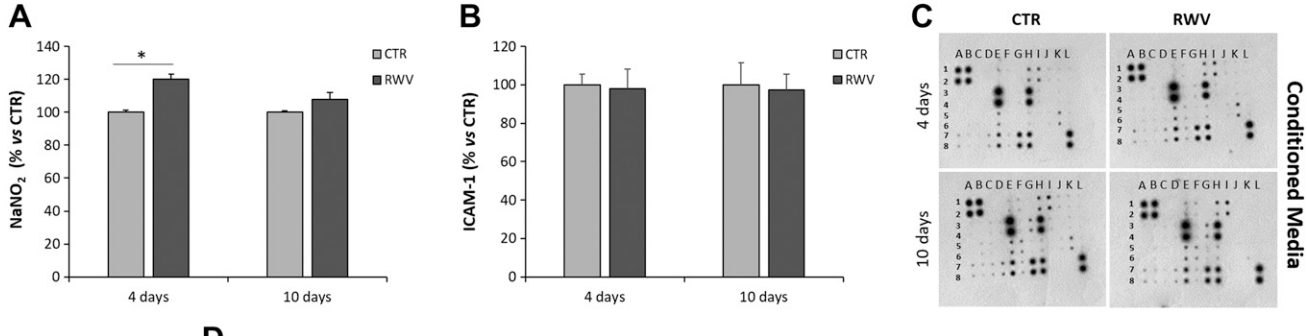


D

| | A | B | C | D | E | F | G | H | I | J | K | L |
|---|---|---|---|---|---|---|---|---|---|---|---|---|
| 1 2 | POS | POS | NEG | NEG | Eotaxin-1 | Eotaxin-2 | GCSF | GM-CSF | ICAM-1 | INF-γ | CCL1 | IL-1α |
| 3 4 | IL-1β | IL-2 | IL-3 | IL-4 | IL-6 | IL-6R | IL-7 | IL-8 | IL-10 | IL-11 | IL-12 p40 | IL-12 p70 |
| 5 6 | IL-13 | IL-15 | IL-16 | IL-17 A | IP-10 | MCP-1 | MCP2 | M-CSF | MIG | MIP-1α | MIP-1β | MIP-1δ |
| 7 8 | RANTES | TGF-β1 | TNFα | TNFβ | TNFRI | TNFRII | PDGF-BB | TIMP-2 | BLANK | BLANK | NEG | POS |

**Figure 6.** NO production and inflammatory response in HUVECs exposed to simulated microgravity. HUVECs were cultured in RWV or in CTR for 4 and 10 d. *A*) NO was measured by the Griess method. Data are shown as percentages of $NaNO_2$ release in HUVECs cultured in the RWV *vs.* CTR. *B*) ICAM-1 levels were determined on 80 μg of cell extracts by ELISA. *C*) Inflammatory protein array was performed on conditioned medium. Representative membranes are shown. *D*) Map of the membrane array. $^{*}P < 0.05$.

survival under mechanical unloading. Moreover, HSP70 binds SOD2 in ECs and chaperons it to the mitochondria (32), thus limiting mitochondrial oxidative stress. Accordingly, we did not detect any significant accumulation of ROS in our experimental model.

After 96 h of culture in the RWV, HSP70 returns to basal levels, whereas other stress proteins are up-regulated. Indeed, after 10 d, the amounts of SIRT2, PON2, SOD2, and HSP27 and its phosphorylated form are higher in HUVECs in simulated microgravity than in the 1G conditions. The dysregulation of the anti- and pro-oxidant enzymes we observe in simulated microgravity is not the result of quiescence but seems to be specifically determined by gravitational unloading.

SIRT2, a member of the sirtuin family, is a $NAD^+$-dependent deacetylase, highly expressed in vascular ECs (33). SIRT2 increases endothelial viability and decreases the levels of ROS by elevating the expression of catalase, glutathione peroxidase, and SOD2 (32). Accordingly, SOD2 is up-regulated in simulated microgravity, and PON2 also increases in HUVECs in the RWV. PON2 is part of the paraxonase family and, besides its lactonase activity, reduces superoxide leakage from the inner mitochondrial membrane (34), thus representing an important defense mechanism against oxidative stress. PON2 also decreases endoplasmic reticulum stress-induced caspase activation (35). We also show an up-regulation of HSP27 and P-HSP27. Wild-type HSP27 lowers the levels of ROS by raising intracellular glutathione (36), whereas P-HSP27 prevents apoptosis interfering with the caspase cascade (33). In addition, HSP27 maintains the stability of actin fibers (37), a function that might be relevant under gravitational unloading to preserve the remaining components of the cytoskeleton.

Besides their own specific function, the common denominator of SIRT2, PON2, SOD2, and HSP27 is their potent antioxidant and antiapoptotic potential. Indeed, despite the marked increase of TXNIP in HUVECs after 10 d in simulated microgravity, we do not observe any accumulation of ROS. Our results suggest that the increased amounts of SIRT2, PON2, SOD2, and HSP27 counterbalance the oxidant action of TXNIP. On the contrary, oxidative stress has been reported in murine fetal fibroblasts and in rat neuronal PC12 cells in simulated microgravity (26, 27) as the result of an imbalance between pro- and antioxidant enzymes. These differences might be due to a more efficient antioxidant arsenal in ECs than in other cell types. In *Caenorhabditis elegans*, an invaluable model that has allowed major advances in our knowledge in many biologic processes, simulated microgravity induces oxidative stress, but also importantly activates the antioxidant defense system in an attempt to reverse the adverse effects of free radicals on nematodes. Therefore, in *C. elegans*, as well as in ECs, both the molecular machineries for the control of oxidative stress and the antioxidant defense system are dysregulated in simulated microgravity.

TXNIP up-regulation is interesting because it confirms what Versari *et al.* (19) described in SPHINX, although limited to RNA level. TXNIP expression is induced by a variety of stresses, including ionizing and exciting radiations, $H_2O_2$, and mechanical forces (38). In fact, TXNIP acts as a blood flow mechanosensor (39) and is overexpressed when blood flow is disturbed (39). We hypothesize that the alteration of mechanical forces because of microgravity triggers TXNIP up-regulation. In general, TXNIP overexpression renders the cells more susceptible to oxidative stress (40); however, in our experimental model, this is not the case, because we do not detect any increase of ROS or any sign of DNA oxidative damage. As previously mentioned, the pro-oxidant effect of TXNIP is likely to be counterbalanced by the complex and articulated increase of various stress proteins with antioxidant activity. Beyond its role as an endogenous inhibitor of TXR, TXNIP also exerts TXR-independent functions, such as regulation of metabolism and cell growth (41). In HUVECs under stress, TXNIP stimulates the transactivation of VEGF receptor type 2, which is fundamental for endothelial survival (30). It is feasible that TXNIP orchestrates several cellular responses that enable HUVECs to survive microgravity-related stress.

Interestingly, p21 is also increased in HUVECs cultured in the RWV for 10 d. Apart from its role in growth arrest, p21 is induced by a wide range of stress stimuli through p53-dependent and -independent pathways (42). Indeed, p21 exerts a protective action against stress because of its well-described antiapoptotic effects (42).

Our data suggest that the complex and dynamic adaptive response of HUVECs to simulated microgravity contributes to the maintenance of their function. Indeed, we did not detect any alteration in the synthesis and secretion of inflammatory cytokines and chemokines or in the amounts of ICAM-1. NO, crucial to maintain endothelial function (43), was elevated in HUVECs exposed to simulated microgravity for 48 h (8). Here we show that NO is increased after 4 d in the RWV and returns to control levels at d 10.

In general, it is noteworthy that culture in the RWV yields results that closely reflect those obtained in space (19). This consideration raises 2 challenging points. First, it is reasonable to use these bioreactors for benchtop microgravity research to design potentially successful experiments in real microgravity. Second, it is mandatory to study the modulation of proteins in cells cultured in space, because our results clearly demonstrate that, despite no alterations of the levels of transcript, the amounts of the corresponding proteins change. Some evidence has been provided about altered posttranscriptional mechanisms induced by microgravity. By a proteomic approach, it was demonstrated that human T lymphocytes in simulated microgravity down-regulate the 26S proteasome subunit 6 and the proteasome activator complex subunit 3, thus suggesting an impairment of the proteasome machinery (44). Accordingly, culture in the RWV reduced the activity of the proteasome in U937 cells (15). Similarly, a gradual decrease of the total activity of the proteasome was reported in ECs cultured in the RWV for 48 and 96 h (14). More studies are necessary to give new insights into the molecular mechanisms that contribute to cell adaptation.

Briefly, we conclude that early upon exposure to microgravity, HUVECs up-regulates HSP70, which activates a transient adaptive response gradually replaced by the increase of other stress proteins that maintain a new homeostatic status. The sequential up-regulation of different proteins is aimed initially at driving the adaptation to mechanical unloading and finally at establishing and maintaining a novel phenotype that preserves cell viability and function. Fj

## ACKNOWLEDGMENTS

This work was supported, in part, by the Italian Space Agency [Coculture of Endothelial Cells and Osteoblast in Space: Effects on Osteoblast Activity (ENDOSTEO) Project]. The authors declare no conflict of interest.

## AUTHOR CONTRIBUTIONS

A. Cazzaniga and L. Locatelli performed research; S. Castiglioni and J. A. M. Maier designed research; J. A. M. Maier wrote the manuscript; and all authors analyzed data.

## REFERENCES

1. Demontis, G. C., Germani, M. M., Caiani, E. G., Barravecchia, I., Passino, C., and Angeloni, D. (2017) Human pathophysiological adaptations to the space environment. *Front. Physiol.* **8**, 547
2. Najrana, T., and Sanchez-Esteban, J. (2016) Mechanotransduction as an adaptation to gravity. *Front Pediatr.* **4**, 140
3. Baratchi, S., Khoshmanesh, K., Woodman, O. L., Potocnik, S., Peter, K., and McIntyre, P. (2017) Molecular sensors of blood flow in endothelial cells. *Trends Mol. Med.* **23**, 850–868
4. Aubert, A. E., Beckers, F., and Verheyden, B. (2005) Cardiovascular function and basics of physiology in microgravity. *Acta Cardiol.* **60**, 129–151
5. Maier, J. A., Cialdai, F., Monici, M., and Morbidelli, L. (2015) The impact of microgravity and hypergravity on endothelial cells. *BioMed Res. Int.* **2015**, 434803
6. Yee, A., Bosworth, K. A., Conway, D. E., Eskin, S. G., and McIntire, L. V. (2008) Gene expression of endothelial cells under pulsatile nonreversing vs. steady shear stress; comparison of nitric oxide production. *Ann. Biomed. Eng.* **36**, 571–579
7. Carlsson, S. I., Bertilaccio, M. T., Ballabio, E., and Maier, J. A. (2003) Endothelial stress by gravitational unloading: effects on cell growth and cytoskeletal organization. *Biochim. Biophys. Acta* **1642**, 173–179
8. Versari, S., Villa, A., Bradamante, S., and Maier, J. A. M. (2007) Alterations of the actin cytoskeleton and increased nitric oxide synthesis are common features in human primary endothelial cell response to changes in gravity. *Biochim. Biophys. Acta* **1773**, 1645–1652
9. Grenon, S. M., Jeanne, M., Aguado-Zuniga, J., Conte, M. S., and Hughes-Fulford, M. (2013) Effects of gravitational mechanical unloading in endothelial cells: association between caveolins, inflammation and adhesion molecules. *Sci. Rep.* **3**, 1494
10. Griffoni, C., Di Molfetta, S., Fantozzi, L., Zanetti, C., Pippia, P., Tomasi, V., and Spisni, E. (2011) Modification of proteins secreted by endothelial cells during modeled low gravity exposure. *J. Cell. Biochem.* **112**, 265–272
11. Janmaleki, M., Pachenari, M., Seyedpour, S. M., Shahghadami, R., and Sanati-Nezhad, A. (2016) Impact of simulated microgravity on cytoskeleton and viscoelastic properties of endothelial cell. *Sci. Rep.* **6**, 32418
12. Ravagnan, L., Gurbuxani, S., Susin, S. A., Maisse, C., Daugas, E., Zamzami, N., Mak, T., Jäättelä, M., Penninger, J. M., Garrido, C., and Kroemer, G. (2001) Heat-shock protein 70 antagonizes apoptosis-inducing factor. *Nat. Cell Biol.* **3**, 839–843
13. Mariotti, M., and Maier, J. A. M. (2009) Human micro- and macrovascular endothelial cells exposed to simulated microgravity upregulate HSP70. *Microgravity Sci. Technol.* **21**, 141–144
14. Mariotti, M., and Maier, J. A. M. (2008) Gravitational unloading induces an anti-angiogenic phenotype in human microvascular endothelial cells. *J. Cell. Biochem.* **104**, 129–135
15. Maier, J. A. (2006) Impact of simulated microgravity on cell cycle control and cytokine release by U937 cells. *Int. J. Immunopathol. Pharmacol.* **19**, 279–286
16. Hatton, J. P., Gaubert, F., Lewis, M. L., Darsel, Y., Ohlmann, P., Cazenave, J. P., and Schmitt, D. (1999) The kinetics of translocation and cellular quantity of protein kinase C in human leukocytes are modified during spaceflight. *FASEB J.* **13** (Suppl), S23–S33
17. Kapitonova, M. Y., Muid, S., Froemming, G. R., Yusoff, W. N., Othman, S., Ali, A. M., and Nawawi, H. M. (2012) Real space flight travel is associated with ultrastructural changes, cytoskeletal disruption and premature senescence of HUVEC. *Malays. J. Pathol.* **34**, 103–113
18. Kapitonova, M. Y., Kuznetsov, S. L., Froemming, G. R., Muid, S., Nor-Ashikin, M. N., Otman, S., Shahir, A. R., and Nawawi, H. (2013) Effects of space mission factors on the morphology and function of endothelial cells. *Bull. Exp. Biol. Med.* **154**, 796–801
19. Versari, S., Longinotti, G., Barenghi, L., Maier, J. A. M., and Bradamante, S. (2013) The challenging environment on board the International Space Station affects endothelial cell function by triggering oxidative stress through thioredoxin interacting protein overexpression: the ESA-SPHINX experiment. *FASEB J.* **27**, 4466–4475
20. Cotrupi, S., Ranzani, D., and Maier, J. A. M. (2005) Impact of modeled microgravity on microvascular endothelial cells. *Biochim. Biophys. Acta* **1746**, 163–168
21. Dejeans, N., Maier, J. A., Tauveron, I., Milenkovic, D., and Mazur, A. (2010) Modulation of gene expression in endothelial cells by hyperlipaemic postprandial serum from healthy volunteers. *Genes Nutr.* **5**, 263–274
22. Cazzaniga, A., Maier, J. A. M., and Castiglioni, S. (2016) Impact of simulated microgravity on human bone stem cells: new hints for space medicine. *Biochem. Biophys. Res. Commun.* **473**, 181–186
23. Castiglioni, S., Cazzaniga, A., Locatelli, L., and Maier, J. A. M. (2017) Silver nanoparticles in orthopedic applications: new insights on their effects on osteogenic cells. *Nanomaterials (Basel)* **7**
24. Castiglioni, S., Cazzaniga, A., Trapani, V., Cappadone, C., Farruggia, G., Merolle, L., Wolf, F. I., Iotti, S., and Maier, J. A. (2015) Magnesium homeostasis in colon carcinoma LoVo cells sensitive or resistant to doxorubicin. *Sci. Rep.* **5**, 16538
25. Leidi, M., Mariotti, M., and Maier, J. A. (2010) EDF-1 contributes to the regulation of nitric oxide release in VEGF-treated human endothelial cells. *Eur. J. Cell Biol.* **89**, 654–660
26. Wang, J., Zhang, J., Bai, S., Wang, G., Mu, L., Sun, B., Wang, D., Kong, Q., Liu, Y., Yao, X., Xu, Y., and Li, H. (2009) Simulated microgravity promotes cellular senescence via oxidant stress in rat PC12 cells. *Neurochem. Int.* **55**, 710–716
27. Liu, Y., and Wang, E. (2008) Transcriptional analysis of normal human fibroblast responses to microgravity stress. *Genomics Proteomics Bioinformatics* **6**, 29–41
28. Beck, M., Moreels, M., Quintens, R., Abou-El-Ardat, K., El-Saghire, H., Tabury, K., Michaux, A., Janssen, A., Neefs, M., Van Oostveldt, P., De Vos, W. H., and Baatout, S. (2014) Chronic exposure to simulated space conditions predominantly affects cytoskeleton remodeling and oxidative stress response in mouse fetal fibroblasts. *Int. J. Mol. Med.* **34**, 606–615
29. Ballatori, N., Krance, S. M., Notenboom, S., Shi, S., Tieu, K., and Hammond, C. L. (2009) Glutathione dysregulation and the etiology and progression of human diseases. *Biol. Chem.* **390**, 191–214
30. Spindel, O. N., Yan, C., and Berk, B. C. (2012) Thioredoxin-interacting protein mediates nuclear-to-plasma membrane communication: role in vascular endothelial growth factor 2 signaling. *Arterioscler. Thromb. Vasc. Biol.* **32**, 1264–1270
31. Quintá, H. R., Galigniana, N. M., Erlejman, A. G., Lagadari, M., Piwien-Pilipuk, G., and Galigniana, M. D. (2011) Management of cytoskeleton architecture by molecular chaperones and immunophilins. *Cell. Signal.* **23**, 1907–1920

32. Afolayan, A. J., Teng, R. J., Eis, A., Rana, U., Broniowska, K. A., Corbett, J. A., Pritchard, K., and Konduri, G. G. (2014) Inducible HSP70 regulates superoxide dismutase-2 and mitochondrial oxidative stress in the endothelial cells from developing lungs. *Am. J. Physiol. Lung Cell. Mol. Physiol.* **306**, L351–L360
33. Liu, J., Wu, X., Wang, X., Zhang, Y., Bu, P., Zhang, Q., and Jiang, F. (2013) Global gene expression profiling reveals functional importance of sirt2 in endothelial cells under oxidative stress. *Int. J. Mol. Sci.* **14**, 5633–5649
34. Altenhöfer, S., Witte, I., Teiber, J. F., Wilgenbus, P., Pautz, A., Li, H., Daiber, A., Witan, H., Clement, A. M., Förstermann, U., and Horke, S. (2010) One enzyme, two functions: PON2 prevents mitochondrial superoxide formation and apoptosis independent from its lactonase activity. *J. Biol. Chem.* **285**, 24398–24403
35. Horke, S., Witte, I., Wilgenbus, P., Krüger, M., Strand, D., and Förstermann, U. (2007) Paraoxonase-2 reduces oxidative stress in vascular cells and decreases endoplasmic reticulum stress-induced caspase activation. *Circulation* **115**, 2055–2064
36. Vidyasagar, A., Wilson, N. A., and Djamali, A. (2012) Heat shock protein 27 (HSP27): biomarker of disease and therapeutic target. *Fibrogenesis Tissue Repair* **5**, 7
37. Sun, H. B., Ren, X., Liu, J., Guo, X. W., Jiang, X. P., Zhang, D. X., Huang, Y. S., and Zhang, J. P. (2015) HSP27 phosphorylation protects against endothelial barrier dysfunction under burn serum challenge. *Biochem. Biophys. Res. Commun.* **463**, 377–383
38. Han, S. H., Jeon, J. H., Ju, H. R., Jung, U., Kim, K. Y., Yoo, H. S., Lee, Y. H., Song, K. S., Hwang, H. M., Na, Y. S., Yang, Y., Lee, K. N., and Choi, I. (2003) VDUP1 upregulated by TGF-beta1 and 1,25-dihydorxyvitamin D3 inhibits tumor cell growth by blocking cell-cycle progression. *Oncogene* **22**, 4035–4046
39. Spindel, O. N., Burke, R. M., Yan, C., and Berk, B. C. (2014) Thioredoxin-interacting protein is a biomechanical regulator of Src activity: key role in endothelial cell stress fiber formation. *Circ. Res.* **114**, 1125–1132
40. Lane, T., Flam, B., Lockey, R., and Kolliputi, N. (2013) TXNIP shuttling: missing link between oxidative stress and inflammasome activation. *Front. Physiol.* **4**, 50
41. DeBalsi, K. L., Wong, K. E., Koves, T. R., Slentz, D. H., Seiler, S. E., Wittmann, A. H., Ilkayeva, O. R., Stevens, R. D., Perry, C. G., Lark, D. S., Hui, S. T., Szweda, L., Neufer, P. D., and Muoio, D. M. (2014) Targeted metabolomics connects thioredoxin-interacting protein (TXNIP) to mitochondrial fuel selection and regulation of specific oxidoreductase enzymes in skeletal muscle. *J. Biol. Chem.* **289**, 8106–8120
42. Cmielová, J., and Rezáčová, M. (2011) p21Cip1/Waf1 protein and its function based on a subcellular localization [corrected]. *J. Cell. Biochem.* **112**, 3502–3506; erratum: 113, 1450
43. Tousoulis, D., Kampoli, A. M., Tentolouris, C., Papageorgiou, N., and Stefanadis, C. (2012) The role of nitric oxide on endothelial function. *Curr. Vasc. Pharmacol.* **10**, 4–18
44. Risso, A., Tell, G., Vascotto, C., Costessi, A., Arena, S., Scaloni, A., and Cosulich, M. E. (2005) Activation of human T lymphocytes under conditions similar to those that occur during exposure to microgravity: a proteomics study. *Proteomics* **5**, 1827–1837

*Received for publication August 1, 2018.*
*Accepted for publication January 15, 2019.*

| | |
|---|---|
| **Title:** | The FASEB journal |
| **Article ID:** | 0892-6638 |
| **Publication:** | Publication1 |
| **Publisher:** | CCC Republication |
| **Date:** | Jan 1, 1987 |





## Order Completed

Thank you for your order.

This Agreement between Laura Locatelli ("You") and Fedn of Am Societies for Experimental Bio (FASEB) ("Fedn of Am Societies for Experimental Bio (FASEB)") consists of your order details and the terms and conditions provided by Fedn of Am Societies for Experimental Bio (FASEB) and Copyright Clearance Center.

| | |
|---|---|
| License number | Reference confirmation email for license number |
| License date | Aug, 21 2019 |
| Licensed content publisher | Fedn of Am Societies for Experimental Bio (FASEB) |
| Licensed content title | The FASEB journal |
| Licensed content date | Jan 1, 1987 |
| Type of use | Thesis/Dissertation |
| Requestor type | Academic institution |
| Format | Print, Electronic |
| Portion | chapter/article |
| The requesting person/organization | Laura Locatelli |
| Title or numeric reference of the portion(s) | article |
| Title of the article or chapter the portion is from | THE DYNAMIC ADAPTATION OF PRIMARY HUMAN ENDOTHELIAL CELLS TO SIMULATED MICROGRAVITY |
| Editor of portion(s) | Babette Walker |
| Author of portion(s) | Cazzaniga |
| Volume of serial or monograph | 33 |
| Page range of portion | |
| Publication date of portion | May 2019 |
| Rights for | Main product |
| Duration of use | Life of current edition |
| Creation of copies for the disabled | no |
| With minor editing privileges | no |
| For distribution to | Other territories and/or countries |
| In the following language(s) | Original language of publication |
| With incidental promotional use | no |
| Lifetime unit quantity of new product | Up to 499 |
| Title | UNRAVELING THE MECHANISMS INVOLVED IN ENDOTHELIAL RESPONSE TO MICROGRAVITY |
| Institution name | University of Milan |
| Expected presentation date | Jan 2020 |
| Requestor Location | Laura Locatelli<br>via G.B. Grassi 74<br><br>Milan, other 20157 |

| | |
|---|---|
| | Italy<br>Attn: |
| Billing Type | Invoice |
| Billing address | Laura Locatelli<br>via G.B. Grassi 74<br><br>Milan, Italy 20157<br>Attn: Laura Locatelli |
| Total (may include CCC user fee) | 0.00 USD |
| Total | 0.00 USD |

CLOSE WINDOW

# MITOPHAGY CONTRIBUTES TO ENDOTHELIAL ADAPTATION TO SIMULATED MICROGRAVITY

Laura Locatelli, Alessandra Cazzaniga, Clara De Palma, Sara Castiglioni and Jeanette A.M. Maier*

Dept Biomedical and Clinical Sciences L. Sacco, Università di Milano, Via G.B. Grassi 74, Milano I-20157

*Corresponding Author:
Jeanette AM Maier
Dipartimento di Scienze Biomediche e Cliniche L. Sacco,
Università di Milano,
Via GB Grassi 74, 20157 Milano, Italy,
jeanette.maier@unimi.it
Tel 39-02-50319648, fax 39-02-50319659

**NON STANDARD ABBREVIATIONS**

EC: Endothelial Cells

HUVEC: Human Umbilical Vein Endothelial Cells

RWV: Rotating Wall Vessel

FBS: Fetal Bovine Serum

ECGF: Endothelial Cell Growth Factor

CTR: 1G condition Control

CQ: Chloroquine

LC3 B: microtubule-associated proteins 1A/1B light chain 3B

P62: Sequestosome 1

CYP D: Cyclophilin D

MTCO1: Mitochondrially Encoded Cytochrome C Oxidase I

VDAC: Voltage-Dependent Anion Channels

BNIP3: BCL2 Interacting Protein 3

GAPDH: glyceraldehydes-3-phosphate dehydrogenase

ISS: International Space Station

**ABSTRACT**

Exposure to real or simulated microgravity is sensed as a stress by mammalian cells, which activate a complex adaptive response. In human primary endothelial cells, we have recently shown the sequential intervention of various stress proteins which are crucial to prevent apoptosis and maintain cell function. We here demonstrate that mitophagy contributes to endothelial adaptation to gravitational unloading. After 4 and 10 days of exposure to simulated microgravity in the Rotating Wall Vessel, the amount of BNIP3, a marker of mitophagy, is increased and, in parallel, mitochondrial content and oxygen consumption are reduced, suggesting that HUVEC acquire a thrifty phenotype to meet the novel metabolic challenges generated by gravitational unloading. Moreover, we suggest that microgravity induced-disorganization of the actin cytoskeleton triggers mitophagy, thus creating a connection between cytoskeletal dynamics and mitochondrial content upon gravitational unloading.

key words: mitochondria, HUVEC, cytoskeleton, RWV

## INTRODUCTION

Microgravity affects health and this results from an array of adaptive responses that ultimately influence homeostasis [1, 2]. It is particular relevant that microgravity alters the behavior of endothelial cells (EC) [3], the gatekeepers of vascular integrity and function, crucial to provide continued and adequate perfusion to all the tissues to sustain their own needs [4]. EC react to many different stimuli. Being located at the interface between the blood and the tissues, these cells are susceptible to the action of a large variety of soluble factors. Moreover, they sense mechanical forces, such as shear stress, a frictional force acting in the direction of blood flow, pressure-stretch, which acts perpendicularly to the vascular wall [5], and gravity [6]. Indeed, many studies have demonstrated that both real and simulated microgravity affect the behavior of human umbilical vein endothelial cells (HUVEC) [7-14], a consolidated model of macrovascular EC. Microgravity models the organization of the cytoskeleton, the proliferative rate, the production of inflammatory and vasoactive molecules [7-14], partly through the activation of a complex and dynamic adaptive response which prevents apoptosis and generate a novel balance so that cell functions are preserved [15]. In face of all this body of knowledge, no data are available on HUVEC bioenergetics in microgravity. In physiological conditions, EC obtain most of the energy by converting glucose to lactate [16], with two principal goals, i) to protect themselves from oxidative stress and ii) to preserve oxygen for the diffusion into the perivascular tissues [16, 17]. Therefore, in EC mitochondria, rod-shaped organelles that convert oxygen and nutrients into ATP, mainly serve as a biosynthetic center to produce the precursors necessary for the synthesis of various molecules required for cellular necessities [18]. Moreover, mitochondria integrate signals from the environment, perceive cellular stresses, are vital in cell death signaling and many other functions, thus playing a crucial role in orchestrating EC behavior [19]. Different stimuli are able to modulate mitochondrial content and function. Mitochondrial content is determined by the balance between mitochondrial biogenesis and degradation through the process called mitophagy, i.e. the autophagic removal of damaged or superfluous mitochondria, while their organization, fundamental in determining their function, is the result of the balance between fusion and fission [20]. Mitochondrial dynamics is strictly linked to cytoskeletal organization, which has a relevant role in maintaining mitochondrial network and function [21].

Because research in space is limited by the high costs and low flight opportunities, several ground-based tools have been developed for simulating microgravity on Earth [22], all based on eliminating a preferential direction of the gravity vector by continuous rotation. It is interesting to point that experiments performed in different bioreactors yielded the same results and often validate data

obtained in space [10, 15, 22, 23]. We have utilized the NASA-developed Rotating Wall Vessel (RWV), which generates a vector-averaged gravity similar to that of near-Earth free-fall orbit [3]. In a previous study we have shown the complex activation of endothelial adaptive response after 4 and 10 days in the RWV [15]. Here we utilize the same time points and demonstrate that simulated microgravity activates mitophagy thus reducing mitochondrial content and oxygen consumption in HUVEC.

## MATERIALS AND METHODS

*Cell culture*

HUVEC were from ATCC and serially passaged in M199 containing 10% fetal bovine serum (FBS), Endothelial Cell Growth Factor (ECGF) (150 μg/ml), glutamine (2 mM), sodium pyruvate (1 mM), and heparin (5 U/ml) on 2% gelatin coated dishes. All culture reagents were from Gibco (Thermo Fisher Scientific, Monza, Italy). To generate microgravity, we utilized the RWV (Synthecon Inc, Houston, TX, USA) after seeding HUVEC on beads (Cytodex 3, Sigma Aldrich, St Louis, Missouri, USA) [7, 10, 24]. As 1G condition (CTR), HUVEC grown on beads were cultured in the vessels not undergoing rotation.

In some experiments, to allow the accumulation of autophagosomes HUVEC were treated with 40μM of chloroquine (CQ) (Sigma Aldrich, St Louis, Missouri, USA) for 1h and then collected for protein extraction and western blot. To inhibit autophagy/mitophagy [25], HUVEC in the RWV were treated with 40 μM of chloroquine for 4 days and collected for western blot and immunofluorescence. In other experiments, HUVEC in 1G condition were treated with 0.5 μM of Cytochalasin D (Sigma Aldrich, St Louis, Missouri, USA).

*Oxygen Consumption Measurements*

The respiratory chain capacity was determined by high-resolution respirometry on HUVEC grown in 1G condition (CTR) or in the RWV for 4 and 10 days. The beads were collected from the RWV vessels, trypsinized and $1x10^6$ cells for each sample were used. The mitochondria respiration rates were measured using the O2K oxygraph chambers (Oroboros, Instruments, Innsbruck, Austria). The cells were transferred into oxygraph chambers and resuspended in the respiration medium MiR06 (0.5 mM EGTA, 3 mM $MgCl_2$, 60 mM K-lactobionate, 20 mM taurine, 10 mM $KH_2PO_4$ 20 mM Hepes, 110 mM sucrose and 1 g/l bovine serum albumin fatty acid-free, 280 U/ml catalase (pH 7.1)). The sequential addition of pyruvate (10 mM), malate (2 mM), oligomycin (0.5 μM), the uncoupler FCCP (Carbonyl cyanide-*4*-(trifluoromethoxy) phenylhydrazone, 0.5 μM), rotenone (0.5 μM) and antimycin A (AA) (2.5 μM) allows the measurement of basal, leak and maximal respiration respectively. All the reagents used for respirometry assay were purchased from Sigma.

Oxygen consumption was measured also on extracted mitochondria of HUVEC grown in 1G condition (CTR) or in the RWV for 4 days. The cells were trypsinized, permeabilized, resuspended in isolation buffer (100mM KCl, 50mM TRIS, 5mM $MgCl_2$, 1.8mM ATP, 1mM EDTA) and centrifuged at 600xg for 10 minutes at 4°C. Then the supernatant was centrifuged at 10000xg for 15 minutes at 4°C to allow the sedimentation of the mitochondria which were resuspended in Mito

Preservation Medium (MiR06 supplemented with 20 mM Histidine, 20 μM Vitamin E succinate, 3mM Glutathione, 1μM Leupeptin, 2 mM Glutamate, 2mM Malate, 2 mM Mg-ATP) and 150 μg of mitochondria were used for high-resolution respirometry analysis. The efficiency of the different components of the respiratory chain was measured: complex I respiration (state2), maximal oxidative phosphorylation capacity of complex I (state3), complexes I and II (state3+Succ), complex II function (state3+Succ+Rot) and proton leak across the inner mitochondrial membrane (state4). Then respiratory chain was inhibited by antimycin A (2.5 μM) to obtain the residual oxygen flux that was subtracted to each steady state to correct oxygen fluxes. The respiratory control ratio was calculated as the ratio between state3 and state4 showing a general measure of mitochondrial function. The oxygen consumption measurements were performed three times and the results are shown as the mean ± standard deviation.

*Western blot*

HUVEC were lysed in 10 mM Tris-HCl (pH 7.4) containing 3 mM $MgCl_2$, 10 mM NaCl, 0.1% SDS, 0.1% Triton X-100, 0.5 mM EDTA and protein inhibitors, separated on SDS-PAGE and transferred to nitrocellulose sheets at 400 mA for 2 h at 4°C. Western analysis was performed using antibodies against LC3 B (Cell Signaling, Euroclone, Pero, Italy), p62 and Cyclophilin D (Invitrogen, Carlsbad, California, USA), MTCO1 and VDAC (Abcam, Cambridge, UK), BNIP3 (Sigma Aldrich, St Louis, Missouri, USA) and glyceraldehydes-3-phosphate dehydrogenase (GAPDH) (Tebu Bio-Santa Cruz, Magenta, Italy). After extensive washing, secondary antibodies labelled with horseradish peroxidase (Amersham Pharmacia Biotech Italia, Cologno Monzese, Italy) were used. Immunoreactive proteins were detected by the SuperSignal chemiluminescence kit (Pierce, Life Technologies- ThermoFisher Scientific, Waltham, MA, USA) [26]. All the experiments were performed at least 3 times and a representative blot is shown. Images were analysed using ImageJ.

*Immunofluorescence and confocal imaging*

After 4 and 10 days in the RWV, HUVEC were trypsinized and cytospun on Frosted microscope glasses, fixed in phosphate-buffered saline containing 4% paraformaldehyde and 2% sucrose pH 7.6, permeabilized with Triton 0.3%, incubated with anti-Cyclophilin D or anti-LC3 immunopurified IgGs overnight at 4°C, and stained with an Alexa Fluor 488 and 546 secondary antibody (ThermoFisher Scientific, Waltham, MA, USA) respectively. Finally, cells were mounted with ProLong™ Gold Antifade Mountant (Invitrogen, Carlsbad, California, USA) and images were acquired using a 40X objective in oil by a SP8 Leica confocal microscope

*Statistical analysis.* Statistical significance was determined using the Student's *t* test and set at *p* values less than 0.05. In the figures *$p<0.05$; **$p<0.01$; ***$p<0.001$.

## RESULTS

*Mitochondrial content in HUVEC exposed to simulated microgravity*

To have an overview of the mitochondrial content, we performed immunofluorescence on HUVEC cultured in the RWV or in 1G condition (CTR). After 4 and 10 days, the cells were trypsinized and cytospun on a glass coverslip. To label the mitochondria we used an antibody against Cyclophilin D (CYP D), a protein that is part of the permeability transition pore in the inner membrane of the mitochondria. Images were then acquired using a confocal microscope with different magnifications. Fig 1A shows that HUVEC grown in the RWV have fewer mitochondria than their control (CTR).

To confirm these results at the biochemical level, we investigated the total amounts of CYP D, Mitochondrially Encoded Cytochrome C Oxidase I (MTCO1), a protein encoded by mitochondrial DNA, and Voltage-Dependent Anion Channels (VDAC), located on the outer mitochondrial membrane [27]. MTCO, VDAC and CYP D are all significantly downregulated in HUVEC cultured in the RWV for 4 and 10 days (Fig 1B).

*Mitochondrial function in HUVEC exposed to simulated microgravity*

We investigated mitochondrial function in HUVEC using O2K oxygraph chambers. To this purpose, $1x10^6$ cells for each sample were treated with different molecules to assess the efficiency of the different components of the respiratory chain. Different respiration states were measured. Maximal respiration represents the maximal activity of the electron transport chain, while basal respiration corresponds to oxygen consumption at steady state. Leak respiration measures oxygen consumption not linked to ATP production. HUVEC exposed to simulated microgravity tend to have a minor basal and leak capacity, without reaching statistical significance, compared to their controls, while their maximal respiratory capacity is significantly reduced (Fig 2A).

We also evaluated the function of isolated mitochondria in HUVEC in 1G condition or exposed to simulated microgravity (RWV) for 4 days. The respiratory control ratio, a general measurement of mitochondrial function, was similar in controls and in cells in the RWV when the same amounts of mitochondria were used, indicating that mitochondria are as efficient in cells cultured in the RWV as in 1G condition (CTR) (Fig 2B).

*Autophagy/Mitophagy in HUVEC exposed to simulated microgravity*

We hypothesized that the decreased number of mitochondria in HUVEC exposed to simulated microgravity could be due to an acceleration of the autophagic flow and, specifically, to mitophagy.

Initially, on the basis of studies indicating the activation of autophagy in HUVEC in simulated microgravity [28-30], we evaluated two markers of autophagy by western blot, i.e. microtubule-associated proteins 1A/1B light chain 3B (LC3 B) and Sequestosome 1 (p62). LC3 B is involved in the formation of autophagosomal vacuoles, while p62 is expressed with the cargo within the vesicle. Since LC3 B is cleaved when autophagy occurs, we measured the ratio between the cleaved (LC3 B-II) and total (LC3 B-I) forms of the protein. Western Blot revealed no significant modulation of these proteins in HUVEC exposed for 4 days to simulated microgravity *vs* their controls (Fig 3A). We hypothesized that autophagy in simulated microgravity was fast to the point that the autophagosomes were very rapidly degraded, preventing any possibility of detecting an increase of LC3 B-II or p62 changes. Therefore, on the basis of previous studies [31], we decided to treat cells with chloroquine, an inhibitor of autophagy that blocks the binding of autophagosomes to lysosomes by altering the acidic environment of the lysosomes [31]. This means that chloroquine allows the accumulation of autophagosomes and facilitates the detection of both LC3 B-II and p62 even in the case of very fast autophagic flow. HUVEC were cultured for 4 and 10 days in 1G condition (CTR) and in the RWV. 1 h before ending the experiment, chloroquine (40 μM) was added to culture media. Then the cells were lysed and evaluated for markers of autophagy by western blot. Fig 3B reveals that HUVEC cultured in the RWV significantly increased LC3 B-II and p62 compared to controls, suggesting that the decreased amount of mitochondria in simulated microgravity could be due to an increased autophagy. Of note, we also detected higher amounts of the marker of mitophagy BCL2 Interacting Protein 3 (BNIP3), which targets mitochondria to autophagosomes by interacting directly with LC3 [32], in HUVEC cultured in the RWV for 4 and 10 days *vs* their controls (Fig 3B).

*The role of mitophagy in modulating mitochondrial content in HUVEC exposed to simulated microgravity*

To link mitophagy to the decrease of mitochondrial content in simulated microgravity, we inhibited autophagy/mitophagy using chloroquine [25]. After performing dose- and time-dependent cell viability experiments, 40 μM emerged as the ideal concentration of chloroquine to inhibit mitophagy without affecting HUVEC survival up to 4 days of treatment (data not shown). Immunofluorescence for LC3 B (Fig 4A) was performed to demonstrate that chloroquine actually inhibits the degradation of the autophagosomes. Then, immunofluorescence and western blot for the mitochondrial protein CYP D were performed on HUVEC grown in 1G condition (CTR), in simulated microgravity (RWV) and in simulated microgravity in presence of chloroquine (RWV+CQ) for 4 days. When autophagy is blocked by chloroquine, HUVEC cultured in the RWV

and their controls have a similar mitochondrial content, thus demonstrating that autophagy is responsible for the degradation of mitochondria in simulated microgravity (Fig 4B).

*The role of cytoskeletal disorganization in driving mitophagy and reducing mitochondrial content*

We asked whether cytoskeletal disorganization, which occurs upon exposure to microgravity [3, 7, 8, 10], might play a role in driving mitophagy. We mimicked cytoskeletal disruption in 1G condition using Cytochalasin D, a toxin that binds actin and induces its depolymerization. We performed dose- and time-dependent experiments to test cell viability, and found that 0.5 µM Cytochalasin D is not cytotoxic up to 96 h (data not shown). HUVEC were treated with 0.5 µM Cytochalasin D for 24 h. We observed massive disorganization of actin fibers associated with modifications of cell shape (Fig 5A), a picture that closely recalls the results obtained in microgravity [3, 7, 8, 10]. Both immunofluorescence and western blot show a decrease of CYP D, indicating a reduced mitochondrial mass. Interestingly, Cytochalasin D upregulates BNIP3 (Fig 5B), thus suggesting that cytoskeletal disruption leads to increased mitophagy which results in a decreased content of mitochondria.

## DISCUSSION

The rise of human activities on the international space station (ISS) and in expected long-term space missions has boosted novel studies to unravel biochemical and structural alterations occurring in cells exposed to microgravity. It is now clear that cells and tissues activate adaptive responses to cope with the absence of gravity, the only environmental factor which has remained constant since when life began on Earth. In particular, the endothelium, the inner lining of blood vessels, dynamically adapts to microgravity through the sequential intervention of various stress proteins and acquires novel features that maintain cellular homeostasis [15]. Also autophagy, a process which allows the cell to raze redundant and/or dysfunctional components, is considered a survival adaptive response, thus contributing to stress resistance [33]. Accordingly, various types of stress - such as heat shock and mechanical cues - activate autophagy in various cell types [34, 35]. Therefore, it is not surprising that simulated microgravity induces autophagy [28-30]. In HUVEC, clinorotation, a simulated model of microgravity, enhances autophagosome formation [28] via downregulation of mTOR by a murine double minute 2/p53 dependent mechanisms [29]. In agreement with these results we report that simulated microgravity generated by the RWV induces autophagy in HUVEC. Our novel finding is that increased autophagy results in mitochondria degradation, since blocking autophagy with chloroquine prevents mitochondrial loss. In addition to increased amounts of LC3 B-II, also BNIP3, a mitochondrial stress sensor and a crucial player in mitophagy [32], is upregulated in HUVEC exposed to microgravity. Mitophagy has a housekeeping role in degrading damaged mitochondria and also entails the clearance of healthy mitochondria under stress [36].

In Hodgkin's lymphoma cells microgravity stimulates autophagy through an increased production of ROS [30]. In HUVEC in simulated microgravity we rule out a role of ROS, since we found only a modest and transient increase of free radicals after 2 h of culture in the RWV [15]. To unveil the mechanisms involved in activating mitophagy/autophagy, we focused on the cytoskeleton, which has been proposed as a sensor of changes of gravity [37]. Since i) cytoskeletal dynamics have an important role in autophagy [38], ii) mitochondria interact with the cytoskeletal components [21], iii) mitophagy is regulated by cytoskeletal components [39], and iv) microgravity rapidly and steadily disassembles HUVEC cytoskeleton [3, 7, 8, 10], we anticipate that a link might exist between autophagy, mitochondria content and cytoskeletal remodelling in our experimental model. Indeed, Cytochalasin D closely mimics microgravity-induced cytoskeletal disorganization and also reduces mitochondrial content through mitophagy. We conclude that the remodelling of the

cytoskeleton in microgravity plays a role in activating mitophagy, therefore resulting in reduced mitochondrial content.

In HUVEC in the RWV mitophagy culminates with a reduction of mitochondrial mass which is associated with a reduced consumption of oxygen. However, mitochondria are as efficient in HUVEC in simulated microgravity and their controls. Since endothelial mitochondria are biosynthetic factories rather than powerhouse, the decreased mitochondrial mass might constrain synthetic pathways as an adaptive response to reach a new balance that allows survival and maintains fundamental functions. We propose that HUVEC in simulated microgravity acquire a thrifty phenotype and are less prone to face an overload of substrates. A lower amount of mitochondria might also protect HUVEC from an overproduction of reactive oxygen species, thus integrating the complex modulation of stress proteins aimed at counteracting the upregulation of the pro-oxidant protein TXNIP [15].

Mitochondria are emerging as relevant targets of microgravity. Indeed, mitochondrial mass was reduced also in Hodgkin's lymphoma cells cultured in a clinostat [30]. In osteoblasts cultured in simulated microgravity using the Random Positioning Machine mitochondrial functions were impaired [40], with important metabolic consequences, but no quantification of mitochondrial mass was performed. On the contrary, rat cardiomyocytes cultured in the RWV upregulated mitochondrial proteins to maintain the energetics of the cells at the expense of protein synthesis [41] and oligodendrocytes, the myelin-forming cells in the central nervous system, increased mitochondrial respiration in simulated microgravity, suggesting an increase in Kreb's cycle flux [42]. Considering the peculiar and highly specific function each cell type exerts, it is not surprising that distinct cells differently regulate mitochondrial mass and activity. Indeed, mitochondria exhibit tissue-specific characteristics, including their number and their capacity of ATP synthesis [43]. Therefore, it is feasible to propose that, while endothelial cells, which are quiescent in normal conditions, can reduce their mitochondria without detrimental effects on their viability, other highly differentiated cells optimize their energetics to meet the challenge generated by gravitational unloading. If the scenario is complex in *in vitro* systems, it becomes even more intricate in humans. A significant decrease in the mtDNA/nDNA was described in hair samples from ten astronauts after six months on the ISS [44]. In contrast, within the "NASA Twin Study", higher levels of mtDNA were revealed in peripheral blood mononuclear cells after 1 year in space [2]. Space is a harsh extreme environment where astronauts are exposed to stresses other than microgravity, such as cosmic radiations, tight work schedule, isolation, etc. It is therefore complicated to interpret human results, which should be read also in the light of individual diversity. It is even harder to compare them with data obtained *in vitro*.

In conclusion, we propose that microgravity-induced cytoskeletal disorganization triggers the activation of autophagy/mitophagy, thus leading to mitochondrial loss (Figure 6). These events might be relevant to deal with the novel metabolic demands generated in microgravity and to reach a novel balance that maintains endothelial survival and fundamental function.

**ACKNOWLEDGEMENTS**
This work was supported, in part, by the Italian Space Agency (ENDOSTEO project).
No potential conflict of interest was reported by the authors.

**AUTHOR CONTRIBUTIONS**
L. Locatelli performed most of the experiments; A. Cazzaniga helped with culture in the RWV; C. De Palma conducted respirometry; S. Castiglioni and J. A. M. Maier designed research; J. A. M. Maier wrote the manuscript; and all authors analysed data.

**REFERENCES**


1. White R.J., Averner M. (2001) Humans in space. Nature409(6823), 1115-1118.
2. Garrett-Bakelman F.E., Darshi M., Green S.J., Gur R.C., Lin L., Macias B.R., McKenna M.J. et al. (2019) The NASA Twins Study: A multidimensional analysis of a year-long human spaceflight. Science364(6436).
3. Maier J.A., Cialdai F., Monici M., and Morbidelli L. (2015) The impact of microgravity and hypergravity on endothelial cells. BioMed Res. Int, 434803.
4. Cahill P.A., Redmond E.M. (2016) Vascular endothelium - Gatekeeper of vessel health. Atherosclerosis248, 97-109.
5. Michiels C. (2003) Endothelial cell functions. J Cell Physiol196(3), 430-43.
6. García-Cardeña G., Gimbrone M.A. Jr. (2006) Biomechanical modulation of endothelial phenotype: implications for health and disease. Handb Exp Pharmacol176 Pt 2, 79-95.
7. Carlsson S.I., Bertilaccio M.T., Ballabio E., Maier J.A. (2003) Endothelial stress by gravitational unloading: effects on cell growth and cytoskeletal organization. Biochim Biophys Acta1642, 173-9.
8. Kapitonova M.Y., Muid S., Froemming G.R., Yusoff W.N., Othman S., Ali A.M., Nawawi H.M. (2012) Real space flight travel is associated with ultrastructural changes, cytoskeletal disruption and premature senescence of HUVEC. Malays. J. Pathol34, 103–113.
9. Kapitonova M.Y., Kuznetsov S.L., Froemming, G.R., Muid S., Nor-Ashikin M.N., Otman S., Shahir A.R., and Nawawi H. (2013) Effects of space mission factors on the morphology and function of endothelial cells. Bull. Exp. Biol. Med154, 796–801.
10. Versari, S., Villa, A., Bradamante, S., Maier, J.A.M. (2007) Alterations of the actin cytoskeleton and increased nitric oxide synthesis are common features in human primary endothelial cell response to changes in gravity. Biochimica et Biophysica Acta1773, 1645-52.
11. Versari S., Longinotti G., Barenghi L., Maier J.A.M., Bradamante S. (2013) The challenging environment on board the International Space Station affects endothelial cell function by triggering oxidative stress through thioredoxin interacting protein overexpression: the ESA-SPHINX experiment. FASEBJ27, 4466–4475.
12. Grenon S.M., Jeanne M., Aguado-Zuniga J., Conte M.S., and Hughes-Fulford M. (2013) Effects of gravitational mechanical unloading in endothelial cells: association between caveolins, inflammation and adhesion molecules. Sci. Rep3, 1494.

13. Griffoni C., Di Molfetta S., Fantozzi L., Zanetti C., Pippia P., Tomasi V., Spisni E. (2011) Modification of proteins secreted by endothelial cells duringmodeled lowgravity exposure. J. Cell. Biochem112, 265–272.
14. Janmaleki M., Pachenari M., Seyedpour S.M., Shahghadami R., Sanati-Nezhad A. (2016) Impact of simulated microgravity on cytoskeleton and viscoelastic properties of endothelial cell. Sci Rep6, 32418.
15. Cazzaniga A., Locatelli L., Castiglioni S., Maier J.A.M. (2019) The dynamic adaptation of primary human endothelial cells to simulated microgravity. FASEBJ33(5):5957-5966.
16. De Bock K., Georgiadou M., Carmeliet P. (2013) Role of endothelial cell metabolism in vessel sprouting. Cell Metab18(5):634-47.
17. Helmlinger G., Endo M., Ferrara N., Hlatky L., Jain R.K. (2000) Formation of endothelial cell networks. Nature405 (6783), 139–141.
18. Rohlenova K., Veys K., Miranda-Santos I., De Bock K., Carmeliet P. (2018) Endothelial Cell Metabolism in Health and Disease. Trends Cell Biol28(3):224-236.
19. Caja S., Enríquez J.A. (2017) Mitochondria in endothelial cells: Sensors and integrators of environmental cues. Redox Biol12:821-827.
20. Kluge M.A., Fetterman J.L., Vita J.A. (2013) Mitochondria and endothelial function. Circ Res112(8):1171-88.
21. Moore A.S., Holzbaur E.L.F. (2018) Mitochondrial-cytoskeletal interactions: dynamic associations that facilitate network function and remodeling. Curr Opin Physiol3:94-100.
22. Grimm D., Wehland M., Pietsch J., Aleshcheva G., Wise P., van Loon J., Ulbrich C., Magnusson N.E., Infanger M., Bauer J. (2014) Growing tissues in real and simulated microgravity: new methods for tissue engineering. Tissue Eng Part B Rev20(6):555-66.
23. Martinez E.M., Yoshida M.C., Candelario T.L., Hughes-Fulford M. (2015) Spaceflight and simulated microgravity cause a significant reduction of key gene expression in early T-cell activation. Am J Physiol Regul Integr Comp Physiol308(6):R480-8.
24. Cotrupi S., Ranzani D., and Maier J.A.M. (2005) Impact of modeled microgravity on microvascular endothelial cells. Biochim. Biophys. Acta1746, 163–168.
25. Georgakopoulos N.D., Wells G., Campanella M. (2017) The pharmacological regulation of cellular mitophagy. Nat Chem Biol13(2):136-146.
26. Castiglioni S., Cazzaniga A., Trapani V., Cappadone C., Farruggia G., Merolle L., Wolf F. I., Iotti S., and Maier J.A. (2015) Magnesium homeostasis in colon carcinoma LoVo cells sensitive or resistant to doxorubicin. Sci. Rep5, 16538.

27. Elrod J.W., Molkentin J.D. (2013) Physiologic functions of cyclophilin D and the mitochondrial permeability transition pore. Circ J77(5):1111-22.
28. Wang Y.C., Lu D.Y., Shi F., Zhang S., Yang C.B., Wang B., Cao X.S., Du T.Y., Gao Y., Zhao J.D., Sun X.Q. (2013) Clinorotation enhances autophagy in vascular endothelial cells. Biochem Cell Biol91(5):309-14.
29. Li C.F., Sun J.X., Gao Y., Shi F., Pan Y.K., Wang Y.C., Sun X.Q. (2018) Clinorotation-induced autophagy via HDM2-p53-mTOR pathway enhances cell migration in vascular endothelial cells. Cell Death Dis9(2):147.
30. Jeong A.J., Kim Y.J., Lim M.H., Lee H., Noh K., Kim B.H., Chung J.W., Cho C.H., Kim S., Ye S.K. (2018) Microgravity induces autophagy via mitochondrial dysfunction in human Hodgkin's lymphoma cells. Sci Rep8(1):14646.
31. Klionsky D.J., Abdelmohsen K., Abe A., Abedin M.J., Abeliovich H., Acevedo Arozena A. et al. (2016) Guidelines for the use and interpretation of assays for monitoring autophagy (3rd edition). Autophagy12(1):1-222.
32. Rikka S., Quinsay M.N., Thomas R.L., Kubli D.A., Zhang X.., Murphy A.N., Gustafsson Å.B. (2011) Bnip3 impairs mitochondrial bioenergetics and stimulates mitochondrial turnover. Cell Death Differ18(4):721-31.
33. Murrow L., Debnath J. (2013) Autophagy as a stress-response and quality-control mechanism: implications for cell injury and human disease. Annu Rev Pathol8:105-37.
34. Dokladny K., Myers O.B., Moseley P.L. (2015) Heat shock response and autophagy--cooperation and control. Autophagy11(2):200-13.
35. King J.S. (2012) Mechanical stress meets autophagy: potential implications for physiology and pathology. Trends Mol Med18(10):583-8.
36. Egan D.F., Shackelford D.B., Mihaylova M.M., Gelino S., Kohnz R.A., Mair W., Vasquez D.S., Joshi A., Gwinn D.M., Taylor R., Asara J.M., Fitzpatrick J., Dillin A., Viollet B., Kundu M., Hansen M., Shaw R.J. (2011) Phosphorylation of ULK1 (hATG1) by AMP-activated protein kinase connects energy sensing to mitophagy. Science331(6016):456-61.
37. Vorselen D., Roos W.H., MacKintosh F.C., Wuite G.J., van Loon J.J. (2014) The role of the cytoskeleton in sensing changes in gravity by nonspecialized cells. FASEB J28(2):536-47.
38. Kast D.J., Dominguez R. (2017) The Cytoskeleton-Autophagy Connection. Curr Biol27(8): R318-R326.
39. Strzyz P. (2018) Autophagy: Mitochondria encaged. Nat Rev Mol Cell Biol19(4):212.
40. Michaletti A., Gioia M., Tarantino U., Zolla L. (2017) Effects of microgravity on osteoblast mitochondria: a proteomic and metabolomics profile. Sci Rep7(1):15376.

41. Feger B.J., Thompson J.W., Dubois L.G., Kommaddi R.P., Foster M.W., Mishra R., Shenoy S.K., Shibata Y., Kidane Y.H., Moseley M.A., Carnell L.S., Bowles D.E. (2016) Microgravity induces proteomics changes involved in endoplasmic reticulum stress and mitochondrial protection. Sci Rep6:34091.
42. Espinosa-Jeffrey A., Nguyen K., Kumar S., Toshimasa O., Hirose R., Reue K., Vergnes L., Kinchen J., Vellis J. (2016) Simulated microgravity enhances oligodendrocyte mitochondrial function and lipid metabolism. J Neurosci Res94(12):1434-1450.
43. Kunz W.S. (2003) Different metabolic properties of mitochondrial oxidative phosphorylation in different cell types--important implications for mitochondrial cytopathies. Exp Physiol88(1):149-54.
44. Indo H.P, Majima H.J., Terada M., Suenaga S., Tomita K., Yamada S., Higashibata A., Ishioka N., Kanekura T., Nonaka I., Hawkins C.L., Davies M.J., Clair D.K., Mukai C. (2016) Changes in mitochondrial homeostasis and redox status in astronauts following long stays in space. Sci Rep6:39015.

**LEGENDS TO THE FIGURES**

Figure 1: *Visualization and quantification of mitochondria in HUVEC in simulated microgravity.*

HUVEC were grown in RWV or in 1G condition (CTR) for 4 and 10 days.

(A) After trypsinization, the cells were cytospun on glass coverslips and stained with Dapi to label nuclei and CYP D to visualize the mitochondria. Images were acquired using a 40X objective in oil by a SP8 Leica confocal microscope.

(B) Western blots for different mitochondrial markers were performed. GAPDH was used as a control of loading. The experiments were repeated at least three times. Representative blots (left) and relative quantification obtained by ImageJ (right) are shown.

Figure 2: *High resolution respirometry on HUVEC and on isolated mitochondria after exposure to simulated microgravity.*

HUVEC were cultured in 1G condition (CTR) or in the RWV for 4 and 10 days.

(A) High resolution respirometry was performed on $1x10^6$ cells and basal, leak and maximal respiration were measured as described.

(B) Mitochondria were extracted from HUVEC grown for 4 days in 1G condition (CTR) or in the RWV and oxygen consumption was measured on a purified fraction of mitochondria (150 µg). The efficiency of the different complexes of the respiratory chain was measured. Glutamate (10 mM) and malate (2 mM) were used to measure complex I respiration (state2) and ADP (2.5 mM) to reveal its maximal oxidative phosphorylation capacity (state3). Then, complexes I and II together were tested using succinate (10 mM) (state3+Succ) and rotenone (0.5 µM) was used to inhibit complex I in order to study complex II (state3+Succ+Rot). Oligomycin (2 µg/ml), an inhibitor of the ATP synthase, was used to measure proton leakage (state4). The respiratory control ratio was calculated as the ratio between state3 and state4 and used as a general indicator of mitochondrial function.

The experiments were repeated three times ± standard deviation.

Figure 3: *The induction of autophagy in HUVEC in simulated microgravity.*

Autophagy was monitored in the presence or in the absence of chloroquine for 1 h.

(A) HUVEC were grown in 1G condition (CTR) or in the RWV for 4 days. Western blot for two markers of autophagy, i.e. LC3 B and p62, was performed.

(B) HUVEC were cultured 1G condition (CTR) or in the RWV for 4 and 10 days. 1 h before cell lysis, the cells were treated with chloroquine for 1 h. Western blot was performed as I (A).

GAPDH was used as a marker of loading. The experiments were repeated at least three times. Representative blots (left) and relative quantification obtained by ImageJ (right) are shown.

Figure 4: M*itochondrial content in HUVEC exposed to simulated microgravity after inhibiting autophagy*.

HUVEC were cultured with (RWV+CQ) or without (CTR and RWV) chloroquine (40 µM) for 4 days.

(A) Immunofluorescence with antibodies against LC3 B was performed to show the inhibition of autophagy by chloroquine. Nuclei were stained by DAPI.

(B) Mitochondria were visualized utilizing antibodies against CYP D (upper panel) and Western blot was performed on cell lysates (lower panel). GAPDH was used as a control of loading. The experiment was repeated three times and a representative blot is shown. Densitometry was performed using Image J.

Figure 5: M*itochondrial content and mitophagy in HUVEC exposed to Cytochalasin D.*

HUVEC were treated or not with Cytochalasin D for 24 h.

(A) Cells were stained to detect CYP D (left) and actin (middle). The merge is shown in the right panels.

(B) BNIP3 and CYP D were analyzed by western blot. GAPDH was used as a control of loading. The experiments were repeated at least three times. Representative blots and relative quantification obtained by ImageJ are shown.

# Figure 1

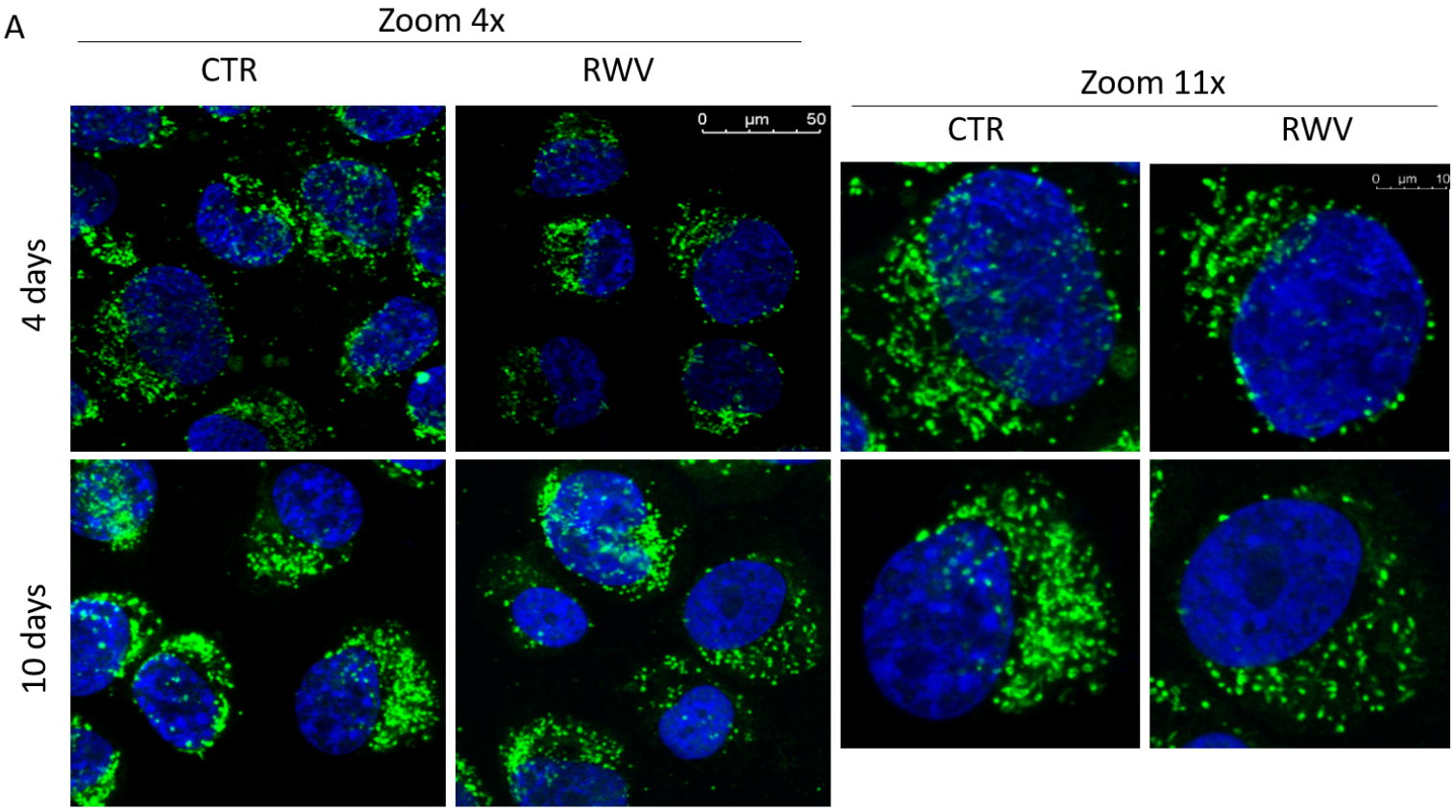
A
Zoom 4x
CTR
RWV
Zoom 11x
CTR
RWV
4 days
10 days
0 µm 50
0 µm 10

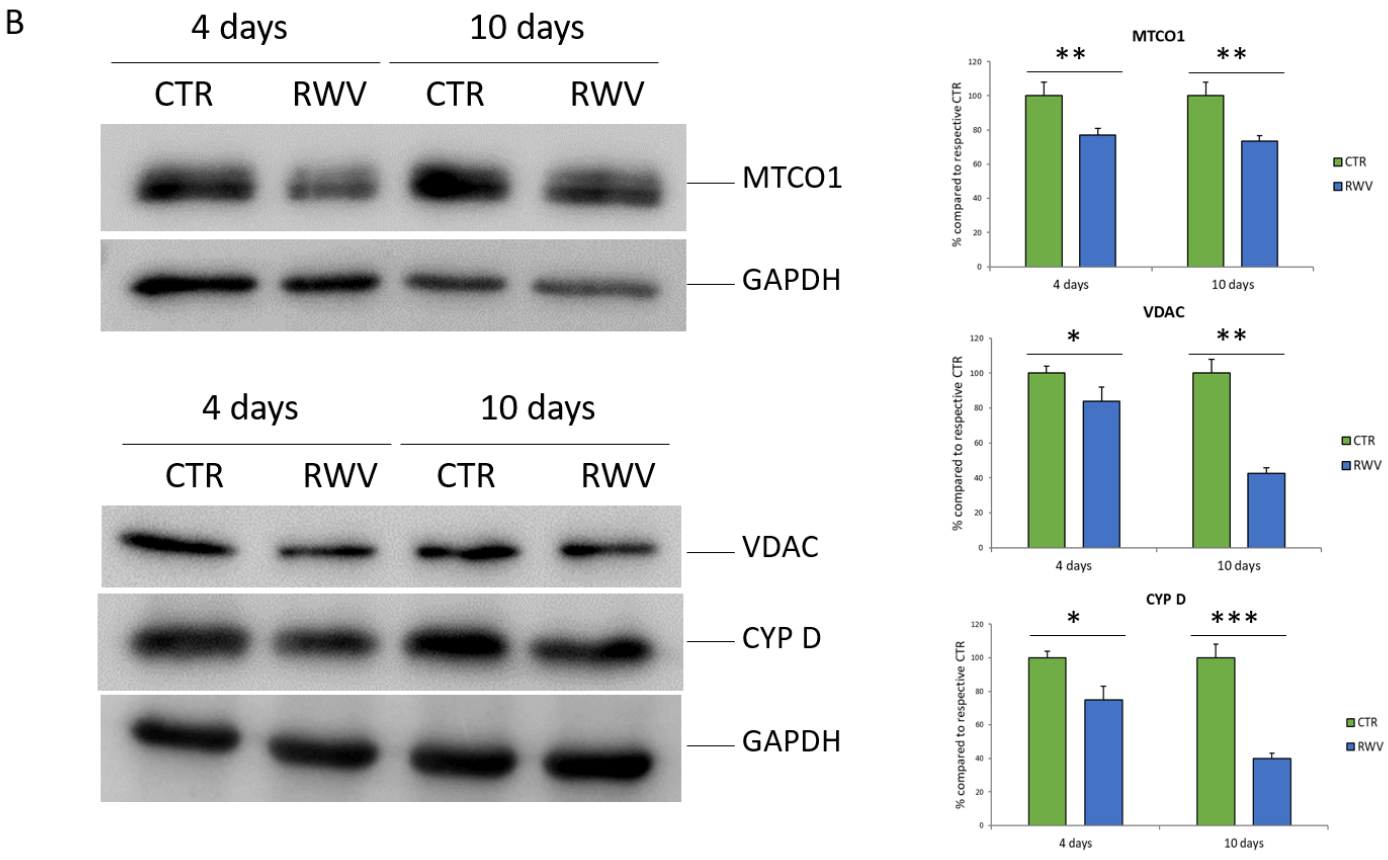
B
4 days
10 days
CTR
RWV
CTR
RWV
MTCO1
GAPDH
4 days
10 days
CTR
RWV
CTR
RWV
VDAC
CYP D
GAPDH
MTCO1
% compared to respective CTR
**
**
4 days
10 days
CTR
RWV
VDAC
% compared to respective CTR
*
**
4 days
10 days
CTR
RWV
CYP D
% compared to respective CTR
*
***
4 days
10 days
CTR
RWV

# Figure 2

A

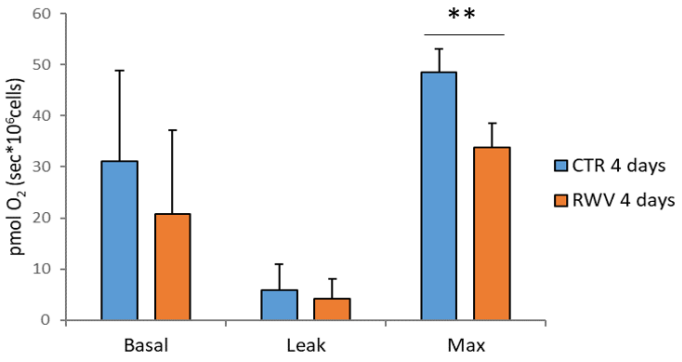
pmol O2 (sec*10^6cells)
60
50
40
30
20
10
0
**
Basal
Leak
Max
CTR 4 days
RWV 4 days

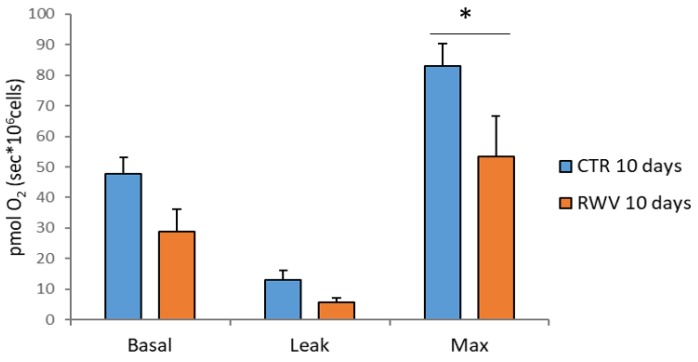
pmol O2 (sec*10^6cells)
100
90
80
70
60
50
40
30
20
10
0
*
Basal
Leak
Max
CTR 10 days
RWV 10 days

B

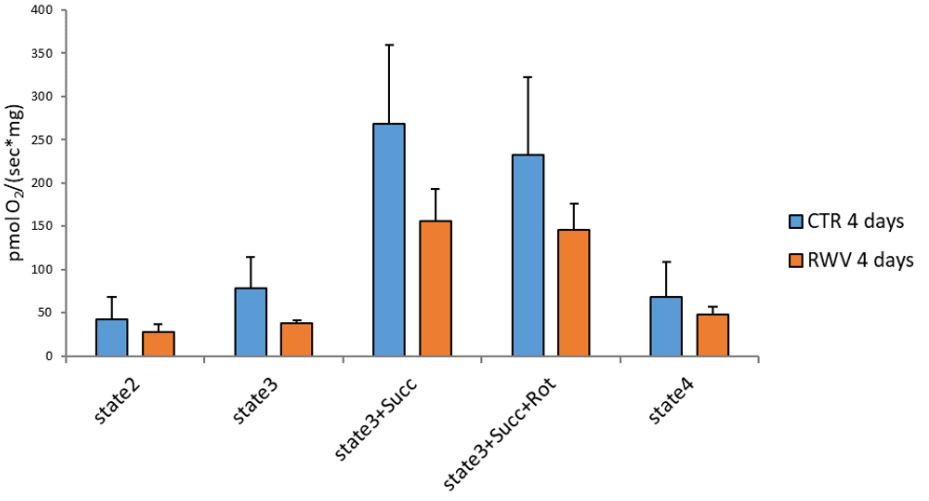
pmol O2/(sec*mg)
400
350
300
250
200
150
100
50
0
state2
state3
state3+Succ
state3+Succ+Rot
state4
CTR 4 days
RWV 4 days

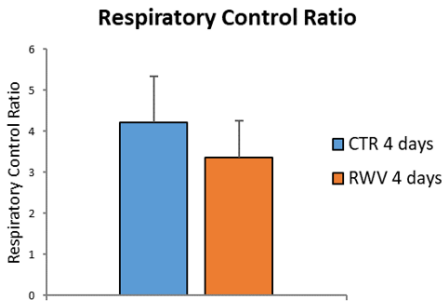
Respiratory Control Ratio
Respiratory Control Ratio
6
5
4
3
2
1
0
CTR 4 days
RWV 4 days

# Figure 3

A

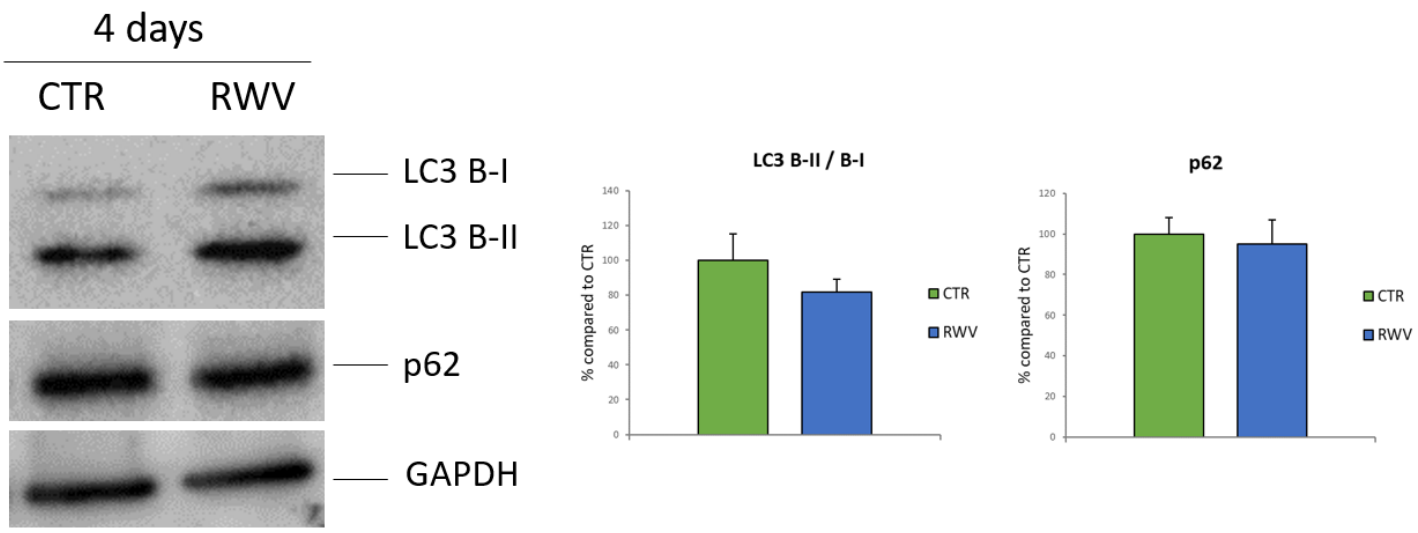
4 days
CTR
RWV
LC3 B-I
LC3 B-II
p62
GAPDH
LC3 B-II / B-I
% compared to CTR
CTR
RWV
p62
% compared to CTR
CTR
RWV

B

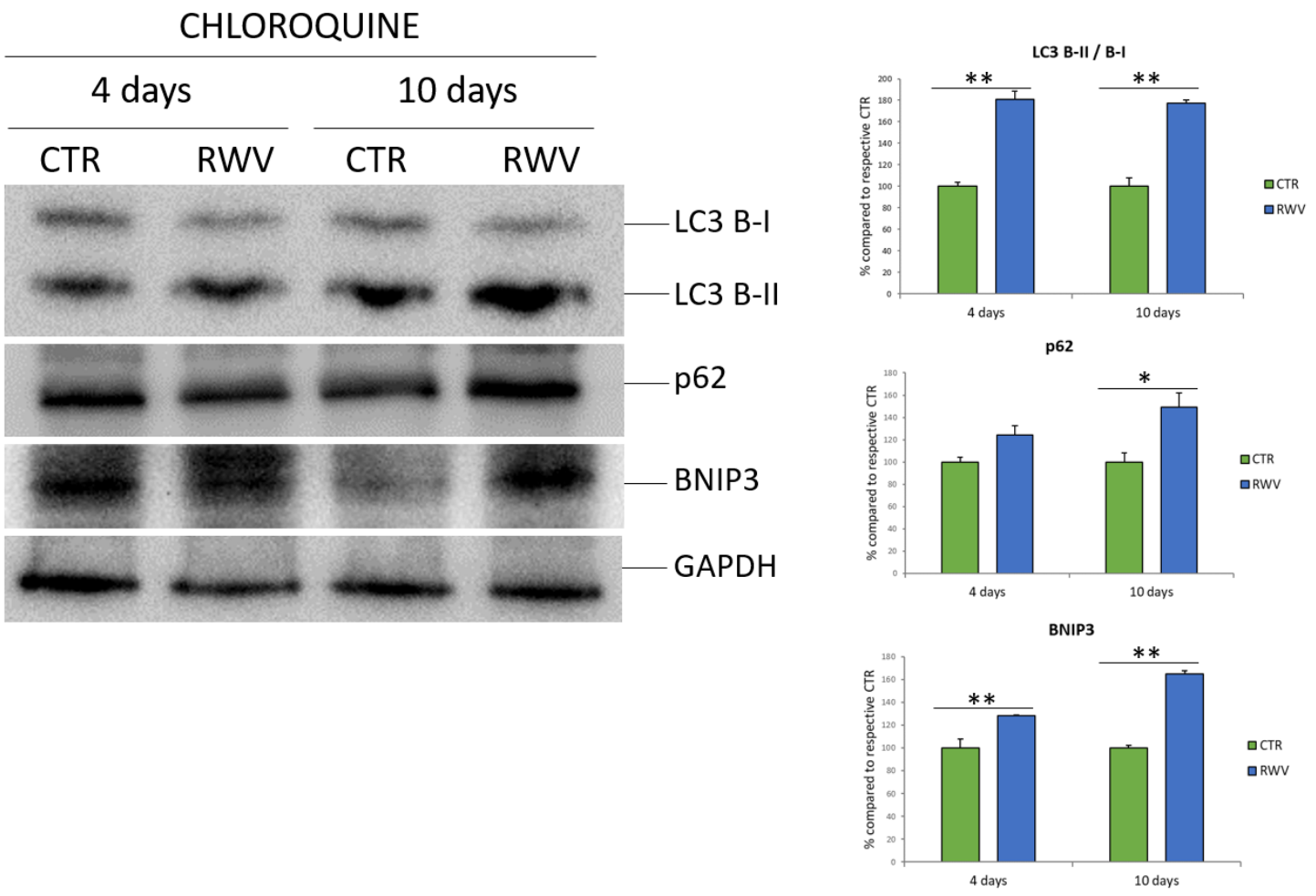
CHLOROQUINE
4 days
10 days
CTR
RWV
CTR
RWV
LC3 B-I
LC3 B-II
p62
BNIP3
GAPDH
LC3 B-II / B-I
**
**
% compared to respective CTR
CTR
RWV
4 days
10 days
p62
*
% compared to respective CTR
CTR
RWV
4 days
10 days
BNIP3
**
**
% compared to respective CTR
CTR
RWV
4 days
10 days

# Figure 4

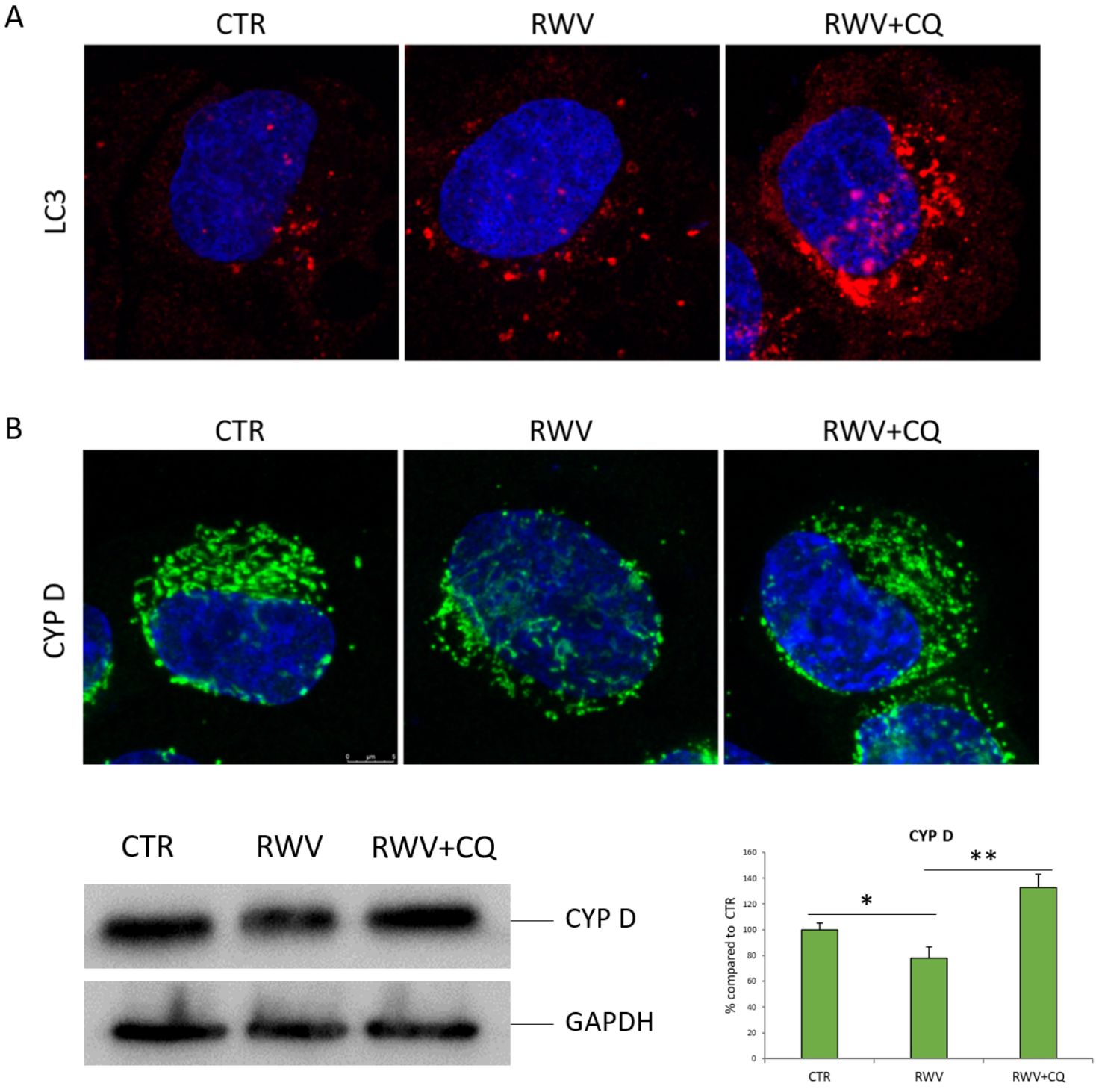
A
CTR
RWV
RWV+CQ
LC3
B
CTR
RWV
RWV+CQ
CYP D
CTR
RWV
RWV+CQ
CYP D
GAPDH
CYP D
% compared to CTR
160
140
120
100
80
60
40
20
0
*
**
CTR
RWV
RWV+CQ

# Figure 5

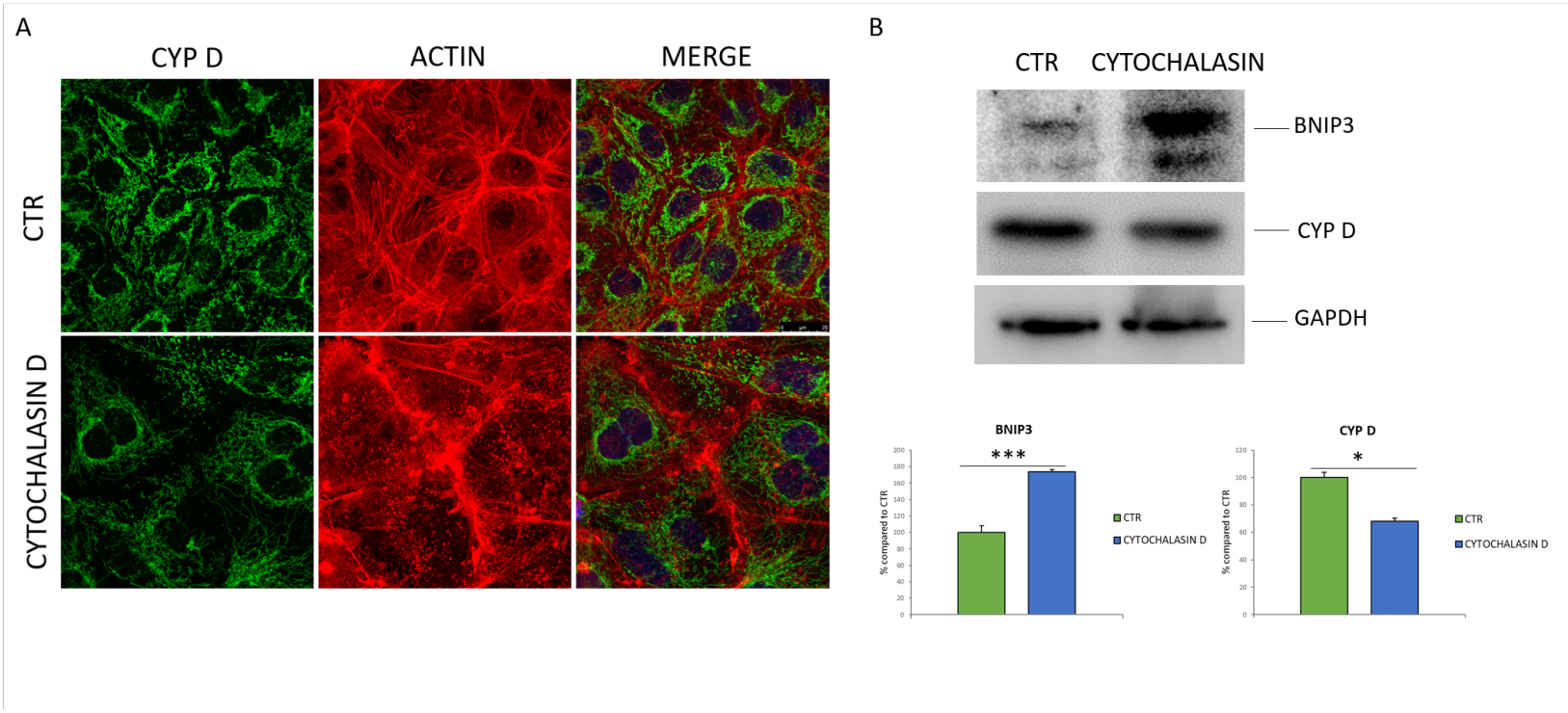
A
CYP D
ACTIN
MERGE
CTR
CYTOCHALASIN D
B
CTR
CYTOCHALASIN
BNIP3
CYP D
GAPDH
BNIP3
***
% compared to CTR
CTR
CYTOCHALASIN D
CYP D
*
% compared to CTR
CTR
CYTOCHALASIN D

# Figure 6

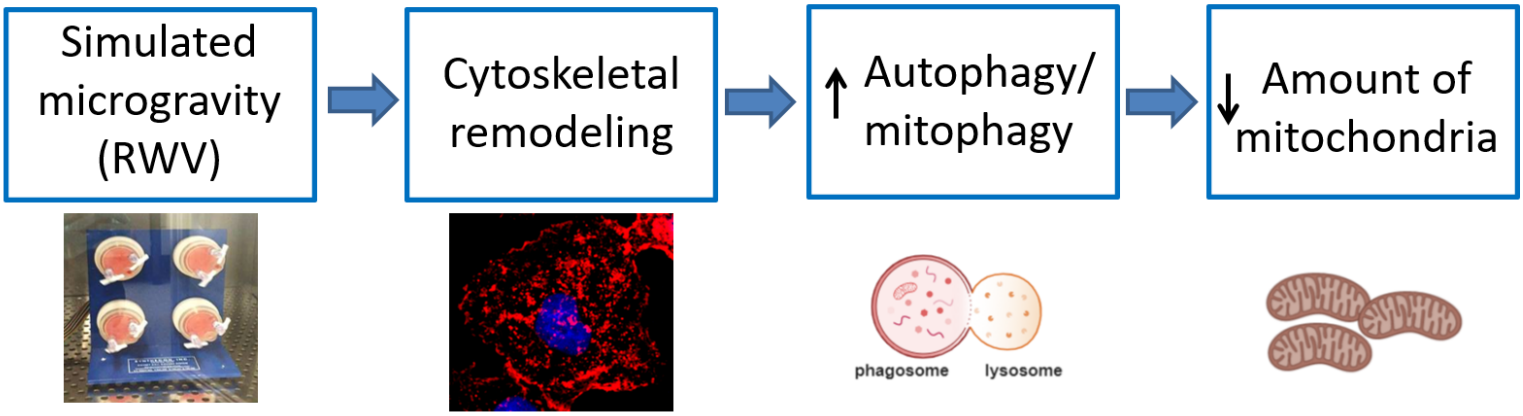
Simulated microgravity (RWV)
Cytoskeletal remodeling
↑ Autophagy/ mitophagy
↓ Amount of mitochondria
phagosome
lysosome